Copyright is owned by the Author of the thesis. Permission is given for a copy to be downloaded by an individual for the purpose of research and private study only. The thesis may not be reproduced elsewhere without the permission of the Author.

Genetic analysis of candidate genes that regulate the *Epichloë festucae-Lolium perenne* mutualistic symbiotic interaction

A thesis presented in partial fulfillment of the requirements for the degree of

Doctor of Philosophy (PhD)
in Genetics

at Massey University, Manawatu,
New Zealand.

Berit Hassing
2019

Abstract

Fungi and plants interact with each other in a multitude of different ways and these interactions can result in different outcomes. The most extreme of these are mutually beneficial interactions, where both partners benefit from the interaction, and pathogenic interactions, where the interaction partners battle each other until one succumbs. For any of these interactions, the fungus relies on two means of communication: (i) it needs to be able to communicate with the host to prevent or elicit defence responses, dependent on the desired outcome, and (ii) it needs to be able to communicate within the hyphal network to ensure nutrient transfer, coordinated growth and development. Here, aspects of these types of communication were analysed in the interaction between the filamentous ascomycete *Epichloë festucae* and perennial ryegrass (*Lolium perenne*). *Epichloë* ssp. are endophytes of cool-season grasses and these interactions are generally mutually beneficial, where the plant benefits through an increased resistance to biotic and abiotic stress, while the fungus feeds on nutrients in the apoplastic space and obtains a means for horizontal and vertical transmission.

Recent studies have highlighted the role of fungal small secreted proteins, so called effectors, in preventing host defence responses in pathogenic as well as beneficial plant-fungal interactions. Here, a list of candidate effectors produced by *E. festucae* was generated and corresponding genes were analysed with regard to genomic location, making use of a fully assembled genome sequence, and expression during growth in axenic culture, *in planta* and in several symbiosis-deficient mutants. While no association of effector candidate-encoding genes with AT-rich regions, telomeres or clusters was found, they were significantly more likely to contain miniature inverted repeat transposable elements (MITEs) in their promotor sequence. As they were also found to be highly upregulated *in planta*, it was hypothesised that MITEs are involved in the regulation of effector gene expression in *E. festucae*. Three candidate effectors and one glycosylphosphatidylinositol (GPI)-anchored protein with a similar expression profile were functionally analysed and found to be secreted. While localisation studies suggested that they remain attached to the fungal cell wall post secretion, genetic deletion or overexpression did not alter the fungus-host interaction, suggesting that these proteins play minor or functionally redundant roles at the observed life stages.

Growth of the endophyte *in planta* is highly regulated and many major signalling pathways are involved in this process, among these signalling via superoxide and other reactive oxygen species (ROS) produced by NADPH oxidase complexes (Nox).

Disruption of these pathways results in stunting of the infected host plant and proliferative growth of the fungus. In mammals and plants, lipid signalling is involved in many crucial cellular processes and multiple studies suggest that it is also involved in the regulation of Nox complexes. Therefore, the role of lipid signalling in fungal growth and the interaction with *L. perenne* was analysed with special focus on a potential role in regulation of the Nox complexes. Of interest here, were the lipid second messengers phosphatidic acid (PA) produced by phospholipase D (PLD), and phosphatidylinositol 4,5-bisphosphate produced by the homolog of the mammalian tumour suppressor protein PTEN.

E. festucae generates two structurally different PLDs, and of these, PldB was found to be required for normal hyphal growth and cell-to-cell fusion. Inoculation of *pldB* deletion strains into *L. perenne* resulted in severe stunting of the plant accompanied by proliferative growth of the fungus. A PA biosensor was generated and demonstrated a localisation to the cytosol instead of to the plasma membrane as observed in WT. Interestingly, nitroblue tetrazolium (NBT) staining revealed that *pldB* deletion strains produced less superoxide. Deletion of the PTEN homolog, *tepA*, did not alter growth of the fungus in culture, but resulted in a mild stunting of the host plant. While lipid biosensors did not localise differently in *tepA* deletion or overexpression strains, staining of *tepA* deletion strains with NBT resulted in an increased signal intensity compared to staining of WT. This might indicate that phosphoinositide 3,4,5-trisphosphate, the substrate of TepA, is involved in the regulation of superoxide production. Together, these observations highlight the importance of lipid signalling for fungal growth and mutualistic interactions, and indicate a connection to superoxide production.

Acknowledgements

First and foremost, I would like to thank my supervisor Barry Scott for giving me the opportunity to do my PhD in his lab, and for the support and incredible amount of feedback I have received over the years. You have given me more opportunities than I could have asked for. To my co-supervisor Carl Mesarich, thank you for getting on board after my confirmation exam and for your support. Your new ideas and feedback have improved all of the projects considerably. Thank you to my co-supervisor Carla Eaton, for helping me get set up and for giving me the opportunity for work on the exciting lipid signalling projects.

I would like to thank André Fleißner for collaborating with us on the PLD project, your contribution adds significant value to this part of our work. To Yvonne Becker, for introducing me to our favourite *Epichloë festucae* all this time ago and for adding very interesting and valuable data to the Ssp project. Thank you David Winter, for contributing considerably to the Ssp and the PLD project, and for your willingness to teach and help a biologist with statistics. To Kimberly Green, for adding to the PLD project, for your valuable comments, and for your friendship and support over the last years; I wish you all the best for your future. I would also like to thank the team at the MMIC: Matthew Savoian, Niki Minard, Pani Vijayan and Jordan Taylor, for your help and interesting discussions. To Ann Truter, Cynthia Cresswell, Fiona Richmond, Debbie McKnight and Mohsen Bagheri, your help was sincerely appreciated.

Thank you Arvina; without your organisational skills, advice and help this would not have been possible. Thank you very much also to the past and present members of the Scottbase lab: Alex, Daniel, Yonathan, Aleysha and Ellie. A special thank you to Taryn, Nazanin and our unofficial member Anika; your friendship, support and advice in all work and life situations has contributed significantly to this work. I could not have asked for a better workgroup.

Thank you very much to the Huggins, Wilson and Gibbie family; your kindness and generosity has made me feel welcomed from the start and your support has been so important over these last years. To Caitlin, Daniel and Ben for the love, support and encouragement; you have impacted my life in so many ways and I look forward to the next adventures.

I would like to thank Massey University, the Bio-Protection Research Centre and the Royal Society of New Zealand Marsden Fund for funding this study.

Finally, I would like to thank my family. Thank you for always believing in me and for supporting me in every possible way, despite me being so far away.

An letzter und wichtigster Stelle möchte ich mich bei meiner Familie bedanken. Mama, Papa, Oma, Opa und Bekky, eure Unterstützung hat diese Doktorarbeit erst möglich gemacht. Danke dass ihr trotz der Entfernung immer dabei seid und stets an mich glaubt. Danke für die offenen Ohren und die guten Ratschläge für alle Lebenslagen. Ihr seid die Besten und ich vermisse euch.

Table of Contents

Chapter 1: Introduction 1

***Epichloë* endophytes: model systems to study mutualistic plant–fungus interactions 3**

Life and growth of *E. festucae in planta* 4

Endophytic growth and asexual transmission 4

The epiphyllous hyphal network 5

The sexual life cycle 6

Benefits of the interaction 7

The *E. festucae* genome 8

Regulation of the interaction 9

The Nox complex 9

MAP kinase pathways 13

Is hyphal fusion required for successful interactions? 14

Epigenetic regulation 14

Additional regulators 14

Identification of small secreted proteins as candidate regulators of the mutualistic interaction 15

The plant immune system and the role of fungal effectors 17

Infection structures and growth *in planta* 18

Invasion patterns 19

Invasion pattern receptors 20

Effectors 21

The genetics of effectors 24

Are effectors required in the interaction between *E. festucae* and *L. perenne?* 25

The requirements of signalling to the host and signalling within the hyphal network 26

The composition of fungal membranes 27

Are lipid second messengers required for fungal growth and the mutualistic interaction? 28

Phosphatidic acid (PA) 29

Phospholipase D 30

Phosphoinositides 31

The phosphatidylinositol 3,4,5-trisphosphate 3-phosphatase PTEN 33

The activation of the Nox complex through lipid signalling **34**
Aims and objectives **35**
About the structure of this thesis **37**

Chapter 2: Analysis of *Epichloë festucae* small secreted proteins in the interaction with *Lolium perenne* **39**
Abstract **41**
Introduction **43**
Materials and Methods **46**
Results **56**
Candidate effectors of *E. festucae* 56
Sequence analysis of downregulated effector candidates 61
GpiB, SspM, SspN and SspO are secreted 63
Analysis of secretion and processing of GpiB, SspM, SspN and SspO in *E. festucae* 64
Functional analysis of *gpiB*, *sspM*, *sspN* and *sspO* 65
Culture and *in planta* phenotype of overexpression strains 72
SspM, SspN and SspO localize extracellularly 75
SspM, SspN, SspO and GpiB do not elicit a defense response in *N. benthamiana* or *N. tabacum* and do not suppress INF1-triggered immunity in *N. benthamiana* 77
Discussion **80**
Supporting information **88**
Acknowledgements **91**
References **92**

Chapter 3: Phosphatidic acid produced by phospholipase D is a key signalling molecule for hyphal cell-to-cell fusion and the mutualistic interaction between *Epichloë festucae* and perennial ryegrass **101**
Summary **103**
Introduction **105**
Materials and Methods **109**
Results **114**
The *Epichloë festucae* genome encodes two putative phosphatidylcholine-hydrolyzing phospholipase Ds 114
PldB is required for normal colony growth and hyphal fusion 116
Localisation of PldA and PldB 120
Interaction partners of PldB 122

PldB is crucial for the *E. festucae-L. perenne* interaction and expressoria formation 122
Deletion of *pldB*, but not *pldA*, results in decreased localisation of a phosphatidic acid biosensor to the plasma membrane 129
Absence of PldB results in mislocalised ROS production 131
The absence of PldB has no effect on Nox complex component localisations 134
Discussion 135
Acknowledgements 143
References 144
Supporting Information 156

Chapter 4: A fungal homolog of the mammalian tumour suppressor protein PTEN is required for the mutualistic interaction between the filamentous ascomycete *Epichloë festucae* and perennial ryegrass 183
Abstract 185
Introduction 186
Materials and Methods 190
Results 195
Epichloë festucae encodes a homolog of the mammalian tumour suppressor protein PTEN 195
Epichloë festucae TepA localises to the cytoplasm and to septa 197
Generation of *Epichloë festucae tepA* deletion and overexpression strains 199
Deletion and overexpression of *Epichloë festucae tepA* does not influence growth in culture 199
Deletion of *Epichloë festucae tepA* influences fungal growth *in planta* 201
Deletion or overexpression of *Epichloë festucae tepA* does not change localisation of lipid biosensors 206
Deletion or overexpression of *Epichloë festucae tepA* does not change localisation of the Nox complex components 208
Deletion or overexpression of *Epichloë festucae tepA* might increase ROS production 211
Discussion 213
Acknowledgements 219
References 220
Supplemental Information 228

Chapter 5: Conclusions and Future Work 239

***E. festucae* small secreted proteins 241**
Conclusions 241
Future work 242
The role of lipid signalling in the mutualistic interaction between *E. festucae* and *L. perenne* 244
Conclusions 244
Future work 245
Bibliography 249
Appendix 271

Table of Figures

Chapter 1: Introduction 1

Figure 1: The life cycle of *Epichloë festucae*. 5

Figure 2: Growth of *Epichloë* species *in planta.* 7

Figure 3: Comparison between the mammalian gp91^{phox} (Nox2) complex and the fungal NoxA (Nox1) complex. 10

Figure 4: The invasion model. 18

Figure 5: Examples of well characterized effectors produced by *Cladosporium fulvum*, *Ustilago maydis*, *Laccaria bicolor* and other species. 22

Figure 6: Simplified overview of glycerophospholipid second messenger synthesis. 29

Chapter 2: Analysis of *Epichloë festucae* small secreted proteins in the interaction with *Lolium perenne* 39

Fig 1. Physical properties of genes encoding effector candidates in *E. festucae*. 58

Fig 2. Analysis of gene expression in WT *E. festucae* and symbiotic mutants of *E. festucae.* 60

Fig 3. Schematic representation of the small secreted proteins SspM, SspN, SspO (effector candidates) and the GPI-anchored protein GpiB and their corresponding genes. 62

Fig 4. Analysis of the GpiB, SspM, SspN and SspO secretion signals in a *S. cerevisiae* complementation assay. 63

Fig 5. Western blot analysis of GpiB-His, SspM-His, SspN-His and SspO-His extracted from *E. festucae* mycelia and culture medium. 65

Fig 6. Culture phenotype of WT and deletion mutant strains. 67

Fig 7. Plant phenotype of *L. perenne* infected with *E. festucae* WT and *gpiB*, *sspM*, *sspN* and *sspO* deletion mutant strains. 68

Fig 8. Light microscopy and transmission electron micrographs of the *in planta* cellular phenotype of *E. festucae* WT and *gpiB*, *sspM*, *sspN* and *sspO* deletion mutant strains. 70

Fig 9. Confocal depth series images of in planta cellular phenotype of *E. festucae* WT and *gpiB*, *sspM*, *sspN* and *sspO* deletion mutant strains. 72

Fig 10. Plant phenotype of *Lolium perenne* infected with *E. festucae* WT and *gpiB*, *sspM*, *sspN* and *sspO* OE strains. 73

Fig 11. Confocal depth image series of in planta cellular phenotype of *E. festucae* WT and *gpiB*, *sspM*, *sspN* and *sspO* OE strains. 75
Fig 12. Confocal micrographs of the localization of SspM-mCherry-NLS, SspN-mCherry-NLS and SspO-mCherry-NLS in endophytic and epiphyllous hyphae of *E. festucae* in mature *L. perenne* plants. 76
Fig 13. *A. tumefaciens* transient expression assays of GpiB, SspM, SspN and SspO in the non-host plants *N. benthamiana* and *N. tabacum*..... 79
S1 File. Methods for computational analysis. 88
S1 Fig. Amino acid sequence alignments of *E. festucae* GpiB, SspM, SspN and SspO. 88
S2 Fig. Strategy for deletion of the *E. festucae* gpiB, sspM, sspN and sspO genes and confirmation by Southern analysis. 88
S3 Fig. Confocal laser scanning microscopy of aniline blue and WGA-AF488 stained ovaries..... 90
S4 Fig. qPCR and RT-qPCR results of the *gpiB*, *sspM*, *sspN* and *sspO* OE strains. 90
S5 Fig. Verification of the heterologous production of GpiB, SspM, SspN and SspO in *N. benthamiana* via western blotting. 90

Chapter 3: Phosphatidic acid produced by phospholipase D is a key signalling molecule for hyphal cell-to-cell fusion and the mutualistic interaction between *Epichloë festucae* and perennial ryegrass..... 101

Figure 1: Structure of *Epichloë festucae* PldA and PldB and phylogenetic analysis of phospholipase D in fungi. 115
Figure 2: Culture phenotype of wild-type *Epichloë festucae* and *pldA* and *pldB* mutant strains. 118
Figure 3: Cytoplasmic mixing of wild-type and *pldB* deletion strains of *Epichloë festucae* expressing cytoplasmic GFP and mCherry. 119
Figure 4: Localisation of GFP-PldA and GFP-PldB in *Epichloë festucae* grown in axenic culture and *in planta*. 121
Figure 5: Plant phenotype of *Lolium perenne* infected with wild-type and *pldA* and *pldB* mutant strains. 124
Figure 6: Light microscopy and transmission electron microscopy of *Lolium perenne* pseudostem cross sections infected with wild-type and *pldA and pldB* mutant strains of *Epichloë festucae*. 126

Figure 7: Confocal depth image series of the cellular phenotype of *Lolium perenne* infected with *Epichloë festucae* wild-type, *pldA* and *pldB* mutant strains. 129
Figure 8: Localisation of the phosphatidic acid biosensor in *Epichloë festucae* wild-type and *pldA* and *pldB* deletion strains growing in axenic culture and *in planta.* 130
Figure 9: Analysis of superoxide production in *Epichloë festucae* wild-type, *pldA* and *pldB* deletion stains. 133
Supporting Information Fig. S1: Amino acid sequence alignment of *Epichloë festucae* PldA and PldB with homologs from other Ascomycete fungi. 169
Supporting Information Fig. S2: Strategy for the deletion of *Epichloë festucae pldA* and *pldB* and verification of deletion by Southern blot analysis. 171
Supporting Information Fig. S3: qRT-PCR analysis of *Epichloë festucae pldA* and *pldB* overexpression strains. 173
Supporting Information Fig. S4: Quantification of hyphal fusion events in *Epichloë festucae* wild-type and *pldA* and *pldB* deletion strains. 174
Supporting Information Fig. S5: Verification of the expression of GFP-PldA, GFP-PldB, PldA-mCherry and PldB-mCherry fusion proteins in *Epichloë festucae* by western blot. 175
Supporting Information Fig. S6: PldB of *Epichloë festucae* does not interact with components of the Nox complex or regulators identified in mammalian cells. 176
Supporting Information Fig. S7: Number of hyphae per intercellular space in *Epichloë festucae* WT and *pldA* and *pldB* mutant strain-infected *Lolium perenne* plants. 177
Supporting Information Fig. S8: Cellophane membrane penetration by *Epichloë festucae* wild-type, *pldB*, *noxA* and *noxB* deletion strains. 178
Supporting Information Fig. S9: Verification of the expression of the phosphatidic acid biosensor in the *Epichloë festucae* wild-type and *pldA* and *pldB* deletion strains by western analysis. 179
Supporting Information Fig. S10: Localisation of Nox complex components in *Epichloë festucae* wild-type and *pldA* and *pldB* deletion strains. 181

Chapter 4: A fungal homolog of the mammalian tumour suppressor protein PTEN is required for the mutualistic interaction between the filamentous ascomycete *Epichloë festucae* and perennial ryegrass 183

Figure 1: Domain structure and protein sequence alignment of *Epichloë festucae* TepA with *H. sapiens* PTEN and its homologs from other fungi. 196

Figure 2: Localisation of TepA during axenic growth of *Epichloë festucae*. ... 199
Figure 3: Culture phenotype of *Epichloë festucae* wild-type and *tepA* mutants. 201
Figure 4: Whole-plant interaction phenotype of *Lolium perenne* plants infected with *Epichloë festucae* WT and *tepA* mutant strains. 203
Figure 5: Examination of pseudostem sections of *Lolium perenne* plants infected with *Epichloë festucae* wild-type and *tepA* deletion strains by light- and transmission electron microscopy..... 203
Figure 6: Confocal depth series of longitudinal sections of *Lolium perenne* infected with *Epichloë festucae* wild-type and *tepA* mutant strains. 206
Figure 7: Localisation of PA, PtdIns[4,5]P_2 and PtdIns[3,4,5]P_3 in *Epichloë festucae* wild-type and *tepA* mutant strains. 208
Figure 8: Localisation of Nox complex components in *Epichloë festucae* wild-type and *tepA* mutant strains. 210
Figure 9: Detection of superoxide in *Epichloë festucae* wild-type and *tepA* mutant strains. 212
Supplemental Figure S1: Verification of the expression of GFP-TepA and TepA-mCherry fusion proteins in *Epichloë festucae* by western blot analysis. 234
Supplemental Figure S2: Strategy for the deletion of *Epichloë festucae tepA* and Southern blot analysis. 235
Supplemental Figure S3: Expression analysis of *Epichloë festucae tepA* overexpression strains by qRT-PCR. 236
Supplemental Figure S4: Growth analysis *Lolium perenne* plants infected with *Epichloë festucae* wild-type and *tepA* overexpression strains. 237

Chapter 5: Conclusions and Future Work 239

Bibliography 249

Appendix 271

List of Tables

Chapter 1: Introduction 1

Table 1: *Epichloë festucae* differentially regulated genes coding for small secreted proteins identified by Eaton *et al*., (2015). 16

Chapter 2: Analysis of *Epichloë festucae* small secreted proteins in the interaction with *Lolium perenne* 39

S1 Table. Biosample references 90

S2 Table. Biological material. 90

S3 Table. Primers used in this study. 91

S4 Table. Summary of the presented information about *E. festucae* effector candidates. 91

S5 Table. Gene expression analysis of wild-type *in planta* versus wild-type in culture. 91

S6 Table. Distribution of *gpiB* and the *ssps* within *Epichloë* and related species. 91

S7 Table. Vertical transmission of ssp mutants in *L. perenne*. 91

Chapter 3: Phosphatidic acid produced by phospholipase D is a key signalling molecule for hyphal cell-to-cell fusion and the mutualistic interaction between *Epichloë festucae* and perennial ryegrass 101

Supporting Information Table S1: Biological material. 156

Supporting Information Table S2: Primer sequences. 160

Supporting Information Methods S1: Construct design. 163

Chapter 4: A fungal homolog of the mammalian tumour suppressor protein PTEN is required for the mutualistic interaction between the filamentous ascomycete *Epichloë festucae* and perennial ryegrass 183

Supplemental Table S1: Biological material. 228

Supplemental Table S2: Primers used in this study. 231

Chapter 5: Conclusions and Future Work 239

Bibliography 249

Appendix 271

Table of Appendices

Appendix 1: DRC 16 Form for Chapter 2 273
Appendix 2: DRC 16 Form for Chapter 3. 274
Appendix 3: DRC 16 Form for Chapter 4. 275
Appendix 4: *gpiB* (pBH1), *sspM* (pBH2), *sspN* (pBH3) and *sspO* (pBH4) deletion constructs. 276
Appendix 5: *gpiB* (pBH29), *sspM* (pBH30), *sspN* (pBH31) and *sspO* (pBH32) overexpression constructs. 277
Appendix 6: cytoplasmic GFP (pBH28) and *sspM* (pBH19), *sspN* (pBH22) and *sspO* (pBH25) localization constucts. 278
Appendix 7: *gpiB* (pBH5), *sspM* (pBH11), *sspN* (pBH7) and *sspO* (pBH9) pSUC2T7M13OR constucts. 279
Appendix 8: *gpiB* (pBH44), *sspM* (pBH45), *sspN* (pBH46) and *sspO* (pBH47) pICH86988 constucts. 280
Appendix 9: *gpiB* (pBH56), *sspM* (pBH57), *sspN* (pBH58) and *sspO* (pBH59) expression constructs with 6xHis-tag. 281
Appendix 10: *pldA* and *pldB* deletion (pCE131, pEC121) and overexpression (pCE129, pBH48) constructs. 282
Appendix 11: *pldA* and *pldB* GFP fusion (pBH37, pBH54) and mCherry fusion (pBH38, pBH52) constructs. 283
Appendix 12: *pldB* complementation (pBH51) and PA-biosensor (pBH51) constructs. 284
Appendix 13: *pldB* (pBH60, pBH61), *mssD* (pBH63, pBH62) and *pkcA* (pBH64, pBH65) yeast two-hybrid constructs. 285
Appendix 14: *tepA* depetion (pBH43) and overexpression (pCE122) constructs. 286
Appendix 15: *tepA* GFP fusion (pBH41) and mCherry fusion (pBH42) constructs. 287

List of Abbreviations

aa Amino acid

AA arachidonic acid

Amp Ampicillin

Amp^R Ampicillin resistant

Af Aspergillus fumigatus

An Aspergillus nidulans

Bc Botrytis cinerea

BLAST Basic local alignment search tool

BLASTn Nucleotide database search using a nucleotide query

BLASTp Protein database search using a protein query

bp Base pair(s)

cDNA Complementary DNA

CFW Calcofluor white

CLSM Confocal Laser Scanning Microscopy

Cp Claviceps purpurea

CWI Cell wall integrity

Cys Cysteine

DAG diacylglycerol

DIC Differential interference contrast

DIG Digoxigenin

DNA Deoxyribonucleic acid

dNTP Deoxynucleotide triphosphate

EDTA Ethylene diamine tetra-acetic acid

GFP Green fluorescent protein

Fg Fusarium graminearum

g Gram

gDNA Genomic DNA

GEF Guanine nucleotide exchange factor

Gen Geneticin

Gen^R Geneticin resistant

GFP Green fluorescent protein

GPI Glycosylphosphatidylinositol

h Hour(s)

H_2O_2 Hydrogen peroxide

Hph Hygromycin resistance gene

Hyg^R Hygromycin resistant

Kan Kanamycin

Kan^R Kanamycin resistant

kb Kilobase(s)

L Litre

LB Lysogeny broth

LPA lysophosphatidic acid

LPC lysophosphatidylcholin

LPA lysophosphatidic acid

M Molar

MAPK(K/K) Mitogen activated protein kinase (kinase/kinase)

µg Microgram

µm Micrometre

µM Micromolar

µL Microlitre

min Minute(s)

mg Milligram

mm Millimeter

mM Millimolar

mL Millilitre

MITE Miniature inverted-repeat transposable element

Mo Magnaporthe oryzae

mRNA Messenger ribonucleic acid

NADH Nicotinamide adenine dinucleotide (reduced form)

NADPH Nicotinamide adenine dinucleotide phosphate (reduced form)

Nc Neurospora crassa

NCBI National Centre for Biotechnology Information

ng Nanogram

Nox NADPH oxidase

Pa Podospora anserina

PA phosphatidic acid

PB1 Protein binding domain 1

PC Plant cell

PCR Polymerase chain reaction

PD Potato dextrose

PEG Polyethylene glycol

pg Picogram

PH pleckstrin homology domain

PLA Phospholipase A

PLC Phospholipase C

PLD Phospholipase D

PM Plasma membrane

pmol Picomole

PMSF Phenylmethylsulfonyl fluoride

PR Pheromone response

PTEN Phosphatase and tensin homolog

PtdIns Phosphatidylinositol

PtdIns[3]P Phosphatidylinositol 3-phosphate

PtdIns[4]P Phosphatidylinositol 4-phosphate

PtdIns[5]P Phosphatidylinositol 5-phosphate

PtdIns[3,4]P_2 Phosphatidylinositol 3,4-bisphosphate

PtdIns[3,5]P_2 Phosphatidylinositol 3,5-bisphosphate

PtdIns[4,5]P_2 Phosphatidylinositol 4,5-bisphosphate

PtdIns[3,4,5]P_3 Phosphatidylinositol 3,4,5-trisphosphate

PX phox homology domain

RG Regeneration

RNA Ribonucleic acid

RNase Ribonuclease

RNA-seq Ribonuclease sequencing

ROS Reactive oxygen species

RPMK Reads per kilo base per million mapped reads

RT Reverse transcriptase

qRT-PCR Quantitative reverse transcriptase-polymerase chain reaction

SAK Stress-activated kinase

SAM Shoot apical meristem

Sc Saccharomyces cerevisiae

SC Synthetic complete

SD Synthetic defined

SDS Sodium dodecyl sulfate

SDS-PAGE Sodium dodecyl sulfate-polyacrylamide gel electrophoresis

Sp Schizosaccharomyces pombe

STRIPAK Striatin interacting phosphatase and kinase

tBLASTn Translated nucleotide database search using a protein query

T-DNA Transfer-deoxyribonucleic acid

TE Transposable element

TEM Transmission electron microscopy

Um Ustilago maydis

V Volts

v/v Volume/volume ratio

WT Wild-type

w/v Weight/volume ratio

°C Degrees Celsius

Chapter 1: Introduction

Epichloë endophytes: model systems to study mutualistic plant–fungus interactions

The fungal family of the Clavicipitaceae contains symbionts of a large range of species, from pathogens of insects (arthropods) and nematodes to mutualists of plants (Schardl, 2001; Spatafora *et al*., 2007). Many of the family members are well known, e.g. the infamous *Claviceps purpurea,* which causes ergotism disease of humans (Tudzynski *et al*., 2001). This study focuses on endophytes of the *Epichloë* genus, which form stable interactions with temperate grasses of the sub-family *Pooideae* (genera *Lolium* and *Festuca*) (Schardl, 2001; Schardl *et al*., 2004). Many *Epichloë* species are able to the increase the tolerance of the host to biotic and abiotic stress. They can produce a remarkable selection of secondary metabolites that provide defense against herbivores, as well as provide drought tolerance (Hahn *et al*., 2008). Due to these advantages, and the requirement of grass to feed livestock, *Epichloë* endophytes are of great agricultural interest and importance (Scott and Schardl, 1993, Scott *et al*., 2012).

The *Epichloë* genus consists of two clades, the *Epichloë typhina* complex and the "main" complex. While species in the *E. typhina* complex have a broad host range, species in the main complex are often associated with a single host tribe (Clay and Schardl, 2002). The nature of these interactions can be best described as a symbiotic continuum that ranges from mainly antagonistic to mutualistic (Schardl, 2001). The position of each species on the continuum is largely dependent on their mode of transmission, which can be sexual, asexual, or both (Schardl, 2001; Schardl *et al*., 2004). During the asymptomatic asexual mode of transmission, the fungus colonizes the ovules and emerging seeds of its host to be transmitted vertically. Exclusively asexually transmitted species (i.e. those that have lost the ability to transmit sexually) are often the result of interspecies hybridization events or sexual intraspecies hybridization (Moon *et al*., 2004). During the sexual mode of transmission, the fungus builds a dense mycelial network on the emerging inflorescence of the host, which prevent its maturation. Strictly sexually reproducing species completely prevent seed production of the host, a state which is referred to as 'choke' disease, and are therefore antagonistic (Clay and Schardl, 2002).

Epichloë festucae is a sexually transmitted *Epichloë* species that is naturally found in *Festucae* spp. However, is it also able to colonize *Lolium perenne*, a globally important pasture grass (Leuchtmann *et al*., 1994; Schardl *et al*., 2004). While a natural endophyte of *L. perenne, E. festucae var*. *lolii* is intractable to genetic manipulation. *E. festucae*, on the other hand, is amenable to genetic modifications. It can also be grown

in axenic culture in approx. one week, and can be artificially inoculated into *L. perenne* seedlings (Latch and Christensen 1985; Scott *et al*., 2012; Becker *et al*., 2018). These features, together with the fact that the complete genome sequence and a number of transcriptome datasets are available (Eaton *et al*., 2015; Dupont *et al*., 2015; Winter *et al*., 2018; Hassing *et al*., 2019), make *E. festucae* an ideal model system to study mutualistic plant-fungal interactions (Scott and Schardl, 1993; Scott *et al*., 2012).

Life and growth of *E. festucae in planta*

Endophytic growth and asexual transmission

E. festucae, like all *Epichloë* species, relies entirely on its host for the completion of its life cycle. This life cycle includes a sexual as well as an asexual stage (Figure 1). During the asexual stage, fungal hyphae expand from the vegetative tissue to colonize the intercellular spaces of the host developing inflorescences, developing ovules, embryos and surrounding tissues (Figures 2F and 2G) (Schardl *et al*., 2004). In doing so, *E. festucae* is able to undergo vertical transmission through the dissemination of infected seeds (Figure 1) (Clay and Schardl, 2002). Upon seed germination, the fungal hyphae then colonize the shoot cell division zone and leaf primordia by hyphal tip growth to align themselves with the leaf axis, where they become physically attached to the plant cell wall by way of an extracellular matrix (Philipson and Christey, 1986). From there, *E. festucae*, like all *Epichloë* species, systemically colonizes the aerial tissues of the host, where it remains confined to the apoplast space. No colonization of the roots or the vascular bundles has been observed (Schardl *et al*., 2004; Scott *et al*., 2012). To maintain synchronized growth with the host, hyphal compartments are elongated in a process called intercalary growth (Figure 2H). Here, hyphae are stretched along their longitudinal axis by mechanical force through the attachment to elongating plant cells (Figures 2E and H). This stretching is followed by the deposition and reinforcement of cell wall material and generation of septa (Christensen *et al*., 2008). Longitudinal hyphal growth ceases as soon as the plant reaches maturity. Instead, hyphae increase only in diameter, while continuing to be metabolically active (Tan *et al*., 2001; Christensen *et al*., 2008). Occasional fusion between two hyphae can also be observed, with the resulting hyphal network within the plant allowing for efficient signalling and nutrient exchange (Christensen *et al*., 2008; Scott *et al*., 2012; Becker *et al*., 2016). Endophytic hyphae subsist entirely on nutrients available in the apoplast and do not generate specialized feeding structures like, for example, haustoria or arbuscules (Christensen *et al*., 2002).

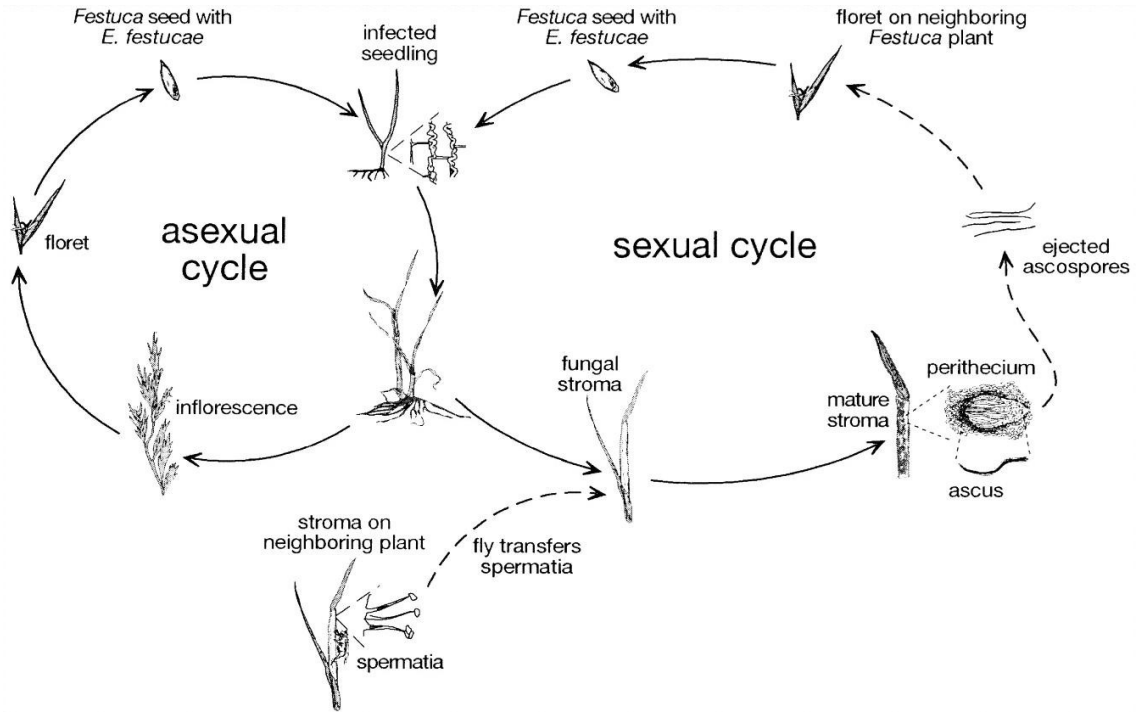

Figure 1: The life cycle of *Epichloë festucae*.

Image reproduced from Clay and Schardl (2002) with permission from the American Naturalist.

The epiphyllous hyphal network

In addition to the endophytic hyphal network, *E. festucae* and other *Epichloë* spp. are able to generate an interconnected epiphytic network on the surface of the leaf (Christensen *et al*., 1997; Moy *et al*., 2000). This epiphytic network results from breaching of the cuticle within the leaf expansion zone by a specialized structure called an expressorium, a swelling of a subcuticular hyphae that is able to rupture the cuticle layer (Becker *et al*., 2016). This exiting of the plant is accompanied by a major remodelling of the fungal cell wall (Becker *et al*., 2016). The epiphyllous network is required for the mutualistic interaction, with the connection between epiphyllous and endophytic hyphae remaining during further growth of the plant (Becker *et al*., 2016). The role of this epiphyllous network is not fully elucidated, but has been proposed to result in increased resistance of the host to other microorganisms by niche exclusion (Moy *et al*., 2000).

The sexual life cycle

The sexual cycle of *Epichloë* spp. is dependent on the physiological state of the host and requires a switch from restrictive to proliferative growth of the fungus (Figures 1, and 2A). While the regulatory signalling mechanism behind this change in growth pattern is not fully understood, the effects are clearly observable. Just prior to the onset of flowering, the fungus proliferates on the leaf sheath surrounding the inflorescence and generates a compact mycelial structure, the stroma (Figures 1, 2A and 2B). This structure prevents maturation of the host inflorescence and the affected tiller will not produce any seeds, which is a feature of antagonistic growth (Clay and Schardl, 2002; Schardl *et al*., 2004; Scott *et al*., 2012). However, most species do not choke all tillers of an infected plants and the effect on the plant fitness is minor. As *Epichloë* spp. are heterothallic, cross fertilization by a strain with the opposite mating type is required to produce sexual ascospores. Conidiospores (spermatia) (Figure 2C) are generated on the young stroma and dispersed by flies of the genus Botanophila, the “third” mutualist of this interaction (Figure 1) (Schardl *et al*., 2004). These flies are attracted by volatiles produced by the fungus (Bultman and Leuchtmann, 2008). While the fly feeds and oviposits on the mycelial structure it transfers spermatia via its faeces to other stromata. The larvae, in turn feed, on the developing perithecia (Figure 2B) (Kohlmeyer *et al*., 1974; Schardl *et al*., 2004; Bultmann and Leuchtmann, 2008).

Upon transfer of the spermatia, the fungus undergoes heterothallic mating, resulting in the development of perithecia containing multiple asci, each filled with four ascospores (Clay and Schardl, 2004; Schardl *et al*., 2004). These ascospores are then ejected into the air and infect the ovules of neighbouring plants to be further transmitted horizontally (Figure 1) (Chung and Schardl, 1997; Schardl *et al*., 2004).

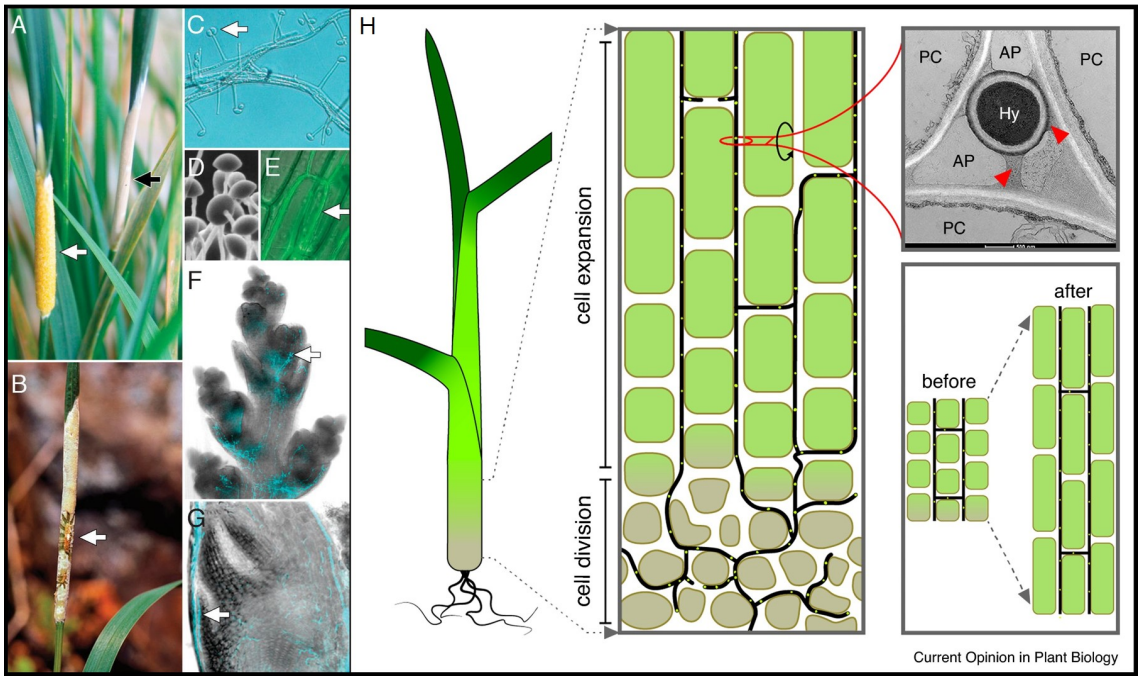

Figure 2: Growth of *Epichloë* species *in planta.*

(A) Stroma of *Epichloë amarillans* before fertilization (black arrow), and after fertilization and maturation (white arrow). (B) Fertilized and partially mature stroma of *E. typhina* (on *Poa trivialis*) with a larval case (arrow) of the symbiotic *Botanophila* sp. fly, surrounded by feeding tracks. (C) Germinating ascospores of *Epichloë elymi* giving rise to conidiophores bearing single or multiple conidia (arrow). (D) Scanning electron micrograph of conidiophores from a mass of germinating *E. amarillans* ascospores. (E) Intercellular growth of *Epichloë festucae* (arrow) in leaf sheath of *Lolium perenne*. Confocal optical slices of transformed *E. festucae* expressing green fluorescent protein overlaid with DIC image. (F) Inflorescence primordium of *L. perenne* with endophytic growth of *E. festucae* (arrow). Confocal optical slices of transformed *E. festucae* expressing cyan fluorescent protein overlaid with DIC image. (G) Endophytic growth of *E. festucae* in *L. perenne* seed, beneath seed coat (arrow), and around and within the embryo. Confocal optical slices of transformed *E. festucae* expressing cyan fluorescent protein overlaid with DIC image. (H) Intercalary growth of *Epichloë* species *in planta* and attachment to an extracellular matrix. Figure and figure legend reproduced from Leuchtmann *et al*. (2014) (A-G) and Scott *et al*. (2018) (H) with permission from Taylor and Francis and Elsevier, respectively.

Benefits of the interaction

Despite the negative impact on the host fitness by the sexual transmission of the fungus, the interaction also increases the host fitness through the production of

protective secondary metabolites (Schardl, 2001; Schardl *et al*., 2004; Schardl *et al*., 2013). The major known classes of secondary metabolites generated by *Epichloë* endophytes are ergot alkaloids, lolines, indole-diterpenes and peramine, of which lolines and peramine mainly have activity against insects and ergot alkaloids and indole-diterpenes affect both insects and mammals (Schardl *et al*., 2013). Among *Epichloë* species is a large chemotypic diversity, thus not every species is able to produce all classes of secondary metabolites and some have been reported to produce none at all (Leuchtmann *et al*., 2000; Schardl *et al*., 2013). One defining feature of these secondary metabolites is that they are exclusively produced *in planta* (Chujo and Scott, 2014). However, their expression is regulated by many factors such as plant hormones, types of herbivory and temperature (Hennessy *et al*., 2016; Fuchs *et al*., 2017; Bastias *et al*., 2017).

In addition to secondary metabolites, many *Epichloë* spp are also able to produce antimicrobial peptides such as Mcf which have activity against clack cutworm, or Efe-AfpA, which has activity against the plant pathogen *Sclerotinia homoeocarpa* (Ambrose *et al*., 2014; Tian *et al*., 2017). Another example is GigA from *E. festucae*, which is cleaved into multiple peptides that are then cyclized. These cyclized peptides, called epichloëcyclins, are suspected to have antimicrobial functions in the apoplast (Johnson *et al*., 2015). Other studies have demonstrated an increase in tolerance of the host to abiotic stress, especially to drought (Bouton *et al*., 1993; Schardl *et al*., 2004). This has been suggested to be due to the induction of compatible solutes production or the induction of increased root growth (Malinowski *et al*., 1999; Hahn *et al*., 2008; Dupont *et al*., 2015)

The *E. festucae* genome

Recently, the complete telomere-to-telomere genome sequence of *E. festucae* strain FI1 has been assembled, which consists of 35 mbp and 8,959 genes distributed on seven chromosomes (Winter *et al*., 2018). As observed for many filamentous fungi, the genome is highly fragmented, consisting of gene-rich/GC-rich regions (GC isochores or GC blocks), as well as gene-poor/AT-rich regions (AT isochores or AT blocks). These AT isochores are rich in repeat sequences, such as transposons and miniature inverted repeat transposable elements (MITEs), and are strongly affected by repeat-induced point mutations (RIP) (Winter *et al*., 2018). Interestingly, the repeat sequences maintain the three-dimensional organization of the genome within the nucleus, where they affect gene expression, as many genes differentially expressed *in planta* are in proximity to these AT isochores (Winter *et al*., 2018). The availability of the complete

genome sequence, as well as topological data, will be a great benefit in better understanding the interaction between *E. festucae* and *L. perenne*.

Regulation of the interaction

Many *E. festucae* genes important for the mutualistic interaction with *L. perenne* have been identified from forward and reverse genetic screens of strain FI1. Many of these genes are connected to the major signalling pathways such as ROS signalling and mitogen activated kinase (MAP) signalling pathways. Other proteins that are required for the mutualistic interaction regulate chromatin structure, iron uptake, or other signalling pathways. The role of these key genes will be described briefly below. As the NADPH oxidase (Nox) complex is of great interest to this study, it will be reviewed in more detail.

The Nox complex

Superoxide and other reactive oxygen species (ROS) are required for signalling in fungi, mammals and plants, and are amongst others generated by NADPH oxidase (Nox) complexes (Bedard and Krause, 2007; Saed-Moucheshi, 2014; Breitenbach *et al*., 2015; Zhang *et al*., 2016). The Nox complex consists of a catalytic subunit, which is integrated into the membrane through six transmembrane helixes, and cytoplasmic activator proteins that interact with the catalytic subunit through its cytoplasmic loops (Bedard and Krause, 2007; Belambri *et al*., 2018). These complexes generate superoxide (O_2^-) by transferring electrons from NADPH across membranes to the electron acceptor oxygen (O_2), making use of $FADH_2$ and two haem groups as cofactors (Bedard and Krause, 2007). The structure and function of the catalytic subunit is highly conserved among higher eukaryotes; however, the activating components differ (Marschall and Tudzynski, 2016). In mammals, the complex localises to the plasma membrane (PM), as well as to mitochondria and the ER (Graham *et al*., 2010; Laurindo *et al*., 2014; Marschall and Tudzynski, 2016). Mammals contain seven subfamilies of Nox proteins: Nox1-Nox5 as well as DUOX1 and DUOX2 (Lambeth *et al*., 2000). The best characterized complex is the Nox2 complex, which is responsible for the phagocytic burst in neutrophils in response to pathogens (Lambeth and Neish, 2014). It consists of the catalytic protein $gp91^{phox}$ (Nox2), the membrane adaptor protein $p22^{phox}$, which together form cytochromeB_{558}, the regulator protein $p67^{phox}$, and the organizer components $p40^{phox}$, $p47^{phox}$ and the small GTPase Rac2 (Figure 3) (Babior, 1999). The activation of the complex requires the phosphorylation of all subunits, the activation of Rac2, and the translocation and interaction of the

cytosolic components to the membrane-bound components. In the resting cell, $p40^{phox}$, $p47^{phox}$ and $p67^{phox}$ form a complex in the cytosol, while Rac2 is in the cytosolic, GDP-bound form and associated with Rho-GDI (GDP dissociation inhibitor). Upon activation, all subunits, except for Rac2 are phosphorylated, and the phosphorylation of $p47^{phox}$ induces a conformational change and release of protein and lipid-binding domains (Belambri *et al.*, 2018). This results in the translocation of the subunits to the membrane, likely due to the lipid-binding domains of $p47^{phox}$ and $p40^{phox}$. Upon activation, Rac2 is released from RhoGDI and recruited to the PM via a geranylgeranyl anchor, where it interacts with a RhoGEF (guanidine exchange factor) to exchange GDP with GTP. Subsequently, Rac2 interacts with Nox2 and $p67^{phox}$ (Scott, 2015; Rastogi *et al.*, 2017; Belambri *et al.*, 2018). In mammalian cells, ROS signalling is required for the oxidative burst against invading pathogens, cell growth, differentiation, motility, cytoskeleton rearrangement and apoptosis (Arbiser *et al.*, 2001; Chiarugi *et al.*, 2003; Bedard and Krause, 2007; Lambeth and Neish, 2014).

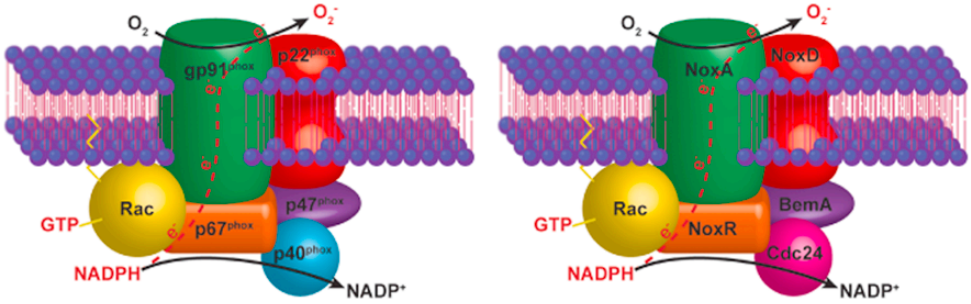

Figure 3: Comparison between the mammalian $gp91^{phox}$ (Nox2) complex and the fungal NoxA (Nox1) complex.

Figure adapted from Scott (2015), with permission from John Wiley and Sons.

Plants have up to 10 NADPH oxidase subfamilies, the so-called respiratory burst oxidase homologs (RBOHs). Similar to mammalian Nox5, they all contain a Ca^{2+}-binding EF-hand motif in their N-terminal region. For activation, they require the small GTPase, Rop (the homolog of mammalian Rac), calcium signalling, as well as the activity of phospholipase D and its product phosphatidic acid (Wong *et al.*, 2007; Ogasawara *et al.*, 2008; Shi *et al.*, 2008; Kaur *et al.*, 2014). ROS signalling is required for root hair and pollen tube growth, plant hormone signalling, seed germination, response to pathogens and abiotic stress (Torres *et al.*, 2002; Bhattacharjee, 2005; Potocký *et al.*, 2007; Müller *et al.*, 2009; Swanson and Gilroy, 2010; Müller *et al.*, 2012; Kaur *et al.*, 2014).

A homolog of the mammalian Nox complexes was first identified in *Aspergillus nidulans*, where it is required for fruiting body development (Lara-Ortiz *et al*., 2003). Since then, it has been shown that fungi in general contain three different subfamilies of the catalytic Nox proteins, and single species contain one to three different Nox proteins (Aguirre *et al*., 2005; Kim *et al*., 2014; Marschall and Tudzynski, 2016). The fungal NoxA (Nox1) and NoxB (Nox2) proteins are homologs of gp91^{phox}, whereas the fungal NoxC protein is more like mammalian Nox5 and plant RBOHs in that it contains a Ca^{2+}-binding EF-hand motif (Aguirre *et al*., 2005; Marschall and Tudzynski, 2016). The most well know fungal Nox complexes are the NoxA and NoxB complexes, which are required for different developmental functions (Figure 3). The fungal NoxA complex consists of the catalytic subunit NoxA, the membrane integrated adaptor protein NoxD (homolog of p22^{phox}), RacA (homolog of Rac2) and the regulator protein NoxR (homolog of p67^{phox}) (Lara-Ortiz *et al*., 2003; Tanaka *et al*., 2006; Takemoto *et al*., 2006; Cano-Dominguez *et al*., 2008; Tanaka *et al*., 2008; Siegmund *et al*., 2013; Lacaze *et al*., 2014; Siegmund *et al*., 2015; Marschall and Tudzynski, 2016). While NoxR contains the domains necessary for the interaction with RacA (four tetratricopeptide repeat (TPR) motifs) and NoxA (NoxA activation domain), it lacks the SH3 protein interaction domains required for the interaction with p40^{phox} and p47^{phox}. In addition, the phox and Bem1 (PB1) domain is very different from the same domain in p67^{phox}, where it is required for the interaction with p40^{phox} (Takemoto *et al*., 2006; Scott, 2015). These observations are consistent with the lack of p40^{phox} and p47^{phox} in fungi (Figure 3) (Tudzynski *et al*., 2012; Scott, 2015). However, interaction studies with NoxR have identified the protein BemA, potentially a functional homolog of p47^{phox}, and Cdc24 as components of the fungal Nox complex (Takemoto *et al*., 2011; Marschall and Tudzynski, 2016). Like p40^{phox} and p47^{phox}, both BemA and Cdc24 contain lipid-binding domains. Signalling via Cdc42 has also been shown to influence Nox activity (Kayano *et al*., 2018). The NoxA complex is required for hyphal fusion in *E. festucae*, *Neurospora crassa*, *Sordaria macrospora* and *Botrytis cinerea*, fruiting body development in *Podospora anserina, S. macrospora* and *N. crassa*, sclerotia formation *B. cinerea*, *Sclerotinia sclerotiorum* and *C. purpurea*, appressorium development in *Magnaporthe oryzae* and *P. anserina*, and hyphal growth in plant–symbiotic fungi (Lara Ortiz *et al*., 2003; Malagnac *et al*., 2004; Tanaka *et al*., 2006; Cano-Dominguez *et al*., 2008; Roca *et al*., 2012; Read *et al*., 2012; Tudzynski *et al*., 2012; Kayano *et al*., 2013; Ryder *et al*., 2013; Dirschnabel *et al*., 2014; Scott, 2015; Becker *et al*., 2016). In *E. festucae*, deletion of *noxA, noxR* and *racA* results in a loss of hyphal fusion, increased conidiation, and a disruption of the symbiotic interaction (Tanaka *et al*., 2006; Takemoto *et al*., 2006; Takemoto *et al*., 2011; Kayano *et al*., 2013). Deletion strains of

noxA and *noxR* were also unable to form expressoria (Becker *et al*., 2016). The deletion of *bemA* resulted in reduced fusion in culture and a mild stunting of the host plant, indicating that BemA is not essential for NoxA activity (Takemoto *et al*., 2011). Interestingly, the disruption of the small GTPase Cdc42 did not influence growth in axenic culture, or the whole plant phenotype (Kayano *et al*., 2018). Microscopic analysis of the cellular phenotype *in planta*, however, revealed that mutant hyphae frequently exhibited hyphal breakage (Kayano *et al*., 2018).

Studies in *P. anserina* and *B. cinerea* demonstrated a colocalisation of the respective NoxA and NoxD homolog in the nuclear envelope, endoplasmic reticulum (ER), in vesicles and vacuoles (Siegmund *et al*., 2013; Lacaze *et al*., 2014; Siegmund *et al*., 2015). However, a BcNoxA construct confined to the ER by the addition of an ER retention signal was unable to fully complement the phenotype, indicating that transport to a different membrane via the Golgi apparatus and vesicles is required for NoxA function (Siegmund *et al*., 2015; Scott, 2015). Cytoplasmic components of the Nox complex in *E. festucae* were found to localise to the vesicles, septa, puncta at the hyphal tip, as well as the apical hyphal membrane (Tanaka *et al*., 2008; Kayano *et al*., 2013; Kayano *et al*., 2018).

The fungal NoxB complex utilizes the tetraspannin Pls1 as a membrane adaptor protein instead of NoxD (Egan *et al*., 2007; Lambou *et al*., 2008; Siegmund *et al*., 2015; Green *et al*., in press). The observation of similar phenotypes in *noxR* and *noxR/noxB* double deletion strains suggest that NoxR also regulates the activity of NoxB (Scott, 2015; Marschall and Tudzynski, 2016). Other components of the NoxB complex have not been identified to date, but might be shared with the NoxA complex in a similar way as NoxR. NoxB is required for fruiting body development in *B. cinerea*, *S. sclerotiorum* and *C. purpurea,* germination of melanised ascospores and plays a key role in appressorium development in *M. oryzae*, *B. cinerea* and *Verticilium dahliae* (Gourgues *et al*., 2004; Malagnac *et al*., 2004; Egan *et al*., 2007; Cano-Dominguez *et al*., 2008; Segmüller *et al*., 2008; Kim *et al*., 2011; Ryder *et al*., 2013; Zhao *et al*., 2016). In *E. festucae* the deletion of *noxB* and *plsA* results in severely stunted host plants and strains are unable to form expressoria (Becker *et al*., 2016; Green *et al*., 2019 (in press)).

In *B. cinerea*, NoxB and Pls1 were found to localise to nuclear membranes, the ER and vacuoles, comparable to the localisation of NoxA and NoxD (Siegmund *et al*., 2013). However, NoxB confined to the ER was unable to complement the phenotype in *B. cinerea*, indicating that it functions elsewhere (Marschall *et al*., 2016). The localisation of NoxB and PlsA in *E. festucae* have not been analysed to date.

MAP kinase pathways

Generally, MAP kinase pathways are required for signal transduction from the cell wall to the nucleus, where they activate gene expression. Each pathway consists of specific receptors, adaptor proteins, three MAP kinases that get sequentially phosphorylated, and specific transcription factors. Often the MAP kinases rely on the presence of a pathway-specific scaffolding protein for more efficient phosphorylation. Three MAP kinase pathways have been described in filamentous fungi (Rispail *et al*., 2009; Hamel *et al*., 2012; Martínez-Soto and Ruiz-Herrera, 2017). Not only are these pathways required for normal growth and mutualism in *E. festucae*, but also for a multitude of other processes from fungal development (such as sporulation and cell wall integrity), cell signalling and stress response, to both mutualistic and pathogenic interactions (Zhao *et al*., 2007; Hamel *et al*., 2012; Martínez-Soto and Ruiz-Herrera, 2017).

The genes *mkkA*, *mpkA* and *so* in *E. festucae* encode the MAP kinase kinase protein, the MAP kinase protein, and the scaffold protein (Soft) of the cell wall integrity (CWI) pathway, respectively (Charlton *et al*., 2012; Becker *et al*., 2015). Analysis of the deletion strains in axenic culture revealed a loss of hyphal fusion, increased conidiation and the formation of intrahyphal hyphae (Becker *et al*., 2015). Analysis of the cellular *in planta* phenotype showed an increase of hyphal biomass, formation of hyphal bundles, colonization of vascular bundles and increased chitin exposure in the cell wall (Charlton *et al*., 2012; Becker *et al*., 2015). Similar observations were also made for two membrane-associated proteins, SymB and SymC, that are suspected to be involved in signalling through the CWI or other MAP kinase pathways (Green *et al*., 2017).

Another important MAPK signalling pathway in *E. festucae* is the stress-activated or high osmolarity glycerol (HOG) pathway, which, in *E. festucae*, is known as the stress-activated MAP kinase (SAK) pathway. Eaton *et al*. (2008) identified the MAP kinase SakA, the homolog of the yeast MAP kinase Hog1. Deletion mutants of *sakA* are more sensitive towards osmotic stress and temperature and inoculation of these strains into *L. perenne* resulted in severely stunted plants, including an increase of hyphal biomass and the elicitation of plant defences (Eaton *et al*., 2008; Eaton *et al*., 2010).

The third major MAP kinase signalling pathway in filamentous fungi is the pheromone response (PR) pathway, and the specific scaffolding protein, IdcA (HAM-5), has been shown to be required for a mutualistic interaction between *E. festucae* and *L. perenne* (Eaton *et al*., 2013; Hamel *et al*., 2012).

Is hyphal fusion required for successful interactions?

In addition to the mutants of the CWI pathway described above, the deletion of the gene coding for the transcription factor *proA*, and of a protein involved in the striatin-interacting phosphatase and kinase (STRIPAK) signalling complex, *mob3,* results in the lack of hyphal fusion and a switch to a pathogen like behaviour of the endophyte (Tanaka *et al*., 2013; Green *et al*., 2016). The number of hyphal fusion and interaction-defective mutants of *E. festucae* has led to the hypothesis that hyphal fusion is required for a mutualistic interaction. Observation of similar phenotypes upon disruption of different signalling pathways suggests that these pathways are components of a larger signalling network that is required for cell-to-cell fusion and mutualism (Green *et al*., 2016).

Epigenetic regulation

In addition to proteins involved in MAP kinase signalling, other proteins have been shown to be required for a mutualistic interaction. One of these is the *E. festucae* heterochromatin protein I (HepA), a histone-binding protein that recruits histone H3K9 methylase, resulting in histone methylation and heterochromatin spreading (Chujo *et al*., 2019). Deletion of the *hepA* gene disrupted proper heterochromatin formation and resulted in derepression of secondary metabolism genes in culture, as well as severely stunted host plants when reinoculated into *L. perenne* seedlings (Chujo *et al*., 2019). Derepression of secondary metabolism genes in culture was also obtained upon deletion of the genes coding for the H3K9 and H3K27 methyltransferases ClrD and EzhB. Inoculation of *L. perenne* with these mutants resulted in a slight stunting in *ezhB* mutant infected plants while *clrD* mutants were unable to infect. These studies demonstrate the importance of correct heterochromatin state and gene expression for a successful interaction (Chujo and Scott, 2014).

Additional regulators

Deletion of the pH-regulated transcription factor *pacC* and the calcineurin subunit A, a calcium dependent protein phosphatase, altered the interaction with the host, implicating an important role of pH and calcium signalling for mutualistic growth (Lukito *et al*., 2015; Mitic *et al*., 2018). Lastly the disruption of the siderophore synthesis gene *sidN* resulted in an altered host phenotype, including colonization of vascular bundles. This was speculated to occur due to the reduced ability for iron uptake (Johnson *et al*., 2013).

These observations highlight the complexity of the interaction between *E. festucae* and *L. perenne*, and raise the question as to which other regulatory mechanisms are required for a successful interaction.

Interestingly, approx. 600 fungal genes are differentially regulated during endophytic growth of *E. festucae* (fold difference ≥2), whereas over 38% of all *L. perenne* genes are differentially regulated when an endophyte is present, compared to endophyte-free growth (Dupont *et al*., 2015; Hassing *et al*., 2019). Therefore, the presence of the endophyte induces major reprogramming of the host transcriptome. Many of the upregulated genes encode proteins associated with trichome development, stomatal closure and secondary metabolite production, whereas those downregulated are involved in primary metabolism, drought and biotic-related stress, DNA synthesis and repair, as well as pathogenesis (Dupont *et al*., 2015). Curiously, an earlier study demonstrated a dramatic increase of expression of pathogenesis-related genes in *L. perenne* plants infected with the previously mentioned *sakA* deletion mutant (Eaton *et al*., 2010). These observations indicate that the endophyte actively reprograms the host metabolism and prevents the expression of pathogenesis-related genes. This reflects the function of effector proteins, which are essential in many pathogenic and mutualistic interactions between fungi and their plant hosts (Lo Presti *et al*., 2015).

Identification of small secreted proteins as candidate regulators of the mutualistic interaction

To identify additional genes required for a mutualistic interaction between *E. festucae* and *L. perenne*, Eaton *et al*. (2015) carried out a three-way transcriptome analysis comparing the *E. festucae* WT gene expression *in planta* with gene expression of *sakA*, *noxA* or *proA* deletion strains *in planta*, respectively. This study identified 182 genes with a common expression pattern in all three symbiosis-deficient mutants. Of these, 143 genes were found to be upregulated in non-functional interactions and 39 downregulated. Interestingly, genes involved in primary metabolism, membrane transport, cell wall biosynthesis, host cell wall degradation were generally upregulated and those involved in secondary metabolism and host signalling were downregulated. These changes reflect the proliferative growth and pathogen-like behaviour of the respective mutants within the host as reported previously (Tanaka *et al*., 2006; Eaton *et al*., 2010; Takemoto *et al*., 2013; Eaton *et al*., 2015). An additional transcriptome

study of the *hepA* deletion mutant *in planta* has since reduced the number of core differentially regulated genes to 111 (Chujo *et al*., 2019).

Interestingly, 14 differentially regulated genes encoding for proteins smaller than 200 amino acids and containing a putative secretion signal were first identified in the original study by Eaton *et al*. (2015) and remained unchanged after the addition of the *hepA* mutant dataset (Chujo *et al*., 2019) (Table 1). Ten of these genes were consistently upregulated and the other four were consistently downregulated. Given the dramatic changes in the host transcriptome observed by Dupont *et al*. (2015), and the identification of effectors in many pathogenic and mutualistic interactions, proteins encoded by these genes were hypothesised to be effector candidates with potentially important roles in regulating or establishing the mutualistic interaction. Thus, the first results chapter of this thesis focuses on the effector candidates of *E. festucae* in general, and on the detailed analysis of four candidate effectors in particular. In the following section, I will review the current knowledge about the plant immune system and the role of effectors in plant-fungus interactions. Here the term symbiont is used as a term to describe the microorganism that enters the plant without discrimination between the type of interaction.

Table 1: *Epichloë festucae* differentially regulated genes coding for small secreted proteins identified by Eaton *et al*., (2015).

The Δ*hepA* data was obtained from Chujo *et al*. (2019).

		Fold difference				
Model	**Name**	**Δ*noxA***	**Δ*proA***	**Δ*sakA***	**Δ*hepA***	**Regulation**
EfM3.008680	*sspB*	2.76	2.27	2.55	2.48	+
EfM3.008740	*sspC*	2.99	5.34	3.59	3.21	+
EfM3.026630	*sspD*	3.03	5.7	13.11	16.68	+
EfM3.040200	*sspE*	3.92	5.17	6.12	4.39	+
EfM3.041770	*sspF*	7.89	9.31	22.68	30.8	+
EfM3.062230	*sspG*	28.89	37.69	71.46	169.98	+
EfM3.075920	*sspH*	15.75	35.43	534.96	65.76	+
EfM3.072390	*sspI*	3.34	3.57	10.8	7.59	+
EfM3.057440	*sspJ*	3.34	5.02	6.23	3.32	+
EfM3.012120	*sspK*	2.35	2.89	3.85	4.65	+
EfM3.018200	*sspL*	2.12	2.85	2.71	2.45	-
EfM3.016770	*sspM*	2.45	9.6	412.73	74.49	-
EfM3.062700	*sspN*	6.33	7.73	59.53	99.86	-
EfM3.014350	*sspO*	2.91	16.58	8.85	122.3	-

The plant immune system and the role of fungal effectors

The interaction between plants and microorganisms is multifaceted and can change during the life cycle of the interaction partners, as well as due to environmental cues. Generally, one differentiates between mutualistic interactions, where both partners benefit from the interaction, pathogenic interactions, where only the microorganism benefits whilst keeping the host plant alive, and necrotrophic interactions, where the microorganism benefits whilst killing the host plant and feeding on its dead tissue. Often the type of interaction depends on the stage of the lifecycle of the symbiont. Each of these symbionts interacts with the host immune system in a different way, dependent on the required outcome. Each interaction can either be compatible, resulting in an ongoing interaction, or incompatible, leading to the end of the interaction. In nature, compatible interactions are the exception, as most plants are resistant to most pathogen species. When they do occur, these compatible interactions, however, can have detrimental effects on agriculture (Heath, 2000; Lo Presti *et al*., 2015).

Unlike mammalian organisms which have an adaptive immune system with specialized and mobile immune cells, plants rely on the perception of invaders via receptors of each single cell and the resulting signalling. Many models have been generated to describe the plant immune system and the response to symbionts of which the most prominent is the zig-zag model (Jones and Dangl, 2006). This model strictly differentiates between pathogen- or microbe-associated molecular patterns (PAMPs or MAMPs) and effectors produced by the symbiont that result in PAMP/MAMP-triggered immunity (PTI/MTI) or effector-triggered immunity (ETI) (Jones and Dangl, 2006). MAMPs are symbiont-derived, conserved and often indispensable molecules such as chitin or flagellin. MAMPs are perceived through pathogen recognition receptors (PRRs) on the cell surface, resulting in MTI, including defence signalling and the production of antimicrobial compounds. To infect their host plants, symbionts must interfere with or suppress MTI through the deployment of effectors. This leads to effector-triggered susceptibility (ETS). During evolution, these effectors are ultimately recognized by extracellular or intracellular receptors, resulting in ETI, which typically involves a localised cell death response, termed the hypersensitive response (HR), rendering the host plant resistant. To successfully infect their host plants, ETI then needs to be supressed through the deployment of further effectors (Jones and Dangl, 2006). However, this model is not readily applicable to mutualistic or necrotrophic interactions, often results in confusing terminology and does not give credit to the observation that many plant and symbiont protein interactions take place

at the same time (Thomma *et al*., 2011; Pritchard and Birch, 2014; Cook *et al*., 2015). Therefore, a more general model, the invasion model, is described here in more detail (Figure 4) (Cook *et al*., 2015).

In the invasion model, plant-derived invasion pattern receptors (IPRs), including both extracellular and intracellular receptors, perceive invasion patterns (IPs). These IPs are externally encoded or are modified-self ligands that can indicate an invasion to the plant, including MAMPs, effectors and damage-associated molecular patterns (DAMPs; see below) (Cook *et al*., 2015). This leads to an IP-triggered response (IPTR), which can either result in the end or the continuation of the symbiosis, and is mediated by three possible mechanisms: failure to supress IPTR, suppression of IPTR, or the utilization of the IPTR. In incompatible biotrophic interactions, the symbiont is unable to prevent the IPTR and is therefore excluded by the host, in compatible biotrophic interactions, the IPTR is prevented through the deployment of effectors, and in necrotrophic interactions the IPTR is utilized to the benefit of the symbiont (Figure 4). Thus, this model describes interactions as a continuum instead of a multi-step process. In the following section, each of the components of this model will be briefly described.

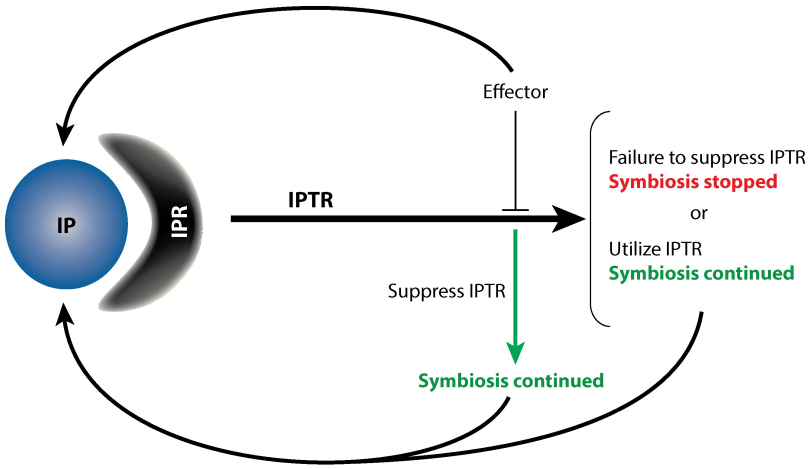

Cook DE, et al. 2015.
Annu. Rev. Phytopathol. 53:541–63

Figure 4: The invasion model.

Figure adapted from Cook *et al*. (2015), with permission from Annual Reviews in Phytopathology. IP: invasion pattern, IPR: invasion pattern receptor, IPTR: invasion pattern-triggered response.

Infection structures and growth *in planta*

While many *Epichloë* spp. are vertically transmitted, this is not the case for many other symbionts. Most interactions begin with the infection of the host and this is achieved

though the formation of species-specific infection structures. Many phytopathogenic fungi, such as *U. maydis* and *M. oryzae*, develop specialized hyphal structures, called appressoria, to invade the plant (Mendgen *et al*., 1996; Tucker and Talbot, 2001). *Cladosporium fulvum* and others enter the plant through stomata (Thomma *et al*., 2005). Inside the host, some fungi grow exclusively by intracellular growth utilizing invasive hyphae (IH), e.g. *U. maydis*, whereas others grow exclusively by intercellular growth, such as *C. fulvum* and *E. festuca*e, feeding from nutrients in the apoplast (Schardl *et al*., 2004; Thomma *et al*., 2005). Other fungi grow intercellularly but insert feeding structures called haustoria into the plant cell. Haustoria are mainly used by obligate biotrophs belonging to the powdery mildews (Ascomycota), the downy mildews (Oomycota), and rust fungi (Basidomycota) (Voegele and Mendgen, 2003).

Invasion patterns

IPs are every possible externally encoded or modified-self ligand, thus this term incudes MAMPs, perceived effectors, modified plant molecules, as well as DAMPs.

MAMPs are molecules of the symbiont with a conserved structure, which are not generated by the host. Often, they are parts of structural molecules that are essential for the symbionts and cannot be modified easily (Boller and He, 2009; Choi and Klessig, 2016). Common fungal MAMPs are chitin (Shimizu *et al*., 2010), ergosterol (Granado *et al*., 1995), β-glucan (Klarzynski *et al*., 2000) and xylanase (Ron and Avni, 2004).

DAMPs are host-derived molecules that are modified or released upon damage inflicted by invaders (Choi and Klessig; 2016). The most well studies DAMPs are polypeptides that are produced from larger proteins such as systemin, produced by tomato, which is generated by wound induced processing of a pre-cursor protein (Constabel *et al*., 1998). Other DAMPs are oligogalacturonides, resulting from fragmented pectin (Denoux *et al*., 2008), and extracellular ATP (Choi *et al*., 2014; Choi and Klessig, 2016). In addition, the term IP includes the proteins that might result in the production of these DAMPs such as proteases and cell wall-degrading enzymes that are produced by the invader to facilitate invasion (Cook *et al*., 2015). Interestingly, both MAMPs and DAMPs are recognized by plant membrane receptors and mount the same immune response (Saijo *et al*., 2017).

Many effectors are recognized by specialized intracellular plant immune receptors, either directly or indirectly, to initiate ETI/IPTR. Effectors that are recognized by a receptor are often referred to avirulence (Avr) proteins, as their corresponding immune receptor (often termed a resistance (R) protein), renders the symbiont avirulent (unable to infect). A prominent example is the effector AvrPi-ta produced by

M. oryzae, that is directly recognized by the receptor Pi-ta expressed by rice plants (Jia *et al*., 2000; Petit-Houdenot and Fudal, 2017).

Invasion pattern receptors

Extracellular IPs can be perceived by membrane-bound pattern recognition receptors (PRRs) with extracellular sensing domains and intracellular effectors by intracellular nucleotide-binding and leucine-rich repeat (NB-LRR) receptors.

PRRs generally belong to one of two classes: “receptor-like kinases” (RLK) and “receptor-like proteins” (RLP). RLK consist of an extracellular ligand-binding domain (ectodomain), a single transmembrane domain, and an intracellular threonine/serine kinase domain. RLPs also contain an extracellular domain and a transmembrane domain, but the short intracellular domain does not contain any signalling function (Zipfel, 2008; Saijo *et al*., 2017). PRRs can be further subdivided based on the nature of their ectodomain: leucine rich-repeat (LRR) domains preferentially bind proteins or peptides such as bacterial flagellin, lysin motifs (LysM) bind to carbohydrate-based ligands, such as chitin, lectin-type domains bind extracellular ATP or lipopolysaccharide (LPS) and epidermal-growth factor-like domains bind oligogalacturonides (Ranf *et al*., 2015; Couto and Zipfel, 2016).

Both RLKs and RLPs form complexes with regulatory receptor kinases to induce defence signalling and these have been reported to be specific to the ectodomain (Couto and Zipfel, 2016). The receptor complex directly activates a multitude of defence responses such as iron flux changes at the PM, increase of cytosolic Ca^{2+} and production of ROS. In addition, MAP kinase signalling pathways and Ca^{2+}-dependent signalling results in transcriptional changes that lead to an accumulation of antimicrobial compounds such as chitinases, glucanases and non-proteinaceous antimicrobial molecules (Zipfel *et al*., 2008; Lo Presti *et al*., 2015; Couto and Zipfel, 2016). Subsequently, the plant cell wall is reinforced and changes in hormone biosynthesis occur. Primary plant hormones involved in defence signalling are jasmonates (JA), salicylic acid (SA) and ethylene, where SA mainly confers resistance to biotrophic fungi and JA to necrotrophic fungi. However, these pathways are connected by active cross talk (Kazan and Lyons, 2014). These responses are usually sufficient to prevent invasion by non-adapted microbes, whereas adapted symbionts are able to prevent this host detection by making use of effectors (Couto and Zipfel, 2016). These effectors, however, can be detected through intracellular NB-LRR receptors, that once activated, can induce a stronger defence response.

NB-LRR receptors consist of an NB-ARC and a C-terminal LRR domain, and often contain an additional N-terminal TIR (Toll, Interleukin-1, resistance protein) or a

coiled-coil domain (CC), distinguishing the two major classes of NB-LRR proteins (Meyers *et al*., 2003). Some NB-LRR protein contain membrane anchors or palmitoylation or myristoylation sites, which directly target the protein to a specific intracellular membrane site, e.g. the Golgi apparatus (Bernoux *et al*., 2011). The recent advances in genome sequencing have revealed the large number of NB-LRR receptors in plants. *Arabidopsis thaliana*, for example, has 159 NB-LRR receptor-coding genes (Guo *et al*., 2011). Their domain structure allows NB-LRR receptors to simultaneously bind Avr proteins as well as activate defence signalling (Petit-Houdenot and Fudal, 2017). While they adopt a closed, autoinhibited conformation in a resting state, sensing of the Avr protein with the LRR domain results in conformational change, an exchange of ADP to ATP and a signalling competent receptor (Takken and Goverse, 2012). Four different models of the detection of Avr proteins by NB-LRR receptors have been described to date and were found to coexist (Petit-Houdenot and Fudal, 2017). In the direct recognition model, the NB-LRR receptor interacts with the effector and activates defence signalling (Jia *et al*., 2000). In the guard mechanism, the NB-LRR protein monitors the status of an effector target (guardee) and is activated in response to its modification (Dangl and Jones, 2001). Another indirect mechanism of detection is described in the decoy model, where the NB-LRR protein detects modifications in a plant protein that mimics the original effector target and traps the effector protein (van der Hoorn and Kamoun, 2008). In the most recent model, domains that mimic the target protein are integrated into the NB-LRR receptor and act as decoy (Cesari *et al*., 2014).

Activation of the NB-LRR receptors results in defence signalling and usually in localised HR at the infection site (Jones and Dangl, 2006). However, the signalling pathways are not well understood. While some NB-LRR receptors have been found to localise to the nucleus, others remain in the cytosol to fulfil their signalling function and they all have been described to have distinct signalling pathways (Qi and Innes, 2013).

Effectors

The defining features of effector proteins are their small size and the lack of clear sequence similarity to proteins with described functions (Lo Presti *et al*., 2015; Franceschetti *et al*., 2017). This observation is often thought to be the consequence of evolutionary pressure that drives rapid diversification of the effector genes (Franceschetti *et al*., 2017). Effector genes are often exclusively expressed *in symbio* and the expression is tightly regulated with the infected organ, the stage of the infection as well as with the respective host (Skibbe *et al*., 2010; Lahrmann *et al*., 2013). To ensure transport to the plant-fungal interface, most effector genes encode N-terminal

secretion signals. Frequently, the effector protein sequence is rich in cysteines, which typically form disulphide bridges to stabilize their structure in the harsh apoplastic environment. Large scale genome sequencing has identified hundreds of effectors in each phytosymbiont, with the number varying between different species (Lo Presti *et al*., 2015).

Effectors have been identified in bacteria, oomycetes, fungi and nematodes, and in different types of interactions, namely mutualistic, biotrophic, hemibiotrophic and necrotrophic interactions (Quentin *et al*., 2013; Lo Presti *et al*., 2015). In the following section, I will focus on effectors secreted by fungi.

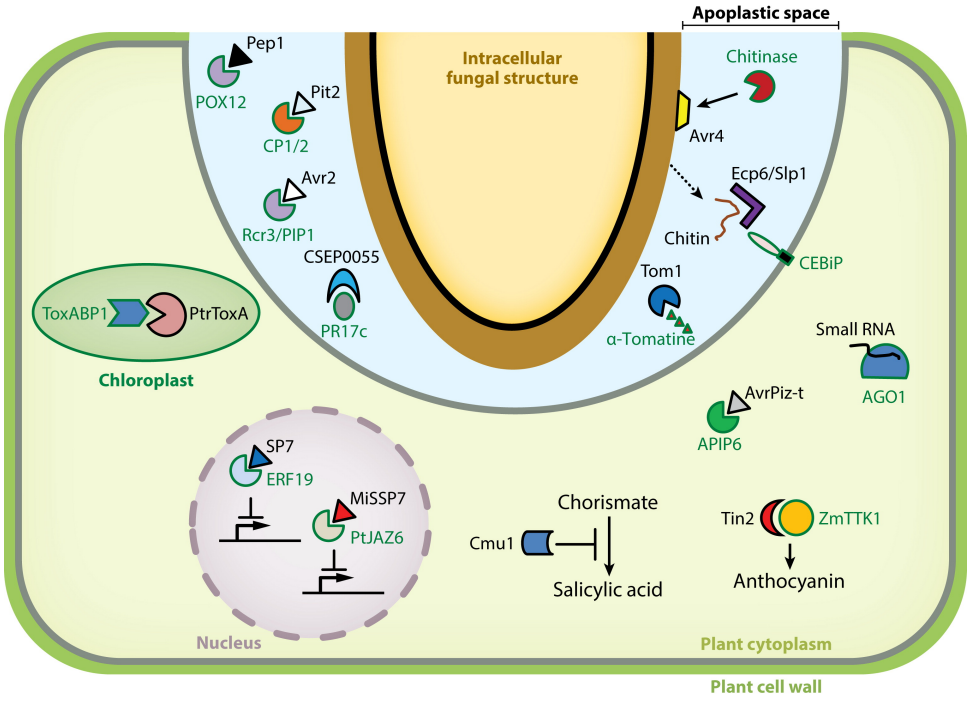

AR Lo Presti L, et al. 2015.
Annu. Rev. Plant Biol. 66:513–45

Figure 5: Examples of well characterized effectors produced by *Cladosporium fulvum*, *Ustilago maydis*, *Laccaria bicolor* and other species.

Figure adapted from Lo Presti *et al*. (2015), with permission from Annual Reviews of Plant Biology.

Apoplastic effectors

Multiple apoplastic effectors with a wide range of functions have been described. Here, a few prominent effectors will be introduced in more detail.

A large class of effectors suppress chitin perception by the plant. To this end, *C. fulvum* secretes two effectors, Avr4 and Ecp6 (van den Burg *et al*., 2006; de Jonge *et al*., 2010). While Avr4 binds to the fungal cell wall to protect it from degradation by

plant chitinases, Ecp6, a LysM domain-containing protein, competes with PRRs for binding of chitin fragments (Figure 5) (van den Burg *et al*., 2006; de Jonge *et al*., 2010). To date, functional homologs of both Avr4 and Ecp6 have been identified in multiple other species, e.g. *M. oryzae* (Slp1) and *Zymoseptoria triciti* (Mg1LysM and Mg3LysM), highlighting the importance of the suppression of chitin perception (Bolton *et al*., 2008; Stergiopoulos *et al*., 2010; Marshall *et al*., 2011; Mentlak *et al*., 2012; Kohler *et al*., 2016).

Another central node for the suppression of immune responses is the inhibition of plant proteases, which are readily secreted upon plant infection (Döhlemann and Hemetsberger, 2013). *C. fulvum* secretes the effector protein Avr2, which inhibits the tomato cysteine protease Rcr3 (Figure 5) (Rooney *et al*., 2005). *U. maydis* produces the effector Pit2, an inhibitor of the maize cysteine protease CP2 (Figure 5) (Döhlemann *et al*., 2011). Homologs of Pit2 were identified in other fungi, but they only share the 14 aa conserved motif described as the functional protease inhibitor domain (Müller *et al*., 2013; Misas Villamil *et al*., 2019). Interestingly, many fungi also secrete proteases themselves, such as *F. oxysporum*, which secretes a serine protease (Sep1) and a metalloprotease (Mep1) that act synergistically to cleave host chitinases (Jashni *et al*., 2015; Franceschetti *et al*., 2017).

The *U. maydis* apoplastic effector Pep1 is also required for successful colonization of the host by inhibiting the maize peroxidase POX1 (Figure 5). This inhibition prevents the oxidative burst of the plant in response to infection and thereby early immune responses (Döhlemann *et al*., 2009). *C. fulvum* secretes Tom1, a tomatinase that degrades the toxic tomato glycoalkaloid α-tomatine (Figure 5) (Ökmen *et al*., 2013).

Cytoplasmic effectors

Some fungi also secrete effectors that are then translocated into the plant cells, such as *U. maydis* and *M. oryzae*, whereas other fungi seem to produce exclusively apoplastic effectors, e.g. *C. fulvum.* While effectors of oomycetes and downy mildews contain the well-studied RxLR (R: arginine, L: leucine, X: any amino acid) motif and/or the crinkle and necrosis (CRN) motif required for translocation, the mechanism of translocation in fungi is not clear (Whisson *et al*., 2007; Lo Presti *et al*., 2015).

The *M. oryzae* effector AvrPiz-t is translocated into the host cytosol and inhibits the rice RING3 ubiquitin ligase APIP6 (Figure 5). This interaction results in decreased ROS production and an increased susceptibility to *M. oryzae* (Park *et al*., 2012).

To date, two effectors have been described that influence the metabolic activity of their host. Tin2, produced by *U. maydis,* prevents the degradation of the kinase

ZmTTK1, and this stabilization promotes anthocyanin production instead of lignin synthesis, as both pathways use the same precursor molecule (Figure 5) (Tanaka *et al*., 2014). The secreted chorismate mutase Cmu1 of *U. maydis* influences the defence hormone signalling of its host (Figure 4). It interacts with maize chorismate mutases and channels chorismate into the shikimate pathway and towards the production of aromatic amino acids. Thereby, it reduces the production of salicylic acid. In addition, it has been found to spread to neighbouring cells and prepare them for infection by metabolic priming (Djamei *et al*., 2011).

Effectors in mutualistic interactions

Less is known about the role of effector proteins in mutualistic interactions, and only a few effector candidates have been studied to date. The ectomycorrhizal fungus *Laccaria bicolor* forms a symbiosis with *Populus trichocarpa*. In response to diffuse root factors, *L. bicolor* secretes the "mycorrhizial-induced small secreted protein 7" (MiSSP7). This effector is then translocated into the nucleus of host cells where it interacts with PtJAZ6, a negative regulator of JA-induced defence responses (Figure 5). This interaction stabilises PtJAZ6 and thereby prevents expression of JA-responsive defence genes. In contrast to other biotrophic fungi that promote JA accumulation to favour colonization and prevent the more detrimental effects of other hormones, e.g. SA, mutualistic ectomycorrhizal fungi are inhibited by JA (Plett *et al*., 2011; Plett *et al*., 2014a; Plett *et al*., 2014b).

The ectomycorrhizal fungus *Rhizophagus irregularis* secretes the effector SP7 into the apoplast of its host *Medicago truncatulata*, from where it is then translocated into host nuclei (Figure 5). There, it was found to interact with the pathogenicity-related transcription factor ERF19, which typically induces the expression of defence-related genes. This interaction is proposed to reduce the activity of the transcription factor and thereby reduce the expression of defence-related genes (Kloppholz *et al*., 2011).

Recently the role of the effector FGB1, fungal-specific β-glucan-binding lectin, was elucidated in the interaction between the root endophyte *Piriformospora indica* and different plant hosts. It was found to have a dual role in modifying the fungal cell wall composition as well as supress β-glucan induced defence responses and thereby influencing fungal infection (Wawra *et al*., 2016).

The genetics of effectors

During the evolution of pathogenic interactions, plants are selected for incompatible interactions, whereas fungi are selected for compatible interactions (Lo Presti *et al*., 2015). In this arms race, both R proteins as well as effectors, are likely to be under

strong positive selection (Jones and Dangl, 2006; Dodds and Rathjen., 2010; Selin *et al*., 2016). This often results in the genes involved being highly polymorphic between closely related species, possessing single-nucleotide polymorphisms (SNPs), insertions and deletions within their gene sequence (Guttman *et al*., 2014; Selin *et al*., 2016). The recent increase in the availability of complete genome sequences allows the analysis of the localisation of the effector-encoding genes within genomes, and how this location can influence effector evolution.

Many effector genes have been found to accumulate in plastic genome regions, such as regions rich in repeats and transposable elements (TE), accessory chromosomes and telomeres (Lo Presti *et al*., 2015). Indeed, a compartmentalization of the genome is observed in some species, indicating a "two-speed" genome in which some regions evolve quicker than others (Dong *et al*., 2015). In some species, effectors have been found to form clusters, which might result from gene duplication without a subsequent gene dispersal (Schirawski *et al*., 2010). In some instances, horizontal gene transfer of effector genes has resulted in an increase of virulence of the recipient strain (Friesen *et al*., 2006).

Are effectors required in the interaction between *E. festucae* and *L. perenne?*

Many observations suggest that effectors play a role in the interaction between *E. festucae* and *L. perenne*, as has been shown in other mutualistic interactions. For example, the artificial inoculation of *L. perenne* seedlings with *E. festucae* does not initiate a plant defence response, and the immune system is also not triggered during later stages of the infection (Eaton *et al*., 2010). Recent studies suggest that changes in the cell wall structure might be involved and required for a successful interaction (Becker *et al*., 2016). In addition, transcriptome studies involving endophyte-free vs. endophyte-infected *L. perenne* plants revealed significant metabolic changes in endophyte-infected plants, including the downregulation of defence-related genes (Dupont *et al*., 2015). However, infection of seedlings with strains that are unable to form a mutualistic interaction results in the upregulation of defence-related genes (Eaton *et al*., 2010).

With the aim of identifying effectors required for a mutualistic interaction, as observed in interactions of *L. bicolor*, *G. intraradices* and *P. indica* with their respective host plants, four effector genes downregulated in four different non-functional interactions were chosen here for further analysis (Eaton *et al*., 2015). Initial analysis

revealed that the gene named *sspL* encoded a glycosylphosphatidylinositol (GPI)-anchored protein, which was therefore renamed to *gpiB.* As GPI-anchored proteins, however, have previously been shown to play a role in plant-fungal interactions (Rittenour and Harris, 2013), and as it showed the same expression pattern as the three remaining candidates, it was included in the analysis presented here as the first results chapter.

The requirements of signalling to the host and signalling within the hyphal network

While the first section of this thesis focuses on signalling of the endophyte to modify host responses, the second part focuses on signalling mechanisms within the fungus that are required for the mutualistic interaction. Multiple examples of the importance of correct signalling process and how they influence growth of the fungus in culture as well as *in planta* have been presented above. Especially crucial is sensing of the environment and signal transduction via MAP kinase pathways and signalling via ROS (Tanaka *et al*., 2006; Eaton *et al*., 2008; Eaton *et al*., 2010; Scott *et al*., 2015; Green *et al*., 2016; Green *et al*., 2017; Becker *et al*., 2015). These pathways require an interplay between membrane bound and cytosolic proteins and many studies in plant and mammalian systems show that lipid signalling is a major player in the targeted membrane recruitment of proteins (Selvy *et al*., 2011; Balla, 2013). The field of lipid signalling has received considerable interest in *Saccharomyces cerevisiae* and other yeasts, but not many studies focus on it in filamentous fungi, despite the significant roles in mammalian and plant organisms (Strahl and Thorner, 2007; Ischebeck *et al*., 2010; Selvy *et al*., 2011; Balla, 2013) The second and third results chapters explore the role of lipid signalling for growth and development of *E. festucae* in culture as well as *in symbio*. Here the focus lies especially on the lipid signalling molecules phosphatidic acid (PA) generated by phospholipase D (PLD), and on phosphatidylinositol 4,5-bisphosphate (PtdIns[4,5]P_2) generated from phosphatidylinositol 3,4,5-trisphosphate (PtdIns[3,4,5]P_3) by a fungal homolog of the mammalian phosphatidylinositol 3,4,5-trisphosphate 3-phosphatase PTEN. As studies in mammals and plants suggest a role of these specific lipid signalling molecules in the regulation of the Nox complex their influence on the fungal Nox complex is analysed as well (Zhang *et al*., 2009).

The composition of fungal membranes

In all kingdoms of life, lipids fulfil three essential functions: 1. They serve as energy storage, often in the form of lipid droplets, 2. Amphipathic lipids, consisting of a polar headgroup and a non-polar tail, are able to form membranes, 3. Amphipathic lipids can act as first and second messengers in signal transduction and recognition processes (van Meer *et al*., 2008). Membranes are essential in forming selective barriers between the inside and the outside of the cell, as well as in forming specific organelles that attract specific proteins. This compartmentalization enables the segregation of chemical reactions, resulting in higher efficiency and providing a means for regulating distribution of the products (van Meer *et al*., 2008). Membrane bilayers generally have an asymmetric distribution of their lipid components in the inner and outer leaflet, due to the activity of membrane-integrated flippases (Nakano *et al*., 2009). Membranes mainly consist of amphiphilic glycerophospholipids and sphingolipids, as well as non-polar sterols, which are required for membrane fluidity and lateral diffusion of lipids (Dufourc *et al*., 2008). Most lipids and lipid precursors are generated in the ER (Henneberry *et al*., 2002).

Cellular membranes contain five major glycerophospholipids: phosphatidylcholine (PC), phosphatidylethanolamine (PE), phosphatidylserine (PS), phosphatidylinositol (PtdIns) and phosphatidic acid (PA) (van Meer *et al*., de Craene *et al*., 2017). These lipids consist of a diacylglycerol (DAG) backbone with different, phosphorylated headgroups (van Meer *et al*., 2008). DAG is composed of a glycerol backbone, esterified with two fatty acid acyl chains in positions 1 and 2. The main structural phospholipid is PC, DAG with a choline headgroup, due to its cylindrical structure. Other glycerophospholipids have an asymmetric cone shape, resulting in membrane curvature (Figure 6) (van Meer *et al*., 2008).

Sphingolipids consist of a ceramide backbone with different headgroups. As their lipid tails are saturated, they can form tightly packed, gel like membranes (van Meer *et al*., 2008). As sphingolipids and lipid messengers derived from sphingolipids are not the focus of this work, the remaining introduction will focus on second messengers derived from glycerophospholipids. However, sphingolipids are at the centre of many studies, as they play a major role in so called lipid rafts (Bieberich, 2018).

Lipid second messenger can be generated though the hydrolysis or modification of different glycerophospholipids. The main lipid second messengers are PA, DAG, phosphoinositides, several different inositol phosphates, lysophospholipids (LPL, different headgroups possible, e.g. choline resulting in LPC) and arachidonic acid

(AA) of which AA and LPL contain only one fatty acid chain and inositol phosphates contain none. Therefore, they are no longer membrane bound and can diffuse into the cytosol, where they can be further modified (Figure 6) (Eyster *et al*., 2007; Newton *et al*., 2016; de Craene *et al*., 2017).

Are lipid second messengers required for fungal growth and the mutualistic interaction?

When considering the big picture of lipid signalling, there are a few key points: most of these lipids are interrelated and can be generated from each other in a few sequential steps and there is a significant amount of interaction in these pathways, where some lipids regulate the production of others by regulating the respective enzyme activity (Figure 6) (Eyster, 2007). This increases the difficulty in studying lipid signalling, as the modification of one lipid species likely affects other ones.

As the focus of this study is PA generated by *E. festucae* phospholipase D, and PtdIns[4,5]P_2 generated from PtdIns[3,4,5]P_3, by the fungal homolog of the mammalian PTEN protein, these molecules and enzymes will be the focus of the following section. Other lipid second messengers will be largely excluded despite their important roles in cellular functions (Eyster, 2007).

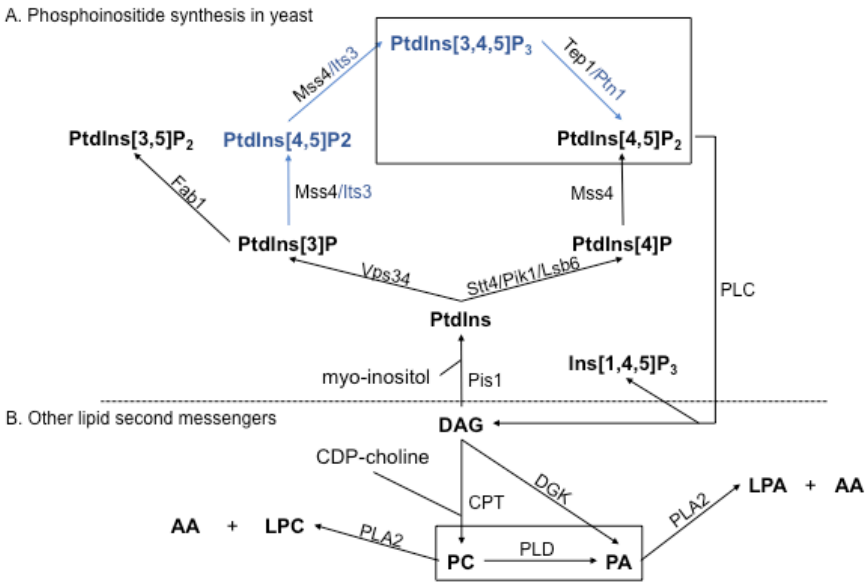

Figure 6: Simplified overview of glycerophospholipid second messenger synthesis.

While (A) is specific to *S. cerevisiae* and contains a pathway for PtdIns[3,4,5]P_3 synthesis as suggested for *S. pombe* (Mitra *et al*., 2014) (B) shows the synthesis of other second messengers in general. For simplification all reactions including enzymes are only depicted in one direction, however some are reversible through the action of other enzymes. (A) Phosphoinositide synthesis in yeast according to Strahl and Thorner (2007) and PtdIns[3,4,5]P_3 synthesis as suggested for *S. pombe* by Mitra *et al*. (2014). Reactions in *S. pombe* indicated in blue arrows and writing. PtdIns: phosphatidylinositol, PLC: phospholipase C. (B) General overview of other glycerophospholipid second messengers. DAG: diacylglycerol, CPT: cholinephosphotransferase, DGK: diacylglycerol kinase, PC: phosphatidylcholine, PLD: phospholipase D; PA: phosphatidic acid, PLD2: phospholipase A2, LPA: lysophosphatidic acid, AA: arachidonic acid. Molecules acting as second messengers are marked in bold, boxed areas are of interest in this study.

Phosphatidic acid (PA)

PA is an important constituent of eukaryotic membranes and makes up 1-4% of the total lipids. It is the smallest of the phospholipids, and only contains an anionic phosphate headgroup, which is relatively small compared to the DAG backbone. This structure gives the molecule an inverted cone shape, which affects membrane topology by inducing negative curvature. The negative charge attracts proteins with positive, polybasic motifs (Selvy *et al*., 2011; Tanguy *et al*., 2019).

While PA can be generated *de novo* from glycerol-3 phosphate, signalling-competent PA is generated from existing glycerophospholipids in three main pathways: through the hydrolysis of PC by PLD, through the phosphorylation of DAG by DAG kinase and through the acylation of lysophosphatidic acid (LPA) by the lysophosphatidic acid acyltransferase (Gibellini and Smith, 2010; Selvy *et al*., 2011). The phospholipase A2 (PLA2) can hydrolyse PA to LPA by removing an acyl residue, while a PA phosphatase can dephosphorylate PA to DAG (Figure 6).

While no clear PA binding domain has been identified to date, PA has been found to interact with a multitude of proteins in mammalian cells (Jang *et al*., 2012). Among these, PA regulates the localisation and activity of small GTP-binding proteins of the ADP ribosylation factor (Arf) and Rho (Ras homologous) families as well as other GTP-binding proteins, multiple kinases, including multiple members of the phosphokinase C family and the phosphatidylinositol 4-phosphate 5-kinase and several phosphatases (Ktistakis *et al*., 1996; Zeniou-Meyer *et al*., 2007; Selvy *et al*., 2011; Jang *et al*., 2012; Kassas *et al*., 2017; Tanguy *et al*., 2019). Through these interactions, PA has been shown to influence the actin cytoskeleton rearrangement, exocytosis, phagocytosis and vesicle trafficking, and most of these functions are attributed to PA generated by PLD (Tanguy *et al*., 2019). In plants, PA has been found to be involved in the regulation of the actin and microtubule cytoskeleton, response to pathogens, including ROS production, stress response, stomatal opening and the response to abscisic acid (Zhang *et al*., 2009; Zhao, 2015; Yao and Xue, 2018). In yeast, PA has mainly been studied through the effect of the deletion of the yeast homolog of PLD, Spo14. By this means, a role for PA in vesicle fusion during sporulation, suppression of growth and membrane trafficking defects in mutants defective in Sec14, exocytosis and transcriptional regulation of glycerophospholipid synthesis has been identified (Xie *et al*., 1998; Rudge *et al*., 2004; Carman and Henry, 2007). In filamentous fungi, PA has not received much attention to date, and here as well, only the effect of the deletion of PLD has been studied in two different species. While some fungal PLD isoforms were required for virulence of *Aspergillus fumigatus* and for virulence and sexual development in *F. graminearum,* other isoforms did not result in any morphological changes (Hong *et al*., 2003; Li *et al*., 2012; Ding *et al*., 2017).

Phospholipase D

Members of the PLD family are classified based on the presence of the conserved HxKxxxxDx$_6$GSxN (HKD) motif, which forms the active site of the protein and indicates that theoretically all members of this family can hydrolyse phosphodiester bonds via a similar reaction mechanism (Ponting and Kerr, 1996; Selvy *et al*., 2011). However,

enzymes that lack this motif, but still are able to carry out this reaction, have been described as well (Selvy *et al*., 2011). While many PLDs of prokaryotes only contain one HKD motif, PLDs of eukaryotes usually contain two, which is indicative of a gene duplication event (Koonin, 1996). Despite PLDs generally not sharing a high degree of sequence homology, four conserved motifs (I-IV) have been described in PLD sequences, of which motifs II and IV contain the HKD motif. In addition, PLDs of higher eukaryotes usually contain a polybasic PtdIns[4,5]P_2-binding motif as well as N-terminal regulatory domains, such as a phox homology (PX) and a pleckstrin homology (PH) domain, involved in lipid binding, or a Ca^{2+}-binding C2 domain (Sciorra *et al*., 1999; Selvy *et al*., 2011). The C-terminal tail is divergent between different PLD isoforms and likely involved in regulation of protein activity (Selvy *et al*., 2011).
Mammals contain two PA generating PLDs, PLD1 and PLD2, which share a similar domain structure, but only 50% sequence homology (Hammond *et al*., 1995; Selvy *et al*., 2011). Both contain an N-terminal PH and PX domain, as well as the PtdIns[4,5]P_2-binding domain and the four conserved motifs. The plant PLDs can be categorized into six subfamilies, of which all contain an N-terminal C2 domain, indicating Ca^{2+}-dependent regulatory mechanisms, with the exception of PLDζ, which has a PH and PX domain (Wang *et al*., 2000). *S. cerevisiae* only encodes one PLD isoform named Spo14, which has a domain structure comparable to mammalian PLD isoforms (Xie *et al*., 1998). In filamentous fungi, up to three isoforms have been identified in one species to date, of which one is generally similar to Spo14 in structure, whereas other ones lack obvious N-terminal regulatory domains (Hong *et al*., 2003; Li *et al*., 2012; Ding *et al*., 2017).

As PA produced by PLD has been shown to be required for a multitude of functions in mammals and plants, including Nox complex activation, and virulence in filamentous fungi, the PLD homologs of *E. festucae* were analysed in this study.

Phosphoinositides

PtdIns is generated from DAG-cytidine diphosphate and myoinositol by a phosphatidylinositol synthase, resulting in an inositol ring esterified to DAG. This serves as the backbone of all other phosphoinositides, which are made through the activity of kinases and phosphatases on the -OH groups in positions 3,4 and 5 of the inositol ring. This allows the production of seven different species of phosphoinositides: PtdIns[3]P, PtdIns[4]P, PtdIns[5]P, PtdIns[3,4]P_2, PtdIns[4,5]P_2, PtdIns[3,5]P_2 and PtdIns[3,4,5]P_3. To date, only mammalian cells have been found to generate all seven phosphoinositides. In plants, neither PtdIns[3,4]P_2 nor PtdIns[3,4,5]P_3 have been detected to date, and similarly, fungi do not seem to produce PtdIns[3,4]P_2 nor

PtdIns[5]P (Balla, 2013). Unlike in plants, however, one study reports the biochemical identification of PtdIns[3,4,5]P_3 in *Schizosaccharomyces pombe* upon the deletion of the phosphatase, which specifically dephosphorylates this species *in vitro* (Figure 6) (Mitra *et al*., 2004). This might indicate that fungi are able to generate PtdIns[3,4,5]P_3, albeit in very low quantities. While plants also encode homologs of this phosphatase, no PtdIns[3,4,5]P_3 have been detected to date (Stevenson *et al*., 2000).

The synthesis of phosphoinositides is complex, interconnected and requires multiple kinases and phosphatases, of which some are very specific for one certain lipid species, whereas others can modify multiple substrates. Interestingly, many of these enzymes have many isoforms, these however are located at specific membranes, such as the Golgi or the PM, and therefore are not functionally redundant (Balla, 2013). Due to the complexity of phosphoinositide metabolism this topic will not be discussed in detail and only briefly mentioned with each of the phosphoinositides. The focus here will be on proteins and lipids identified in *S. cerevisiae*. The degradation of phosphoinositides can either occur though dephosphorylation through phosphatases or though hydrolysis by PtdIns-specific phospholipase C (PLC) enzymes, whose action results in the release of the inositol headgroup and DAG of which both act as second messengers. The phosphoinositide kinases are assigned to classes, based on their biochemical properties, as well as into subgroups on the basis of the reaction they perform (Strahl and Thorner, 2007).

Phosphoinositides act by interacting with membrane-bound proteins, such as transporters, or by recruiting proteins to specific membranes, making use of a large number of lipid-binding domains, such as PH, PH, FYVE, PDZ domains, as well as stretches of polybasic aa. As they are asymmetrically distributed in cellular membranes, they additionally serve as a means of generating membrane identity (Falkenburger *et al*., 2010; Balla, 20013; de Craene *et al*., 2017).

PtdIns[4]P

In yeast, PtdIns[4]P is mainly located in the Golgi, where it is generated by the PtdIns 4-kinase Pik1, as well as at the PM, where it is generated by the PtdIns 4-kinase Stt1. Deletion of either of the corresponding genes is lethal (Figure 6) (Audhya *et al*., 2000). In addition, yeast contains another PM-associated PtdIns 4-kinase, Lsb6, which is not essential. PtdIns[4]P can also be generated through the dephosphorylation of PtdIns[4,5]P_2 by the 5-phosphatases Inp51/Sjl1, Inp52/Sjl2, Inp53/Sjl3 and Inp54 (de Creane *et al*., 2017). PtdIns[4]P at the Golgi is required for transport between the ER and the Golgi, and the PM pool is required for actin organisation and integrity of the yeast cell wall (Audhya *et al*., 2000; Godi *et al*., 2004).

PtdIns[4,5]P_2

In *S. cerevisiae*, the main pool of PtdIns[4,5]P_2 is located at the inner leaflet of the PM, where it is generated by the only PtdIns 5-kinase, Mss4, through the phosphorylation of PtdIns[4]P. Like Pik1 and Stt4, Mss4 is required for cell viability (Desrivières *et al*., 1998). In mammalian cells, PtdIns[4,5]P_2 can also be generated though the dephosphorylation of PtdIns[3,4,5]P_3, by the phosphatidylinositol 3,4,5-trisphosphate 3-phosphatase PTEN (Figure 6). Despite the presence of a PTEN homolog in *S. cerevisiae*, there is no evidence to date that suggests it to be a functional lipid phosphatase, whereas the deletion in fission yeast resulted in measurable amounts of PtdIns[3,4,5]P_3. PtdIns[4,5]P_2 plays an important role in actin cytoskeleton rearrangement as well as in endocytosis, which is actin dependent in yeast (Sun *et al*., 2007). In mammalian cells, PtdIns[4,5]P_2 is involved in the regulation of iron channels and transporters, exocytosis, endocytosis, chemotaxis, phagocytosis and many additional processes (Botelho *et al*., 2000; Holz *et al*., 2000; Suh and Hille, 2008; Weiger and Parent; 2012; Tóth *et al*., 2012; Balla, 2013).

PtdIns[3]P

In yeast cells, PtdIns[3]P is generated by a single PtdIns 3-kinase Vps34 (Herman and Emr, 1990). Unlike many of the other lipid kinases, Vps3 is only essential at elevated temperatures (Figure 6). In addition, it can be generated from PtdIns[3,5]P_2 by dephosphorylation though Fig4, Ip52/Sjl2, Inp53/Sjl3 and Sac1. Vps34 is activated though interaction with other proteins and the resulting complexes and thereby PtdIns[3]P are involved in endosomal trafficking and vacuolar sorting or autophagy (Kihara *et al*., 2001).

PtdIns[3,5]P_2

In *S. cerevisiae* cells, PtdIns[3,5]P_2 is generated through the sequential action of Vps34 and Fab1, which specifically phosphorylates PtdIns[3]P (Figure 6) (Yamamoto *et al*., 1995). Similar to Vps34, Fab1 is activated by other proteins, and deletion of *FAB1* results in temperature and stress sensitivity and defects in vacuolar morphology and segregation (Yamamoto *et al*., 1995; Bonangelio *et al*., 2002; de Craene *et al*., 2017).

The phosphatidylinositol 3,4,5-trisphosphate 3-phosphatase PTEN

The mammalian protein phosphatase and tensin homolog (PTEN) is both a PtdIns[3,4,5]P_3 phosphatase as well as a protein phosphatase, able to dephosphorylate tyrosine, serine and threonine residues. It addition to the phosphatase domain it contains a N-terminal PtdIns[4,5]P_2-binding, a C2 domain, a PDZ domain (binds protein

with a PDZ domain) and an autoregulatory C-terminal tail. Each of these domains as well as extensive phosphorylation and other secondary modifications are required for correct localisation and regulation of this protein (Nguyen *et al*., 2014; Bermúdez-Brito *et al*., 2015; Chen *et al*., 2018). In mammalian cells, PTEN plays a critical role in regulating cell growth and proliferation by dephosphorylating PtdIns[3,4,5]P_3, which is generated by a phosphoinositide 3-kinase from PtdIns[4,5]P_2 after stimulation by growth factor-induced signalling (Li *et al*., 1997; Manning and Cantley; 2007; Chen *et al*., 2018). PtdIns[3,4,5]P_3 recruits the kinase Akt, which phosphorylates and deactivates a negative regulator of the target of rapamycin (TOR). The activation of TOR results in cell growth and proliferation (Manning and Cantley, 2007). Mutations in the gene encoding PTEN result in Cowden disease and Bannayan–Riley–Ruvalcaba syndrome, which are characterized by benign tumours and a high risk of cancer (Sansal and Sellers, 2004). Therefore, *PTEN* is referred to as a tumour suppressor gene (Li *et al*., 1997). In addition to its role in cell growth, PtdIns[3,4,5]P_3 is also required for cell polarity and chemotaxis in mammalian cells, as well as in the slime mould *Dictyostelium* (Iijima and Devreotes, 2002; Iijima *et al*., 2004; Heit *et al*., 2008; Weiger and Parent, 2012; Balla, 2013). Homologs of PTEN were found in fungi as well as in plants with the exception of the homolog in fission yeast, the phosphatase activity has not been verified to date. Indeed, the PTEN homolog has only been studied in two filamentous fungi, namely *F. graminearum* and *U. maydis*, where they play a role in virulence and sporulation. Therefore, this study focussed on the role of the *E. festucae* PTEN homolog and its impact on lipid concentrations in axenic growth as well as in the interaction with *L. perenne*. In addition, the influence on the activity of the Nox complex was analysed, which has previously been shown to be activated by PtdIns[4,5]P_2.

The activation of the Nox complex through lipid signalling

As described, lipid signalling is required for a plethora of cellular functions, and among these, several studies suggest a role of PA and PtdIns[4,5]P_2 in the activation of the Nox complex. Indeed, lipid binding of the mammalian subunits $p40^{phox}$ and $p47^{phox}$ is required for Nox complex activity, and $p47^{phox}$ has been shown to both bind PA and has weak affinity for PtdIns[4,5]P_2 (Kanai *et al*., 2001; Karthanassis *et al*., 2002). While fungi do not encode homologs of $p40^{phox}$ and $p47^{phox}$, they do have cytosolic proteins that are required for Nox activity, namely BemA and Cdc24, both of which contain a lipid-binding domain (Takemoto *et al*., 2011). The PX domain of Cdc24, in particular, has previously been shown to be required to membrane translocation of this protein (Toenjes *et al*., 1999). Furthermore, exogenous addition of PtdIns[4,5]P_2 and PA

increased Nox activity in plant PM preparations, respectively, while addition of PA also increased activity of mammalian Nox (Palicz *et al*. 2001; Potocký *et al*., 2012). In addition, multiple other lines of evidence indicate a role of lipid signalling in the activation of the Nox complex, such as the activation of PKC, required for the phosphorylation of the cytosolic subunits, both through PtdIns[4,5]P_2 and PA (Chauhan *et al*., 1991; Regier *et al*., 1999).

Aims and objectives

Given that the presence of *E. festucae* in *L. perenne* results in significant changes in the host transcriptome, including the downregulation of defence-related genes, and that artificial inoculation of the endophyte does not result in a host defence response, it is likely that the endophyte is able to suppress the host immune response. A recent study identified three proteins that might play a role in this process.

Lipid signalling is a key player in many cellular processes in mammalian and plant cells, but is largely unexplored in fungi. Of special interest here are the signalling lipids PtdIns[4,5]P_2 and phosphatidic acid, produced by the fungal homolog of the mammalian PTEN protein and Phospholipase D. Both signalling molecules have previously been shown to be involved in the regulation of the Nox complex, which is essential for a mutualistic interaction between *L. perenne* and *E. festucae*.

To address the role of effectors and lipid signalling in the interaction *between E. festucae* and *L. perenne*, the following aims and objectives were pursued:

The first aim was to analyse effector candidates produced by *E. festucae* using bioinformatic tools as well as to characterise three candidates and a GPI-anchored protein in depth and investigate their role in the interaction between *E. festucae* and *L. perenne*.

1. Generate a list of the effector candidates produced by *E. festucae*, analyse their location in the genome regarding distribution patterns, and identify their expression patterns.
2. Verify the secretion of GpiB and the candidate effectors SspM, SspN and SspO making use of a secretion-signal complementation assay in *S. cerevisiae* and by western blot analysis.
3. Generate *gpiB*, *sspM*, *sspN* and *sspO* deletion and overexpression strains of *E. festucae*.
4. Analyse phenotypes of the mutant strains in culture.
5. Analyse phenotypes of the mutant strains in *planta*.

6. Identify the localisation of SspM- mCherry-NLS SspO-mCherry-NLS, SspN-mCherry-NLS and SspO-mCherry-NLS fusion proteins *in planta* and investigate their potential translocation into the plant cell.
7. Investigate whether expression of GpiB, SspM, SspN or SspO in non-host plants initiates plant defence responses.
8. Investigate whether expression of GpiB, SspM, SspN or SspO in non-host plants can supress an INF1-triggered immune response.

The second aim was to analyse the role of PA produced by phospholipase D in fungal growth in culture and *in planta.* In addition, the influence on the Nox complex was to be determined.

1. Identify homologs of *S. cerevisiae* Spo14 in *E. festucae*
2. Generate *pldA* and *pldB* deletion and overexpression strains of *E. festucae*.
3. Analyse phenotypes of the mutant strains in culture.
4. Analyse the ability of *pldB* deletion strains to undergo hyphal fusion.
5. Analyse the localisation of PldA and PldB during axenic growth and *in planta.*
6. Identify interaction partners of PldB.
7. Analyse phenotypes of the mutant strains in *planta.*
8. Analyse the localisation of a PA biosensor in *pldA* and *pldB* deletion strains.
9. Analyse the influence of the deletion of *pldA* and *pldB* on superoxide production and on the localisation of the subunits of the Nox complex.

The third aim was to analyse the role of the homolog of the mammalian PTEN protein in growth of *E. festucae* in culture and *in planta*. Furthermore, the effect of the deletion of the PTEN homolog on the membrane composition and on Nox complex activity was to be analysed.

1. Identify the *E. festucae* PTEN homolog.
2. Analyse the localisation of PTEN in axenic culture.
3. Generate *tepA* deletion and overexpression strains.
4. Analyse phenotypes of the mutant strains in culture.
5. Analyse phenotypes of the mutant strains in *planta.*
6. Investigate the localisation of lipid biosensors in *tepA* mutant strains.
7. Analyse the influence of the overexpression and deletion of *tepA* on superoxide production and on the localisation of the subunits of the Nox complex.

About the structure of this thesis

Each of the following result chapters is presented as a manuscript including an abstract, introduction, materials and methods, results, discussion, acknowledgements, references and supplementary material. As the first manuscript is available online and many of the supplementary files consist of excel spreadsheets a hyperlink for each file is provided in the "Supporting information" section of this particular manuscript. References within the introduction are listed in the final bibliography. The "statement of contribution" forms (DRC16) and plasmid maps of plasmids designed in this study can be found in the appendices.

Chapter 2: Analysis of *Epichloë festucae* small secreted proteins in the interaction with *Lolium perenne*

Analysis of *Epichloë festucae* small secreted proteins in the interaction with *Lolium perenne*

Berit Hassing[1,2], David Winter[1,2], Yvonne Becker[3], Carl H. Mesarich[1,4], Carla J. Eaton[1,2], Barry Scott[1,2]*

[1]School of Fundamental Sciences, Massey University, Palmerston North, New Zealand

[2]Bio-Protection Research Centre, Massey University, Palmerston North, New Zealand

[3] Institute for Epidemiology and Pathogen Diagnostics, Julius Küehn-Institute, Federal Research Centre for Cultivated Plants, Braunschweig, Germany

[4]School of Agriculture and Environment, Massey University, Palmerston North, New Zealand

* Corresponding author

E-mail: d.b.scott@massey.ac.nz (BS)

Abstract

Epichloë festucae is an endophyte of the agriculturally important perennial ryegrass. This species systemically colonises the aerial tissues of this host where its growth is tightly regulated thereby maintaining a mutualistic symbiotic interaction. Recent studies have suggested that small secreted proteins, termed effectors, play a vital role in the suppression of host defence responses. To date only a few effectors with important roles in mutualistic interactions have been described. Here we make use of the fully assembled *E. festucae* genome and EffectorP to generate a suite of 141 effector candidates. These were analysed with respect to their genome location and expression profiles *in planta* and in several symbiosis-defective mutants. We found an association between effector candidates and a class of transposable elements known as MITEs, but no correlation with other dynamic features of the *E. festucae* genome, such as transposable element-rich regions. Three effector candidates and a small glycosylphosphatidylinositol (GPI)-anchored protein were chosen for functional analysis based on their high expression *in planta* compared to in culture and their differential regulation in symbiosis defective *E. festucae* mutants. All three candidate effector proteins were shown to possess a functional signal peptide and two could be detected in the extracellular medium by western blotting. Localization of the effector candidates *in planta* suggests that they are not translocated into the plant cell, but rather, are localized in the apoplastic space or are attached to the cell wall. Deletion

and overexpression of the effector candidates, as well as the putative GPI-anchored protein, did not affect the plant growth phenotype or restrict growth of *E. festucae* mutants *in planta*. These results indicate that these proteins are either not required for the interaction at the observed life stages or that there is redundancy between effectors expressed by *E. festucae*.

Introduction

Plant-pathogenic fungi deploy a number of virulence factors, termed effector proteins, to promote colonization of their hosts. These effector proteins, which can be targeted to the host apoplast (extracellular effectors) or to various compartments of the plant cell (intracellular effectors), typically promote colonization by altering host physiology or by modulating host immune responses [1]. Well-characterized examples of extracellular fungal effector proteins include Avr2, Avr4 and Ecp6 from the tomato leaf mould pathogen *Cladosporium fulvum* [2-4], as well as Pit2 and Rsp3 from the corn smut pathogen *Ustilago maydis* [5, 6]. More specifically, Avr4 binds to chitin molecules present in the cell wall of invading hyphae to prevent hydrolysis by host chitinases [2, 7], while Ecp6 sequesters chitin oligosaccharides released from the cell wall of invading hyphae to prevent detection by host chitin immune receptors [4, 8]. Rsp3 binds to the cell wall of invading hyphae to protect them against two antimicrobial mannose-binding host proteins [6], while both Pit2 and Avr2 inhibit host cysteine proteases to prevent degradation of fungal proteins [3, 9-11]. A well-characterized example of an intracellular fungal effector protein is Cmu1 from *U. maydis*, which functions as a chorismate mutase to redirect the metabolism of chorismate away from the production of the defense signaling hormone salicylic acid [12].

Like plant-pathogenic fungi, plant-beneficial fungi must also deploy effector proteins to promote host colonization [13, 14]. However, to date only a small number of effectors from this group of fungi have been identified and functionally characterized. Furthermore, of those that have been functionally characterized all are from mycorrhizal fungi. One such example is MiSSP7 from *Laccaria bicolor*, an ectomycorrhizal fungus of poplar roots. In plants (including poplar), JAZ proteins repress the expression of jasmonic acid (JA)-related defense genes, with the degradation of these proteins leading to the activation of JA-related defense genes [15]. During infection of poplar, MiSSP7 is transported into the plant nucleus where it interacts with and stabilizes the JAZ protein PtJAZ6 to prevent its degradation, and thus prevent the expression of JA defence-related genes [16, 17]. A second example is SP7, which is produced by the arbuscular mycorrhizal fungus, *Glomus intraradices*. SP7, which like PtJAZ6 is also transported into the plant nucleus, influences defense gene signaling by interacting with the pathogenicity-related transcription factor ERF12 [18]. A third example is Fgb1 has been characterized from the endophytic root-colonizing fungus, *Piriformospora indica*. Fgb1 is a β-glucan-binding lectin that modulates the fungal cell composition and prevents β-glucan-triggered immunity in

plants, presumably through a similar mechanism to that shown for as Ecp6 and other LysM domain-containing effectors from plant-pathogenic fungi [19].

There is little amino acid sequence conservation between effector proteins of plant-associated fungi, and most lack obvious functional domains. Together, these features render their identification and functional characterization difficult. Some features, however, are common to many effector proteins. For example, most have an amino (N)-terminal signal peptide for secretion, are small (<300 amino acid residues in length) and rich in an even number of cysteines, and are highly expressed during host colonization [1, 20]. Furthermore, many of these effector proteins are encoded by genes located in dynamic regions of the fungal genome (e.g. those regions rich in transposable elements; TEs), where increased mutation rates can result in the increased diversification of effector genes; a beneficial trait in the 'arms race' with the host [1, 21, 22]. One group of TEs are miniature inverted-repeat transposable elements (MITES)[23], which are small non-autonomous DNA transposable elements that have been proposed to have a role in regulating the expression of plant induced genes in phytopathogenic and mutualistic fungi [24-27].

Here we present an analysis of effector candidates from *Epichloë festucae*, an endophytic fungus of the cool-season grass, *Lolium perenne*. The interaction between *Epichloë spp.* and cool-season grasses is of agricultural importance due to the array of secondary metabolites produced by the endophyte that protect the host from various biotic stresses, such as insect and mammalian herbivory [28]. Unlike mycorrhizal fungi, which only infect the roots of their host plants, *E. festucae* and other *Epichloe* spp. exclusively colonize plant aerial tissues and are only found in association with their host. These endophytes can be vertically transmitted through host seeds [29, 30] or horizontally transmitted by ascospore transfer. The latter occurs following sexual development on host inflorescences, and results in the formation of stromata that prevent the maturation of these inflorescences to cause 'choke' disease [31, 32]. While some *Epichloë* spp. have a high degree of host specificity, others, such as *E. typhina,* can infect a variety of grass species [33]. Within the host tissue, the fungal growth is highly restricted and confined to the intercellular spaces. Deletion of key signaling genes results in the loss of this restricted growth and, in doing so, the 'breakdown' of the symbiosis [34-40]. Here, we make use of the fully assembled *E. festucae* genome [26] and EffectorP [41] to identify a suite of candidate effectors in this mutualistic endophyte, and analyse their genomic location to identify potential patterns of distribution. In addition, we use multiple transcriptome datasets to generate an expression profile for these candidate effectors, with the aim of identifying effectors with a potential role in the *E. festucae-L. perenne* interaction. Based on these

analyses, three candidate effectors were selected for functional characterization. As glycosylphosphatidylinositol (GPI)-anchored proteins play an important role in plant–fungus interactions [42, 43] we also selected a GPI anchored protein with a similar expression profile to the abovementioned candidate effectors for functional characterization.

Materials and Methods

Bioinformatics

A detailed record of the bioinformatic and statistical analyses performed in this study is provided in S1 File. Here we briefly describe each step of these analyses.

Classification of proteins and amino acid composition

The program SignalP v4.1 [44] was used to identify those *E. festucae* proteins of ≤200 amino acid residues in length that contain an N-terminal secretion signal, while EffectorP v 1.0 [41] was used to predict which of these proteins is an effector. The latter uses a machine learning approach based on sequence properties common to known effectors. Taking these results together, each protein was then classified into one of three non-overlapping classes: (i) candidate effectors (proteins with ≤200 amino acid residues, a signal peptide and an EffectorP probability of >0.5), (ii) secreted proteins (proteins with a signal peptide that do not meet the other abovementioned criteria for effectors), and (iii) non-secreted proteins (all other proteins). The hypothesis that secreted proteins are more cysteine-rich than average was tested using a logistic regression. Specifically, a model with the proportion of cysteine residues as the response variable and membership of the three protein-classes described above as a predictor was fitted using R 3.0.1 [45].

Genomic landscape of candidate effectors

Bedtools v 2.26.0 [46] and the recently published *E. festucae* Fl1 genome [26], were used to calculate the distance between each protein-coding gene and its nearest AT-rich isochore, minature inverted TE (MITE) and telomere. Logistic regression was used to test whether secreted proteins and candidate effectors are more likely to appear near to a MITE (within 2 kb), an AT-rich isochore (within 5 kb) or a sub-telomeric region (within 50 kb) than other proteins. A Monte Carlo approach was used to test whether genes encoding candidate effectors fall into clusters within the Fl1 genome. Specifically, Bedtools was used to calculate the minimum distance between each effector-encoding gene and another gene of the same type (i.e. the minimum distance to another candidate effector gene). The mean distance between candidate effector genes was compared to a null distribution of this statistic. We simulated this null distribution by calculating the same statistic for 1000 random gene-sets, each the same size as the set of candidate effectors.

Gene expression analyses

The hypothesis that genes encoding candidate effectors are differentially expressed *in planta* compared to axenic culture was tested by logistic regression, using previously published RNAseq data as input [36, 47]. A model in which the probability that genes demonstrate significant (corrected p-value < 0.01) and substantial (> 2 $\log_2$ fold) differences in expression between culture and *planta* conditions compared between candidate effectors, secreted proteins and all other proteins was fitted using R. Similarly, the hypothesis that repression of candidate effector genes is disrupted in Δ*hepA*, a mutant of the heterochromatin protein 1 (HP1) gene [48, 49], was tested using logistic regression. Finally, the *in planta* expression of candidate effector genes was compared across four separate symbiosis-deficient mutants, including Δ*noxA*, Δ*proA* and Δ*sakA* [36, 47] and Δ*hepA* (Chujo & Scott, personal communication. The Δ*hepA* transcriptome data used here is available from the Sequence Read Archive (SRA) under Bioproject PRJNA447872. A list of the individual biosample numbers is provided in S1 Table.

Strains and growth conditions

Escherichia coli strains were grown overnight in Lysogeny Broth (LB) or on LB agar supplemented with 100 µg/ml ampicillin or 50 µg/ml kanamycin at 37°C, as described by [50]. *Agrobacterium tumefaciens* strains were grown for one day in LB broth or for two days on LB agar supplemented with 50 µg/ml kanamycin at 30°C, as previously described [51]. *Saccharomyces cerevisiae* strains were grown at 30°C on YPDA (2% peptone, 1% yeast extract 0.01% adenine hemisulfate, 2% glucose, 2% agar; adjusted to pH 5.7). For *S. cerevisiae* complementation assays cells were plated on CMD tryptophan dropout medium (0.67% yeast nitrogen base, 0.064% W/L dropout supplement, 0.00033% leucine, 2% sucrose, 0.1% glucose, 2% agar, pH 5.7). To test for secretion of the SUC2 secretion signal fusion protein, fresh colonies of *S. cerevisiae* were streaked on CMDRAA medium (0.67% yeast nitrogen base, 0.064% W/L dropout mixture, 0.00033% leucine, 0.00033% tryptophan, 2% raffinose, 2 µg/ml antimycin A, 2% agar, pH 5.8) and compared with growth on YPDA control plates [52, 53]. *E. festucae* strains were grown on 2.4% Potato-Dextrose Agar (PDA) supplemented with 150 µg/ml hygromycin B or 250 µg/ml geneticin or in 2.4% Potato-Dextrose Broth (PDB) for up to seven days [54, 55]. For microscopy analyses, strains were grown on 3% water agar overlaid with 1.5% water agar [40]. All strains used in this study can be found in S2 Table.

Plant growth and endophyte inoculation

E. festucae strains were inoculated into endophyte-free seedlings of perennial ryegrass (*L. perenne* cv Samson) using the method previously described [56]. Inoculated plants were grown in root trainers at 22°C in a controlled growth room with a photoperiod of 16 h light (approximately 100 μE/m^2/s) and 8 h dark. *N. benthamiana* and *N. tabacum* were grown at approx. 28°C in a controlled growth room with a photoperiod of 16 h light (approximately 100 μE/m^2/s) and 8 h dark for 6–7 weeks. For agroinfiltration experiments (see below), plants were transferred to a greenhouse and grown at 25°C with natural lighting.

DNA isolation, PCR and sequencing

High quality genomic DNA was extracted from freeze-dried mycelia of *E. festucae* as previously described [57]. Plasmid DNA was extracted from *E. coli* using the High Pure plasmid isolation kit (Roche). DNA resolved by agarose gel electrophoresis was purified using the Wizard SV Gel and PCR Clean-Up System (Promega) or the Zymoclean Gel DNA Recovery kit (Zymo Research). PCR amplification of short DNA products was conducted with the OneTaq (NEB) polymerase according to the manufacturer's instructions. Each reaction was set up as follows: 1× Standard OneTaq Reaction Buffer, 200 μM dNTPs, 0.2 μM for each forward and reverse primer, 0.025 units/μl OneTaq Polymerase and 20-300 ng of template DNA. If crude DNA was used as a template, 3% DMSO was added. PCRs were performed with the following Thermocycler (Eppendorf) settings: 1 min at 94°C for initial denaturation, then 30-35 cycles of 30 s at 94°C (denaturation), 30 s at 45-65°C (annealing), 1 min/kb at 68°C (extension) followed by 3-5 min at 68°C (final extension). Amplification of DNA fragments for Gibson Assembly [58] was performed with Phusion High Fidelity polymerase (ThermoFisher Scientific). Each reaction was set up as follows: 1× Phusion HF buffer, 200 μM dNTPs, 0.5 μM of each forward and reverse primer, 0.02 U/μl Phusion polymerase and 20-300 ng of template DNA. PCRs were performed with the following Thermocycler settings: 1 min at 98°C for initial denaturation, then 30-35 cycles of 30 s at 98°C (denaturation), 30 s at 59-68°C (annealing), 30 s/kb at 72°C (extension), followed by 3-5 min at 72°C (final extension). Where long primers (>30 bp) were used, a 2-step PCR was performed with the same reaction set up, but with different cycler settings: 1 min at 98°C for initial denaturation, then 5 cycles of 30 s at 98°C (denaturation), 30 s at 55°C (annealing), 30 s/kb at 72°C (extension), followed by 25 cycles of 30 s at 98°C (denaturing) and 30 s/kb at 72°C (extension). Subsequently the reaction was incubated for 3-5 min at 72°C (final extension). PCR products were purified using the Wizard SV Gel and PCR Clean-Up System (Promega). Primers were

sourced from Integrated DNA Technologies. Primer sequences can be found in the Supplemental Table S2. Sequencing reactions were performed using the Big-DyeTM Terminator Version 3.1 Ready Reaction Cycle Sequencing Kit (Applied BioSystems, Carlsbad, California, USA), and separated using an ABI3730 genetic analyser (Applied Bio Systems). Sequence data was assembled and analysed using MacVector sequence assembly software, v14.5.2.

Preparation of constructs

The *gpiB* replacement construct, pBH1, was prepared as follows. Firstly, the 1,639 bp 5' and 1,389 bp 3' flanks of *gpiB* were amplified from wild type (WT) *E. festucae* strain Fl1 genomic DNA by PCR using BH1/BH2 and BH3/BH4 primer pairs, respectively. The 1,394 bp hygromycin resistance cassette (P*trpC-hph)* sequence was then amplified from pSF15.15 DNA using the hph_F/hph_R primer pair. The 5,483 bp backbone vector, pRS426, was amplified by PCR using the pRS426_F/pRS246_R primer pair. All PCRs were performed with Phusion High-Fidelity DNA polymerase (NEB). The fragments were then assembled via Gibson Assembly [58] and the correct assembly was verified using a diagnostic restriction enzyme digest and sequencing. The replacement constructs for *sspM* (pBH2), *sspN* (pBH3) and *sspO* (pBH4) were generated in the same way. The 1,377 bp 5' and 1,333 bp 3' flanks of *sspM* were amplified with the BH11/BH12 and BH9/BH10 primer pairs, respectively; the 1,431 bp 5' and 1,433 bp 3' flanks of *sspN* were amplified with the BH15/BH16 and BH13/BH14 primer pairs, respectively; and the 1,443 bp 5' and 1,318 bp 3' flanks of *sspO* were amplified with the BH5/BH6 and BH7/BH8 primer pairs, respectively.

The *S. cerevisiae* complementation vector pSUC2T7M13ORI [52] was fully sequenced using primers BH25 to BH42 and BH61 to BH63. The nucleotide sequences encoding the secretion signals from SspN (54 bp), SspO (54 bp), SspM (54 bp) and GpiB (57 bp) were then amplified from *E. festucae* strain Fl1 genomic DNA with the BH21/BH22, BH70/BH71, BH68/BH69 and BH64/BH65 primer pairs, respectively, using OneTaq polymerase. In doing so, these primers added a 5' *Eco*RI and 3' *Xho*I restriction site to each amplified sequence. Due to difficulties in working with small fragments, different cloning strategies were effective for the different fragments. The *sspN* fragment was cloned into the TOPO-TA vector according to the manufacturer's instructions. Following this cloning step, pSUC2TM13ORI and the TOPO-TA vector containing the *sspN* secretion signal-encoding nucleotide sequence were digested with *Eco*RI and *Xho*I restriction enzymes and purified. The pSUC2TM13ORI vector backbone and secretion signal-encoding nucleotide sequence were then ligated using T4 ligase to generate pBH7. The *gpiB*, *sspM* and *sspO*

secretion signal-encoding nucleotide sequences were directly digested with *Eco*RI and *Xho*I and purified, omitting the sub-cloning step into the TOPO-TA vector. Subsequently the nucleotide sequences were then directly ligated into *Eco*RI and *Xho*I digested pSUCTM13ORI generating pBH5 (*gpiB*), pBH11 (*sspM*) and pBH9 (*sspO*) respectively.

The four overexpression constructs were generated by Gibson Assembly [58] of two fragments, respectively. The 2,844 bp backbone fragment, containing a hygromycin resistance cassette, was amplified from pBH12 with the primer pair BH75/76. The nucleotide fragments encoding *gpiB*, *sspM*, *sspN* or *sspO* downstream of the P*tef* promoter as well as an ampicillin resistance gene (*bla*) and an *oriT* were amplified from pBH14, pBH18, pBH21 or pBH24 respectively. For amplification, the primer pairs BH72/BH120 (3,476 bp), BH72/BH121 (3,725 bp), BH72/122 (3,525 bp) or BH72/BH123 (3,493 bp) were used, respectively. Assembly of the respective fragments generated the plasmids pBH29 (*gpiB*), pBH30 (*sspM*), pBH31 (*sspN*) and pBH32 (*sspO*).

Constructs encoding the genes of interest, C-terminally fused to an 8xHis tag, were generated via Gibson Assembly [58]. Again, each plasmid was assembled from two fragments. The 2,488 bp backbone was amplified from pBH30 using the BH176/BH75 primer pair. The forward primer, BH176, was designed in a way that it added the 8xHis tag followed by a stop codon to the fragment. The *sspM*-, *sspN*- and *sspO*- encoding fragments were amplified from pBH30, pBH31 and pBH32 with the primer pairs BH72/BH177 (3,728 bp), BH72/BH178 (3,528 bp) and BH72/179 (3,496 bp) respectively. The reverse primers BH177/BH178/BH179 were designed in such a way that the stop codon was removed and an overhang to the 8xHis tag was generated. The *gpiB*-containing fragment was generated based on a previously generated construct, pBH34. To prevent the loss of the 8xHis tag due to the addition of the GPI anchor at the omega site [59], the 8xHis tag was added 30 bp upstream of the omega site. To this end, the vector was assembled in two pieces amplified from pBH34: the 2,823 bp fragment amplified by PCR with BH181/BH75 primer pair containing the C-terminus of *gpiB* as well as the hygromycin resistance cassette, and the 3,377 bp fragment amplified by PCR with the BH72/BH180 primer pair encoding an ampicillin resistance gene, an OriT and the *gpiB* N-terminus. The primers BH180 and BH181 generated the 8xHis tag and thereby overhangs with each other. This generated the plasmids pBH56 (*gpiB*), pBH57 (*sspM*), pBH58 (*sspN*) and pBH59 (*sspO*).

For the localization constructs, the plasmid pBV579 (PN4241) encoding mCherry fused to a T-virus nuclear localization signal, was used [60]. The constructs

were generated via Gibson Assembly [58] from three different fragments, generating C-terminal translational fusions between the *ssp* of interest and mCherry-NLS separated by a (GGGS)x2 linker to facilitate independent folding of the protein of interest and mCherry. All constructs incorporated the native *ssp* promoter. The 5,060 bp backbone of the vector was amplified by PCR from pBH12 with the BH76/BH78 primer pair. The 834 bp mCherry-NLS fragment was amplified by PCR from pBV579 with the BH79/BH80 primer pair, where the primer BH79 added the linker. The *sspM*, *sspN* and *sspO* and the corresponding promoter encoding fragments were amplified by PCR from WT genomic DNA using the primer pairs BH88/BH86 (827 bp), BH91/BH89 (977 bp) and BH93/BH94 (798 bp) respectively. Assembly of the fragments generated the plasmids pBH19, pBH22 and pBH25. All plasmids can be found in S2 Table and all primers in S3 Table.

Transformation of organisms

Chemically competent *E. coli* DH5α were transformed by heat-shock for 1 min at 42°C, followed by a 2 min incubation step on ice. Cells were allowed to recover for 1 h at 37°C in SOC medium and subsequently plated on LB agar containing ampicillin or kanamycin. *S. cerevisiae* YTK12 cells were made competent using the lithium acetate method [61], transformed by heat-shock for 30 min at 40°C [62] and plated on defined CMD tryptophan dropout medium (see above). *A. tumefaciens* GV3101 [63] cells were made competent and transformed by electroporation (25 mF, 2.5 kV, 200 Ω) [64]. Cells were allowed to recover in SOC medium and then plated on LB agar containing kanamycin. *E. festucae* Fl1 protoplasts were generated as previously described [65]. Protoplasts were transformed with up to 5 µg of the construct using the method previously described [66]. Protoplasts were allowed to regenerate overnight on regeneration agar (RG) and overlaid with RG agar containing either hygromycin B or geneticin the next day.

Protein extraction, protein purification and western blotting

For protein extraction, *E. festucae* strains were grown for at least 3 days in liquid PD at 22°C. Cultures were filtered through a nappy liner, washed, and snap frozen in liquid nitrogen and ground to a fine powder. Depending on the amount of mycelium, 400–800 µl of lysis buffer (50 mM NaH_2PO_4, 300 mM NaCl, 10 mM imidazole, 0.1% (v/v) IGEPAL CA360, 0.2 mM PMSF, 10 µl/ml protease inhibitory cocktail (Sigma Aldrich), 5 mM β-mercaptoethanol) was added and samples were vortexed for 10 min. Subsequently, samples were centrifuged at 14,000 g for 15 min at 4°C and the supernatant was stored at -20°C. The growth medium of each strain (50–80 ml) was

collected and filtered through a 0.45 µm filter. Samples were concentrated to approx. 2 ml with Vivaspin 20 MWCO 30,000 spin columns (GE Healthcare Life Sciences) according to the manufacturer's instructions and washed twice with 10 ml lysis buffer. Samples were stored at -20°C.

The protein purification was performed with Ni-NTA spin columns (Qiagen) according to the manufacturer's instructions with the exception of the elution buffer (50 mM NaH_2PO_4, 300 mM NaCl, 10–500 mM imidazole, 0.1% (v/v) IGEPAL CA360), 0.2 mM PMSF, 10 µl/ml protease inhibitory cocktail (Sigma Aldrich)). Samples were loaded onto 15% (w/v) SDS polyacrylamide gels, electrophoresed at 100 V for 1.5 h then electrophoretically transferred at 30 V for 1 h to PMSF membranes (Roche). The primary antibody, rabbit α-His (Abcam, ab9108), was used in a 1:2,000 dilution and the secondary goat α-rabbit-HRP (Abcam, ab6721) in a 1:10,000 dilution. Detection was performed with the Amersham ECL western blotting detection reagent (GE Healthcare Life Sciences).

For the verification of Ssp and GpiB production in *N. benthamiana*, total protein was extracted from the infiltrated area. First the tissue was snap frozen, then ground to a fine powder in liquid nitrogen and subsequently resuspended in an equal volume of GTEN buffer (10% glycerol, 100 mM Tris pH 7.5, 1 mM EDTA, 150 mM NaCl, 10 mM DTT, 0.2% IGEPAL CA360, 10 µl/ml protease inhibitory cocktail (Sigma Aldrich), 1% PVP). Afterwards, samples were centrifuged at 14,000 rpm for 15 min at 4°C and the supernatant was stored at -20°C. Samples were loaded onto a 15% SDS polyacrylamide gel and transferred onto PMSF membranes (Roche) as described above. The primary antibody, a mouse α-FLAG antibody (Sigma, F6165), was used in a 1:2,000 dilution followed by the secondary goat α-mouse–HRP (Santa Cruz Biotechnology, Dallas, TX, USA) antibody in a 1:1,000 dilution.

RNA extraction and qPCR

For the determination of the gene copy number, high quality gDNA was extracted as described above and qPCR was performed with SYBR Green (Invitrogen) on a LightCycler 480 System (Roche) as per the manufacturer's instructions. Each sample was analysed with two technical replicates. The single copy genes *hepA* (EfM3.043690) and *pacC* (EfM3.009480) were used as reference genes and the copy number was calculated relative to WT as described previously [67].

For the determination of relative expression levels, RNA was extracted from freeze-dried mycelium using TRIzol reagent (Invitrogen). Subsequently, cDNA synthesis was performed with the QuantiTect Reverse Transcriptase kit (Qiagen). The

qRT-PCR was performed as described above. Each sample was analysed with two technical replicates. The genes coding for translation elongation factor 2 (EF-2, EfM3.021210) and 40S ribosomal protein S22 (S22, EfM3.016650) were chosen as reference genes as previously described [68]. The expression level was calculated relative to WT as described previously [67]. All primers used for qPCR and qRT-PCR can be found in the S3 Table.

Analysis of transmission of *E. festucae* mutants into *L. perenne* seeds

Twenty endophyte free seedlings of *L. perenne* cv. Samson were inoculated with three independent deletion strains of *gpiB* (T111, T133, T148), *sspM* (T52, T99, T163), *sspN* (T10, T30, T52) and *sspO* (T78, T195, T210) [56, 69]. Twenty seeds were inoculated with PD agar as mock control. Plants were grown in root trainers in the greenhouse for 7 weeks at 20°C with a photoperiod of 16 h of light and tested for presence of the endophyte by immunoblotting [70]. Five immunoblot positive plants of each strain were transferred to new pots 10 weeks post-infection and grown in the greenhouse for an additional two weeks. For vernalisation, plants were transferred to a growth cabinet and cultivated for 7 weeks at 6°C with a short-day photoperiod of 8 h light and 16 h dark. Starting from four weeks until ten weeks after vernalisation, plants produced inflorescences. Ovaries were collected, stored in 95% EtOH and stained [69] when pollen was visible and ovaries were mature. Stained ovaries were stored in 70% glycerol until microscopic observation. Seeds were collected, dried and stored in the fridge until further use. For microscopy and immunoblotting of seeds, the seeds were surface sterilised [56, 69], germinated on wet filter paper overnight and cross sections used for immunoblotting.

Microscopy

For microscopy of *E. festucae* culture growth, a small piece of a fresh colony was inoculated on the edge of a glass slide covered with a thin layer of 1.5% H_2O agar placed on an agar plate with 3% H_2O agar. Strains were incubated for 6 days before examination with an Olympus IX71 inverted fluorescence microscope using the filter sets for DIC and CFW/DAPI. For staining of the cell wall, a drop of a 3 mg/ml of Calcoflour White was added to the sample just before microscopy.

For the examination of growth and morphology of hyphae *in planta*, pseudostem tissue was stained with aniline blue diammonium salt (Sigma) and Wheat Germ Agglutinin conjugated to AlexaFluor488 (WGA-AF488, Molecular Probes/Invitrogen). First, infected tissue was incubated in 100% EtOH overnight at 4°C followed by an incubation in 10% KOH overnight at 4°C. Samples were washed at least

3 times with PBS (pH 7.4) before incubation in the staining solution (0.02% aniline blue, 10 ng/ml WGA-AF488, 0.02% Tween-20 (Invitrogen) in PBS (pH 7.4)) for 10 min. Samples were vacuum-infiltrated with the staining solution for 30 min and then stored at 4°C until analysis. Examination of these samples was performed with a Leica SP5 DM6000B confocal microscope (488 nm argon and 561 nm DPSS laser, 40× oil immersion objective, NA= 1.3) (Leica Microsystems). For TEM pseudostem samples were fixed with 3% glutaraldehyde and 2% formaldehyde in 0.1 M phosphate buffer, pH 7.2 for 1 h, as described previously [71]. The fixed samples were examined with a Philips CM10 TEM and the images were acquired using a SIS Morada digital camera. Sections of the resin-embedded samples were also stained with 0.05% toluidine blue in phosphate buffer and heat-fixed at approx. 100°C for 10 s. These samples were examined with a Zeiss Axiophot Microscope with Differential Interference Contrast (DIC) Optics and Colour CCD camera.

For the *in planta* localization of the Ssp-mCherry-NLS fusion proteins, unfixed pseudostem samples were examined with a Leica SP5 DM6000B confocal microscope (488 nm argon and 561 nm DPSS laser, 40× oil immersion objective, NA= 1.3).

Preparation of binary vectors, agroinfiltration and suppression assay

All binary backbone vectors for transformation into *Agrobacterium* are listed in S2 Table. The plasmids pBH44-47 were generated via Golden Gate cloning using pICH86988 as the backbone. The nucleotide sequences of *gpiB, sspM, sspN and sspO* were amplified by PCR without their native secretion signal from WT *E. festucae* cDNA with primer pairs adding additional base pairs for the necessary overhang and a *Bsa*I restriction site (*gpiB*: BH165/BH166, *sspM*: BH167/BH168, *sspN*: BH170/BH171, *sspO*: BH172/BH173) as described. The *N. tabacum* secretion signal PR1α was obtained from pUC19B (S. Marillonet, pers.comm.). The digestion and ligation were conducted either in one step or in two separate steps. The one-step reaction was performed in a total volume of 20 µl with 1 µl T4 ligase (NEB) and 1 µl BSA (NEB) and equimolar amounts of all three inserts (approx. 50 ng total). The reaction was performed in a Thermocycler (Eppendorf) with the following settings: 25 cycles of 37°C for 3 s and 16°C for 4 s, followed by 5 s inactivation at 50°C and 80°C each. For the two-step reaction, the digest was performed in a volume of 10 µl with 1 µl BSA (NEB) and equimolar amounts of each insert. The reaction was performed at 37°C for 3 h. Subsequently the reaction was inactivated by heating to 50°C. For the ligation, the volume was topped up to 20 µl per reaction including 1 µl T4 ligase (NEB). The reaction was incubated at 16°C in a Thermocycler (Eppendorf) overnight followed by

an 80°C inactivation step. A diagnostic restriction digest and DNA sequencing confirmed the sequence of all vectors. Electro-competent *A. tumefaciens* GV3101 cells were generated and transformed as described. Cells were allowed to recover in SOC medium and subsequently plated on LB agar containing kanamycin. To perform the infiltrations, fresh strains were inoculated in 3 ml LB medium with kanamycin and incubated at 30°C overnight. The next day, cultures were spun down and resuspended in 1 ml infiltration buffer (10 mM $MgCl_2$, 10 mM MES-KOH, 100 µM acetosyringone). These cultures were adjusted to an OD_{600} of 0.4 in the necessary amount of infiltration buffer (usually 5–10 ml) and incubated at room temperature for at least 3 h before infiltration. To confirm the expression of each of the constructs, total protein was extracted from infiltrated *N. benthamiana* tissue and a western blot was performed.

For HR suppression assays *A. tumefaciens* strains carrying plasmids encoding the potential suppression gene pBH44 (*gpiB*), pBH45 (*sspM*), pBH46 (*sspN*), pBH47 (*sspO*), pBIN-Plus-Avr3a (suppression control), pICH86966-N-3xFlag-GFP (control), pBC302-3-R3a (HR control) were infiltrated 24h before infiltration with pBC302-3-INF1 and pBIN-Plus-Avr3a (HR control).

Results

Candidate effectors of *E. festucae*

The recent availability of the complete telomere-to-telomere genome sequence of *E. festucae* strain FI1, which is 35 Mb in size and encodes 8,465 predicted genes on seven chromosomes [26], provided us with the opportunity to study the organization, structure and genome context of genes encoding candidate effector proteins. First, we established which of the 8,465 predicted genes likely encode secreted proteins. For this purpose, we defined a secreted protein as any protein with a predicted amino N-terminal secretion signal, as determined using the SignalP server, that targets the protein outside of the fungal plasma membrane [44]. This definition does not exclude those proteins with a predicted transmembrane domain or GPI anchor modification site. In total, 682 genes (8.1%) were predicted to encode a secreted protein. We then analysed which of the 682 predicted secreted proteins encode candidate effectors using the EffectorP server, which predicts effectors using a machine learning approach [41]. In addition, we applied a size cutoff of ≤200 amino acids, as most fungal effectors fall within this range [72]. Out of 175 predicted secreted proteins meeting this length requirement, 141 were predicted to be candidate effectors by EffectorP. For subsequent analyses the 8,465 predicted proteins were subdivided into 'effector candidates' (n=141), 'secreted', comprising all putatively secreted proteins that are not classified as effector candidates (n= 541), and 'non-secreted' made up of all putatively non-secreted proteins (n= 7,783) (S4 Table).

To gain further insight into the possible functions of the 141 effector candidates, and to determine which of these predicted proteins have homologs across the *Sordariomycetes*, a BLASTp analysis was performed against fungal reference proteins at NCBI. Of the 141 effector candidates, 83 were found to have sequence homology to proteins present in the NCBI database (E-value cut off of ≤1e-10), but 56 of these were to uncharacterized or hypothetical proteins. Among the 'hits' to characterized proteins were ten cell wall-associated proteins, including hydrophobins and carbohydrate-binding proteins, two toxins and other small secreted proteins (S4 Table). The majority of 'hits' were to proteins from species in the Hypocreales (21 *Claviceps spp*., 21 *Metarhizium spp*., 14 *Pochonia spp*., 6 *Moelleriella spp*., 6 *Ustilaginoiea spp*.), with the remaining hits to proteins from other species within the Sordariomycetes. For 58 of the effector candidates, no homologs could be identified (E-value>1e-10), but analysis against a custom made Clavicipitaceae endophyte database

(epichloe.massey.ac.nz)[47] found potential homologs for 20 of these proteins. The remaining 38 Ssps are apparently unique to *Epichloë spp.* (S4 Table).

Given many fungal effectors are cysteine-rich, a property that enables the formation of disulfide bonds and protein folding to maintain structural integrity in the protease-rich apoplast [73, 74], the frequency of cysteine residues in the effector candidates was compared with that of the secreted and non-secreted categories. As expected the candidate effectors were significantly more cysteine-rich (3.6% of residues) than either secreted (frequency= 1.7%, *P*= <1e-18) or non-secreted (frequency= 1.4%, *P* < 1e-18) (S1 File).

In smut fungi, secreted genes are predominantly arranged in clusters within the genome and are highly upregulated during tumor formation [75, 76]. We therefore tested whether the genes encoding the *E. festucae* effector candidates were clustered by mapping them to each of the seven chromosomes (Fig 1A). From this low-resolution analysis, it appears that the genes encoding effector candidates of *E. festucae* are evenly distributed throughout the genome. This conclusion was supported by an analysis comparing the within category gene distances, which concluded that genes encoding effector candidates are not clustered in the *E. festucae* genome (Fig 1A). Of all the genes encoding candidate effectors, only eight (four gene pairs) were found within 1 kb of each other. In fact, the mean distance between candidate effector genes was not significantly different from that expected from a random subset of the 141 genes (*P*= 0.236).

E. festucae is one of several filamentous fungi that has a genome comprised of distinct gene-poor AT isochores and gene-rich GC isochores [21, 26]. Because the AT-rich regions are subject to an unusually high mutation rate [77-80] they are frequently referred to as 'birthplaces' for new genes such as those encoding effectors and secondary metabolites [81]. In *Leptosphaeria maculans* 20% of all genes in AT isochores encode small secreted proteins (SSPs, effector candidates), whereas they make up just 4.2% of all genes in GC isochores [21]. In contrast to *L. maculans*, there was no enrichment of genes encoding effectors in or near to AT isochores of the *E. festucae* genome (*P*= 0.369) (Fig 1B). Similarly, there was no enrichment of genes in the secreted category in AT isochores (*P*= 0.812) (Fig 1B). Indeed, of the 548 genes located in or within 1,000 bp of an AT isochore, only 1.5% and 4.7% encoded a protein from the candidate effector and secreted categories, respectively.

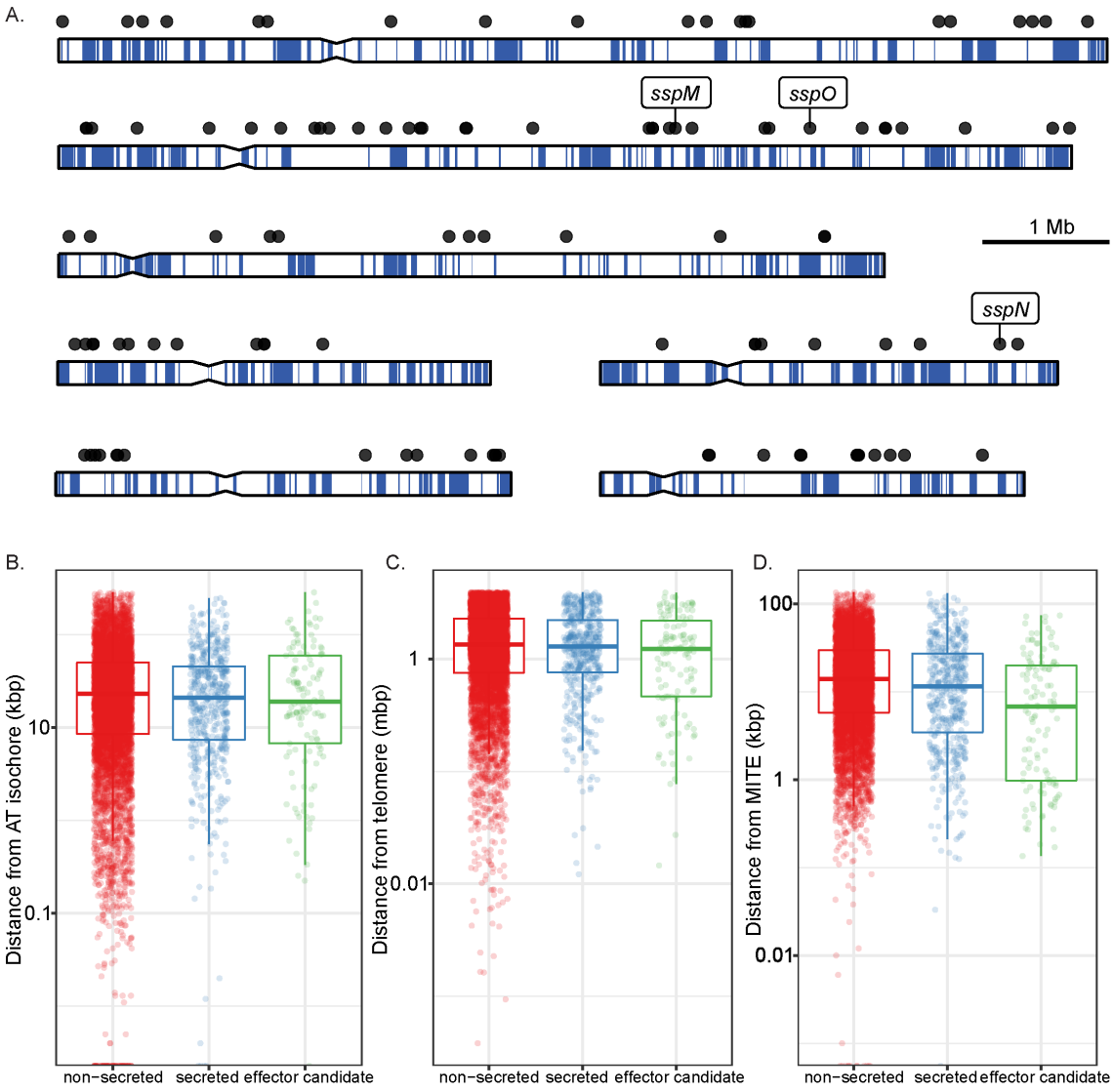

Fig 1. Physical properties of genes encoding effector candidates in *E. festucae*.
(A) Location of genes encoding effector candidates (black circles) on the seven chromosomes of *E. festucae* strain FI1. The blue line indicates AT richness in a 1,000 bp window. (B) Distance of each *E. festucae* gene from AT-rich regions (isochores). (C) Distance of each *E. festucae* gene from telomeres. (D) Distance of each *E. festucae* gene from MITES. Genes are divided into the categories 'non-secreted' (n= 7783), 'secreted' (n= 541) and 'effector candidates' (n= 141).

Given some fungal effector genes, such as the *AVR-Pita* gene from *Magnaporthe oryzae* [82], are found in close proximity to telomeres, we took advantage of the telomere-to-telomere *E. festucae* genome sequence to determine if genes encoding candidate effectors are located close to telomeres. These regions of the genome are also subject to higher mutation rates than the remainder of the genome and potential sites for the evolution of environment adaptation genes such as those

encoding effectors [83, 84]. However, genes encoding effector candidates were not significantly closer to telomeres than other genes present in the *E. festucae* genome (*P*< 0.787) (Fig 1C).

Transposable elements are increasingly seen as important regulators of gene expression [85, 86], and miniature inverted-repeat transposable elements (MITES) have been postulated to play a role in the expression of *E. festucae* genes *in planta* [24, 26]. For this reason, the distance between genes encoding effector candidates and MITES was analyzed in the *E. festucae* genome. This analysis revealed that genes encoding effector candidates are more likely to contain a MITE within 2 kb of their transcription start site than non-secreted proteins (*P*= 3.56e-18, Fig 1D). Genes encoding other secreted proteins were also more likely to contain a MITE immediately upstream of their transcription start site than non-secreted proteins (*P*= 1.66e-7). No particular MITE family is over-represented within 2 kb of these genes.

Apart from the physical organization of effector genes within fungal genomes, the expression of these genes often follows distinct host colonization patterns and are generally more highly expressed *in planta* than in axenic culture [72, 87, 88]. We therefore analysed the transcript expression profiles of the three different gene categories between *E. festucae* grown *in planta* and in axenic culture (S5 Table). Genes encoding effector candidates were significantly more highly expressed *in planta* (mean $\log_2$ fold difference= 1.20, *P*< 2e-16) (Fig 2A). Other secreted proteins were also moderately more highly expressed *in planta* (mean $\log_2$ fold difference= 0.20, *P*= 0.004) (Fig 2A).

Given genes encoding effector candidates are preferentially silenced in axenic culture compared to *in planta* we examined whether this might be due to the chromatin state as shown for *L. maculans* where RNAi-induced silencing of DIM-5, a histone H3 lysine 9 trimethyl transferase, and heterochromatin protein 1 (HP1), led to de-repression of effector gene expression in axenic culture [89]. We therefore compared expression of *E. festucae* genes encoding effector candidates in a *hepA* (homolog of *HP1*) mutant versus wild type. We found candidate effector genes were moderately more highly expressed in the *hepA* mutant (mean $\log_2$ fold difference= 0.310, P= 4.13e-9) (Fig 2B). For some genes, this change in gene expression was substantial. Eleven percent of candidate effectors showed $\log_2$ fold difference in expression greater than 2, a significantly higher proportion than observed in larger secreted (1.5% of genes, P= 5e-14) or non-secreted proteins (3% of genes, P= 1e-4).

Previously we showed that disruption of the usually asymptomatic interaction between *L. perenne* and *E. festucae* by infecting the host with symbiotic mutants of *E. festucae* results in major changes in the fungal transcriptome [47]. We therefore tested

whether effector candidate gene expression changed in the Δ*sakA*, Δ*noxA,* Δ*proA* and Δ*hepA* symbiotic mutants using previously generated transcriptome data sets [47](Tetsuya & Scott, personal communication). Generally, genes encoding effector candidates were upregulated in each of the dysfunctional interactions (mean difference of 0.411 log2 fold units, P = 5.28 x 10-8) (Fig 2C). A closer investigation showed that ten genes encoding effector candidates SspB-SspK were consistently upregulated across all four different mutant interactions and three genes encoding effector candidates SspM-SspO were consistently down regulated [47](Tetsuya & Scott, personal communication).

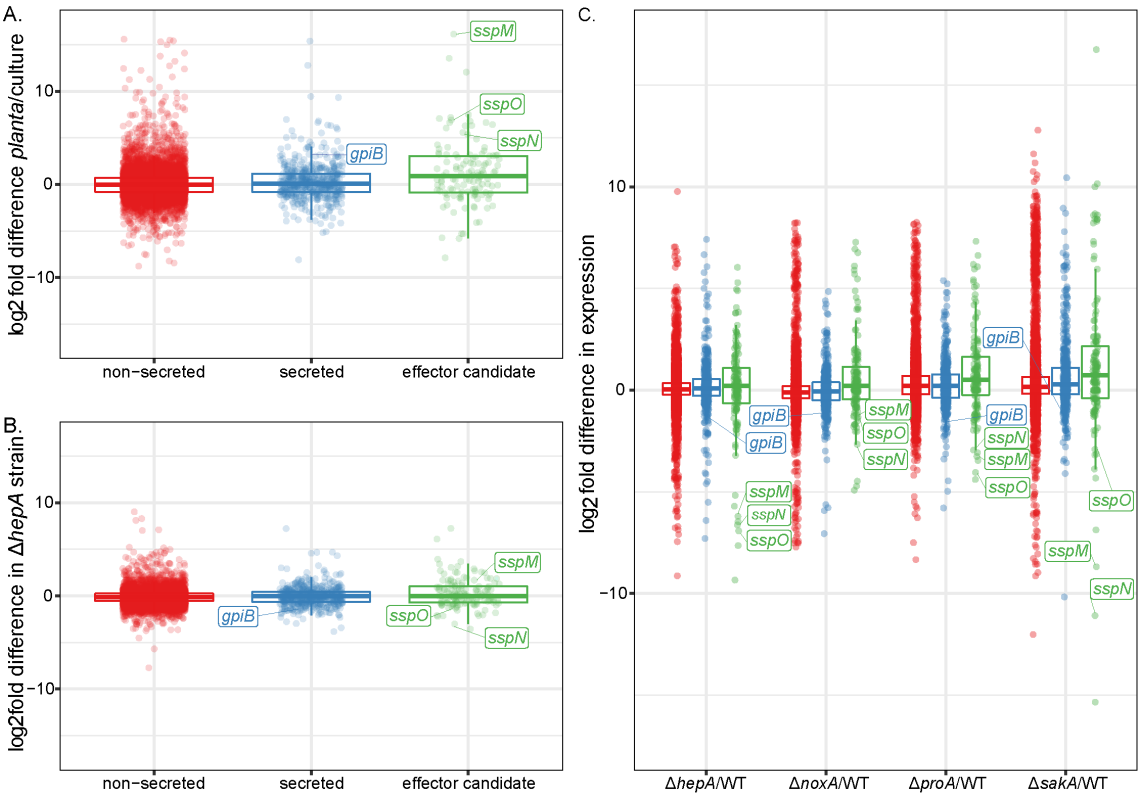

Fig 2. Analysis of gene expression in WT *E. festucae* and symbiotic mutants of *E. festucae.*

(A) Log_2 fold difference in gene expression between WT *E. festucae* grown *in planta* and in culture. (B) Log_2 fold difference in gene expression between WT and a *hepA* deletion strain grown in culture. (C) Log_2 fold difference in gene expression between WT and Δ*noxA,* Δ*proA,* Δ*sakA* and Δ*hepA* strains grown *in planta*. Number of genes in each category: 'non-secreted', n= 7783; 'secreted', n= 541; and 'effector candidates', n= 141.

In summary, the genes encoding effector candidates from *E. festucae* do not show a distinct distribution pattern as has been described for some other fungi, but

seem to be evenly dispersed throughout the genome. These genes do not cluster, and are not preferentially located in AT-rich isochores or telomeres. However, these genes are enriched with respect to their proximity to MITES. As found for many other fungi, a significant number of genes encoding effector candidates from *E. festucae* are preferentially upregulated *in planta*. Furthermore, many of these genes are upregulated in symbiotic mutants of *E. festucae* that disrupt the restrictive pattern of growth observed for WT *E. festucae*.

Sequence analysis of downregulated effector candidates

To gain further insight into the role of *E. festucae* effectors in the symbiotic interaction with *L. perenne*, the three genes described above (*sspM*, EfM3.016770; *sspN*, EfM3.062700; and *sspO*, EfM3.014350) that were found to be downregulated in all four symbiotic mutant interactions, were selected for genetic analysis [47](Tetsuya & Scott, personal communication). The fact that they were among the top 100 genes upregulated *in planta* compared to axenic culture was an additional criterium for selecting these three genes (Fig 2A, S4 Table). A fourth gene, *gpiB* (EfM3.018200), encoding a putative GPI-anchored protein, was also selected for functional analysis because it had an identical expression profile to *sspM*, *sspN* and *sspO* [47], and because GPI-anchored proteins are known to have important roles in fungal virulence [42, 43].

cDNA sequencing confirmed that the proposed gene models for each of these four genes were correct. In the case of *sspN*, where two alternatively spliced forms were proposed the second of these (mRNA-2) corresponded to the cDNA sequence. The *gpiB* gene (EfM3.018200) is predicted to encode a protein of 126 aa with an unmodified MW of 12.61 kDa (8.7 kDa without secretion signal and C-terminus beyond the omega cleavage site), while the *sspM* gene (EfM3.016770) is predicted to encode a protein of 177 aa with an unmodified MW of 18.87 kDa (17.1 kDa without secretion signal). The protein encoded by *sspN* (EfM3.062700) is predicted to be 127 aa in length with an unmodified MW of 14.98 kDa (13.19 kDa without secretion signal), while the protein encoded by *sspO* (EfM3.014350) is predicted to be 104 aa in length with an unmodified MW of 11.11 kDa (9.4 kDa without secretion signal) (Fig 3).

Analysis of the selected protein sequences with InterproScan [90], SMART [91], T-Reks [92] and HHPRED [93] did not identify any conserved domains with known function, but did predict a number of different structural features and secondary modifications (Fig 3). GpiB contains a predicted *N*-glycosylation motif as well as a putative C-terminal GPI anchor. The SspM protein contains a possible pre-pro domain ending with a classical LxKR kexin cleavage site motif and a predicted *N*-glycosylation

site. SspN is a repeat-containing protein, consisting of 7.5 almost perfect repeats of 15 aa. Like SspM, it also contains a putative kexin cleavage site. Analysis of the SspO sequence did not reveal any obvious structural features. Both SspM and SspO are rich in cysteines; SspO containing eight and SspM containing six downstream of the cleavage site, whereas SspN and GpiB are cysteine-free (Fig 3).

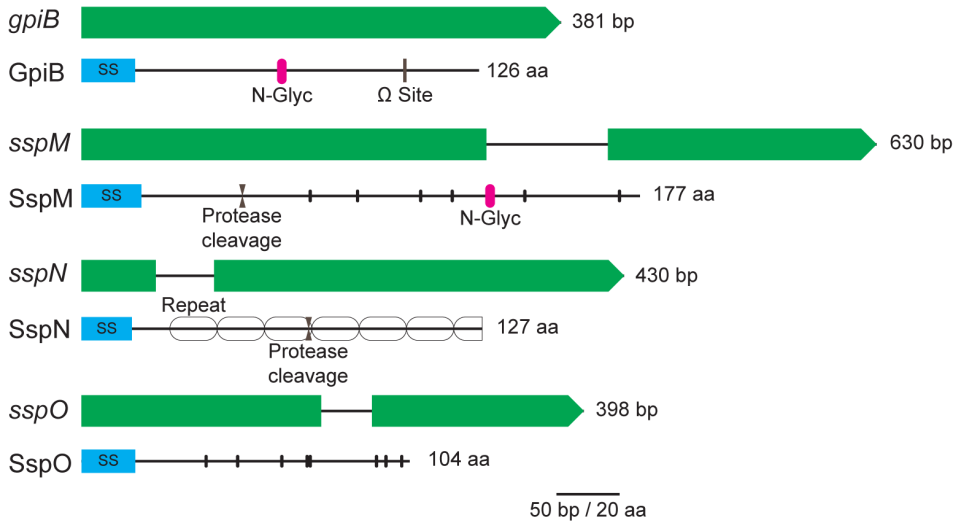

Fig 3. Schematic representation of the small secreted proteins SspM, SspN, SspO (effector candidates) and the GPI-anchored protein GpiB and their corresponding genes.

GpiB (EfM3.018200) is encoded by a 381 bp gene that lacks introns, and is predicted to encode a protein of 126 aa. The gene encoding the predicted 177 aa SspM (EfM3.016770) is 630 bp in size and contains one intron. SspN (EfM3.062700) is encoded by a gene of 430 bp, with one intron, and encodes a predicted protein of 127 aa. SspO (EfM3.014350) is encoded by a 398 bp gene, containing one intron, and is predicted to encode a protein of 104 aa. N-terminal secretion signals (SS) are indicated by blue boxes and post-translational modifications and structural motifs by pink bars (*N*-glycosylation), grey bars (GPI anchor modification site), facing arrows (protease cleavage site), hollow ovals (repeats) and small black bars (cysteine residues).

A BLASTn analysis of the four selected genes revealed a patchy distribution within the *Epichloë* species, with only *gpiB* present in all analyzed genomes available on the Kentucky Endophyte Database [94]. The observed distribution patterns did not correlate with specific hosts or the sexual phenotype of the fungus (S6 Table). Alignment of the protein sequences of interest with the corresponding homologs in other *Epichloë* species showed that GpiB and SspO are highly conserved (S1A and S1D Figs). Interestingly, SspM was highly conserved from the N-terminus to the

proposed kexin cleavage site and less conserved beyond this site (S1B Fig). The repeat structure of SspN was also conserved, with homologs mainly differing in their number of repeats (S1C Fig). A BLASTp analysis identified homologs of the Ssps and GpiB in species outside of *Epichloë* (S4 Table); however, none of these are functionally characterized.

GpiB, SspM, SspN and SspO are secreted

To experimentally verify secretion of the three selected candidate effectors and the GPI anchored protein, GpiB, a complementation assay was performed in *S. cerevisiae*. The nucleotide sequence encoding the secretion signal predicted by SignalP was ligated in frame to the N-terminus of the *S. cerevisiae* invertase *SUC2* encoded on the pSUC2T7M13ORI vector [52]. These constructs were then transformed into the *SUC2*-negative yeast strain YTK12 and tested for growth on CMDRAA medium, which contains raffinose as the sole carbon source. All four test strains expressing the secretion signal-Suc2 fusion protein grew on this medium whereas the strain expressing Suc2 without a secretion signal and the untransformed YTK12 did not (Fig 4). These results indicate that the signal peptides of SspM, SspN, SspO and GpiB are sufficient to mediate secretion in *S. cerevisiae*.

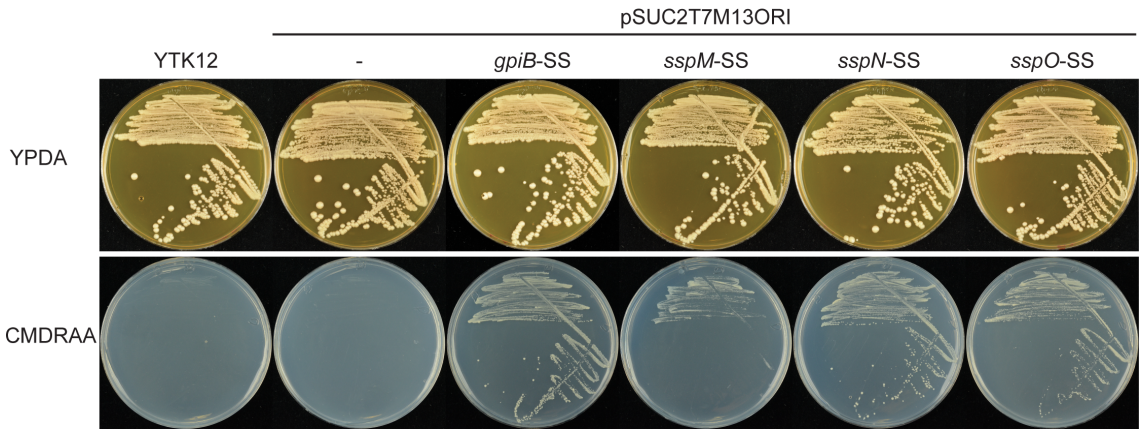

Fig 4. Analysis of the GpiB, SspM, SspN and SspO secretion signals in a *S. cerevisiae* complementation assay.

YTK12 strains transformed with pSUC2T7M13ORI encoding *SUC2* transcriptionally fused to *gpiB, sspM, sspN* or *sspO* secretion signal nucleotide sequence, as well as the empty vector and YTK12-only controls. Only strains expressing the secretion signal-Suc2 fusion proteins were able to grow on defined medium with raffinose as carbon source (CMDRAA). SS, secretion signal. All strains grew on the control plates containing YPDA media.

Analysis of secretion and processing of GpiB, SspM, SspN and SspO in *E. festucae*

As discussed above, many effectors are post-translationally processed (e.g. by proteolytic cleavage) or modified (e.g. by glycosylation) to their final form. To verify the secretion of these proteins in *E. festucae*, and to check if they are modified (Fig 3), His-tagged fusions of GpiB, SspM, SspN and SspO were purified from extracts of *E. festucae* mycelia (intracellular form), as well as from the liquid culture medium (extracellular form), separated by PAGE and analyzed by western blotting (Fig 5). All four proteins were present in extracts from fungal mycelia. The 13 kDa band for GpiB is larger than the predicted His-tagged size of 9.8 kDa, possibly due to the addition of the GPI anchor and/or modification by *N*-glycosylation. A band corresponding to SspN was detected at approx. 14 kDa, which agrees with the predicted His-tagged size of 14.31 kDa for the unprocessed protein, indicating that under the growth conditions used, this protein is not cleaved, even though it has a predicted kexin cleavage site. The signal for SspO was very faint, and slightly larger (12 kDa) than the predicted His-tagged size of 10.5 kDa for this protein. In contrast, two bands of 20 and 16 kDa were detected for SspM, with the band of higher molecular weight being very faint. SspM has a predicted His tagged size of 18.22 kDa in the unprocessed form (with its predicted pro-domain) and 12.7 in the cleaved form (without its predicted pro-domain). Taking into account a probable increase in size due to the predicted *N*-glycosylation, the sizes observed for SspM agrees with the predicted sizes of the kexin-unprocessed and processed forms, respectively. The presence of additional bands on the western is probably the result of non-specific binding to other proteins present in the crude extract separated on these gels.

Analysis of the culture medium identified bands for SspO and SspM, but the latter was only detected when the culture medium was buffered to pH 6.5 with 50 mM HEPES. The bands detected for SspO and SspM were the same size as those seen in the mycelial fraction, with the latter again present as a double band. These results suggest that SspO does not contain any secondary modifications and is secreted into the culture medium, whereas SspM is processed at the predicted kexin site. The absence of bands for GpiB and SspN in the culture medium suggest that these proteins are either unstable in the culture medium or remain attached to the fungal hyphae following secretion.

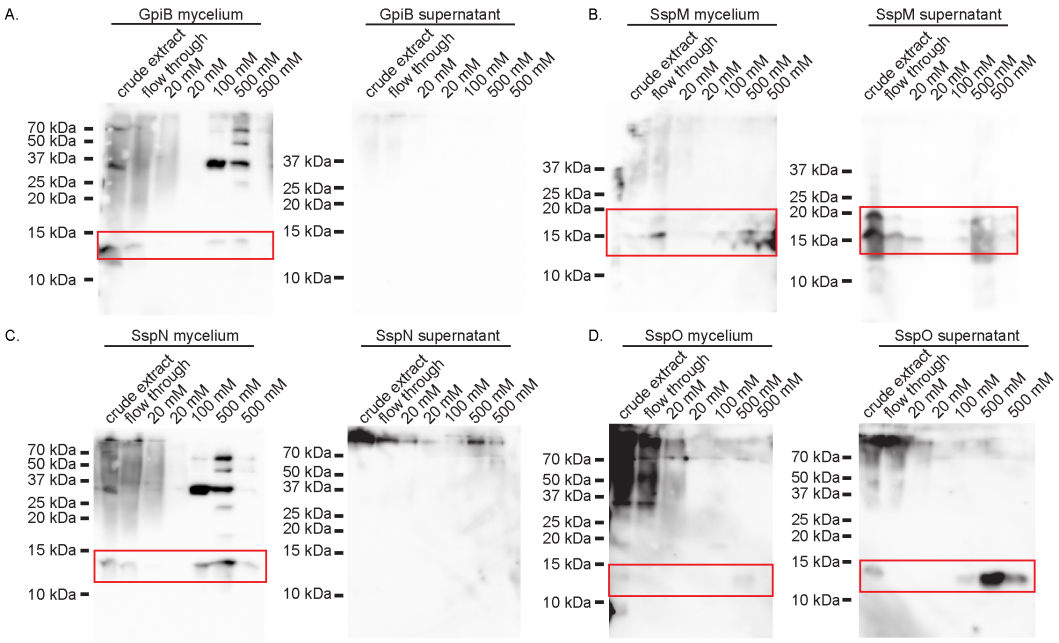

Fig 5. Western blot analysis of GpiB-His, SspM-His, SspN-His and SspO-His extracted from *E. festucae* mycelia and culture medium.

Genes of interest (*gpiB*, *sspM*, *sspN* and *sspO*) were translationally fused to an 8x His tag at the C-terminus and constructs were placed under the control of the P*tef* overexpression promoter. Total protein was extracted from fungal mycelia and the corresponding growth medium, and His-tagged proteins purified on Ni-NTA spin columns eluted with increasing concentrations of imidazole. Samples were separated on a 15% SDS PAGE gel, transferred to membranes and probed with an anti-His antibody. SspM-His was extracted from *E. festucae* strains grown in medium buffered to pH 6.5 with 50 mM HEPES. Predicted sizes of proteins were calculated on the basis that each protein lacked the secretion signal and had the 8x His-tag.

Functional analysis of *gpiB*, *sspM*, *sspN* and *sspO*

To investigate whether *sspM*, *sspN*, *sspO* or *gpiB* are necessary for establishing a mutualistic symbiotic interaction, given their expression is downregulated in three different symbiotic mutants [47], each gene was individually deleted in the WT background using a gene replacement approach. Replacement constructs, pBH1–4, were prepared, and PCR-amplified linear fragments of each were transformed into WT protoplasts. Putative gene replacements were identified by PCR screening approximately 200 independent Hyg^R transformants with primers that flank the site of *hph* integration. Additional PCR screening with primer sets that amplify the left and right flanks of each of the insertion sites was used to confirm the transformants

selected had gene replacements. Southern blot analysis of genomic DNA extracted from these strains identified three independent deletion strains for *gpiB* (T111, T133, T148), *sspM* (T52, T99, T163*) sspO* (T78, T195, T210), and *sspN* replacement (T10, T30, T52) (S2 Fig).

To determine the phenotype of the deletion strains in culture, the whole colony morphology of each independent deletion strain was compared to that of WT, which is typically circular with white fluffy mycelium that thins and flattens towards the edges. This comparison revealed that the whole colony morphology of each deletion strain was indistinguishable from WT (Fig 6). Given this result, the hyphal morphology was more closely analysed by microscopy. *E. festucae* WT had smooth hyphal tips with hyphae arranged in bundles that are thicker in the more mature inner zone of the colony. Hyphae of WT had hyphal bridges, which are formed by tip-to-side fusion [40], as well as hyphal coil structures, which are thought to promote conidiophore formation [40]. When stained with Calcofluor white, which preferentially binds to chitin, the cell walls of WT hyphae uniformly fluoresced. Similar to the whole-colony comparison, each of the deletion strains had an indistinguishable phenotype to that of WT, forming hyphal bundles, with occasional hyphal fusion, and coil formation (Fig 6).

To determine the host interaction phenotype, strains were inoculated into *L. perenne* seedlings and the phenotype of infected plants examined eight weeks post-planting. At this time point, WT infected plants typically have 2–6 tillers that are up to 50 cm in length (Fig 7). Plants infected with the deletion mutants had the same interaction phenotype as those infected with WT, with no statistically significant difference in either the number or length of tillers (Fig 7). To analyse the cellular phenotype of the infected plants, pseudostem cross sections were fixed and embedded in resin, and slices stained with Toluidine blue. WT-infected samples typically have one to two hyphae per intercellular space and never colonize the vascular bundle tissue (Fig 8). The mutant-infected plants had the same cellular phenotype as WT plants, with one to two hyphae per intercellular space and no hyphae within the vascular bundles (Fig 8). Given these results, samples were then prepared for TEM, to give better resolution of the cellular phenotype. The cellular structure of tissue infected with *E. festucae* mutants was indistinguishable from WT (Fig 8). In addition, longitudinal leaf sections were infiltrated with wheat germ agglutinin, a chitin-binding lectin, conjugated to AlexaFluor 488 (WGA-AF488), as well as aniline blue, a β-glucan-binding dye, and analysed by confocal laser scanning microscopy (CLSM). Leaves infected with WT typically had one hypha (red pseudocolor, aniline blue) with regularly spaced septa (blue pseudocolor, WGA-AF488) growing between plant cells (Fig 9).

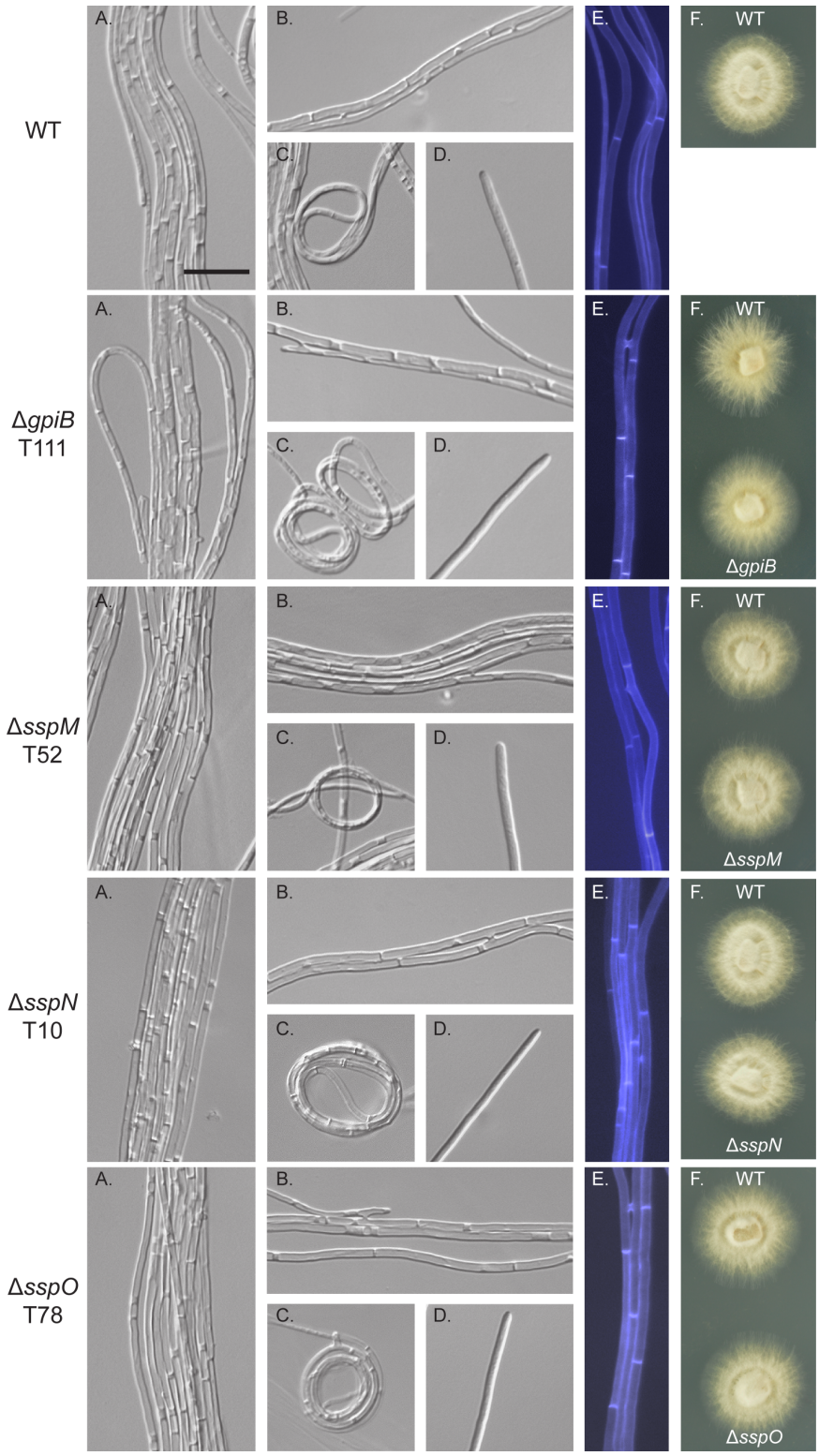

Fig 6. Culture phenotype of WT and deletion mutant strains.

(A)-(D) Representative DIC images captured with the inverted microscope of WT and deletion mutant strains grown on 1.5% water agar for 6 days. (A) Hyphal bundle formation. (B) Hyphal fusion points. (C) Hyphal coils. (D) Hyphal tips. (E) Hyphae stained with Calcofluor white to examine cell wall composition. (F) Colony morphology of WT compared to the deletion strains grown on 2.4% PDA for 7 days. Bar: 20 μm.

These hyphae occasionally branched and where tips of branches meet, fused to establish a hyphal network throughout the leaf tissue (Fig 9). The morphology and growth pattern of the mutant hyphae were indistinguishable from WT (Fig 9).

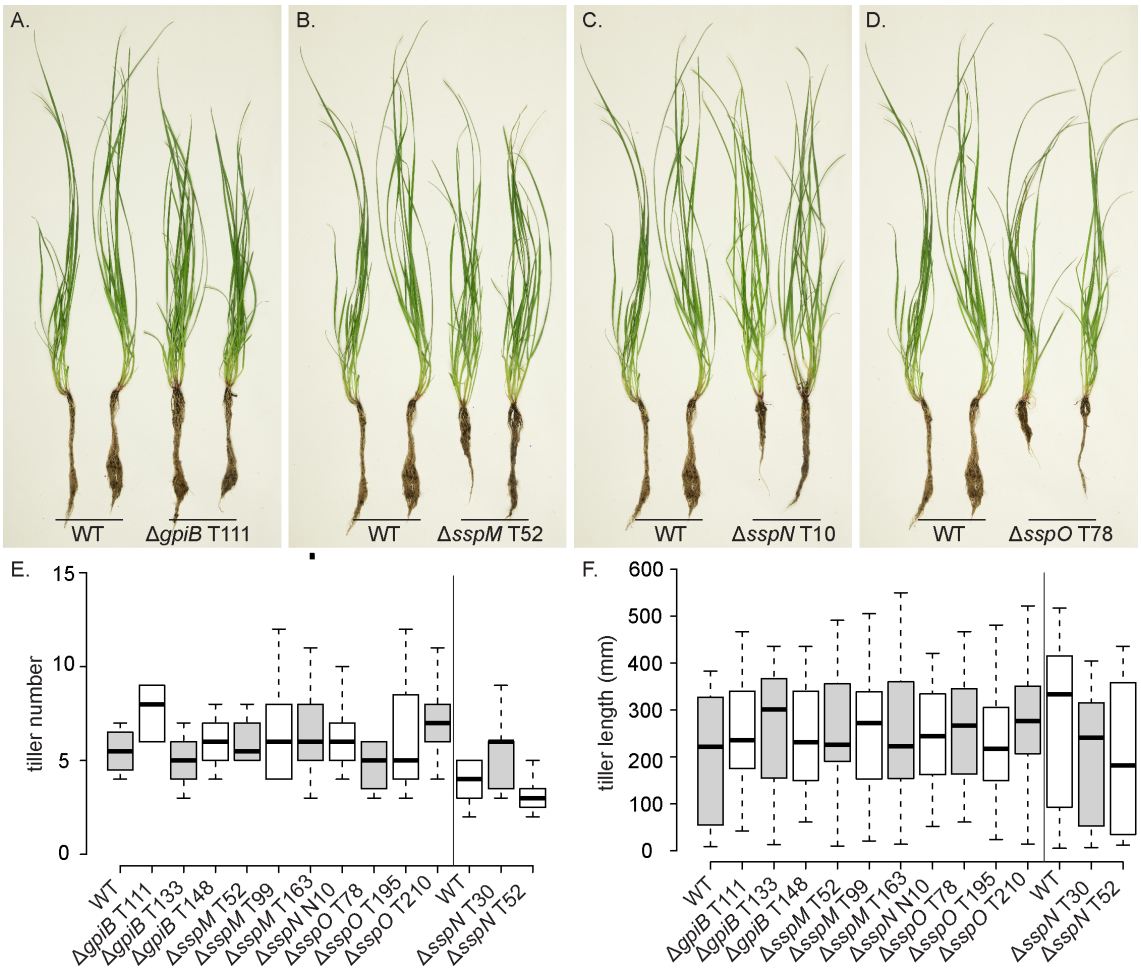

Fig 7. Plant phenotype of *L. perenne* infected with *E. festucae* WT and *gpiB*, *sspM*, *sspN* and *sspO* deletion mutant strains.

(A-D) Whole plant phenotype of WT and deletion mutant-infected *L. perenne* plants 8 weeks post-planting. (E and F) Box plots representing tiller number (E) and length (F) of ryegrass plants 8 weeks post-planting infected with *E. festucae* WT (n=6) and Δ*gpiB* (n=9/9/5), Δ*sspM* (n=10/15/13), Δ*sspN* (n=13/8/8) and Δ*sspO* (n=7/8/9) mutant strains. One-way ANOVAs were used to test for differences in both plant phenotypes between wildtype and modified strains. In each case the ANOVA was fitted with R and a Bonferroni correction was applied to all p-values to account for multiple testing.

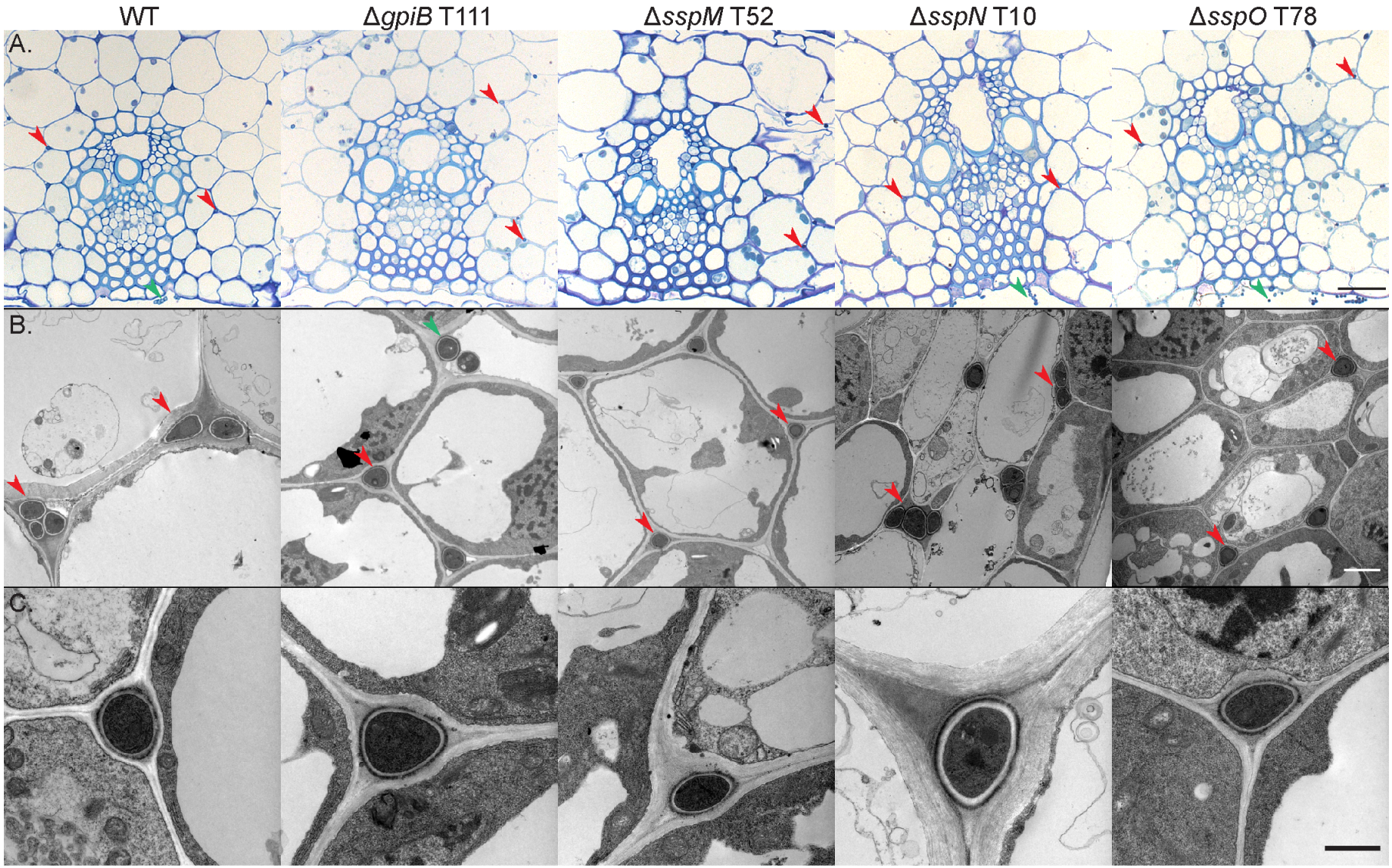
WT
ΔgpiB T111
ΔsspM T52
ΔsspN T10
ΔsspO T78
A.
B.
C.

Fig 8. Light microscopy and transmission electron micrographs of the *in planta* cellular phenotype of *E. festucae* WT and *gpiB*, *sspM*, *sspN* and *sspO* deletion mutant strains.

(A) Light microscope analysis of fixed *L. perenne* pseudostem cross sections stained with Toluidine blue. The focus of the section is on the vascular bundles and surrounding regions; Bar= 10 μm. (B) TEM analysis of hyphal growth in the host apoplast; Bar= 2 μm. (C) Magnified transmission electron micrograph of one single hypha; Bar= 1 μm. Representative images from one of the independent mutants for each gene. Red arrows indicate position of hyphae and green arrows epiphyllous hyphae.

Next we tested whether these mutants could be vertically transmitted into the seeds of *L. perenne*. Plants infected with each of the individual transformants were vernalized and ovaries collected from flowers for CLSM and seed collected from mature inflorescences to test for endophyte in each of these tissues. Endophyte was shown to be present in ovaries of some of the flowers collected from plants infected with Δ*gpiB*, Δ*sspM* and Δ*sspN* mutants but not Δ*sspO* (S3 Fig; S7 Table). Seeds of Δ*gpiB* (2/43), Δ*sspM* (25/90) and Δ*sspN* (14/70) were immunopositive indicating that these three mutants were vertically transmitted (S7 Table). However, none of the seeds infected with Δ*sspO* (0/60) were found to contain endophyte suggesting this mutant was unable to be transferred to the seed.

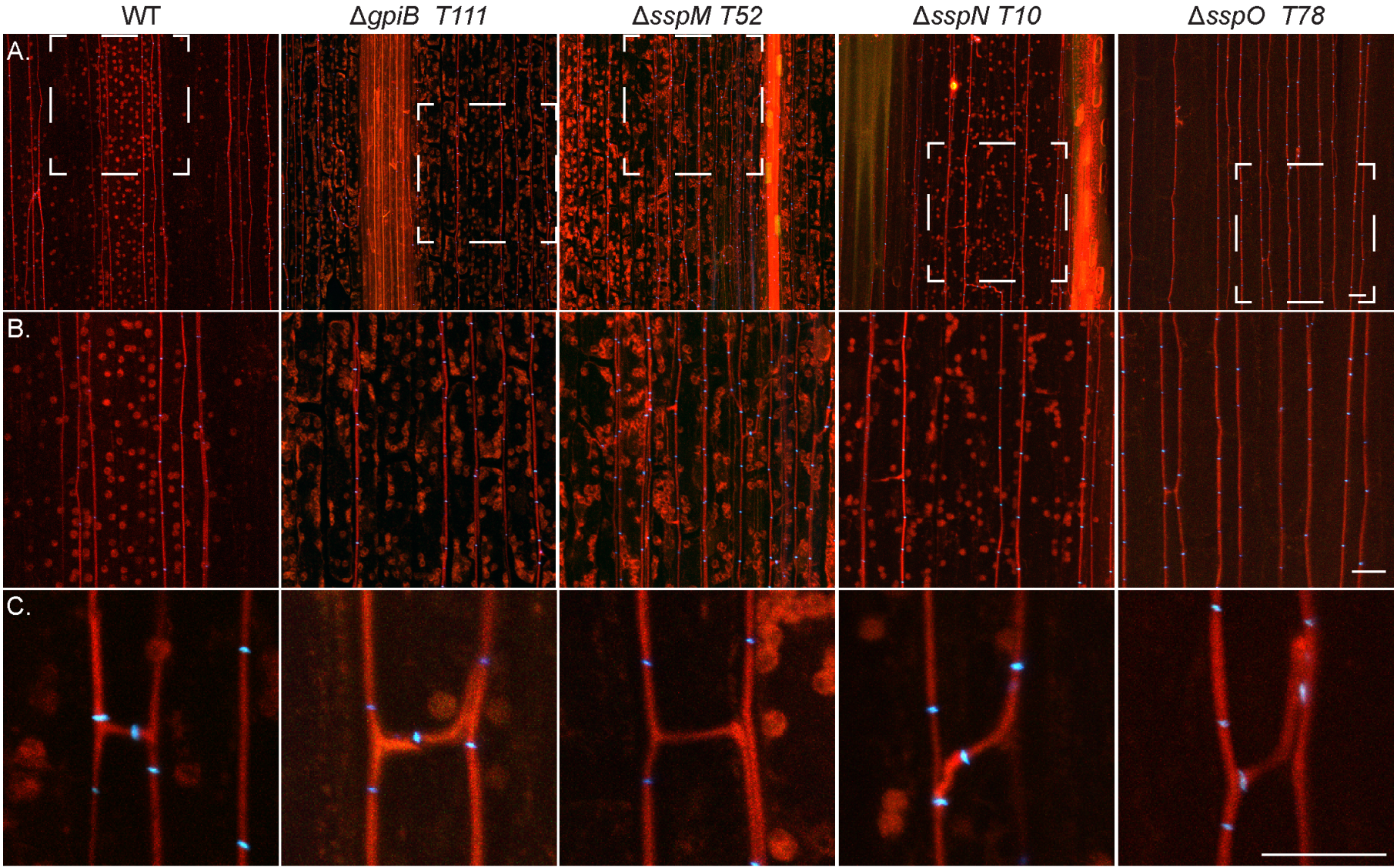
WT
ΔgpiB T111
ΔsspM T52
ΔsspN T10
ΔsspO T78
A.
B.
C.

Fig 9. Confocal depth series images of in planta cellular phenotype of *E. festucae* WT and *gpiB*, *sspM*, *sspN* and *sspO* deletion mutant strains.

Infected *L. perenne* pseudostem samples were stained with aniline blue/WGA-AF488. Hyphae show aniline blue fluorescence of β-glucans (red pseudocolor) and chitin staining of septa with WGA-AF488 (blue pseudocolor). (A) Representative growth of WT and deletion strains *in planta* (*z*= 15 μm); Bar= 20 μm. (B) Magnification of the area boxed with white dashed lines in A, showing representative growth of the strains in more detail (*z*= 15 μm); Bar= 20 μm. (C) Representative hyphal branching and fusion of WT and deletion strains *in planta* (*z*= 5 μm); Bar= 10 μm.

In summary, deletion of *gpiB*, *sspM* and *sspN* did not result in any obvious culture or plant interaction phenotype, suggesting that the proteins encoded by these genes are not essential for any of these growth processes. Similarly, *sspO* appears to be dispensable for most of these growth processes but may be important for vertical transmission within the host grass.

Culture and *in planta* phenotype of overexpression strains

As the deletion of the four genes did not result in any obvious plant interaction phenotype, overexpression (OE) constructs were generated using the translation elongation factor (*tef*) promoter from *Aureobasidium pullulans*, which is commonly used for OE studies [37, 67]. Plasmids encoding the *gpiB*, *sspM*, *sspN* and *sspO* OE constructs (pBH29–32) were prepared and transformed into WT protoplasts and the copy number of 10 independent transformants for each construct determined (S4 Fig). A total of three strains per construct, each with a different copy number, were chosen for further analysis. In addition, the relative expression level of the gene in each of the three independent strains was determined and found to generally correlate with the copy number (S4 Fig). No difference in culture growth or morphology was observed between the OE strains and WT. To test the plant symbiotic phenotype, the OE strains were inoculated into *L. perenne* seedlings and infected plants examined 8 weeks post-planting. No difference in whole plant (Fig 10) or cellular phenotype (Fig 11) was observed between the OE strains and WT. In summary, these results demonstrate that overexpression of *gpiB*, *sspM*, *sspN* or *sspO* has no impact on the culture or whole plant interaction phenotype.

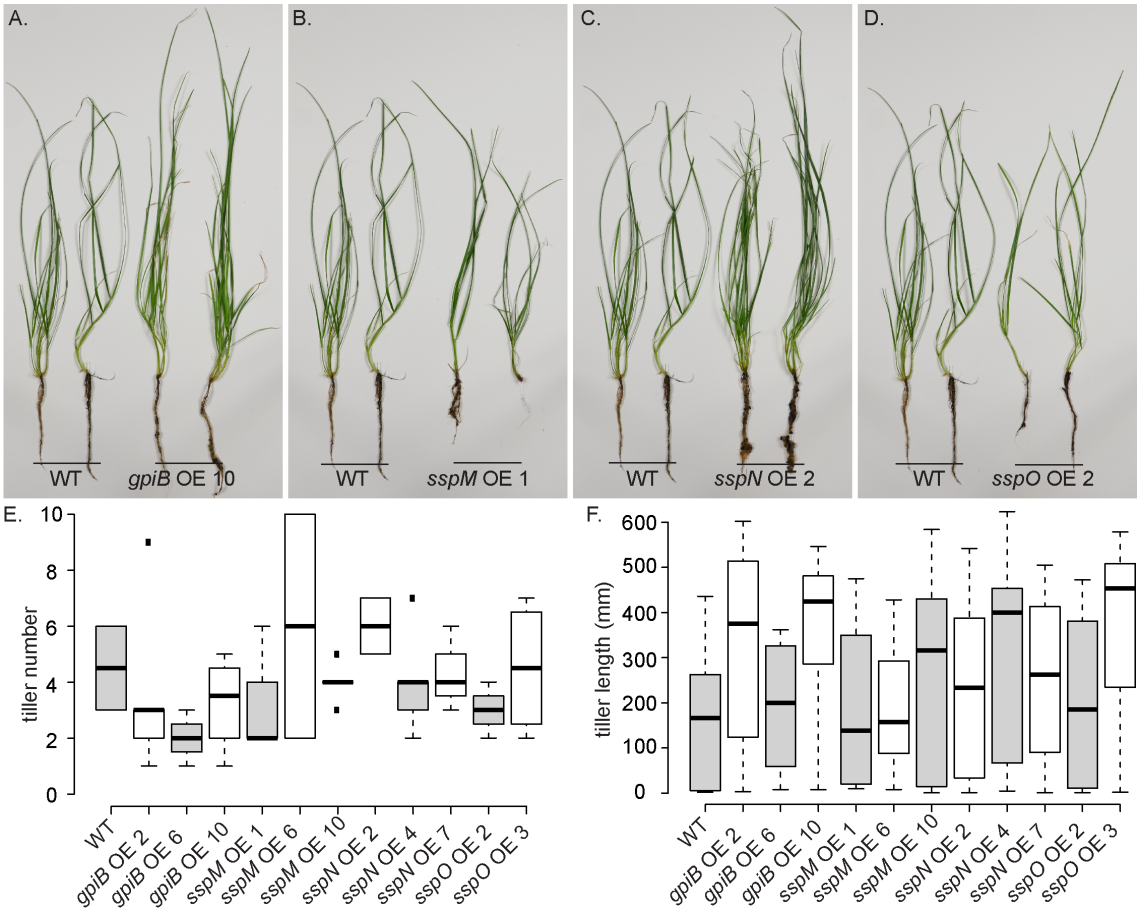

Fig 10. Plant phenotype of *Lolium perenne* infected with *E. festucae* WT and *gpiB*, *sspM*, *sspN* and *sspO* OE strains.

(A-D) Whole plant phenotype of WT and OE strain-infected *L. perenne* plants 8 weeks post-planting. (E and F) Boxplots representing tiller number (E) and length (F) of ryegrass plants eight weeks post-planting with *E. festucae* WT (n= 2) and *gpiB* (n= 2/6/4), *sspM* (n= 3/2/6), *sspN* (n= 2/7/3) and *sspO* (n= 4/4) OE strains. One-way ANOVAs were used to test for differences in both plant phenotypes between wildtype and modified strains. In each case the ANOVA was fitted with R and a Bonferroni correction was applied to all p-values to account for multiple testing.

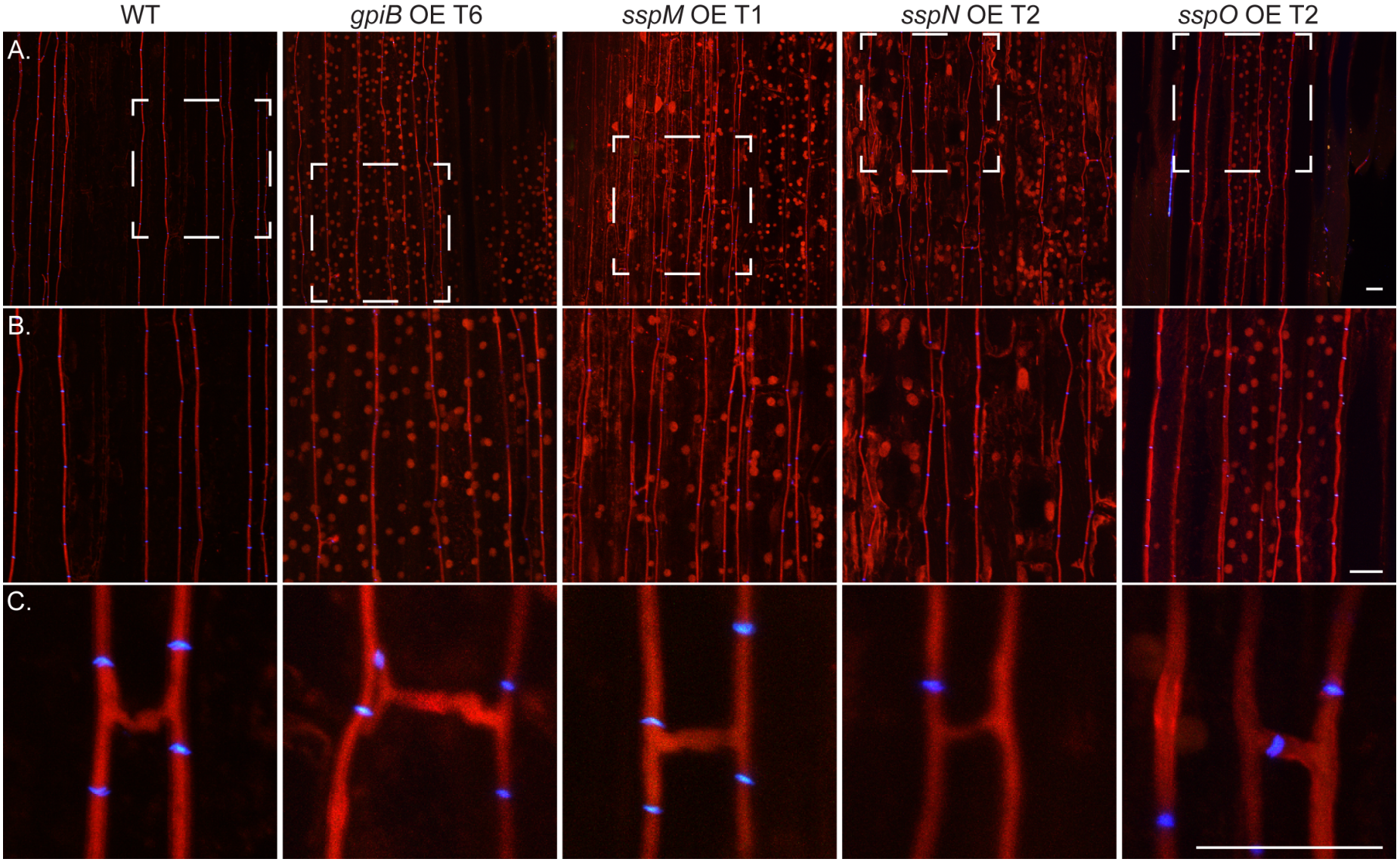
WT
gpiB OE T6
sspM OE T1
sspN OE T2
sspO OE T2
A.
B.
C.

Fig 11. Confocal depth image series of in planta cellular phenotype of *E. festucae* WT and *gpiB*, *sspM*, *sspN* and *sspO* OE strains.

Infected *L. perenne* pseudostem samples were stained with aniline blue/WGA-AF488. Hyphae show aniline blue fluorescence of β-glucans (red pseudocolor) and chitin staining of septa with WGA-AF488 (blue pseudocolor). (A) Representative growth of WT and OE strains *in planta* (*z*= 15 μm); Bar= 20 μm. (B) Magnification of the area boxed with white dashed lines in A, showing representative growth of the strains in more detail (*z*= 15 nm); Bar= 20 μm. (C) Hyphal branching and fusion of WT and OE strains *in planta* (*z*= 5 nm); Bar= 20 μm.

SspM, SspN and SspO localize extracellularly

To test whether SspM, SspN and SspO are translocated to the cytosol of the host, we generated C-terminal mCherry fusion constructs of each protein under the control of their native promoters. These constructs also contained three C-terminal tandem repeats of the simian virus large T-antigen nuclear localization signal to target the fusion proteins to the host nucleus, to enhance the signal in the cell if the proteins are translocated to the plant cytosol [60]. The constructs were transformed into protoplasts of their respective deletion strain, together with a vector encoding cytoplasmic eGFP to facilitate identification of hyphae among the plant cell background. Transformants were screened by PCR for presence of the construct and then inoculated into *L. perenne* seedlings.

Leaf tissue was harvested from mature infected plants and examined by CSLM for mCherry localization. Although the fluorescence from the mCherry fusion proteins was generally weak *in planta*, a signal of sufficient intensity was detected from SspM-mCherry-NLS and SspO-mCherry-NLS in the apoplast on either side of the hyphae. For SspN-mCherry-NLS, the signal was so weak that a localization profile for this protein in endophytic hyphae was not possible. No evidence was found for localization of any of the three constructs to the plant nucleus despite examining many individual sections and fields from different plants inoculated with other transformants. By contrast, the signal for mCherry in epiphyllous hyphae on the leaf surface was relatively strong and distinctly localized along the cell walls for all three constructs, demonstrating that the proteins were secreted *in planta,* but appear to remain attached to the hyphal cell surface (Fig 12). These observations indicate that SspM, SspN and SspO are secreted into the apoplast and may remain attached to the hyphal cell surface post-secretion.

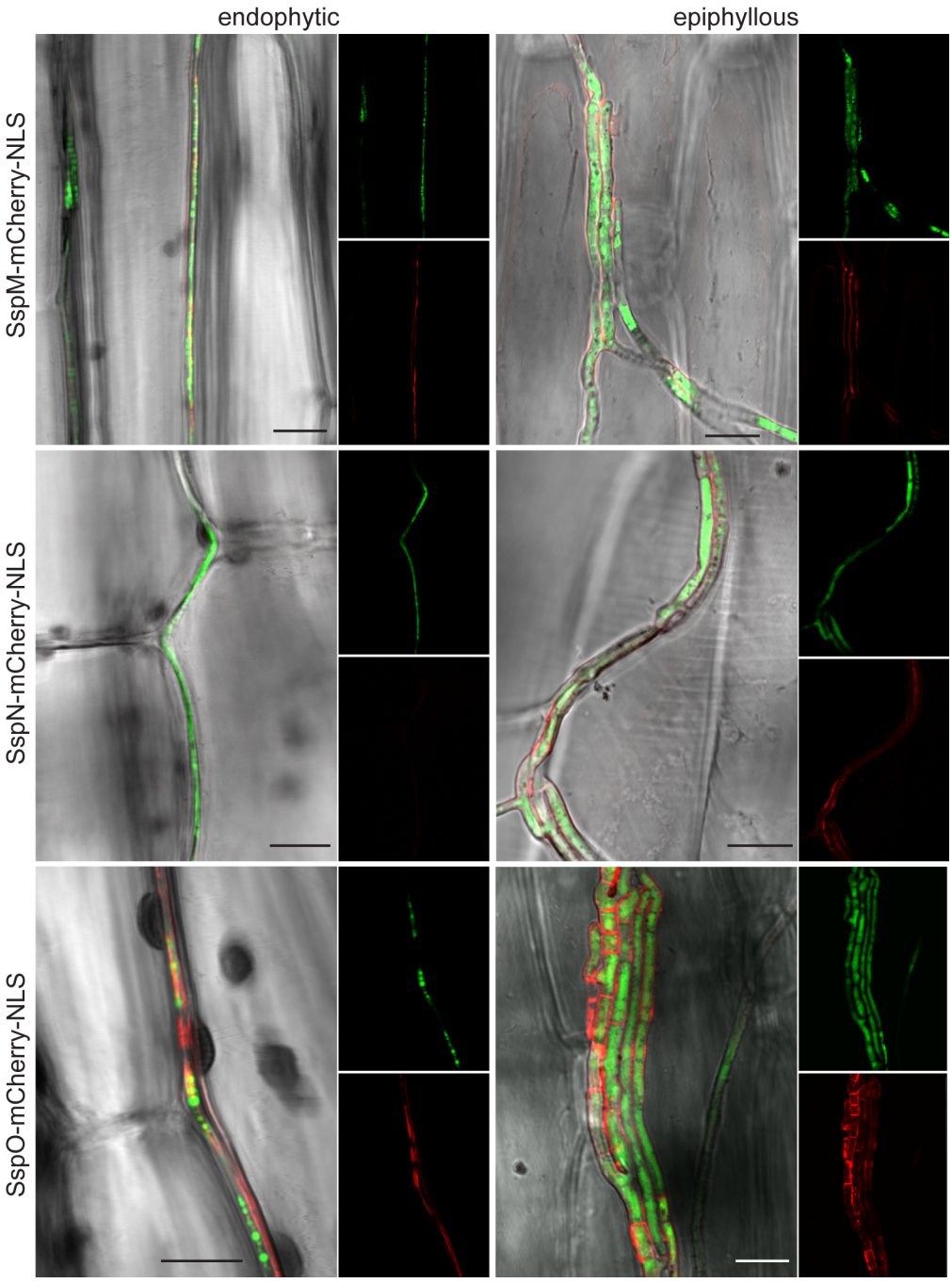

Fig 12. Confocal micrographs of the localization of SspM-mCherry-NLS, SspN-mCherry-NLS and SspO-mCherry-NLS in endophytic and epiphyllous hyphae of *E. festucae* in mature *L. perenne* plants.

Besides the mCherry constructs each transformant contained eGFP to facilitate identification of the hyphae *in planta*; Bar= 10 µm.

.

SspM, SspN, SspO and GpiB do not elicit a defense response in *N. benthamiana* or *N. tabacum* and do not suppress INF1-triggered immunity in *N. benthamiana*

Several fungal effector proteins have been shown to activate the plant immune system (i.e. to trigger a cell death immune response) in non-host plants upon their recognition as 'invasion patterns' by corresponding plant immune receptor proteins [95]. To test whether non-host plants are able to recognize GpiB or the Ssps, as invasion patterns, each was expressed in *N. benthamiana* and *N. tabacum* leaf tissue using an *A. tumefaciens* transient expression assay and screened for an associated cell death response. For this purpose, the cDNA sequence encoding each mature protein (i.e. lacking a native secretion signal) was fused to the nucleotide sequence encoding the *N. tabacum* PR1α secretion signal (for secretion to the plant apoplast) and 3xFLAG (for detection by western blot), and ligated into the pICH86988 expression vector by Golden Gate cloning. The resulting expression vectors were then transformed into *A. tumefaciens* strain GV3101. Strains confirmed to contain the correct construct were infiltrated into leaves of approx. five-week old *N. benthamiana* and *N. tabacum* plants, and the expression of GpiB and the three Ssps verified by western blotting using an antibody to the FLAG-Tag (S5 Fig). Plants were examined for any sign of a cell death response at one-week post-infiltration. As expected, the positive control, INF1 from *Phytophthora infestans* (a PAMP), triggered a strong cell death response in both *N. benthamiana* and *N. tabacum* (Figs 13A and B). As expected, the negative control, pICH86988 empty vector, failed to trigger cell death in these plants (Figs 13A and B). Unlike INF1, however, neither GpiB, nor the three Ssps, triggered cell death in *N. benthamiana* or *N. tabacum* (Figs 13A and B) suggesting that they are not recognized as invasion patterns by these non-host plants.

Many fungal effector proteins are anticipated to suppress activation of the plant immune response [1]. With this in mind, we next examined whether any of the four proteins are able to suppress the cell death response elicited by the INF1 PAMP in *N. benthamiana*, a model plant system for testing for this response. As before, responses were evaluated one-week post-infection. For this experiment, leaves were first infiltrated with the *A. tumefaciens* strain containing an expression vector for GpiB or one of the three Ssps. After 24 h, the same infiltration zone was infiltrated with the *A. tumefaciens* strain containing the INF1 expression vector. As the outcome of this experimental design is very sensitive to environmental influences, appropriate controls were included for each independent experiment. As expected, infiltration of an *A. tumefaciens* strain containing an expression vector for the *P. infestans* effector Avr3a

24 h after the corresponding potato resistance protein R3 resulted in a strong cell death response (Figs 13C and D). As expected, infiltration of an *A. tumefaciens* strain containing an expression vector for eGFP 24 h before INF1, gave a strong cell death response, demonstrating that eGFP is not able to suppress the cell death response caused by INF1 (Figs 13C and D). When Avr3 was infiltrated 24 h before INF1, the PAMP-triggered cell death response normally elicited by INF1 was strongly suppressed (Figs 13C and D), confirming a previous study showing that Avr3a is able to suppress INF1-triggered cell death in *N. benthamiana* [96]. Unlike the results shown for Avr3a, infiltration of the three Ssps or GpiB, did not result in suppression of INF1-triggered cell death (Figs 13C and D).

Taken together, these experiments show that neither the Ssps, nor GpiB, are recognized by the non-host plants *N. tabacum* and *N. benthamiana*, and that these proteins are unable to suppress the cell death response triggered by INF1.

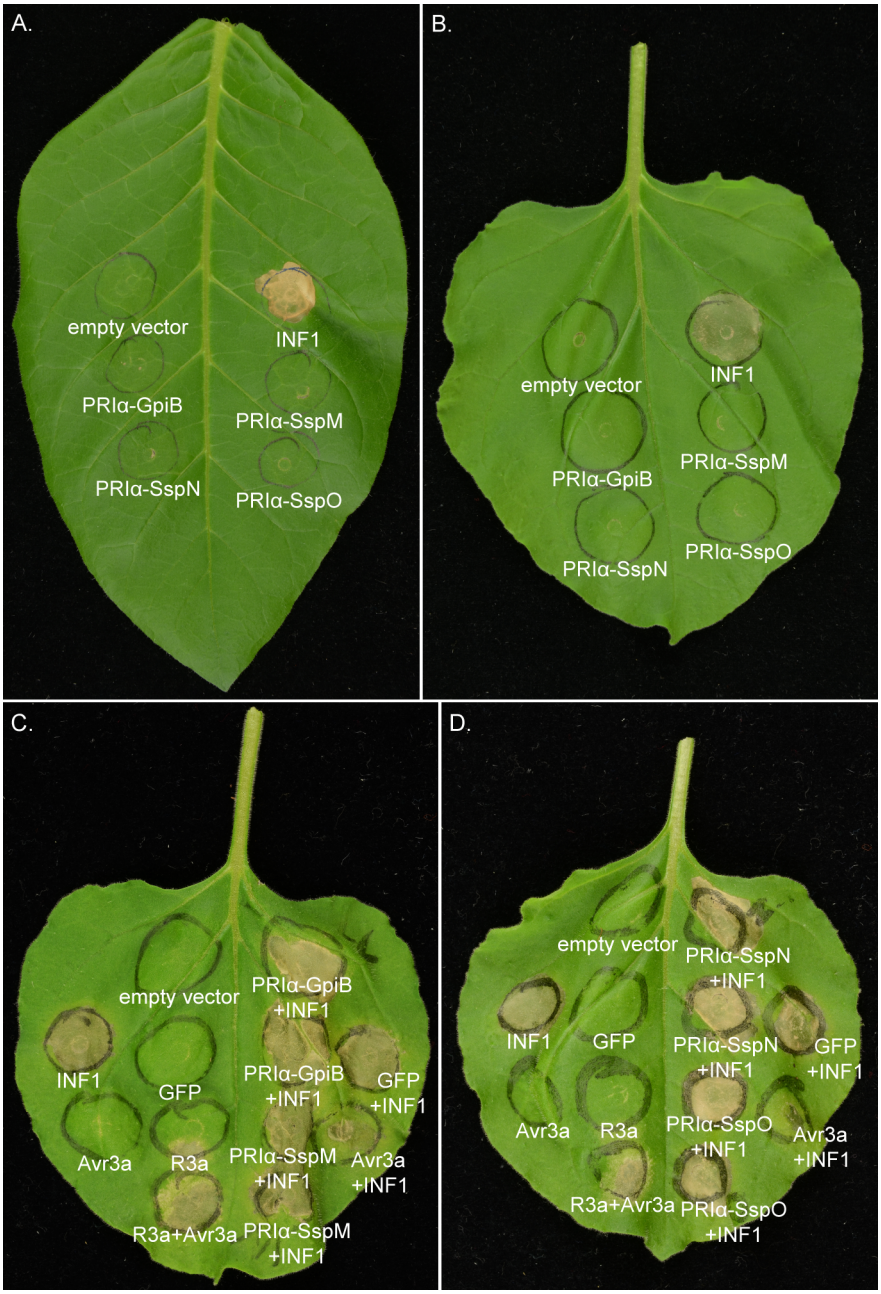

Fig 13. *A. tumefaciens* transient expression assays of GpiB, SspM, SspN and SspO in the non-host plants *N. benthamiana* and *N. tabacum*.

(A) *N. benthamiana* and (B) *N. tabacum* leaf phenotypes in response to *A. tumefaciens* transient expression assays involving GpiB, SspM, SspN, SspO or INF1. INF1 triggers a strong cell death response, whereas the pICH86988 empty vector had no effect. (C and D) INF1-triggered cell death suppression assays in *N. benthamiana* with GpiB and SspM (C) and SspN and SspO (D) plus controls. GpiB or any of the three Ssps were unable to suppress INF1-triggered cell death in *N. benthamiana*. eGFP was used as a negative control, INF1/Avr3a as a suppression control, and Avr3a/R3a as cell death positive control. All photos were taken one-week post-infiltration.

Discussion

Effectors of plant-pathogenic fungi function to promote host colonization, typically by suppressing the plant immune system. Current evidence, based on a small number of functionally characterized effectors from root endophytes [16-19], suggests that effectors from plant-mutualistic fungi play a similar role. In this study, we identified a suite of candidate effectors from the mutualistic symbiotic fungus *E. festucae*. We then performed an in-depth functional analysis in an attempt to uncover a role for three candidate effectors, representing some of the most highly expressed candidate effectors from this fungus *in planta*, in the mutualistic symbiotic interaction of *E. festucae* with *L. perenne*.

Making use of the completely annotated genome of *E. festucae* strain Fl1 and a combination of SignalP, EffectorP and protein size restriction we identified 141 genes encoding candidate effectors. Eighty-three of these genes are homologous to uncharacterized proteins from other Sordariomycete genera, while a further nine have homologs in other *Epichloë* species. The repertoire of effectors present in the genome thus includes conserved proteins that may support somewhat generalized host-adaptation and a number of apparently lineage-specific genes. Effectors are known to contribute to host specificity in other plant-associated fungal species [97-99], and we predict some of the apparently lineage-specific effectors identified here will contribute to specific host interactions in *Epichloë* strains.

Having a complete and finished *E. festucae* genome sequence enabled us to test for association between structural features of the genome and genes encoding effectors. Our results are remarkable for the lack of associations that are well-documented in other fungal species. The *E. festucae* genome has a “patchwork” structure, in which distinct blocks of highly AT-biased DNA comprised almost entirely of TEs are interleaved with gene-rich regions that have balanced GC-content. This genome structure is similar to that found in the pathogenic fungus *L. maculans,* where effector genes are greatly over-represented within AT-rich blocks (comprising 80% of all genes in these regions). Similarly, it has been reported that effector-encoding genes are located in TE-rich regions of the *M. oryzae* [100], *Blumeria graminis* [101] and *F. oxysporum* [102] genomes [103]. In contrast, we found no evidence for enrichment of genes encoding candidate effectors in proximity to AT- and transposable element-rich regions. Indeed, only 5.7% of the candidate effector genes can be found within 1 kb of an AT-rich block and none were found within an AT-rich block.

The lack of association between AT-rich blocks in the *E. festucae* genome and effectors is made more surprising by the evidence that these blocks contribute to plant-

specific gene expression of other genes [26]. We have recently shown that the patchwork structure of the *E. festucae* genome strongly influences the resultant 3D conformation of the chromosomes, where AT-rich blocks mainly interact with other AT-rich blocks to generate a highly condensed chromatin state compared to the GC and gene-rich blocks. Genes specific to *E. festucae* as well as genes highly expressed during the interaction with the plant host were found to be overrepresented in proximity to the AT-rich blocks [26]. The fact effectors are not associated with the blocks, the rapidly evolving sub-telomeric regions, and do not form distinct clusters as found in other species, reflect the difference in evolutionary pressures experienced by symbiotic, rather than pathogenic, fungal species. However, we did find an enrichment of genes encoding secreted proteins in general and SSPs in particular, in proximity to MITEs. MITEs are small, non-autonomous DNA transposable elements abundantly distributed in eukaryotic genomes. Transposable elements are increasingly seen as important for gene regulation, and MITEs have been linked to gene expression traits in a number of species [27, 104]. In *E. festucae*, MITEs have been found in the promoter region of key secondary metabolite gene clusters [24, 105] and are greatly over-represented in the regions upstream of genes preferentially expressed *in planta* [26]. These results, and the demonstration here that genes encoding Ssps are frequently in close proximity to MITEs, suggests that elements either directly or indirectly associated with MITEs may play a key role in regulating the expression of *ssps*.

In the root endophyte *F. oxysporum,* most effector genes are encoded on a dispensable TE-rich pathogenicity chromosome [97, 106]. Recently a MITE from the mimp family was identified in the promoter region of each of the *SIX* effector genes and based on the presence of this mimp in the promoter region of other genes, further secreted proteins could be predicted and subsequently identified in the xylem sap of infected tomato plants [25]. Interestingly, deletion of the mimp element from the promoter region of two of the *SIX* genes did not significantly change the expression of these genes *in planta* or culture, thereby ruling out a direct role of this element in transcriptional regulation [25]. However, a putative transcriptional regulator (repressor) binding element in close proximity to the mimp is important for SIX gene expression. Whether the MITEs identified in *E. festucae* contribute to transcriptional silencing or activation remains to be elucidated.

Expression of effector genes is often induced upon plant infection or at a certain stage of host infection [87, 88]. Consistent with this observation we found a preferential expression of candidate effector-encoding genes *in planta.* Previous work has shown that a major remodeling of the *E. festucae* chromatin state occurs upon the switch from growth in axenic culture to growth *in planta*. In culture the genome is highly

heterochromatic, characterized by high levels of H3K9me3 and H3K27me3, whereas *in planta* the genome contains higher levels of transcriptionally active euchromatin characterized by much lower levels of these two repressive epigenetic marks [68]. While RNAseq data for mutants of the responsible methyltransferases was not available, a set of data was available for a mutant of the gene encoding heterochromatin protein 1 (*hepA*). When a comparison was made between the transcriptome of Δ*hepA* vs WT in axenic culture there was a minor but significant increase in expression of the candidate effector genes. Similar results have been obtained in *L. maculans* where silencing of genes encoding the heterochromatin regulators DIM-5, a H3K9 methyl transferase, and heterochromatin protein 1 (HP1) resulted in the expression of many effector genes in axenic culture, which were repressed in WT [89]. As discussed above, effector genes in *L. maculans* are mainly located within the AT isochore component of the genome, which is in a highly heterochromatic state in axenic culture [89]. In contrast genes encoding *E. festucae* effectors are not associated with the AT-rich blocks of the genome and thus were expected to be less affected by heterochromatin silencing.

Previous studies have shown that the deletion of genes coding for NoxA, a NADPH oxidase [34], ProA, a transcription factor [39], and SakA, a stress-responsive MAP kinase [36], in *E. festucae* result in a severe breakdown in the symbiotic interaction with the host leading to severely stunted plants. Analysis of the fungal transcriptome of these three different interactions identified a core set of 182 *E. festucae* genes that were differentially expressed (DE) in the same direction in all three symbiosis mutants [47]. Among this core gene set were 14 genes encoding secreted proteins, corresponding to 10 that were upregulated and four (*gpiB, sspM*, *sspN* and *sspO*), that were downregulated. The three candidate effector genes analysed here were among the top 100 DE genes *in planta* compared to axenic culture.

In order to verify that the predicted secretion signals of the three effector candidates and the GPI-anchored protein were functional, a yeast complementation assay was carried out [52]. *S. cerevisiae* transformants containing each of the four predicted secretion signals fused to SUC2 all grew on raffinose confirming these signals are functional. In addition, western blots were performed with His-tagged versions of each of the four genes under the control of a *tef* promoter to confirm they were secreted and to check for proteolytic processing and any potential post-translational modifications. Both GpiB and SspM were predicted to be *N*-glycosylated and SspM and SspN contain a kexin cleavage site. Proteins of the expected size for GpiB, SspN and SspO were detected in extracts of fungal mycelia. For SspM, two signals were detected which potentially correspond to the pro-protein and a post-

translationally modified protein. Some effectors, such as *C. fulvum* Avr4 and Avr9 are further processed in the apoplast by either fungal or plant proteases [20]. To determine whether there is protease modification of the SspM *in planta* and whether this processing is necessary for the activation of SspM will require further experimentation using protein extracts obtained from ryegrass apoplastic fluid. Despite the presence of an LxKR kexin recognition motif in SspN, only a single band was detected corresponding to the size of the unprocessed protein. Sequence alignment with closely related species shows that this motif can only be found in strain Fl1, suggesting this might be the result of a recent mutation. One possible reason for lack of cleavage at this site could be lack of accessibility of this motif within the folded protein. Alternatively, it is possible it is only cleaved *in planta* and not in axenic culture. While the function of SspN is not known it does have a repeat domain structure which is a common feature of several effectors characterized to date including Ecp6 from *C. fulvum* [107], which contains multiple LysM domain containing repeats, Sp7 from the mutualist *Glomus intraradices* [18], *Colletotrichium graminicola* EP1[108] and the recently identified effector Rsp3 from *U. maydis* [6]. However, unlike all these proteins, which have been shown by genetic analysis to be very important for the interaction with the host, deletion of *sspN* had no obvious plant interaction phenotype. Some of these repeat-containing effectors function in the apoplast (Ecp6 and Rsp3), whereas others are transported into the host cytoplasm (Sp7 and EP1). Due to the adoption of an extended module-like structure, some repeat-containing proteins such as EP1 are found to be associated with nucleic acids following transport into the host nucleus whereas others mediate protein-protein interactions [108-110]. In addition, some repeat-containing proteins are located on the surface of the cell where they are integrated into the plasma membrane or attached to the cell wall [109]. Rps3 is located on the *U. maydis* cell wall where it interacts with the mannose-binding and anti-fungal activity of the maize protein AFP1 [6]. Some repeat-containing proteins contain kexin cleavage sites between the repeating units resulting in generation of bioactive peptides. A classic example of this in *Epichloë* is GigA, which is processed to generate a series of cyclic peptides called epichloëcyclins of unknown biological function [111]. In *U. maydis*, Rep1, is processed into smaller peptides that form cell wall associated fibrils mediating attachment of the hyphae to hydrophobic surfaces [112, 113].

Although products of all four genes could be detected in the fungal mycelium, only SspM and SspO, which contain six and eight cysteines respectively, were detected in the culture medium. The lack of detection of GpiB in the culture medium was not surprising as the addition of a GPI-anchor generally results in cell wall attachment. GPI-anchored proteins are involved in multiple processes, including

attachment of hyphae to various surfaces, cell wall integrity and virulence [42, 43]. The two protein products observed for SspM in the media were the same size as those observed in the mycelia. The presence of two bands could either indicate that both the modified as well as the unmodified protein fulfill a function in *E. festucae* or that the overexpression of the gene because of multiple integrations resulted in an overproduction compared to the available protease. As the protein however can be detected in the modified version in culture and only one band can be detected in the western blot on SspM expressing *N. benthamiana* protein extracts, a modification by plant proteases to induce activity can probably be excluded. The inability to detect SspN in the culture media could be either due to the instability of the protein resulting from the lack of cysteines that promote stability or due to an attachment of this protein to the cell wall as has been described for multiple repeat-containing proteins as discussed above. A single protein product of the same size as observed in mycelia was detected in the media of cultures containing the SspO construct indicating this protein is not post-translationally modified. The presence of eight cysteines, which have the potential to form four cysteine bridges, is likely to account for the high stability of this protein. Given the observed size for SspM was similar to the expected size, this protein is probably not *N*-glycosylated. However, the product of the His-tagged GpiB was greater than the predicted size, which may be due to addition of the GPI anchor and/or modification by *N*-glycosylation. For a definitive answer, purified proteins could be analyzed by mass spectrometry or subjected to an enzymatic removal of glycosylation followed by a size comparison using SDS-PAGE.

Some pathogens such as *U. maydis* produce apoplastic as well as cytoplasmic effectors [1], whereas other pathogens such as *C. fulvum* seem to only produce apoplastic effectors [72]. In order to determine where the effector candidates of *E. festucae* are targeted during host colonization, translational fusions were generated between each of the candidate genes and mCherry. Given it is difficult to detect effectors in the host cytoplasm, we used the method of adding a nuclear localization signal to target the proteins to the plant nucleus, as this was shown to be very effective for detecting some *M. oryzae* effectors in cells of the host *O. sativa* [60]. Despite examining multiple samples of different aged plants, no signal from any of the candidates was observed in the nuclei of ryegrass leaf cells. Therefore, the effector candidates are likely to reside in the apoplast. Indeed, we were able to show that all three of the effector candidates localized to the cell walls or plasma membrane of the fungal hyphae *in planta*. The clearest signals were obtained by imaging epiphyllous hyphae on the surface of the leaves. While it was more challenging to detect the localization of these proteins inside the leaf, signals of sufficient intensity were detected

for both SspM and SspO on the cell walls of endophytic hyphae. However, no signal could be detected for SspN in endophytic hyphae which could be due to the fact that the promoter of *sspN* is weaker than that of *sspM* and *sspO*. Alternatively, SspN may be more unstable in the apoplast than SspM and SspO as was suggested by the western analysis. Alternatively, *sspN* may be just expressed on the leaf surface. This hypothesis could be tested by fusing the promoter of *sspN* to eGFP and analyzing where fluorescence occurs.

To elucidate the role of these proteins in the interaction we generated deletion and overexpression strains and analysed their phenotype in axenic culture as well as in the interaction with perennial ryegrass. In culture, *E. festucae* forms white, soft looking colonies with a diameter of approx. 2 cm after 7 days of growth. Both deletion and overexpression strains were indistinguishable from the WT. Within the plant host, *E. festucae* grows exclusively in the apoplastic space, where the growth is highly regulated and synchronized with the host [114]. In the host meristematic tissue, *E. festucae* grows by tip growth, but as hyphal cells grow into the cell expansion zone of the leaf, the hyphae switch to intercalary growth, a pattern of growth that prevents mechanical shear and enables the hyphae to maintain the same rate of growth as the host [114, 115]. Ryegrass plants infected with either the deletion or overexpression strains had the same whole plant interaction and cellular growth phenotype as WT with one exception. Mutants Δ*gpiB*, Δ*sspM* and Δ*sspN* were seed transmitted but not Δ*sspO*. Additional long-term experiments will be necessary to determine the mechanism for this interesting Δ*sspO* phenotype. Also it would be interesting to check whether these mutants affect the transition from asexual to sexual development but this is difficult to investigate as initiation of the sexual cycle requires vernalisation of host material, formation of stromata and transfer of spermatia to a stroma of the opposite mating type by a *Botanophila* fly [116]. Furthermore, it is possible that each of these effector candidates contributes to the interaction in a minor incremental way making it difficult to detect a phenotype by deletion of single effector gene unless there is a very sensitive phenotype screen [117, 118].

Functional redundancy of effector proteins could also explain the lack of an altered host interaction phenotype. Redundancy is thought to be the result of multiple effectors having the same or overlapping functions. Notably, a study by Wessling and colleagues [119] found effectors from a single pathogen species converging on interactions with a small subset of host proteins in a process named “interspecies convergence” of which many are involved in high level regulatory processes. Interestingly, even effectors from different species of pathogens can target a similar subset of host proteins with a correlation between the degree of convergence and the

relevance of the host protein. Therefore homology-independent functional redundancy is maintained as an evolutionary benefit and protects against rapid loss of a single effector due to host recognition [119, 120]. For example, both Avr4 and Ecp6 prevent chitin recognition in the *C. fulvum*-tomato interaction, however, the molecular functions are different and there is no sequence homology between these two effectors [2, 4].

In the presence of a corresponding host immune receptor protein, fungal effectors are known to activate the plant immune system. Often, the main output of this activation is the hypersensitive response (HR), which renders the host resistant and the pathogen avirulent [121]. Notably, a subset of fungal effectors can also trigger an HR-like cell death response when expressed in the non-host plants *N. benthamiana* or *N. tabacum* (i.e. following their recognition by unknown immune receptor proteins) using an *A. tumefaciens* transient expression assay. Indeed, multiple effectors of the wheat pathogen *Z. tritici* have been found to induce an HR in *N. benthamiana* [95]. Using this approach, we tested whether the three candidate effectors of *E. festucae* trigger cell death when produced by these two non-host plants but none triggered a cell death response. We also tested whether the effector candidates are able to suppress a defense response triggered by the *P. infestans* elicitor INF1 using an *A. tumefaciens* transient expression assay. INF1 functions in the apoplastic space where it binds to the ELR (elicitin response) receptor, resulting in activation of the plant immune system [122, 123]. Even though these candidate effectors localize to the apoplast, none were able to suppress INF1-triggered immunity.

In *E. festucae*-infected *L. perenne* plants, approx. one third of *L. perenn*e genes were found to be differentially expressed compared to non-infected plants. These changes were found to be in the key areas of ‘stress response’, ‘primary metabolism’ and ‘secondary metabolism’ [124]. Genes in the category ‘primary metabolism’ and ‘stress response’, including PR genes, were found to be mainly downregulated, and genes involved in secondary metabolism were found to be upregulated [124]. These findings, together with the fact that these candidate effectors are so highly expressed in *E. festucae in planta*, suggests that these proteins are likely to have a key role in the interaction. Furthermore, microscopic studies in infected *L. perenne* plants revealed a lack of chitin, a crucial PAMP, in endophytic hyphae [124, 125]. This indicates that chitin is either masked, potentially by a similar mechanism as has been described for Avr4 of *C. fulvum,* or modified.

In this study, we have identified for the first time, a suite of effector candidates from the grass endophyte *E. festucae*. Genes encoding effector candidates were found to associate with MITEs but not with AT-rich regions or TEs, indicating that they might not be under strong selection pressure. Three effector candidates were functionally

analysed but were found to be dispensable for the interaction with *L. perenne* under the growth conditions analysed. Although we could not find any evidence for a role for any of these effectors in the interaction, the list of effector candidates identified provides a good database for selecting other proteins and strategies for functional analysis. Sequencing of additional *Epichloë* species will help identify effector genes conserved across species or unique to one species and thereby provide important insights into the role of these effectors in host specificity in this agriculturally important symbiosis.

Supporting information

S1 File. Methods for computational analysis.

https://doi.org/10.1371/journal.pone.0209463.s001

(PDF)

S1 Fig. Amino acid sequence alignments of *E. festucae* GpiB, SspM, SspN and SspO.

Alignments of GpiB (A), SspM (B), SspN (C) and SspO (D) with homologs from a selection of *Epichloë* species. Red shading: Protease cleavage site; Green shading: omega site; Purple shading: *N*-glycosylation site; Orange shading: cysteine residues. Protein sequences for *E. baconii, E. elymi* and *E. typhina* were obtained from the Kentucky Endophyte database when available or predicted using FGENESH using *Claviceps purpurea* parameters. The deduced amino acid sequence was used for the alignment. Sequences marked with * were manually annotated.

https://doi.org/10.1371/journal.pone.0209463.s002

(TIF)

S2 Fig. Strategy for deletion of the *E. festucae* gpiB, sspM, sspN and sspO genes and confirmation by Southern analysis.

(A) Physical map of the *gpiB* WT genomic locus, linear insert of the *gpiB* replacement construct, pBH1, and the recombinant locus showing restriction enzyme sites for *Nde*I. Grey shading indicates regions of recombination. Numbers indicate the PCR primer pairs used for Gibson assembly (BH1/BH5) and deletion mutant screening (BH43/BH44). (B) PCR screening of deletion candidates with the PCR primer pair BH43/BH44, generated expected bands of 3,997 bp in WT, and 4,602 bp in deletion mutants (C) NBT/BCIP-stained Southern blot of digests (approx. 1 µg) from *E. festucae* WT, Δ*gpiB* T27, Δ*gpiB* T111 (PN3113), Δ*gpiB* T133 (PN3114), Δ*gpiB* T148 (PN3115), Δ*gpiB* T160 and Δ*gpiB* T204 strains probed with digoxigenin (DIG)-11-dUTP-labeled linear insert of pBH1 amplified with the primer pair BH1/BH5. Expected bands of 5,317 bp in WT, and 3,971 bp and 1,951 bp in the deletion mutant.

(D) Physical map of the *sspM* WT genomic locus, linear insert of the *sspM* replacement construct, pBH2, and the recombinant locus showing restriction enzyme sites for *Eco*RI. Grey shading indicates regions of recombination. Numbers indicate the PCR primer pairs used for Gibson assembly (BH9/BH12) and deletion mutant screening (BH45/BH46). (E) PCR screening of deletion candidates with the PCR primer pair

BH45/BH46, generated expected bands of 3,615 bp in WT, and 4,190 bp in deletion mutants. (F) NBT/BCIP-stained Southern blot of digests (approx. 1 μg) of *E. festucae* WT, Δ*sspM* T180, Δ*sspM* T173, Δ*sspM* T163 (PN3118), Δ*sspM* T135, Δ*sspM* T99 (PN3117) and Δ*sspM* T52 (PN3116) strains probed with digoxigenin (DIG)-11-dUTP-labeled linear insert of pBH2 amplified with the primer pair BH9/BH12. Expected bands of 2,205 bp and 1,569 bp in WT and 4,349 bp in the deletion mutant.

(G) Physical map of the *sspN* WT genomic locus, linear insert of the *sspN* replacement construct, pBH3, and the recombinant locus showing restriction enzyme sites for *Bam*HI. Grey shading indicates regions of recombination. Numbers indicate the PCR primer pairs used for Gibson assembly (BH13/BH16) and deletion mutant screening (BH47/BH48). (H and J) PCR screening of deletion candidates with the PCR primer pair BH47/BH48, generated expected band of 3,403 bp in WT, and 4,250 bp in deletion mutants. (I) NBT/BCIP-stained Southern blot of digests (approx. 1 μg) of *E. festucae* WT, Δ*sspN* T151 and Δ*sspN* T10 (PN3119), strains probed with digoxigenin (DIG)-11-dUTP-labeled linear insert of pBH1 amplified with the primer pair BH13/BH16. (K) NBT/BCIP-stained Southern blot of digests (approx. 1 μg) of *E. festucae* WT, Δ*sspN* T52 (PN3121), Δ*sspN* T15, Δ*sspN* T103, Δ*sspN* T51, Δ*sspN* T30 (PN3120) and Δ*sspN* T3 strains probed with digoxigenin (DIG)-11-dUTP-labeled linear insert of pBH3 amplified with the primer pair BH13/BH16. Expected bands of 1,710 bp and 3,631 bp in WT, and 1,710 bp and 4,477, in the deletion mutant.

(L) Physical map of the *sspO* WT genomic locus, linear insert of the *sspO* replacement construct, pBH4, and the recombinant locus showing restriction enzyme sites for *Pst*I. Grey shading indicates regions of recombination. Numbers indicate the PCR primer pairs used for Gibson assembly (BH5/BH9) and deletion mutant screening (BH49/BH50). (M) PCR screening of deletion candidates with the PCR primer pair BH49/BH50, generated expected band of 3,654 bp in WT, and 4,482 bp in deletion mutants. (N) NBT/BCIP-stained Southern blot of digests (approx. 1 μg) of *E. festucae* WT, Δ*sspO* T210 (PN3124), Δ*sspO* T195 (PN3123), ΔsspO T130, Δ*sspO* T102, Δ*sspO* T78 (PN3122) and Δ*sspO* T60 strains probed with digoxigenin (DIG)-11-dUTP-labeled linear insert of pBH4 amplified with the primer pair BH5/BH9. Expected bands of 1,859 bp and 1,678 bp in WT and 4,635 bp in the deletion mutant.

https://doi.org/10.1371/journal.pone.0209463.s003

(TIF)

S3 Fig. Confocal laser scanning microscopy of aniline blue and WGA-AF488 stained ovaries.

The fungal endophytic cell wall was stained with aniline blue (orange pseudo colour) while fungal septa were stained with WGA-AF 488 (blue pseudo colour). A. Ovary of mutant strain Δ*sspM* T52, B. Ovary of mutant strain Δ*sspM* T163. *E. festucae* hyphae are marked by asterisk. Scale bar: 50 µm.

https://doi.org/10.1371/journal.pone.0209463.s004

(TIF)

S4 Fig. qPCR and RT-qPCR results of the *gpiB*, *sspM*, *sspN* and *sspO* OE strains.

(A) Copy number determined by qPCR is expressed relative to the WT copy number. Genes encoding *hepA* (single copy, light grey) and *pacC* (single copy, dark grey) were used as reference genes. (B) Expression level determined by RT-qPCR is expressed relative to the WT gene expression. The 40S ribosomal S22 gene was used as reference gene. Primers used for the analyses are given in S2 Table.

https://doi.org/10.1371/journal.pone.0209463.s005

(TIF)

S5 Fig. Verification of the heterologous production of GpiB, SspM, SspN and SspO in *N. benthamiana* via western blotting.

Total protein of the infiltrated leaf region was extracted and separated by electrophoresis on a 10% SDS gel. The gel was transferred to a membrane and probed with an anti-FLAG antibody. eGFP expressed in *N. benthamiana* served as positive control. Expected sizes: approx. 12.8 kDa for GpiB, 17 kDa for SspN, 13 kDa for SspO and for SspM 17.8 and 21.8 kDa.

https://doi.org/10.1371/journal.pone.0209463.s006

(TIF)

S1 Table. Biosample references

https://doi.org/10.1371/journal.pone.0209463.s007

(XLSX)

S2 Table. Biological material.

https://doi.org/10.1371/journal.pone.0209463.s008

(DOCX)

S3 Table. Primers used in this study.

https://doi.org/10.1371/journal.pone.0209463.s009

(DOCX)

S4 Table. Summary of the presented information about *E. festucae* effector candidates.

https://doi.org/10.1371/journal.pone.0209463.s010

(XLSX)

S5 Table. Gene expression analysis of wild-type *in planta* versus wild-type in culture.

RPKM and fold differences for all gene models (sheet 1), the list of gene models that encode effector candidates (sheet 2), list of gene models that encode putative secreted proteins that are not classified as effector candidate (sheet 3) and a summary of the number of genes that are differentially expressed in the three classes using as criteria a q-value < 0.01 and an absolute L2FD > 2 (sheet 4).

https://doi.org/10.1371/journal.pone.0209463.s011

(XLSX)

S6 Table. Distribution of *gpiB* and the *ssps* within *Epichloë* and related species.

https://doi.org/10.1371/journal.pone.0209463.s012

(XLSX)

S7 Table. Vertical transmission of ssp mutants in *L. perenne*.

https://doi.org/10.1371/journal.pone.0209463.s013

(XLSX)

Acknowledgements

We thank Jordan Taylor, Niki Murray and Matthew Savoian (Manawatu Microscopy and Imaging Centre, Massey University) for assistance with microscopy, Arvina Ram and Karolin Warnecke for technical assistance, Christopher Schardl for provision of the *Epichloë* database sequences, Melissa Guo for provision of strains and advice on *Agrobacterium* infiltration assays, and Sophien Kamoun and Barbara Valent for provision of plasmids.

References

1. **Lo Presti L, Lanver D, Schweizer G, Tanaka S, Liang L, Tollot M, *et al*.** Fungal effectors and plant susceptibility. Annu Rev Plant Biol. 2015;66:513-45. doi: 10.1146/annurev-arplant-043014-114623. PubMed PMID: 25923844.
2. **van den Burg HA, Harrison SJ, Joosten MH, Vervoort J, de Wit PJ.** *Cladosporium fulvum* Avr4 protects fungal cell walls against hydrolysis by plant chitinases accumulating during infection. Mol Plant-Microbe Interact. 2006;19(12):1420-30. PubMed PMID: 17153926.
3. **van Esse HP, Van't Klooster JW, Bolton MD, Yadeta KA, van Baarlen P, Boeren S, *et al*.** The *Cladosporium fulvum* virulence protein Avr2 inhibits host proteases required for basal defense. Plant Cell. 2008;20(7):1948-63. Epub 2008/07/29. doi: 10.1105/tpc.108.059394. PubMed PMID: 18660430; PubMed Central PMCID: PMCPMC2518240.
4. **de Jonge R, van Esse HP, Kombrink A, Shinya T, Desaki Y, Bours R, *et al*.** Conserved fungal LysM effector Ecp6 prevents chitin-triggered immunity in plants. Science. 2010;329(5994):953-35. Epub 2010/08/21. doi: 329/5994/953 [pii]
10.1126/science.1190859. PubMed PMID: 20724636.
5. **Doehlemann G, Reissmann S, Assmann D, Fleckenstein M, Kahmann R.** Two linked genes encoding a secreted effector and a membrane protein are essential for *Ustilago maydis*-induced tumour formation. Mol Microbiol. 2011;81(3):751-66. doi: 10.1111/j.1365-2958.2011.07728.x. PubMed PMID: 21692877.
6. **Ma LS, Wang L, Trippel C, Mendoza-Mendoza A, Ullmann S, Moretti M, *et al*.** The *Ustilago maydis* repetitive effector Rsp3 blocks the antifungal activity of mannose-binding maize proteins. Nature communications. 2018;9(1):1711. doi: 10.1038/s41467-018-04149-0. PubMed PMID: 29703884; PubMed Central PMCID: PMC5923269.
7. **Hurlburt NK, Chen L-H, Stergiopoulos I, Fisher AJ.** Structure of the *Cladosporium fulvum* Avr4 effector in complex with (GlcNAc)6 reveals the ligand-binding mechanism and uncouples its intrinsic function from recognition by the Cf-4 resistance protein. PLoS Pathog. 2018;14(8):e1007263. Epub 2018/08/28. doi: 10.1371/journal.ppat.1007263. PubMed PMID: 30148881; PubMed Central PMCID: PMCPMC6128652.
8. **Sánchez-Vallet A, Saleem-Batcha R, Kombrink A, Hansen G, Valkenburg D-J, Thomma BPHJ, *et al*.** Fungal effector Ecp6 outcompetes host immune receptor for chitin binding through intrachain LysM dimerization. Elife. 2013;2:e00790. Epub 2013/07/11. doi: 10.7554/eLife.00790. PubMed PMID: 23840930; PubMed Central PMCID: PMCPMC3700227.
9. **Mueller AN, Ziemann S, Treitschke S, Assmann D, Doehlemann G.** Compatibility in the *Ustilago maydis*-maize interaction requires inhibition of host cysteine proteases by the fungal effector Pit2. PLoS Pathog. 2013;9(2):e1003177. doi: 10.1371/journal.ppat.1003177. PubMed PMID: 23459172; PubMed Central PMCID: PMC3573112.
10. **Rooney HCE, Van't Klooster JW, van der Hoorn RAL, Joosten MHAJ, Jones JDG, de Wit PJGM.** *Cladosporium* Avr2 inhibits tomato Rcr3 protease required for Cf-2-dependent disease resistance. Science. 2005;308(5729):1783-6. Epub 2005/04/23. doi: 10.1126/science.1111404. PubMed PMID: 15845874.
11. **Shabab M, Shindo T, Gu C, Kaschani F, Pansuriya T, Chintha R, *et al*.** Fungal effector protein AVR2 targets diversifying defense-related cys proteases of tomato. Plant Cell. 2008;20(4):1169-83. Epub 2008/05/03. doi: 10.1105/tpc.107.056325. PubMed PMID: 18451324; PubMed Central PMCID: PMCPMC2390736.

12. **Djamei A, Schipper K, Rabe F, Ghosh A, Vincon V, Kahnt J, *et al*.** Metabolic priming by a secreted fungal effector. Nature. 2011;478(7369):395-8. Epub 2011/10/07. doi: nature10454 [pii]10.1038/nature10454. PubMed PMID: 21976020.
13. **O'Connell RJ, Panstruga R.** Tête à tête inside a plant cell: establishing compatibility between plants and biotrophic fungi and oomycetes. New Phytol. 2006;171(4):699-718. Epub 2006/08/22. doi: 10.1111/j.1469-8137.2006.01829.x. PubMed PMID: 16918543.
14. **Zamioudis C, Pieterse CMJ.** Modulation of host immunity by beneficial microbes. Mol Plant-Microbe Interact. 2012;25(2):139-50. Epub 2011/10/15. doi: 10.1094/MPMI-06-11-0179. PubMed PMID: 21995763.
15. **Pauwels L, Goossens A.** The JAZ proteins: a crucial interface in the jasmonate signaling cascade. Plant Cell. 2011;23(9):3089-100. Epub 2011/10/04. doi: 10.1105/tpc.111.089300. PubMed PMID: 21963667; PubMed Central PMCID: PMCPMC3203442.
16. **Plett JM, Kemppainen M, Kale SD, Kohler A, Legue V, Brun A, *et al*.** A secreted effector protein of *Laccaria bicolor* is required for symbiosis development. Curr Biol. 2011;21(14):1197-203. doi: 10.1016/j.cub.2011.05.033. PubMed PMID: 21757352.
17. **Plett JM, Daguerre Y, Wittulsky S, Vayssieres A, Deveau A, Melton SJ, *et al*.** Effector MiSSP7 of the mutualistic fungus *Laccaria bicolor* stabilizes the Populus JAZ6 protein and represses jasmonic acid (JA) responsive genes. Proc Natl Acad Sci USA. 2014;111(22):8299-304. doi: 10.1073/pnas.1322671111. PubMed PMID: 24847068; PubMed Central PMCID: PMC4050555.
18. **Kloppholz S, Kuhn H, Requena N.** A secreted fungal effector of *Glomus intraradices* promotes symbiotic biotrophy. Curr Biol. 2011;21(14):1204-9. doi: 10.1016/j.cub.2011.06.044. PubMed PMID: 21757354.
19. **Wawra S, Fesel P, Widmer H, Timm M, Seibel J, Leson L, *et al*.** The fungal-specific beta-glucan-binding lectin FGB1 alters cell-wall composition and suppresses glucan-triggered immunity in plants. Nature communications. 2016;7:13188. doi: 10.1038/ncomms13188. PubMed PMID: 27786272.
20. **Stergiopoulos I, de Wit PJGM.** Fungal effector proteins. Annu Rev Phytopathol. 2009;47:233-63. Epub 2009/04/30. doi: 10.1146/annurev.phyto.112408.132637. PubMed PMID: 19400631.
21. **Rouxel T, Grandaubert J, Hane JK, Hoede C, van de Wouw AP, Couloux A, *et al*.** Effector diversification within compartments of the *Leptosphaeria maculans* genome affected by Repeat-Induced Point mutations. Nature communications. 2011;2:202. doi: 10.1038/ncomms1189. PubMed PMID: 21326234; PubMed Central PMCID: PMC3105345.
22. **Raffaele S, Kamoun S.** Genome evolution in filamentous plant pathogens: why bigger can be better. Nat Rev Microbiol. 2012;10(6):417-30. Epub 2012/05/09. doi: 10.1038/nrmicro2790. PubMed PMID: 22565130.
23. **Feschotte C, Mouches C.** Evidence that a family of miniature inverted-repeat transposable elements (MITEs) from the *Arabidopsis thaliana* genome has arisen from a pogo-like DNA transposon. Mol Biol Evol. 2000;17(5):730-7. Epub 2000/04/26. doi: 10.1093/oxfordjournals.molbev.a026351. PubMed PMID: 10779533.
24. **Fleetwood DJ, Khan AK, Johnson RD, Young CA, Mittal S, Wrenn RE, *et al*.** Abundant degenerate miniature inverted-repeat transposable elements in genomes of epichloid fungal endophytes of grasses. Genome Biol Evol. 2011;3:1253-64. Epub 2011/09/29. doi: evr098 [pii] 10.1093/gbe/evr098. PubMed PMID: 21948396; PubMed Central PMCID: PMC3227409.
25. **Schmidt SM, Houterman PM, Schreiver I, Ma L, Amyotte S, Chellappan B, *et al*.** MITEs in the promoters of effector genes allow prediction of novel virulence genes in *Fusarium oxysporum*. BMC Genomics. 2013;14:119. doi: 10.1186/1471-

2164-14-119. PubMed PMID: 23432788; PubMed Central PMCID: PMC3599309.
26. **Winter DJ, Ganley ARD, Young CA, Liachko I, Schardl CL, Dupont PY, *et al*.** Repeat elements organise 3D genome structure and mediate transcription in the filamentous fungus *Epichloë festucae*. PLoS Genet. 2018;14(10):e1007467. Epub 2018/10/26. doi: 10.1371/journal.pgen.1007467. PubMed PMID: 30356280.
27. **Fattash I, Rooke R, Wong A, Hui C, Luu T, Bhardwaj P, *et al*.** Miniature inverted-repeat transposable elements: discovery, distribution, and activity. Genome. 2013;56(9):475-86. Epub 2013/10/31. doi: 10.1139/gen-2012-0174. PubMed PMID: 24168668.
28. **Schardl CL, Scott B, Florea S, Zhang D.** *Epichloë* endophytes: clavicipitaceous symbionts of grasses. In: Deising HB, editor. The Mycota Volume V - Plant Relationships. Berlin: Springer-Verlag; 2009. p. 275-306.
29. **Leuchtmann A, Schardl CL, Siegel MR.** Sexual compatibility and taxonomy of a new species of *Epichloë* symbiotic with fine fescue grasses. Mycologia. 1994;86:802-12.
30. **Schardl CL, Leuchtmann A, Tsai H-F, Collett MA, Watt DM, Scott DB.** Origin of a fungal symbiont of perennial ryegrass by interspecific hybridization of a mutualist with the ryegrass choke pathogen, *Epichloë typhina*. Genetics. 1994;136:1307-17.
31. **Chung K-R, Schardl CL.** Sexual cycle and horizontal transmission of the grass symbiont, *Epichloë typina*. Mycol Res. 1997;101(3):295-301.
32. **Scott B, Schardl C.** Fungal symbionts of grasses: evolutionary insights and agricultural potential. Trends Microbiol. 1993;1(5):196-200.
33. **Chung K-R, Hollin W, Siegel MR, Schardl CL.** Genetics of host specifictiy in *Epichloë typhina*. Phytopathology. 1997;87(6):599-605.
34. **Tanaka A, Christensen MJ, Takemoto D, Park P, Scott B.** Reactive oxygen species play a role in regulating a fungus-perennial ryegrass mutualistic association. Plant Cell. 2006;18:1052-66.
35. **Takemoto D, Kamakura S, Saikia S, Becker Y, Wrenn R, Tanaka A, *et al*.** Polarity proteins Bem1 and Cdc24 are components of the filamentous fungal NADPH oxidase complex. Proc Natl Acad Sci USA. 2011;108(7):2861-6.
36. **Eaton CJ, Cox MP, Ambrose B, Becker M, Hesse U, Schardl CL, *et al*.** Disruption of signaling in a fungal-grass symbiosis leads to pathogenesis. Plant Physiol. 2010;153(4):1780-94. Epub 2010/06/04. doi: pp.110.158451 [pii] 10.1104/pp.110.158451. PubMed PMID: 20519633.
37. **Takemoto D, Tanaka A, Scott B.** A p67(Phox)-like regulator is recruited to control hyphal branching in a fungal-grass mutualistic symbiosis. Plant Cell. 2006;18(10):2807-21. PubMed PMID: 17041146.
38. **Tanaka A, Takemoto D, Hyon GS, Park P, Scott B.** NoxA activation by the small GTPase RacA is required to maintain a mutualistic symbiotic association between *Epichloë festucae* and perennial ryegrass. Mol Microbiol. 2008;68(5):1165-78. PubMed PMID: 18399936.
39. **Tanaka A, Cartwright GM, Saikia S, Kayano Y, Takemoto D, Kato M, *et al*.** ProA, a transcriptional regulator of fungal fruiting body development, regulates leaf hyphal network development in the *Epichloë festucae-Lolium perenne* symbiosis. Mol Microbiol. 2013;90(3):551-68. doi: doi: 10.1111/mmi.12385.
40. **Becker Y, Eaton CJ, Brasell E, May KJ, Becker M, Hassing B, *et al*.** The fungal cell wall integrity MAPK cascade is crucial for hyphal network formation and maintenance of restrictive growth of *Epichloë festucae* in symbiosis with *Lolium perenne*. Mol Plant-Microbe Interact. 2015;28:69-85. doi: doi:10.1094/MPMI-06-14-0183-R.
41. **Sperschneider J, Gardiner DM, Dodds PN, Tini F, Covarelli L, Singh KB, *et al*.** EffectorP: predicting fungal effector proteins from secretomes using machine learning. New Phytol. 2016;210(2):743-61. doi: 10.1111/nph.13794. PubMed PMID: 26680733.

42. **Rittenour WR, Harris SD.** Glycosylphosphatidylinositol-anchored proteins in *Fusarium graminearum*: inventory, variability, and virulence. PLoS One. 2013;8(11):e81603. doi: 10.1371/journal.pone.0081603. PubMed PMID: 24312325; PubMed Central PMCID: PMC3843709.
43. **Zhu W, Wei W, Wu Y, Zhou Y, Peng F, Zhang S, *et al*. BcCFEM1, a CFEM** domain-containing protein with putative GPI-anchored site, is involved in pathogenicity, conidial production, and stress tolerance in *Botrytis cinerea*. Frontiers Microbiol. 2017;8:1807. Epub 2017/10/06. doi: 10.3389/fmicb.2017.01807. PubMed PMID: 28979251; PubMed Central PMCID: PMC5611420.
44. **Petersen TN, Brunak S, von Heijne G, Nielsen H.** SignalP 4.0: discriminating signal peptides from transmembrane regions. Nat Methods. 2011;8(10):785-6. Epub 2011/10/01. doi: nmeth.1701 [pii] 10.1038/nmeth.1701. PubMed PMID: 21959131.
45. R development core team. R: A language and environment for statistical computing. R Foundation for Statistical Computing, Vienna, Austria. 2013;URL https://www.R-project.org/.
46. **Quinlan AR.** BEDTools: The swiss-army tool for genome feature analysis. Curr Protoc Bioinformatics. 2014;47:11.2. 1-34. Epub 2014/09/10. doi: 10.1002/0471250953.bi1112s47. PubMed PMID: 25199790; PubMed Central PMCID: PMCPMC4213956.
47. **Eaton CJ, Dupont P-Y, Solomon PS, Clayton W, Scott B, Cox MP**. A core gene set describes the molecular basis of mutualism and antagonism in *Epichloë* species. Mol Plant-Microbe Interact. 2015;28:218-31. doi: doi.org/10.1094/MPMI-09-14-0293-FI.
48. **Lachner M, O'Carroll D, Rea S, Mechtler K, Jenuwein T.** Methylation of histone H3 lysine 9 creates a binding site for HP1 proteins. Nature. 2001;410(6824):116-20. doi: 10.1038/35065132. PubMed PMID: 11242053.
49. **Maison C, Almouzni G.** HP1 and the dynamics of heterochromatin maintenance. Nat Rev Mol Cell Biol. 2004;5(4):296-304. doi: 10.1038/nrm1355. PubMed PMID: 15071554.
50. **Miller JH.** Experiments in Molecular Genetics. New York: Cold Spring Harbor Laboratory Press; 1972.
51. **Sambrook J, Fritsch EF, Maniatis T.** Molecular cloning: a laboratory manual. Cold Spring Harbor, New York: Cold Spring Harbor Laboratory Press; 1989.
52. **Jacobs KA, Collins-Racie LA, Colbert M, Duckett M, Golden-Fleet M, Kelleher K, *et al*.** A genetic selection for isolating cDNAs encoding secreted proteins. Gene. 1997;198(1-2):289-96. PubMed PMID: 9370294.
53. **Ausubel FM, Brent R, Kingston RE, Moore DD, Seidman JG, Smith JA, *et al*.** Current Protocols in Molecular Biology. New York.: John Wiley & Sons; 1993.
54. **Moon CD, Tapper BA, Scott B.** Identification of *Epichloë* endophytes *in planta* by a microsatellite-based PCR fingerprinting assay with automated analysis. Appl Environ Microbiol. 1999;65:1268-79.
55. **Moon CD, Scott B, Schardl CL, Christensen MJ.** The evolutionary origins of *Epichloë* endophytes from annual ryegrasses. Mycologia. 2000;92:1103-18.
56. **Latch GCM, Christensen MJ.** Artificial infection of grasses with endophytes. Ann Appl Biol. 1985;107(1):17-24.
57. **Byrd AD, Schardl CL, Songlin PJ, Mogen KL, Siegel MR.** The β-tubulin gene of *Epichloë typhina* from perennial ryegrass (*Lolium perenne*). Curr Genet. 1990;18(4):347-54.
58. **Gibson DG, Young L, Chuang RY, Venter JC, Hutchison CA, III, Smith HO.** Enzymatic assembly of DNA molecules up to several hundred kilobases. Nat Methods. 2009;6(5):343-5. Epub 2009/04/14. doi: nmeth.1318 [pii] 10.1038/nmeth.1318. PubMed PMID: 19363495.
59. **Eisenhaber B, Schneider G, Wildpaner M, Eisenhaber F.** A sensitive predictor

for potential GPI lipid modification sites in fungal protein sequences and its application to genome-wide studies for *Aspergillus nidulans, Candida albicans, Neurospora crassa*, *Saccharomyces cerevisiae* and *Schizosaccharomyces pombe*. J Mol Biol. 2004;337(2):243-53. doi: 10.1016/j.jmb.2004.01.025. PubMed PMID: 15003443.

60. **Khang CH, Berruyer R, Giraldo MC, Kankanala P, Park SY, Czymmek K, *et al*.** Translocation of *Magnaporthe oryzae* effectors into rice cells and their subsequent cell-to-cell movement. Plant Cell. 2010;22(4):1388-403. Epub 2010/05/04. doi: tpc.109.069666 [pii]
10.1105/tpc.109.069666. PubMed PMID: 20435900; PubMed Central PMCID: PMC2879738.
61. **Winston F, Dollard C, Ricupero-Hovasse SL.** Construction of a set of convenient *Saccharomyces cerevisiae* strains that are isogenic to S288C. Yeast. 1995;11(1):53-5. Epub 1995/01/01. doi: 10.1002/yea.320110107. PubMed PMID: 7762301.
62. **Gietz RD, Woods RA.** Transformation of yeast by lithium acetate/single-stranded carrier DNA/polyethylene glycol method. Meth Enzymol. 2002;350:87-96. Epub 2002/06/21. PubMed PMID: 12073338.
63. **Koncz C, Martini N, Szabados L, Hrouda M, Bachmair A, Schell J**. Specialized vectors for gene tagging and expression studies. In: Gelvin SB, Schilperoort RA, editors. Plant Molecular Biology Manual. Dordrecht: Kluwer Academic; 1994. p. 1-22.
64. **Weigel D, Glazebrook J.** Transformation of *Agrobacterium* using the freeze-thaw method. CSH Protoc. 2006;pdb.prot4666.
65. **Young CA, Bryant MK, Christensen MJ, Tapper BA, Bryan GT, Scott B.** Molecular cloning and genetic analysis of a symbiosis-expressed gene cluster for lolitrem biosynthesis from a mutualistic endophyte of perennial ryegrass. Mol Gen Genomics. 2005;274:13-29.
66. **Itoh Y, Johnson R, Scott B.** Integrative transformation of the mycotoxin-producing fungus, *Penicillium paxilli*. Curr Genet. 1994;25:508-13.
67. **Lukito Y, Chujo T, Scott B.** Molecular and cellular analysis of the pH response transcription factor PacC in the fungal symbiont *Epichloë festucae*. Fungal Genet Biol. 2015;85:25-37. doi: 10.1016/j.fgb.2015.10.008. PubMed PMID: 26529380.
68. **Chujo T, Scott B.** Histone H3K9 and H3K27 methylation regulates fungal alkaloid biosynthesis in a fungal endophyte-plant symbiosis. Mol Microbiol. 2014;92(2):413-34. Epub 2014/02/28. doi: 10.1111/mmi.12567. PubMed PMID: 24571357.
69. **Becker Y, Green K, Scott B, Becker M.** Artificial inoculation of *Epichloë festucae* into *Lolium perenne*, and visualization of endophytic and epiphyllous fungal growth. Bio-protocol 2018;8:e2990.
70. **Florea S, Schardl CL, Hollin W.** Detection and isolation of *Epichloë* species, fungal endophytes of grasses. Current Protocols Microbiol. 2015;38:19A.1.-A.1.24. Epub 2015/08/04. doi: 10.1002/9780471729259.mc19a01s38. PubMed PMID: 26237108.
71. **Spiers AG, Hopcroft DH.** Black canker and leaf spot of Salix in New Zealand caused by *Glomerella miyabeana* (*Colletotrichum gloeosporioides*). Eur J Forest Pathol. 1993;23:92-102.
72. **Mesarich CH, Ökmen B, Rovenich H, Griffiths SA, Wang C, Karimi Jashni M, *et al*.** Specific hypersensitive response-associated recognition of new apoplastic effectors from *Cladosporium fulvum* in wild tomato. Mol Plant-Microbe Interact. 2018;31(1):145-62. doi: 10.1094/MPMI-05-17-0114-FI. PubMed PMID: 29144204.
73. **Joosten MHAJ, Vogelsang R, Cozijnsen TJ, Verberne MC, de Wit PJGM.** The biotrophic fungus *Cladosporium fulvum* circumvents Cf-4-mediated resistance by producing unstable AVR4 elicitors. Plant Cell. 1997;9(3):367-79.

74. **Luderer R, De Kock MJD, Dees RHL, De Wit PJGM, Joosten MHAJ.** Functional analysis of cysteine residues of ECP elicitor proteins of the fungal tomato pathogen *Cladosporium fulvum*. Mol Plant Pathol. 2002;3(2):91-5. Epub 2002/03/01. doi: 10.1046/j.1464-6722.2001.00095.x. PubMed PMID: 20569313.
75. **Kämper J, Kahmann R, Bolker M, Ma LJ, Brefort T, Saville BJ, *et al*.** Insights from the genome of the biotrophic fungal plant pathogen *Ustilago maydis*. Nature. 2006;444(7115):97-101. doi: 10.1038/nature05248. PubMed PMID: 17080091.
76. **Brefort T, Tanaka S, Neidig N, Doehlemann G, Vincon V, Kahmann R.** Characterization of the largest effector gene cluster of *Ustilago maydis*. PLoS Pathog. 2014;10(7):e1003866. doi: 10.1371/journal.ppat.1003866. PubMed PMID: 24992561; PubMed Central PMCID: PMC4081774.
77. **Cambareri EB, Jensen BC, Schabtach E, Selker EU**. Repeat-induced G-C to A-T mutations in *Neurospora*. Science. 1989;244(4912):1571-5. PubMed PMID: 2544994.
78. **Gladyshev E.** Repeat-induced point mutation and other genome defense mechanisms in fungi. Microbiol Spectrum. 2017;5(4):FUNK-0042-2017. doi: 10.1128/microbiolspec.FUNK-0042-2017. PubMed PMID: 28721856; PubMed Central PMCID: PMC5607778.
79. **Cambareri EB, Singer MJ, Selker EU.** Recurrence of repeat-induced point mutation (RIP) in *Neurospora crassa*. Genetics. 1991;127(4):699-710. Epub 1991/04/01. PubMed PMID: 1827629; PubMed Central PMCID: PMCPMC1204397.
80. **Fudal I, Ross S, Brun H, Besnard AL, Ermel M, Kuhn ML, *et al*.** Repeat-induced point mutation (RIP) as an alternative mechanism of evolution toward virulence in *Leptosphaeria maculans*. Mol Plant-Microbe Interact. 2009;22(8):932-41. Epub 2009/07/11. doi: 10.1094/MPMI-22-8-0932. PubMed PMID: 19589069.
81. **Wong S, Wolfe KH.** Birth of a metabolic gene cluster in yeast by adaptive gene relocation. Nature Genet. 2005;37(7):777-82. PubMed PMID: 15951822.
82. **Orbach MJ, Farrall L, Sweigard JA, Chumley FG, Valent B.** A telomeric avirulence gene determines efficacy for the rice blast resistance gene Pi-ta. Plant Cell. 2000;12(11):2019-32.
83. **Rehmeyer C, Li W, Kusaba M, Kim YS, Brown D, Staben C, *et al*.** Organization of chromosome ends in the rice blast fungus, *Magnaporthe oryzae*. Nucleic Acids Res. 2006;34(17):4685-701. PubMed PMID: 16963777.
84. **Brown CA, Murray AW, Verstrepen KJ.** Rapid expansion and functional divergence of subtelomeric gene families in yeasts. Curr Biol. 2010;20(10):895-903. Epub 2010/05/18. doi: 10.1016/j.cub.2010.04.027. PubMed PMID: 20471265; PubMed Central PMCID: PMC2877759.
85. **Hirsch CD, Springer NM.** Transposable element influences on gene expression in plants. Biochim Biophys Acta Gene Regul Mech. 2017;1860(1):157-65. Epub 2016/05/29. doi: 10.1016/j.bbagrm.2016.05.010. PubMed PMID: 27235540.
86. **Chuong EB, Elde NC, Feschotte C.** Regulatory activities of transposable elements: from conflicts to benefits. Nat Rev Genet. 2016;18(2):71-86. doi: 10.1038/nrg.2016.139. PubMed PMID: 27867194.
87. **Lanver D, Müller AN, Happel P, Schweizer G, Haas FB, Franitza M, *et al*.** The biotrophic development of *Ustilago maydis* studied by RNA-Seq analysis. Plant Cell. 2018;30(2):300-23. doi: 10.1105/tpc.17.00764. PubMed PMID: 29371439; PubMed Central PMCID: PMC5868686.
88. **Kleemann J, Rincon-Rivera LJ, Takahara H, Neumann U, Ver Loren van Themaat E, van der Does HC, *et al*.** Sequential delivery of host-induced virulence effectors by appressoria and intracellular hyphae of the phytopathogen *Colletotrichum higginsianum*. PLoS Pathog. 2012;8(4):e1002643. Epub 2012/04/13. doi: 10.1371/journal.ppat.1002643. PubMed PMID: 22496661;

PubMed Central PMCID: PMCPMC3320591.
89. **Soyer JL, El Ghalid M, Glaser N, Ollivier B, Linglin J, Grandaubert J, *et al*.** Epigenetic control of effector gene expression in the plant pathogenic fungus *Leptosphaeria maculans*. PLoS Genet. 2013;10(3):e1004227. Epub 2014/03/08. doi: 10.1371/journal.pgen.1004227
PGENETICS-D-13-03255 [pii]. PubMed PMID: 24603691; PubMed Central PMCID: PMC3945186.
90. **Jones P, Binns D, Chang HY, Fraser M, Li W, McAnulla C, *et al*.** InterProScan 5: genome-scale protein function classification. Bioinformatics. 2014;30(9):1236-40. Epub 2014/01/24. doi: 10.1093/bioinformatics/btu031. PubMed PMID: 24451626; PubMed Central PMCID: PMC3998142.
91. **Letunic I, Doerks T, Bork P.** SMART: recent updates, new developments and status in 2015. Nucleic Acids Res. 2015;43(Database issue):D257-60. Epub 2014/10/11. doi: 10.1093/nar/gku949. PubMed PMID: 25300481; PubMed Central PMCID: PMC4384020.
92. **Jorda J, Kajava AV.** T-REKS: identification of Tandem REpeats in sequences with a K-meanS based algorithm. Bioinformatics. 2009;25(20):2632-8. Epub 2009/08/13. doi: 10.1093/bioinformatics/btp482. PubMed PMID: 19671691.
93. **Zimmermann L, Stephens A, Nam SZ, Rau D, Kubler J, Lozajic M, *et al*.** A completely reimplemented MPI bioinformatics toolkit with a new HHpred server at its core. J Mol Biol. 2018;430(15):2237-43. Epub 2017/12/21. doi: 10.1016/j.jmb.2017.12.007. PubMed PMID: 29258817.
94. **Schardl CL, Young CA, Hesse U, Amyotte SG, Andreeva K, Calie PJ, *et al*.** Plant-symbiotic fungi as chemical engineers: multi-genome analysis of the *Clavicipitaceae* reveals dynamics of alkaloid loci. PLoS Genetics. 2013;9(2):e1003323.
95. **Kettles GJ, Bayon C, Canning G, Rudd JJ, Kanyuka K.** Apoplastic recognition of multiple candidate effectors from the wheat pathogen *Zymoseptoria tritici* in the nonhost plant *Nicotiana benthamiana*. New Phytol. 2017;213(1):338-50. Epub 2016/10/04. doi: 10.1111/nph.14215. PubMed PMID: 27696417; PubMed Central PMCID: PMC5132004.
96. **Bos JIB, Kanneganti T-D, Young C, Cakir C, Huitema E, Win J, *et al*.** The C-terminal half of *Phytophthora infestans* RXLR effector AVR3a is sufficient to trigger R3a-mediated hypersensitivity and suppress INF1-induced cell death in Nicotiana *benthamiana*. Plant J. 2006;48(2):165-76. Epub 2006/09/13. doi: 10.1111/j.1365-313X.2006.02866.x. PubMed PMID: 16965554.
97. **Ma LJ, van der Does HC, Borkovich KA, Coleman JJ, Daboussi MJ, Di Pietro A, *et al*.** Comparative genomics reveals mobile pathogenicity chromosomes in Fusarium. Nature. 2010;464(7287):367-73. Epub 2010/03/20. doi: nature08850 [pii] 10.1038/nature08850. PubMed PMID: 20237561.
98. **van Dam P, Fokkens L, Schmidt SM, Linmans JH, Kistler HC, Ma LJ, *et al*.** Effector profiles distinguish *formae speciales* of *Fusarium oxysporum*. Environ Microbiol. 2016;18(11):4087-102. doi: 10.1111/1462-2920.13445. PubMed PMID: 27387256.
99. **Inoue Y, Vy TTP, Yoshida K, Asano H, Mitsuoka C, Asuke S, *et al*.** Evolution of the wheat blast fungus through functional losses in a host specificity determinant. Science. 2017;357(6346):80-3. Epub 2017/07/08. doi: 10.1126/science.aam9654. PubMed PMID: 28684523.
100. **Yoshida K, Saitoh H, Fujisawa S, Kanzaki H, Matsumura H, Yoshida K, *et al*.** Association genetics reveals three novel avirulence genes from the rice blast fungal pathogen *Magnaporthe oryzae*. Plant Cell. 2009;21(5):1573-91. Epub 2009/05/21. doi: 10.1105/tpc.109.066324. PubMed PMID: 19454732; PubMed Central PMCID: PMC2700537.
101. **Ridout CJ, Skamnioti P, Porritt O, Sacristan S, Jones JD, Brown JK.** Multiple avirulence paralogues in cereal powdery mildew fungi may contribute to parasite

fitness and defeat of plant resistance. Plant Cell. 2006;18(9):2402-14. doi: 10.1105/tpc.106.043307. PubMed PMID: 16905653; PubMed Central PMCID: PMC1560912.
102. **Houterman PM, Cornelissen BJ, Rep M.** Suppression of plant resistance gene-based immunity by a fungal effector. PLoS Pathog. 2008;4(5):e1000061. Epub 2008/05/10. doi: 10.1371/journal.ppat.1000061. PubMed PMID: 18464895; PubMed Central PMCID: PMC2330162.
103. **Selin C, de Kievit TR, Belmonte MF, Fernando WG.** Elucidating the role of effectors in plant-fungal interactions: progress and challenges. Frontiers Microbiol. 2016;7:600. Epub 2016/05/21. doi: 10.3389/fmicb.2016.00600. PubMed PMID: 27199930; PubMed Central PMCID: PMC4846801.
104. **Lu C, Chen J, Zhang Y, Hu Q, Su W, Kuang H.** Miniature inverted-repeat transposable elements (MITEs) have been accumulated through amplification bursts and play important roles in gene expression and species diversity in *Oryza sativa*. Mol Biol Evol. 2012;29(3):1005-17. Epub 2011/11/19. doi: 10.1093/molbev/msr282. PubMed PMID: 22096216; PubMed Central PMCID: PMC3278479.
105. **Fleetwood DJ, Scott B, Lane GA, Tanaka A, Johnson RD.** A complex ergovaline gene cluster in *epichloë* endophytes of grasses. Appl Environ Microbiol. 2007;73(8):2571-9. PubMed PMID: 17308187.
106. **van Dam P, Fokkens L, Ayukawa Y, van der Gragt M, Ter Horst A, Brankovics B, *et al*.** A mobile pathogenicity chromosome in *Fusarium oxysporum* for infection of multiple cucurbit species. Sci Rep. 2017;7(1):9042. Epub 2017/08/24. doi: 10.1038/s41598-017-07995-y. PubMed PMID: 28831051; PubMed Central PMCID: PMC5567276.
107. **Bolton MD, van Esse HP, Vossen JH, de Jonge R, Stergiopoulos I, Stulemeijer IJE, *et al*.** The novel *Cladosporium fulvum* lysin motif effector Ecp6 is a virulence factor with orthologues in other fungal species. Mol Microbiol. 2008;69(1):119-36. Epub 2008/05/03. doi: 10.1111/j.1365-2958.2008.06270.x. PubMed PMID: 18452583.
108. **Vargas WA, Sanz-Martín JM, Rech GE, Armijos-Jaramillo VD, Rivera LP, Echeverria MM, *et al*.** A fungal effector with host nuclear localization and DNA-binding properties is required for maize anthracnose development. Mol Plant-Microbe Interact. 2016;29(2):83-95. Epub 2015/11/12. doi: 10.1094/MPMI-09-15-0209-R. PubMed PMID: 26554735.
109. **Mesarich CH, Bowen JK, Hamiaux C, Templeton MD**. Repeat-containing protein effectors of plant-associated organisms. Front Plant Sci. 2015;6:872. Epub 2015/11/12. doi: 10.3389/fpls.2015.00872. PubMed PMID: 26557126; PubMed Central PMCID: PMC4617103.
110. **Grove TZ, Cortajarena AL, Regan L.** Ligand binding by repeat proteins: natural and designed. Curr Opin Struct Biol. 2008;18(4):507-15. Epub 2008/07/08. doi: 10.1016/j.sbi.2008.05.008. PubMed PMID: 18602006; PubMed Central PMCID: PMCPMC3500881.
111. **Johnson RD, Lane GA, Koulman A, Cao M, Fraser K, Fleetwood DJ, *et al*.** A novel family of cyclic oligopeptides derived from ribosomal peptide synthesis of an *in planta*-induced gene, gigA, in *Epichloë* endophytes of grasses. Fungal Genet Biol. 2015;85:14-24. doi: 10.1016/j.fgb.2015.10.005. PubMed PMID: 26519220.
112. **Wosten HA, Bohlmann R, Eckerskorn C, Lottspeich F, Bolker M, Kahmann R. A** novel class of small amphipathic peptides affect aerial hyphal growth and surface hydrophobicity in *Ustilago maydis*. EMBO J. 1996;15(16):4274-81. Epub 1996/08/15. PubMed PMID: 8861956; PubMed Central PMCID: PMC452153.
113. **Teertstra WR, van der Velden GJ, de Jong JF, Kruijtzer JA, Liskamp RM, Kroon-Batenburg LM, *et al*.** The filament-specific Rep1-1 repellent of the phytopathogen *Ustilago maydis* forms functional surface-active amyloid-like

fibrils. J Biol Chem. 2009;284(14):9153-9. Epub 2009/01/24. doi: 10.1074/jbc.M900095200. PubMed PMID: 19164282; PubMed Central PMCID: PMCPMC2666566.
114. **Christensen MJ, Bennett RJ, Ansari HA, Koga H, Johnson RD, Bryan GT, *et al*.** *Epichloë* endophytes grow by intercalary hyphal extension in elongating grass leaves. Fungal Genet Biol. 2008;45:84-93.
115. **Voisey CR.** Intercalary growth in hyphae of filamentous fungi. Fungal Biol Rev. 2010;24:123-31.
116. **Bultman TL, Leuchtmann A.** Biology of the *Epichloë-Botanophila* interaction: an intriguing association between fungi and insects. Fungal Biol Rev. 2009;22:131-8.
117. **Stewart EL, McDonald BA.** Measuring quantitative virulence in the wheat pathogen *Zymoseptoria tritici* using high-throughput automated image analysis. Phytopathology. 2014;104(9):985-92. Epub 2014/03/15. doi: 10.1094/PHYTO-11-13-0328-R. PubMed PMID: 24624955.
118. **Stewart EL, Hagerty CH, Mikaberidze A, Mundt CC, Zhong Z, McDonald BA.** An improved method for measuring quantitative resistance to the wheat pathogen *Zymoseptoria tritici* using high-throughput automated image analysis. Phytopathology. 2016;106(7):782-8. Epub 2016/04/07. doi: 10.1094/PHYTO-01-16-0018-R. PubMed PMID: 27050574.
119. **Wessling R, Epple P, Altmann S, He Y, Yang L, Henz SR, *et al*.** Convergent targeting of a common host protein-network by pathogen effectors from three kingdoms of life. Cell Host Microbe. 2014;16(3):364-75. Epub 2014/09/12. doi: 10.1016/j.chom.2014.08.004. PubMed PMID: 25211078; PubMed Central PMCID: PMC4191710.
120. **Win J, Chaparro-Garcia A, Belhaj K, Saunders DG, Yoshida K, Dong S, *et al*.** Effector biology of plant-associated organisms: concepts and perspectives. Cold Spring Harbor Symposia on Quantitative Biology. 2012;77:235-47. Epub 2012/12/12. doi: 10.1101/sqb.2012.77.015933. PubMed PMID: 23223409.
121. **Heath MC.** Nonhost resistance and nonspecific plant defenses. Curr Opin Plant Biol. 2000;3(4):315-9. PubMed PMID: 10873843.
122. **Derevnina L, Dagdas YF, De la Concepcion JC, Bialas A, Kellner R, Petre B, *et al*.** Nine things to know about elicitins. New Phytol. 2016;212(4):888-95. Epub 2016/09/02. doi: 10.1111/nph.14137. PubMed PMID: 27582271.
123. **Du J, Verzaux E, Chaparro-Garcia A, Bijsterbosch G, Keizer LC, Zhou J, *et al*.** Elicitin recognition confers enhanced resistance to *Phytophthora infestans* in potato. Nature Plants. 2015;1(4):15034. Epub 2015/01/01. doi: 10.1038/nplants.2015.34. PubMed PMID: 27247034.
124. **Dupont PY, Eaton CJ, Wargent JJ, Fechtner S, Solomon P, Schmid J, *et al*.** Fungal endophyte infection of ryegrass reprograms host metabolism and alters development. New Phytol. 2015;208(4):1227-40. doi: 10.1111/nph.13614. PubMed PMID: 26305687.
125. **Becker M, Becker Y, Green K, Scott B.** The endophytic symbiont *Epichloë festucae* establishes an epiphyllous net on the surface of *Lolium perenne* leaves by development of an expressorium, an appressorium-like leaf exit structure. New Phytol. 2016;211:240-54. doi: 10.1111/nph.13931. PubMed PMID: 26991322.

Chapter 3: Phosphatidic acid produced by phospholipase D is a key signalling molecule for hyphal cell-to-cell fusion and the mutualistic interaction between *Epichloë festucae* and perennial ryegrass

Phosphatidic acid produced by phospholipase D is a key signalling molecule for hyphal cell-to-cell fusion and the mutualistic interaction between *Epichloë festucae* and perennial ryegrass

Berit Hassing[1,2], Kimberly Green[1,2], David Winter[1,2], Ulrike Brandt[4], Carl H. Mesarich[2,3], Carla J Eaton[1,2], Andre Fleissner[4] and Barry Scott[1,2]

[1]School of Fundamental Sciences, Massey University, Palmerston North, NZ,

[2]Bio-Protection Research Centre, NZ,

[3]School of Agriculture and Environment, Massey University, Palmerston North, NZ.

[4]Institute for Genetics, Technische Universität Braunschweig, Braunschweig, Germany.

Summary

Epichloë festucae is a filamentous fungus that forms a stable and mutually beneficial interaction with the agriculturally important grass *Lolium perenne*. *E. festucae* is exclusively found in the aerial tissues of the host, where it colonises the intercellular spaces of vegetative and reproductive tissues to form a highly regulated hyphal network. Signalling via reactive oxygen species (ROS) is essential for the establishment and maintenance of this symbiotic interaction as disruption of the NADPH oxidase (Nox) complex results in a dramatic switch of *E. festuae* to a pathogen-like behaviour. Phosphatidic acid (PA) produced by phospholipase D (PLD) has been shown to regulate the recruitment and activation of the NADPH oxidase in mammalian and plant cells, but whether similar signalling occurs in filamentous fungi has not been tested. *E. festucae* encodes two structurally different PLD proteins and analysis of deletion mutants revealed that PldB, but not PldA, is required for polarized growth and cell-to-cell fusion, highlighting the importance of PldB and phosphatidic acid during fungal development. A phosphatidic-acid biosensor was found to localise to the plasma membrane in wild-type (WT) and *pldA* deletion strains, but to the cytosol in *pldB* deletion strains, indicating that PA is largely generated though the activity of PldB. While *pldA* mutants were asymptomatic *in planta*, inoculation of *pldB* mutant strains into ryegrass seedlings resulted in hyphal proliferation and host stunting. In addition, *pldB* deletion mutants were unable to form functional expressoria. Analysis of superoxide production within *pldB* deletion mutants revealed differences in the localisation of ROS compared to WT but none of the components of the Nox complex itself were found to be mislocalised. These results indicate that PA produced by PldB is

required for normal superoxide production, regular hyphal growth and establishment of a mutualistic symbiotic interaction with perennial ryegrass.

Introduction

Epichloë festucae is a filamentous ascomycete fungus that has an intimate and largely beneficial interaction with perennial ryegrass. The interaction between *Epichloë* species and cool-season grasses is of great agricultural importance due to the beneficial impact of the endophytes on host responses to biotic and abiotic stresses (Schardl *et al*., 2004). The fungus colonises the apoplast of the infected plant in a very restricted manner, giving rise to a hyphal network *in planta* (Christensen *et al*. 2008). In addition, it forms an epiphyllous network upon exiting the plant through use of an expressorium (Becker *et al*., 2016). The formation of an epiphyllous structure, called a stroma, on the plant inflorescence is important for the sexual transmission of the fungus, which otherwise only transmits vertically by host seed colonisation (Scott and Schardl, 1993; Chung and Schardl, 1997).

Superoxide and reactive oxygen species (ROS) generated by NADPH oxidase (Nox) complexes are of great importance to the mutualistic interaction between *E. festucae* and *L. perenne* (Scott *et al*., 2015). Disruption of these complexes results in the loss of mutualism and a switch to pathogen-like behaviour. The most well-characterised Nox complex is that of mammalian phagocytes, which catalyses an "oxidative burst" in response to pathogen attack (Lambeth and Neish, 2013). This complex consists of the catalytic transmembrane protein $gp91^{phox}$ (also known as Nox2), the membrane-bound adaptor protein $p22^{phox}$, the regulatory subunits $p67^{phox}$, $p40^{phox}$, $p47^{phox}$ and the small GTPase Rac2. The membrane-integrated catalytic core of the Nox complex transfers electrons from NADPH to molecular oxygen, generating superoxide and other ROS. For activation of the complex and production of superoxide, the cytosolic components are recruited to the plasma membrane. This process requires phosphorylation of some of the subunits, activation of Rac1 and various protein-protein and protein-lipid interactions (Belambri *et al*., 2018). Mammalian Nox proteins can be classified into seven groups: Nox1, Nox2 ($gp91^{phox}$), Nox3, Nox4, Nox5, Duox1, and Duox2 (Lambeth *et al*., 2000). Together they are involved in regulating the above-mentioned oxidative burst, cell proliferation, developmental processes and hormone synthesis (Bedard and Krause, 2007; Lambeth and Neish, 2014). Plant respiratory burst homologs (RBOHs) are Nox5-like NADPH oxidases, which contain EF-Hand motifs regulated by Ca^{2+}. These NADPH oxidases are involved in defence against pathogens, adaptation to biotic and abiotic stress, and polarized growth (Marino *et al*., 2012; Kaur *et al*., 2014). Fungi possess up to four different *nox* genes, which can be assigned to three different subfamilies (Aguirre *et al*., 2005). The best-studied fungal Nox complexes are NoxA (also Nox1) and NoxB (also Nox2), which

have overlapping but distinct roles and both contain homologs of gp91^{phox}. In *Aspergillus niduans, Podospora anserina* and *Neurospora crassa* NoxA is required for sexual fruiting body development, whereas NoxB is necessary for the germination of ascospores (Lara-Ortiz *et al*., 2003; Malagnac *et al*., 2004; Cano-Dominguez *et al*., 2008). In addition, NoxA is crucial for hyphal fusion in *E. festucae, N. crassa*, *Botrytis cinerea* and *P. anserina* whereas NoxB is dispensable for hyphal fusion in *N. crassa*, *B cinerea*, *P. anserina* and *E. festucae* (Roca *et al*., 2012; Tudzynski *et al*., 2012; Kayano *et al*., 2013; Tong *et al*., 2014). Both NoxA and NoxB are required for the development of sclerotia in other fungi, and recent studies revealed that both proteins are required for the formation of appressoria in *Magnaporthe oryzae* and expressoria in *E. festucae* (Segmüller *et al*., 2008; Kim *et al*., 2011; Ryder *et al*., 2013; Becker *et al*., 2016). Furthermore, disruption of either of these two complexes results in a breakdown of the *E. festucae*-perennial ryegrass interaction, including loss of restricted growth and premature death of the host (Tanaka *et al*., 2006; Becker *et al*., 2015).

Similar to gp91^{phox} in mammals, multiple proteins are necessary for NoxA activation in fungi, of which some are homologous to their mammalian counterparts. The NoxA complex consists of NoxA, the adaptor protein NoxD (homolog of p22^{phox}), and the regulatory proteins NoxR (homolog of p67^{phox}) and the small GTPase RacA (homolog of Rac2) (Lacaze *et al*., 2015). Homologs of p40^{phox} and p47^{phox} do not appear to be present; instead, the fungal NoxA complex includes the scaffold protein BemA (Takemoto *et al*., 2011). In addition, signalling via the guanine-exchange factor (GEF) Cdc24 and the small GTPase Cdc42 influence the regulation of the Nox complex via direct interactions with some of the cytosolic subunits (Takemoto *et al*., 2011; Kayano *et al*., 2013; Kayano *et al*., 2018). While the localisation of the individual subunits of the NoxA complex has been determined, the localisation of the assembled NoxA complex, as well as its means of activation, has not been identified yet. The structure of the NoxB complex has not been fully elucidated: however NoxR and the tetraspannin Pls1 are required for NoxB signalling (Siegmund *et al*., 2013; Ryder *et al*, 2013; Zhao *et al*., 2016).

In plants, lipid signalling via phosphospholipase D (PLD) synthesised phosphatidic acid (PA) has been shown to be involved in the activation of NADPH oxidase complexes. PLD hydrolyses phosphatidylcholine (PC) to produce PA and free choline. PA has a cone structure due to the smaller headgroup compared to the lipid tail, which induces negative membrane curvature. PA is able to recruit proteins to specific membranes, as well activate proteins through interaction, and is an important second messenger in plant and mammalian cells involved in stress responses,

cytoskeleton rearrangements, growth, and development (Jenkins and Frohman, 2005; Selvy *et al*., 2011).

Plant PLDs can be subdivided into two subgroups based on the nature of their N-terminal regulatory domain; the C2 calcium-binding domain-containing PLDs (PLDα-PLDε) and the phox-homology (PX) and plekstrin-homology (PH) domain-containing PLDs (PLDζ) (Selvy *et al*., 2011). Plant PLDs and PA have been correlated with stress responses, actin polymerization, and root elongation (Lee *et al*., 2003; Huang *et al*., 2006; Hong *et al*., 2009). Depletion of PLDα in *Arabidopsis* leaves and the inhibition of PLD in tobacco pollen tubes reduces NADPH oxidase activity, which can be restored through the exogenous addition of PA *in vitro* and *in vivo* (Sang et el., 2001; Potocký *et al*., 2012). PA is required to induce an oxidative burst in response to a fungal avirulence elicitor, and direct interaction between RBOHD and PA is required to achieve stomatal closure upon abscisic acid signalling (de Jong *et al*. 2004; Zhang *et al*, 2009).

In animal cells, two PLDs have been identified, PLD1 and PLD2, which have a similar domain structure but differ in their regulation, interaction partners, cellular localisation and cellular roles (Selvy *et al*., 2011). Studies have shown that both $p22^{phox}$ and $p47^{phox}$ are phosphorylated by a PA-activated kinase, which in turn results in a conformational change of $p47^{phox}$ and increased binding to $p22^{phox}$ (McPhail *et al*., 1995; Waite *et al*., 1997; Regier *et al*., 1999; Regier *et al*., 2000). Activation of $p47^{phox}$ results in release of autoinhibition of the PX domain, which allows binding to phosphatidylinositol 3,4-bisphosphate (PtdIns[3,4]P_2) and PA, which in turn has been proposed to facilitate membrane recruitment of the cytosolic components (Kanai *et al*., 2001; Karathanassis *et al*., 2002; Ago *et al*., 2003). In a cell-free system, PA is sufficient for the activation of the oxidase, and this process is independent of ATP (Qualliotine-Mann *et al*., 1993; Palicz *et al*., 2001). More recent studies were able to demonstrate that a direct interaction between $gp91^{phox}$ and PA results in conformational changes in $gp91^{phox}$ (Qualliotine-Mann *et al*., 1993; Taylor *et al*, 2004; Taylor *et al*., 2012). Furthermore, Rac1 and Rac2 have been found to bind PA via their polybasic domain, which results in the translocation of Rac1 to the membrane (Chae *et al*., 2008; Faugaret *et al*., 2011). In turn, Rac1 is also able to activate PLD1, suggesting control by a feedback loop (Powner and Wakelam, 2002).

In fungi, the role of PLD-synthesised PA in the recruitment and activation of the Nox complex has not been studied to date. However, given that PA signalling has an impact both in plant and animal cells, a role in fungi is likely. While fungi lack a $p47^{phox}$ homolog, two of the cytosolic components, BemA and Cdc24, contain lipid-binding domains.

Studies to date include an analysis of the role of PLD in vegetative growth, sexual reproduction and virulence. Fungal genomes contain up to three genes encoding PC-hydrolyzing PLDs; some of which contain a PX and PH domain, while others do not (Ding *et al*., 2017). In *S. cerevisiae*, the PLD1 homolog, Spo14, is required for vesicle fusion to the prospore membrane, sporulation, morphogenesis, and polarized growth in response to pheromone (Hairfield *et al*., 2001; Harkins *et al*., 2008). In *Candida albicans*, PLD1 is necessary for the dimorphic transition and full virulence (McLain and Dolan *et al*., 1997; Hube *et al*., 2001; Dolan *et al*., 2004). The filamentous pathogen *A. fumigatus* encodes three PLD isoforms (PLD, PLD1, PLDA), of which PLD is required for internalization of *A fumigatus* into epithelial cells and for full virulence in certain immunosuppressed mice (Li *et al*., 2012). The wheat pathogen *Fusarium graminearum*, also encodes three *pld* genes. While deletion of *pld2* and *pld3* has no effect on growth or morphology; deletion of *Fgpld1* results in reduced colony size, defects in sporulation and sexual development, decreased production of the mycotoxin deoxynivalenol (DON), and reduced virulence on wheat (Ding *et al*., 2017).

The genome of *E. festucae* carries two genes that putatively encode PC-hydrolyzing PLDs, which we have named PldA and PldB. In this study, we analyse the role of these two proteins in axenic growth of the fungus, as well as in the symbiotic interaction with *L. perenne*. Furthermore, we investigate their contribution to ROS production by the Nox complex.

Materials and Methods

Bioinformatic analyses

Protein sequences were obtained from the Kentucky Endophyte Database (Schardl *et al*., 2013) and annotated using InterproScan (Jones *et al*., 2014) and SMART (Letunic *et al*., 2015). Domains in the PLDs were annotated based on publications by Sung *et al*. (1997) and Sciorra *et al*. (1999 and 2002). BLASTp analyses were performed against fungal reference proteins at NCBI. Alignments were generated using MAFFT version 7 (Katoh *et al*., 2017) and were shaded according to percentage identity in Jalview version 1. The Ensembl genome database (Zerbino *et al*., 2018) was used to compare *E. festucae* PldA and PldB proteins to other phospholipase D sequences. We downloaded a pre-computed protein alignment for the gene family with ID "EGGT00050000001203", which includes the *Saccharomyces cerevisiae* PLD protein Spo14 and added *Epichloë* sequences to this alignment using the "profile" method implemented in Muscle v3.8.31 (Edgar, 2004). Finally, we estimated a maximum likelihood phylogeny from the combined alignment using RAxML v 8.2.12 (Stamatakis, 2014) using the BLOSUM62 model of amino acid substitution. Box plots were generated using BoxPlotR (available on http://shiny.chemgrid.org/boxplotr/). Dunn's test for multiple comparisons, as implemented in the R package dunn.test v 1.3.5 (Dinno, 2017) was used to identify significant differences in the number of hyphae per intercellular space between all deletion and over-expression strains. This test was chosen as it corrects for multiple comparisons and is robust for the non-normality shown in the hyphal-count data. One-way ANOVAs were used to test for differences in plant phenotypes between WT and mutant strains. In each case, the ANOVA was fitted with R, and a Bonferroni correction was applied to all p-values to account for multiple testing. Differences in the number of hyphal fusions and NBT staining were calculated with a t-test.

Strains and growth conditions

Escherichia coli strains were grown in Lysogeny Broth (LB) (Miller, 1972) or on 1.5% LB agar supplemented with 100 µg/ml ampicillin or 50 µg/ml kanamycin overnight at 37°C. *S. cerevisiae* strains were grown in YPDA (1% yeast extract, 2% peptone, 0.01% adenine hemisulfate, 2% glucose, 2% agar; adjusted to pH 5.7) liquid medium or on 2% YPDA agar overnight or for up to three days, respectively, at 30°C. Following transformation, strains were selected on SD synthetic -T/L dropout medium (0.67% yeast nitrogen base without amino acids, 0.064% T/L dropout supplement, 18.23% sorbitol, 2% glucose, 1.6% agar, pH 5.7) and incubated at 30°C until colonies

appeared. For a yeast two-hybrid assays, strains were grown in liquid SD-T/L broth, then plated on SD-T/L/H and -T/L/H/A dropout media (0.67% yeast nitrogen base, 0.064% T/L/H or 0.064% T/L/H/A dropout supplement, 18.23% sorbitol, 2% glucose, 1.6% agar, pH 5.7), and were incubated for up to 5 days at 30°C. *E. festucae* strains were grown on Potato-Dextrose (PD) agar (2.4% PD, 1.5% agar) supplemented with 150 µg/ml hygromycin B and/or 200 µg/ml geneticin for up to seven days at 22°C. Strain details can be found in Supporting Information Table S1.

Plant growth and endophyte inoculation

E. festucae strains were artificially inoculated into *Lolium perenne* cv Samson seeds as previously described (Latch and Christensen, 1985). Inoculated plants were grown in root trainers at 22°C with a photoperiod of 16h light and 8h dark with artificial lighting (approximately 100 µE/m^2/s).

DNA isolation, PCR and sequencing

High quality genomic DNA was purified from freeze-dried *E. festucae* mycelia as described by Byrd *et al*. (1990). Plasmid DNA was extracted and purified from *E. coli* strains using the High Pure plasmid isolation kit (Roche). PCR amplification of short DNA fragments (<3000 bp in length) for screening purposes was conducted using OneTaq® DNA polymerase (NEB) and amplification of DNA fragments for cloning purposes was performed with the Phusion™ DNA polymerase (NEB) according to the manufacturer's instructions. DNA fragments generated with long primers (>30 bp) for Gibson assembly were amplified using a hybrid three-step two-step PCR; the first 5 cycles were performed as per manufacturer's instructions followed by 25 cycles of 10 sec at 98°C (denaturation) and 30 sec/kbp at 72°C (extension), followed by 1 min 72°C (final extension). DNA fragments were separated by electrophoresis on a 0.8% (w/v) agarose gel and purified with the Wizard SV Gel and PCR Clean-Up System (Promega). Sequence authenticity was confirmed at the Massey Genome Centre using the Big-Dye™ Terminator Version 3.1 Ready Reaction Cycle Sequencing Kit (Applied BioSystems, Carlsbad, California, USA) and the ABI3730 genetic analyser (Applied Bio Systems). Sequence data was assembled (ClustalW) and analysed using MacVector v14.5.2.

Preparation of constructs

All constructs were designed using MacVector v14.5.2 and synthesised using Gibson assembly as described by Gibson (2009). All relevant primer sequences can be found

in Supporting Infromation Table S2 and a detailed description of the construct design in Supporting Information Methods S1.

Transformation of organisms

Chemically competent *E. coli* DH5α cells were transformed as described previously (Hanahan, 1983). *S. cerevisiae* AH109 cells were made competent using the lithium acetate method, and then transformed with approx. 600 ng of each plasmid via heat-shock at 42°C for 20 min (Giez *et al*., 2002). Cells were directly plated as described. Protoplasts of *E. festucae* strains were generated as described previously (Young *et al*., 2005), and transformed with up to 5 µg of each plasmid (Itoh *et al*, 1993). Protoplasts were allowed to recover overnight on regeneration agar (RG) before being overlaid with 0.8% RG agar including 150 µg/ml hygromycin B and/or 200 µg/ml geneticin. Protoplasts of the *pldB* deletion strains were allowed to recover for two days before being overlaid with 20-50 µg/ml hygromycin B.

Southern blot analysis

Genomic DNA was extracted as described and 1.2 µg was digested with approx. 30 U of the desired restriction enzyme overnight. Development of the Southern blot was conducted with the Dig Easy Hyb Kit (Roche) as per manufacturer's instructions.

Protein extraction and western blot analysis

E. festucae strains were grown shaking in PD liquid medium for 3-4 days at 21°C. Mycelia was harvested, filtered through nappy liners, washed and snap frozen in liquid nitrogen. The mycelium was ground to a fine powder and resuspended in 0.2-1 mL of lysis buffer (50 mM Tris-HCL, 100 mM NaCl, 10 mM EDTA, 0.2 mM PMFS, 0.1 mM DTT, 1 µl/mL NP40, 1 µl/mL Protease inhibitor cocktail (Roche)) and vortexed. Cell debris was collected by centrifugation at 4°C and 14,000 x g for 15 min, and 15-20 µl of the supernatant (protein suspension) resolved on a 7 or 10% SDS-polyacrylamide gel. After electrophoresis proteins were transferred to a PVDF membrane at 100 V for 60-80 min. The membrane was incubated with a 1:3,000 dilution of primary rabbit anti-GFP antibody (Abcam, ab290) or a 1:2,000 dilution of primary rabbit anti-mCherry antibody (Abcam, ab167453) overnight. This was followed by incubation with a 1:10,000 dilution of secondary goat anti-rabbit horseradish peroxidase (HRP) antibody (Abcam, ab6721) for one hour. Detection of HRP was performed using the Amersham ECL Western blotting detection reagent, as per the manufacturer's instructions (GE Healthcare Life Sciences).

RNA extraction and qRT-PCR

RNA was extracted from snap frozen and ground mycelia using TRIzol (Invitrogen), and cDNA synthesis performed with the QuantiTect Reverse Transcriptase kit (Qiagen). The qRT-PCR was performed with SYBR Green (Invitrogen) on a LightCycler 480 System (Roche), as described by the manufacturer. Each sample was analysed with two technical replicates. As reference genes, the *E. festucae* genes coding for translation elongation factor 2 (*EF-2*, M3 model number on the database http://www.endophyte.uky.edu (Schardl *et al*., 2013): EfM3.021210) and 40S ribosomal protein S22 (*S22*, EfM3.016650) (Lukito *et al*., 2015) were chosen. The gene expression level in the overexpression strains was calculated relative to the expression in WT (Lukito *et al*., 2015). Primers BH185-BH188 were used and sequences can be found in Supporting Information Table S2.

Microscopy

For analysis of the hyphal morphology and localisation of proteins of interest, *E. festucae* strains were grown on a microscope slide covered with 1.5% H_2O agar. Strains were incubated for five to seven days and examined with an Olympus IX83 inverted fluorescence microscope. Cell walls were stained using 3 µl of a 3 mg/ml Calcofluor White (CFW) stock solution, and for the examination of the endomembrane system, 3 µl of a 16.3 µM FM4-64 stock solution were added to the colony just before analysis. For the visualization of nuclei 3 µl of a 0.071 mM 4',6-diamidino-2-phenylindole (DAPI) solution was added to the colony and incubated for 3 min before analysis. For the quantification of fusion events, colonies were incubated for 14 days before analysis. For transmission electron microscopy (TEM), infected plant tissue was fixed in 3% glutaraldehyde and 2% formaldehyde in 0.1 M phosphate buffer (pH 7.2) for 1 h and embedded in resin (Spiers and Hopcroft, 1993). Samples were cut, stained and analysed with a FEI Tecnai G2 Biotwin TEM. Sections were also stained with 0.05% toluidine blue in phosphate buffer and heat-fixed at approx. 100°C for 10 s. These sections were examined with a Zeiss Axiophot Microscope with Differential Interference Contrast (DIC) Optics and Colour CCD camera.

To evaluate hyphal growth *in planta*, infected pseudostem samples were stained with aniline blue diammonium salt (Sigma) and wheat germ agglutinin conjugated to AlexaFluor®488 (WGA-AF488, Molecular Probes/Invitrogen), as described previously (Becker *et al*., 2016; Becker *et al*., 2018). Examination of these samples was performed with a Leica SP5DM6000B confocal microscope (488 nm argon and 561 nm DPSS laser, 40× oil immersion objective, NA = 1.3) (Leica Microsystems).

Superoxide detection

For the detection of superoxide, two methods were utilized, Nitroblue tetrazolium (NBT, Sigma) and the ROS-ID® Superoxide detection kit (ENZO Life Sciences). For NBT staining, colonies were grown for seven days as described above and then stained as reported previously by Tanaka *et al*. (2006). Colonies were photographed and imaged with a Zeiss Axiophot microscope with differential interference contrast (DIC) Optics and Colour CCD camera. For the quantification of hyphae exhibiting the normal staining pattern vs. an irregular stain distribution, two colonies of each strain of interest were stained as described. For each strain, three times approx. 50 hyphae were evaluated.

To perform superoxide staining with the ROS-ID ® Superoxide (ENZO LifeSciences) probe, colonies were grown for seven days as described above. The probe was diluted 1:30 (0.16 mM) in H_2O and 3 µl added to the colonies, followed by 10 min incubation in the dark. Subsequently, samples were analysed with an Olympus IX83 inverted fluorescence microscope and excited with yellow light (550 nm). For co-staining with the mitochondrial staining reagent-green (Cytopainter, Abcam ab176830) the stain was diluted 1:500 in H_2O and 3 µl were added to the colonies. Then the ROS-ID ® Superoxide probe was added as described after 20 min of incubation in the dark.

Yeast two-hybrid

All plasmids used in yeast two-hybrid assays can be found in Supporting Information Table S1. Yeast strain AH109 was transformed as described above, and the assay was performed as described by Green (2016). The assay was conducted twice.

Cellophane penetration test

The cellophane penetration assays were performed as described by Green *et al*. (2019, in press). In short, cellophane disks were autoclaved in H_2O and placed on PD agar plates in one, two or three layers. A small quantity of mycelia was inoculated on top of the cellophane layer and incubated for seven days. Then layers were carefully peeled off and the top layer and the plate were photographed. The assay was performed twice.

Results

The *Epichloë festucae* genome encodes two putative phosphatidylcholine-hydrolyzing phospholipase Ds

To identify genes encoding phospholipase D in the *E. festucae* Fl1 genome, a tBLASTn analysis was performed using *S. cerevisiae* Spo14 as a query sequence. This identified two putative homologues: EfM3.055250 (E-value of 1e-89; hereafter referred to as *pldA*) and EfM3.032570 (E-value of 0; hereafter referred to as *pldB*). An expression analysis of these genes, making use of available transcriptome datasets, showed that both genes are moderately expressed in axenic culture (*pldA*: 10.39 RPMK, *pldB*: 35.96 RPMK) (Hassing *et al*., 2019). The expression of *pldB* is downregulated two-fold *in planta* relative to axenic culture, while the expression of *pldA* is not significantly different (Hassing *et al*., 2019). Neither gene was found to be differentially expressed in the symbiotic mutants analysed to date (Δ*sakA*, Δ*noxA*, Δ*proA*, or Δ*hepA*) (Eaton *et al*., 2015; Chujo *et al*., 2019). PldA and PldB are 877 and 1,713 amino acid residues in length, respectively (Figure 1). These protein sequences share 39.8% amino acid sequence identity with each other. Both were found to contain four conserved domains characteristic of PLDs, including the $HXKX_4D(X_6GSXN)$ (HKD) motif in domains II and IV (Pontig and Kerr, 1996; Koonin, 1996), which are necessary for the phosphatidyltransferase activity of the enzyme (Sung *et al*. 1997; Liscovitch *et al*. 1999; Liscovitch *et al*. 2000). In addition, PldB contains a homologous sequence to a polybasic motif between domains II and III that is required for PtdIns[4,5]P_2 binding and PLD activation in mammals and yeast (Sciorra *et al*., 1999; Sciorra *et al*., 2002). PldA, however, lacks this motif, suggesting that it is activated by a different mechanism (Figure 1). Further analysis using InterproScan (Jones *et al*., 2014) and SMART (Letunic *et al*., 2015) demonstrated the presence of a PX and PH-domains N-terminal of the four conserved domains in the sequence of PldB, but not PldA. Both domains are present in mammalian and fungal PLDs, but only in the Pldζ group of PLDs found in plants. These domains have been shown to bind phosphoinositides (PIs), and are required for localising mammalian Pld1 and Pld2 to specific membranes (Morris, 2007; Selvy *et al*., 2011). The lack of these domains in PldA suggests that a different mechanism may be involved in recruiting this protein to membranes. Furthermore, PldB contains five N-linked glycosylation sites (3 N-terminal, 1 central, 1 C-terminal), whereas PldA contains none (Figure 1A).

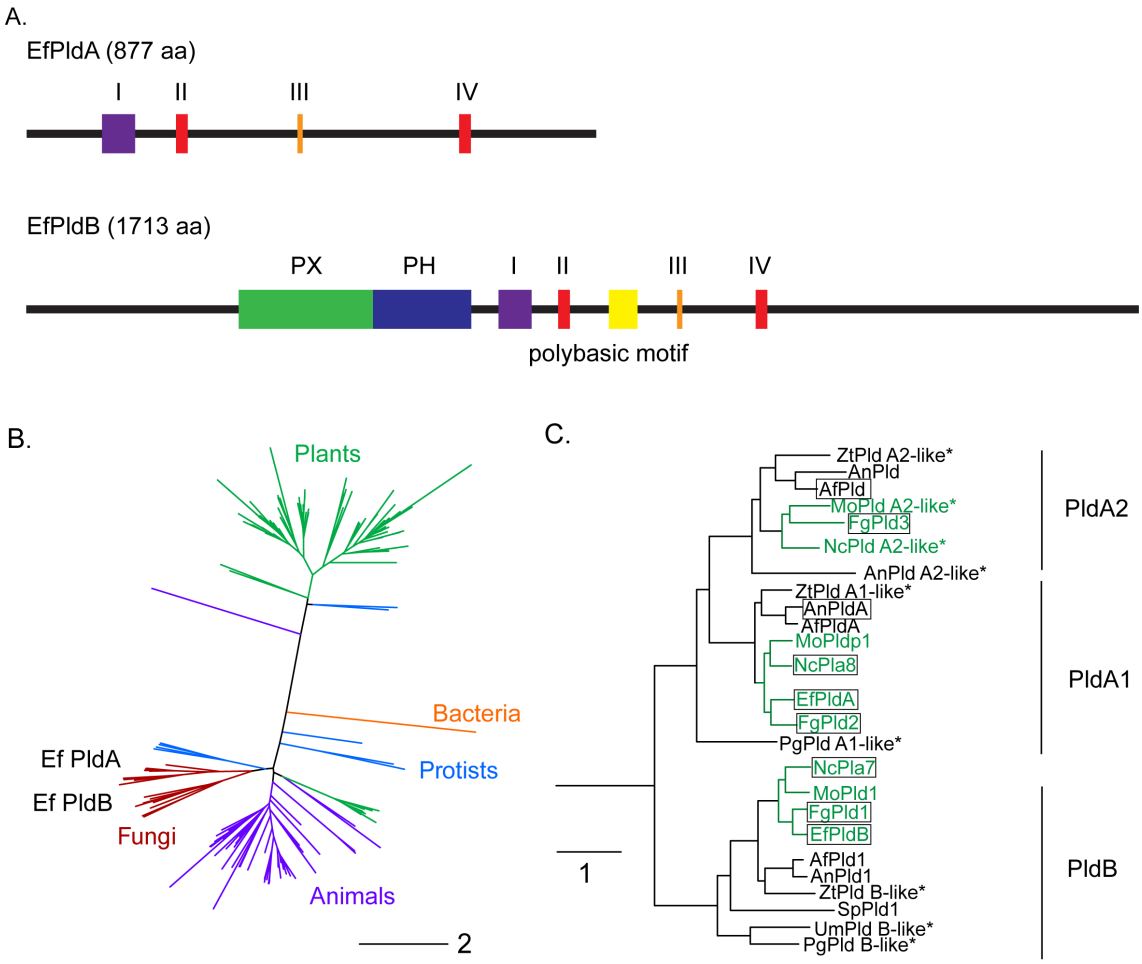

Figure 1: Structure of *Epichloë festucae* PldA and PldB and phylogenetic analysis of phospholipase D in fungi.

(A) Domain structure of PldA and PldB, annotated according to InterProScan (Jones *et al*., 2014), SMART (Letunic *et al*., 2015), and the publications of Sung *et al*. (1997) and Sciorra *et al*. 1999; Sciorra *et al*. 2002); Green box: PX (phox homology) domain; blue box: PH (pleckstrin homology) domain; purple box: motif I; red box: motif II and IV; orange box: motif III; yellow box: polybasic motif; aa: amino acids. (B) Phylogenetic analysis of the distribution of Phospholipases D (PLD) making use of all sequences available on the Esembl genome browser (Zerbino *et al*., 2018). Bar indicates a/a substitutions per site. (C) Phylogenetic analysis of PLDs in filamentous fungi with sequences highlighted in green belonging to the Sordariomycetes. Boxed proteins have previously been characterised. Proteins marked with * are described as “putative/hypothetical Pld” in NCBI databases and have therefore been renamed for clarity. Unique identifiers can be found below. *Ef*: *Epichloë festucae* (EfPldB: EfM3.032570, EfPldA: EfM3.055250); *Fg*: *Fusarium graminearum* (FgPld1: XP_011318823.1, FgPld2: XP_011317835.1, FgPld3: XP_011324813.1); *Mo*: *Magnaporthe oryzae* (MoPld1: XP_003717990.1, MoPldp1 XP_003712119.1, MoPld

A2-like: XP_003712056.1*); *Nc*: *Neurospora crassa* (NcPla7: XP_957594.3, NcPla8: XP_001728077.1, NcPld A2-like: XP_962376.3*); *Af*: *Aspergillus fumigatus* (AfPld1: KEY78740.1, AfPldA; XP_748951.1, AfPldA2 like: XP_755989.2), *An: Aspergillus nidulans* (AnPld1: ANIA_10413, AnPldA; ANIA_06712, AnPld: ANIA_02586, AnPld A2-like: ANIA_07334*), *Zt: Zymoseptoria triciti* (ZtPldB1: XP_003857513*, ZtpldA_like: XP_003848870*, ZtPldA2_like: XP_003855368*), *Pg: Puccinia graminis* (PgPld B-like XP_003322083.2*, PgPldA_like: XP_003330640.2*), *Sp: Schizosaccharomyces pombe* (SpPld1: CBE61318.1), *Um: Ustilago maydis* (UmPld B-like: KIS71943*). Bar indicates a/a substitutions per site.

Phylogenetic analysis of all PLD sequences available on the Ensembl genome browser (Zerbino *et al*., 2018), revealed a separation between plant and mammalian/fungal PLDs, presumably due to the presence of the different protein domains. Using only selected sequences we observed a separation between PldB-like and PldA-like PLDs within the fungal kingdom, demonstrating that both isoforms are conserved among filamentous fungi. However just the PldB-like isoform is present in unicellular yeasts. All analysed fungal genomes with the exception of *E. festucae* contained a third PLD isoform, which separated as a subgroup of PldA-like PLDs, which we have named PldA2-like (Figures 1B & 1C).

An amino acid sequence alignment of PldA and PldB with the corresponding homologs from *N. crassa, M. oryzae, F. graminearum* and *A. fumigatus*, as identified by a reciprocal BLAST analysis, revealed that PldA and PldB homologs have high sequence identity (an average of 68.02% and 58.22%, respectively) (Supporting Information Fig. S1A). For PldB, the sequences were most similar within the catalytic core, whereas the N- and C-terminal regions showed a higher degree of divergence (Supporting Information Fig.S1B).

PldB is required for normal colony growth and hyphal fusion

To investigate whether PldA and PldB are required for normal colony growth in *E. festucae*, each gene was individually deleted from the wild-type (WT) background using a gene replacement approach. For the deletion of *pldA* the linear deletion cassette was amplified by PCR from the corresponding deletion construct (pCE131) and transformed into WT protoplasts. For the deletion of *pldB* the linear deletion cassette was amplified by PCR in two fragments with an overlapping region of approx. 600 bp (pCE121). This split marker approach has been shown to increase transformation efficiency (Rahnama *et al*., 2017). Approximately 200 hygromycin-resistant *pldA* transformants and 500 geneticin-resistant *pldB* transformants were

screened by PCR for the integration of the cassette at the target loci. Positive transformants were subsequently analysed by Southern blot analysis to verify the successful replacement of the target gene. This analysis resulted in the identification of three hygromycin-resistant *pldA* deletion strains (#T47, #T49, #T82) and three geneticin-resistant *pldB* deletion strains (#T26, #T50, #T87) (Supplemental Figure S2A). All three *pldA* deletion strains contained the resistance cassette in the target locus just once. *pldB* deletion strains T26 and T50 contained tandem or tandem and ectopic integrations of the resistance cassette and only T87 contained a single integration at the target locus (Supporting Information Fig. S2B).

Although deletion of *pldA* had no effect on growth and colony morphology, deletion of *pldB* deletion had a dramatic effect with a significant reduction in colony size and an increase of aerial hyphae (Figure 2). Further analysis using microscopy confirmed that the hyphal morphology of the *pldA* deletion strains was indistinguishable from WT (Figure 2). In contrast, *pldB* deletion strains frequently had swollen and highly vacuolated hyphae and hyphal tips (Figure 2). Staining of the colony with the chitin stain CFW revealed occasional accumulation of the stain in the cytoplasm of hyphae, which is indicative of a defect in the recycling of cell wall components (Higuchi *et al*., 2009). Intra-hyphal hyphae (i.e. hyphae growing within hyphae, IHH) were also occasionally detected. Although both strains formed hyphal bundles and coils like WT, no cell-to-cell fusion could be observed in the *pldB* deletion strains (Figures 2 and S4). To verify this cell-to-cell fusion defect, *pldB* deletion strains expressing either GFP or mCherry under the regulation of a constitutive promoter were inoculated in close proximity and analysed for signs of cytoplasmic mixing (Becker *et al*., 2015). WT hyphae with both GFP and mCherry fluorescence were frequently observed, but in the *pldB* deletion strains the hyphae had either GFP or mCherry fluorescence but not both (Figure 3). Introduction of *pldB* gDNA containing both the native promoter and terminator regions into the *pldB* deletion strains fully restored colony growth, hyphal morphology and hyphal fusion, confirming this mutation could be complemented. Like wild type these strains lacked CFW accumulations and IHH (Figure 2).

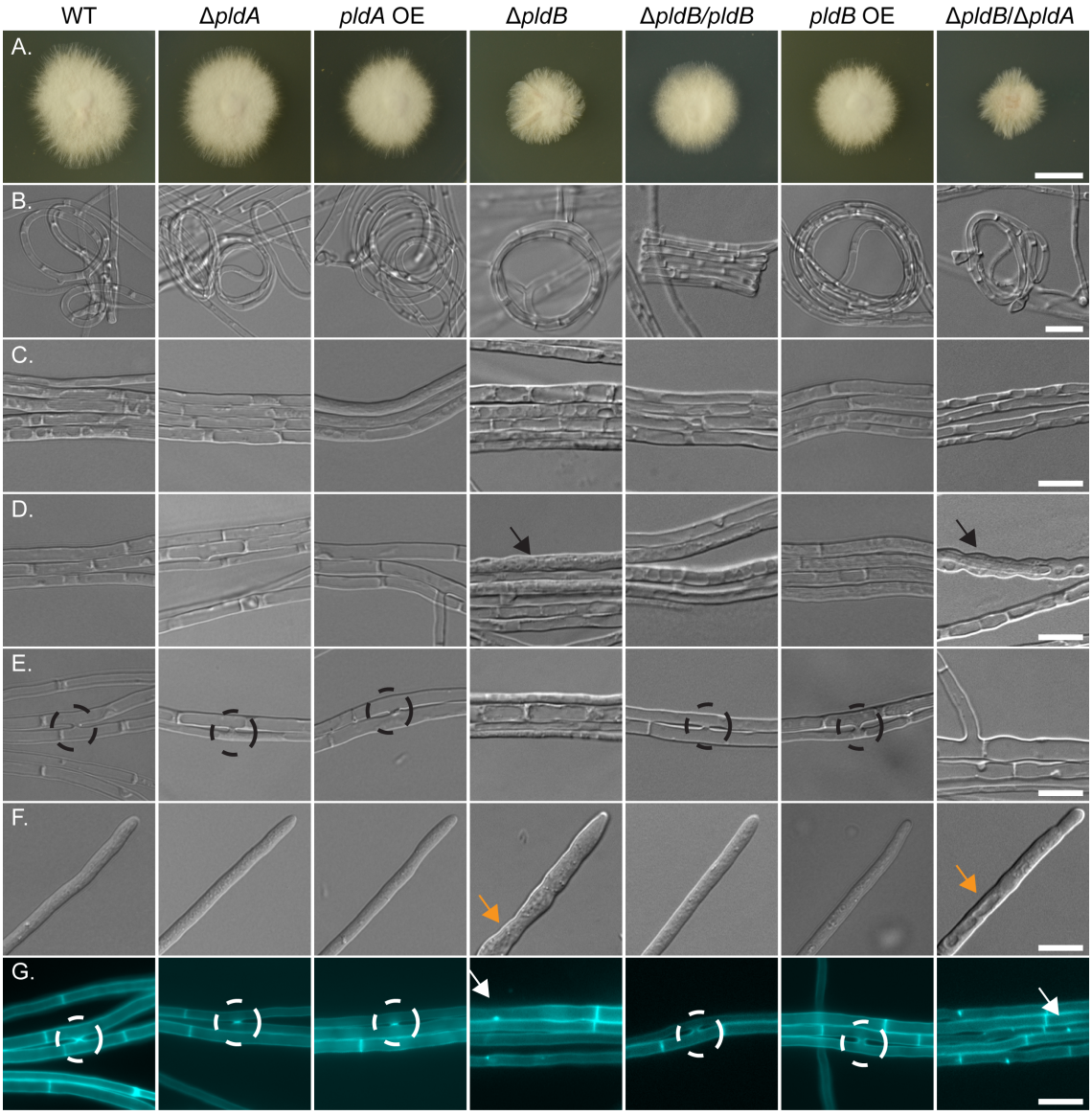

Figure 2: Culture phenotype of wild-type *Epichloë festucae* and *pldA* and *pldB* mutant strains.

The phenotype of wild-type (WT) strain and three independent mutants of each genotype were analysed. The images of Δ*pldA*#T47, *pldA* OE#T4, Δ*pldB*#T87, Δ*pldB*T#87/*pldB*#T4, *pldB* OE#T21, Δ*pldB*/Δ*pldA*#T3 shown are representative of all strains analysed. (A) Representative image of the whole colony morphology after seven days on 2.4% potato-dextrose agar; Bar = 1 cm; (B-G) representative differential interference contrast microscopy images of hyphal morphology after seven days of incubation on 1.5% H_2O agar; Bar = 10 µm; (B) hyphal coil; (C) hyphal bundle; (D) intra-hyphal hyphae; (E) hyphal fusion; (F) hyphal tip; (G) hyphae stained with calcofluor white (CFW) to examine cell wall composition. Black arrows: intra-hyphal hyphae; dashed circle: hyphal fusion; orange arrows: vacuolated hyphal tips; white arrows: cytoplasmic CFW accumulations.

To determine whether there was any functional redundancy between PldA and PldB, double deletion strains were generated. To this end, *pldA* was deleted in the *pldB* T26 and T87 backgrounds. Protoplasts of the *pldB* deletion strains T26 and T87 were transformed with the linear *pldA* replacement construct as described in the Materials and Methods. PCR screening identified two strains carrying a 'clean' *pldA* deletion (Δ*pldB*#T26Δ*pldA*#T5, Δ*pldB*#T87Δ*pldA*#T3; hereafter referred to as Δ*pldB/*Δ*pldA*#T3 and Δ*pldB/*Δ*pldA*#T5) (Supporting Information Fig. S2). The culture phenotype of the double deletion strains was comparable to the single *pldB* deletion strains for whole colony morphology as well as hyphal growth (Figure 2).

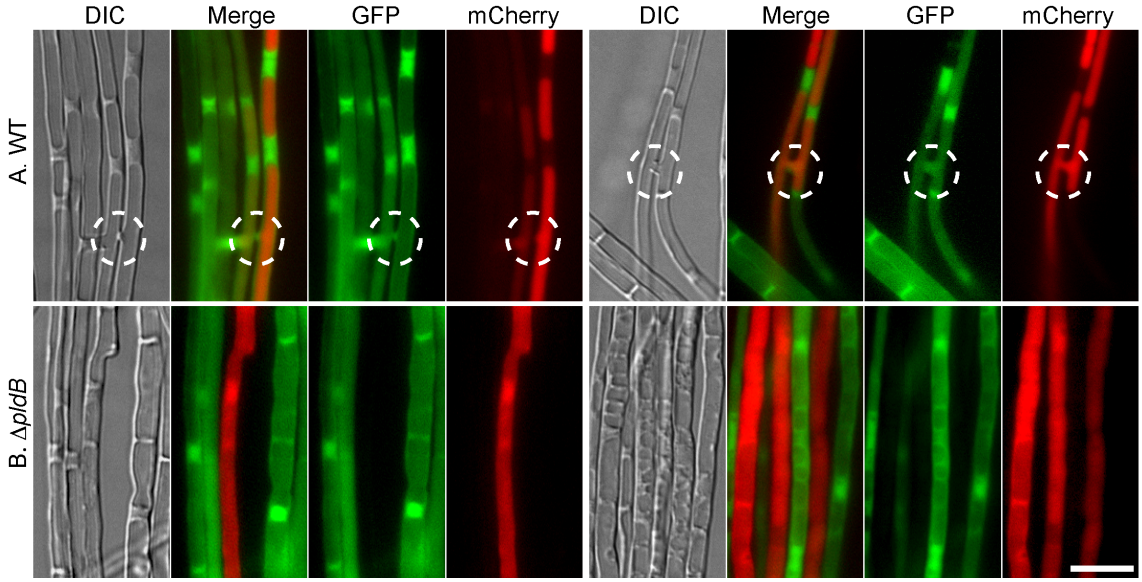

Figure 3: Cytoplasmic mixing of wild-type and *pldB* deletion strains of *Epichloë festucae* expressing cytoplasmic GFP and mCherry.

Wild-type (WT) strains expressing cytoplasmic GFP (pBH28) and mCherry (pCE126) (WT GFP#T1/WT mCherry#T1) (A) and *pldB* deletion strains (Δ*pldB*#T26 GFP#T1/Δ*pldB*#T26 mCherry T2) (B) expressing cytoplasmic GFP or mCherry were co-cultured on 1.5% H_2O agar for 7 days. Strains were examined for hyphae expressing both GFP and mCherry to indicate hyphal fusion followed by cytoplasmic mixing. White, dashed circles: hyphal fusion; Bar = 10 µm.

To determine whether overexpression of these genes would influence fungal growth, *pldA* and *pldB* overexpression strains were generated in the WT background. Overexpression constructs driven by the *A. nidulans gpdA* promoter were generated and transformed into WT protoplasts (pCE129, pBH48). Expression of the corresponding gene was analysed by relative qRT-PCR, and strains with a range of gene overexpression values were chosen for analysis (*pldA* OE strains: T3, T4, T9,

pldB OE strains: T6, T21, T22; Supporting Information Fig. S2). Analysis of the overexpression mutants revealed no differences in the culture phenotype in comparison to the WT strain (Figure 2).

In summary, the deletion of *pldB* was found to result in a severe change in axenic culture phenotype, accompanied by altered hyphal morphology and a lack of cell-to-cell fusion, whereas the deletion of *pldA* resulted in no obvious phenotypic changes.

Localisation of PldA and PldB

PLDs analysed to date have localised to various cellular compartments, such as the Golgi apparatus, vesicles, the plasma membrane (PM), and the cytosol (Colley *et al*., 1997; Hughes and Parker, 2001; Du *et al*., 2003; Selvy *et al*. 2011). To investigate the localisation of *E. festucae* PldA and PldB, N-terminal GFP and C-terminal mCherry translational fusion constructs were designed and transformed into WT protoplasts. Expression of fusion proteins of the expected size was verified by western blot analysis (Supporting Information Fig. S5).

PldA fusion proteins were found to localise to the cytoplasm in hyphal tips, young hyphal bundles as well as in older hyphae. Apparent localisation to septa in older hyphae was likely caused by the accumulation of the cytoplasmic content in the cell periphery due to the size of the vacuole, as indicated by the concave shape of the signal. This was comparable to strains expressing cytosolic GFP driven by the same promoter (Figure 4). PldB fusion proteins were found to localise to the cytoplasm of hyphae of all ages. In young bundles, as well as mature hyphae, the signal was also detected in septa and occasionally associated with the PM (Figure 4). This could indicate a transient localisation to the membrane, as has been described previously (Selvy *et al*., 2011).

Analysis of plant material revealed localisation of the GFP fusion proteins to round organelles in endophytic as well as epiphyllous hyphae. This was comparable to the signal detected from cytoplasmic GFP, and might therefore be an artifact caused by the overexpression of otherwise lowly expressed proteins.

To confirm the functionality of the PldB localisation constructs they were transformed into protoplasts of *pldB* deletion strains (T26 and T87). Introduction of these localisation constructs restored WT like growth in axenic culture confirming they were functional (Data not shown). Expression of the GFP and mCherry fusion proteins of the expected size was verified by western blot (Supporting Information Fig. S5).

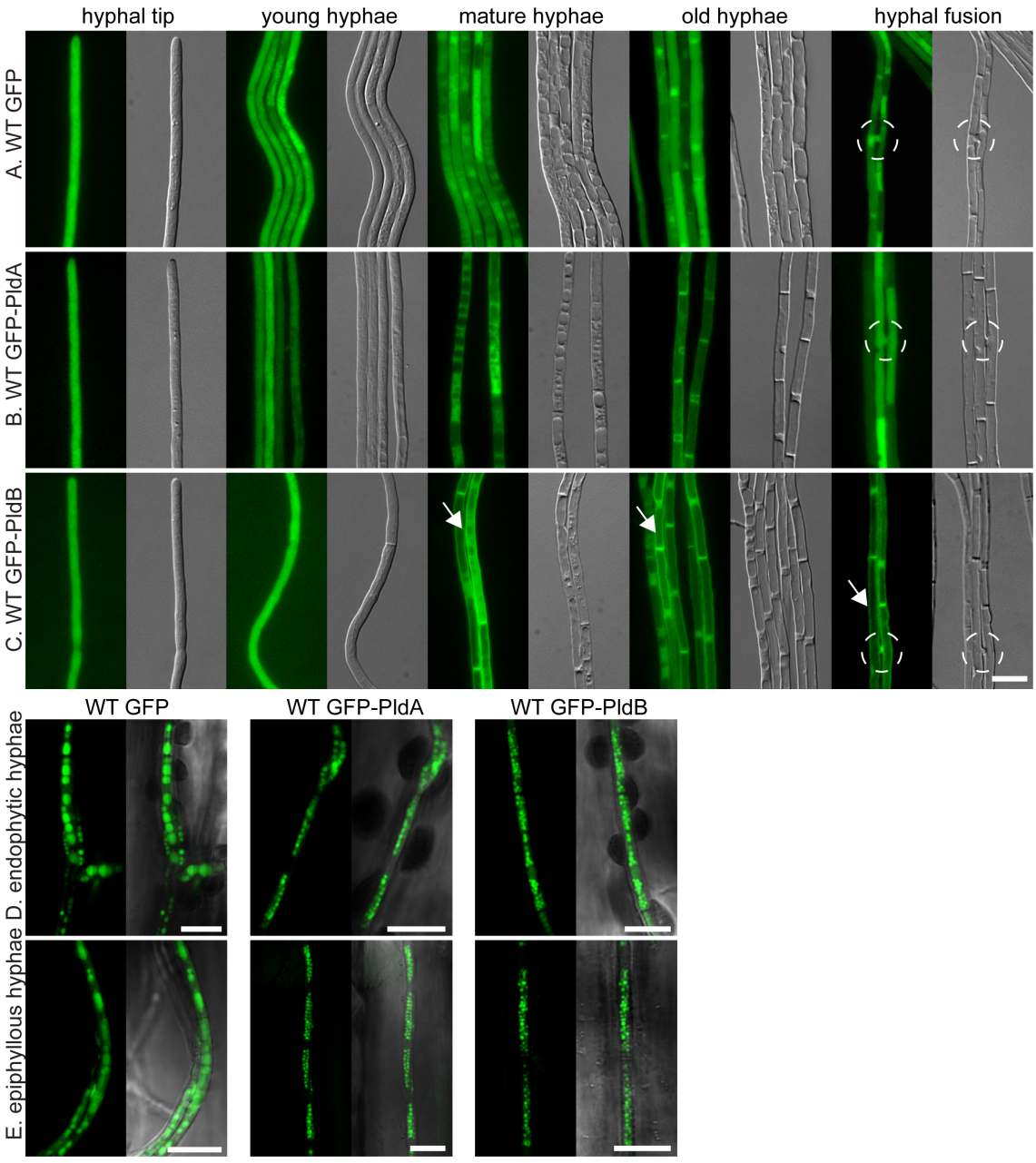

Figure 4: Localisation of GFP-PldA and GFP-PldB in *Epichloë festucae* grown in axenic culture and *in planta*.

(A-C) Wild-type (WT) strains expressing either (A) cytoplasmic GFP (pBH28, #T6), (B) GFP-PldA (pBH37, #T4), or (C) GFP-PldB (pBH54, #T14) fusion proteins were analysed in axenic culture by fluorescence microscopy after approx. five days of incubation. Localisation of the constructs *in planta* was analysed in mature plants (>10 weeks old) infected with cytoplasmic GFP (#T1), GFP-PldA (#T14), or GFP-PldB (#T15) in (D) endophytic hyphae and (E) epiphyllous hyphae by CLSM. White arrow: PM localisation of GFP-PldB; Bar = 10 µm. The images shown here are representative of multiple transformants containing these constructs growing either in axenic culture or *in planta*.

Interaction partners of PldB

In mammalian cells, PA has been found to interact directly with NoxA, and PLD1 and PLD2 have been found to interact with proteins involved in Nox complex activation; e.g. Rho and ARF GTPases, protein kinase C and the phosphoinositide 5-kinase (Selvy *et al*., 2011). Given only PldB was found to be crucial for growth in culture and *in planta*, only PldB was tested for interactions with the corresponding fungal homologs (RacA, Cdc24, Cdc42, PkcA (EfM3.006500), MssD (EfM3.031950)), and the remaining cytosolic components of the Nox complex, NoxR and BemA, by yeast two-hybrid. None of the tested interactions were positive on selection media, indicating that PldB does not interact with any of the cytosolic components of the Nox complex or with homologs of known interactors in mammalian cells (Supporting Infromation Fig. S6).

PldB is crucial for the *E. festucae*-*L. perenne* interaction and expressoria formation

To analyse the role of PldA and PldB in the mutualistic interaction with its grass host, deletion and overexpression strains were inoculated into *L. perenne* seedlings. At eight weeks post-planting, plants infected with *pldA* deletion or overexpression strains, or with *pldB* overexpression strains, were indistinguishable from those infected with the WT fungus. In contrast, plants infected with either of the *pldB* deletion strains were severely and significantly stunted (Figure 5). Statistical analysis of the length and number of tillers verified a significant difference between WT and *pldB* deletion strain-infected plants in regard to tiller length. Plants infected with the strain Δ*pldB*#T87 however also demonstrated a significantly increased number of tillers. Plants infected with the double deletion strain Δ*pldB/*Δ*pldA*#T3 were comparable to those infected with single *pldB* deletion strains, and all examined complementation strains were found to fully restore WT-like plant growth (Figure 5).

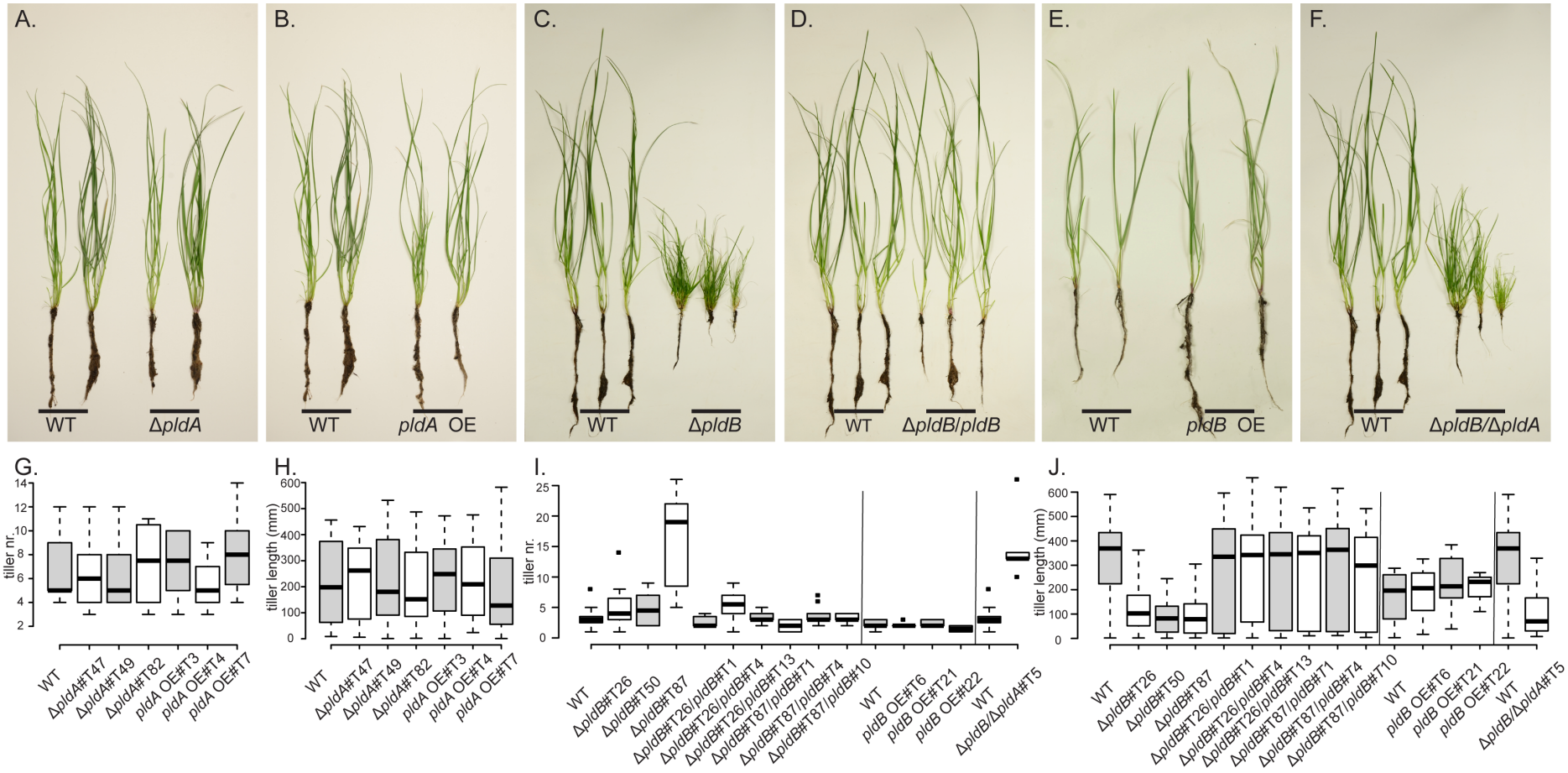
A.
WT
ΔpldA
B.
WT
pldA OE
C.
WT
ΔpldB
D.
WT
ΔpldB/pldB
E.
WT
pldB OE
F.
WT
ΔpldB/ΔpldA
G.
tiller nr.
WT
ΔpldA#T47
ΔpldA#T49
ΔpldA#T82
pldA OE#T3
pldA OE#T4
pldA OE#T7
H.
tiller length (mm)
WT
ΔpldA#T47
ΔpldA#T49
ΔpldA#T82
pldA OE#T3
pldA OE#T4
pldA OE#T7
I.
tiller nr.
WT
ΔpldB#T26
ΔpldB#T50
ΔpldB#T87
ΔpldB#T26/pldB#T1
ΔpldB#T26/pldB#T4
ΔpldB#T26/pldB#T13
ΔpldB#T87/pldB#T1
ΔpldB#T87/pldB#T4
ΔpldB#T87/pldB#T10
WT
pldB OE#T6
pldB OE#T21
pldB OE#t22
WT
ΔpldB/ΔpldA#T5
J.
tiller length (mm)
WT
ΔpldB#T26
ΔpldB#T50
ΔpldB#T87
ΔpldB#T26/pldB#T1
ΔpldB#T26/pldB#T4
ΔpldB#T26/pldB#T13
ΔpldB#T87/pldB#T1
ΔpldB#T87/pldB#T4
ΔpldB#T87/pldB#T10
WT
pldB OE#T6
pldB OE#T21
pldB OE#T22
WT
ΔpldB/ΔpldA#T5

Figure 5: Plant phenotype of *Lolium perenne* infected with wild-type and *pldA* and *pldB* mutant strains.

Plants infected with the wild-type (WT) strain and three independent transformants for each mutation, with the exception of the double deletion strain, were analysed by microscopy. The images shown here are representative of plants infected with all analysed strains. Strains depicted here are the deletion mutants Δ*pldA*#T47, Δ*pldB*#T87, Δ*pldB*/ΔpldA#T5, and Δ*pldB*#T86/*pldB*#T4 and overexpression strains *pldA* OE#T4 and *pldB* OE#T21. (A-F) Plant phenotype of WT and mutant-infected plants 8 weeks post-planting (10 weeks post-inoculation); (G-J) boxplot representation of tiller number (G and I) and tiller length (G and H) of infected plants; (G and H) data of *pldA* mutant-infected plants, WT (n = 5), Δ*pldA* (n = 6/6/4), *pldA* overexpression (n = 6/8/8); (I and J) data of *pldB* mutant-infected plants, WT (n = 11/6/11), Δ*pldB* (n = 8/6/7), *pldB* complementation (n = 11/10/10/9/13/10), *pldB* overexpression (n = 5/6/2) and Δ*pldB*Δ*pldA* double deletion (n = 7). Note that the *pldB* deletion and complementation strains and overexpression strains were analysed in different experiments and therefore can only be compared to the WT of the same experiment. This is indicated by black lines in the graphs. One-way ANOVAs were used to test for differences in plant phenotypes between WT and mutant strains. In each case, the ANOVA was fitted with R, and a Bonferroni correction was applied to all p-values to account for multiple testing. Error bars represent the standard deviation. Only *pldB* and *pldB/pldA* deletion strains had a significantly reduced tiller length (#T26: P = 1.01E-7; #T50: P = 1.22E-8; #T87: P = 2.04E-13; Δ*pldB*/ΔpldA#T5: P = 1.09E-12) and only Δ*pldB*#T87 and Δ*pldB*/ΔpldA#T5 had an increased tiller number (P = 5.57E-12; P = 1.95E-10).

To investigate hyphal growth *in planta*, pseudostem cross sections were fixed and embedded in resin. Sections were stained with toluidine blue, revealing the location of hyphae in the cross section. An average of 1.33 hyphae were found between neighbouring plant cells in the *pldA* deletion, 1.37 in the *pldA* overexpression and 1.27 in the *pldB* overexpression strain-infected plants, values which are all comparable to that of WT-infected samples with an average of 1.28 hyphae (Figure 6 & Supporting Information Fig. S7). However, in plants infected with the *pldB* deletion, an average of 3.02 hyphae were observed in the intercellular space, demonstrating a significant increase in hyphal biomass (P < 0.0000). TEM analysis of the same sections revealed an occasional colonisation of vascular bundles by the *pldB* deletion strains, a phenotype not found for WT or any of the other examined strains (Figure 6). Furthermore, IHH were frequently detected in *pldB* deletion strains, but not in the other

strains and hyphae in the *pldB* deletion strains as well as in the double deletion strains were often found to be less electron dense or completely vacuolated (Figure 6). Some hyphae of WT and *pldA* deletion strains were found to be epiphyllous or located just below the cuticle. In the latter case, the cuticle was not present on the very top of the hyphae, indicative of degradation. Epiphyllous hyphae of the *pldB* deletion strains were also observed, however when hyphae were located below the cuticle, they did not show any signs of degradation. This indicates that *pldB* deletion strains proliferate below the cuticle (Figure 6).

To examine the extend of host colonisation longitudinal pseudostem sections were infiltrated with wheat germ agglutinin conjugated to AlexaFlour 488 (WGA-AF488) (a chitin-binding lectin; blue pseudocolour), and aniline blue, a β-glucan-binding dye (red pseudocolour), and analysed via confocal laser scanning microscopy (CLSM). Only septa of endophytic hyphae generally fluoresce with WGA-AF488 because chitin in the cell wall is either converted into chitosan or masked (Becker *et al*., 2016). However, epiphyllous hyphae fluoresce uniformly with both aniline blue and WGA-AF488. Analysis of plants infected with the *pldA* deletion and *pldA* and *pldB* overexpression strains revealed an *in planta* hyphal cellular phenotype indistinguishable from plants infected with WT (Figure 7). In comparison, plants infected with the *pldB* deletion strains had multiple hyphae between plant cells, which formed bundles and multicellular lobed structures. Furthermore, *pldB* deletion strains were unable to form expressoria. Instead, hyphae proliferated immediately below the cuticle (green pseudocolour), occasionally breaching it, presumably by mechanical force exerted by the mass of hyphae. This resulted in multiple smaller and less numerous epiphyllous hyphal networks (Figure 7). To further investigate the loss of expressoria, strains were tested for their ability to penetrate cellophane layers in axenic culture. Like *noxA* deletion strains, *pldB* deletion strains were still able to penetrate up to three cellophane layers, despite the inability to form expressoria *in planta* (Supporting Information Fig. S8).

The Δ*pldB*/Δ*pldA* double deletion strain exhibited an *in planta* hyphal phenotype comparable to the single Δ*pldB* single deletion strain, while complementation strains exhibited a range of different hyphal growth patterns (Figure 7). Some showed a complete restoration of WT-like growth including the formation of normal expressoria whereas others exhibited an increased hyphal biomass and frequent subcuticular hyphae (data not shown).

Thus, the deletion of *pldB* results in the loss of restrictive growth of *E. festucae* *in planta*, a reduction of the epiphyllous network on the plant surface, and a break-

down of the symbiosis. The deletion or overexpression of *pldA*, however, does not influence growth *in planta*.

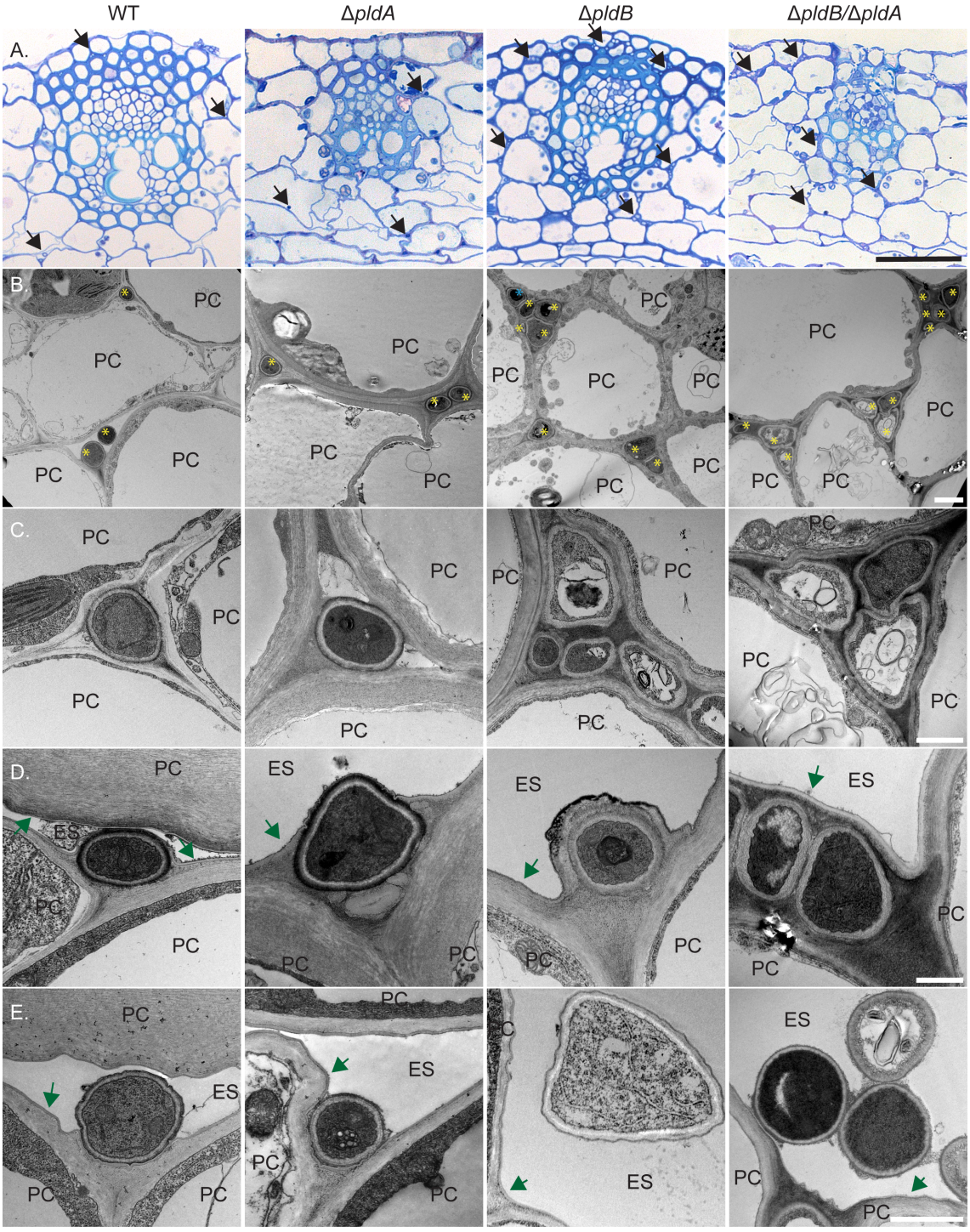

Figure 6: Light microscopy and transmission electron microscopy of *Lolium perenne* pseudostem cross sections infected with wild-type and *pldA and pldB* mutant strains of *Epichloë festucae*.

Plants infected with wild-type (WT) and three independent *pldA* and three independent *pldB* deletion strains were analysed. Here only Δ*pldA*#T47, Δ*pldB*#T26 and

Δ*pldB*/Δ*pldA*#T5 infected plants are shown as representation of all analysed strains. As plants infected with *pldA* and *pldB* overexpression strains were asymptomatic no TEM analysis was performed. (A) Vascular bundles of WT and mutant-infected plants stained with toluidine blue and imaged with a light microscope; Bar = 50 µm; (B) Representative TEM micrograph of growth of WT and mutant strains in infected plants; Bar = 10 µm. (C) Representative TEM micrograph of the hyphal structure of WT and mutant strains in infected plants; Bar = 1 µm. (D) Representative TEM micrograph of a subcuticular hypha of WT and mutant strains in infected plants; Bar = 1 µm. Note the cuticle degradation on top of the WT and Δ*pldA* hyphae. (E) Representative TEM micrograph of epiphyllous hyphae of WT and mutant strains in infected plants; Bar = 1 µm. Black arrow/yellow star: hyphae, blue star: intra-hyphal hypha, green arrow: cuticle, PC: plant cell. ES: extracellular space.

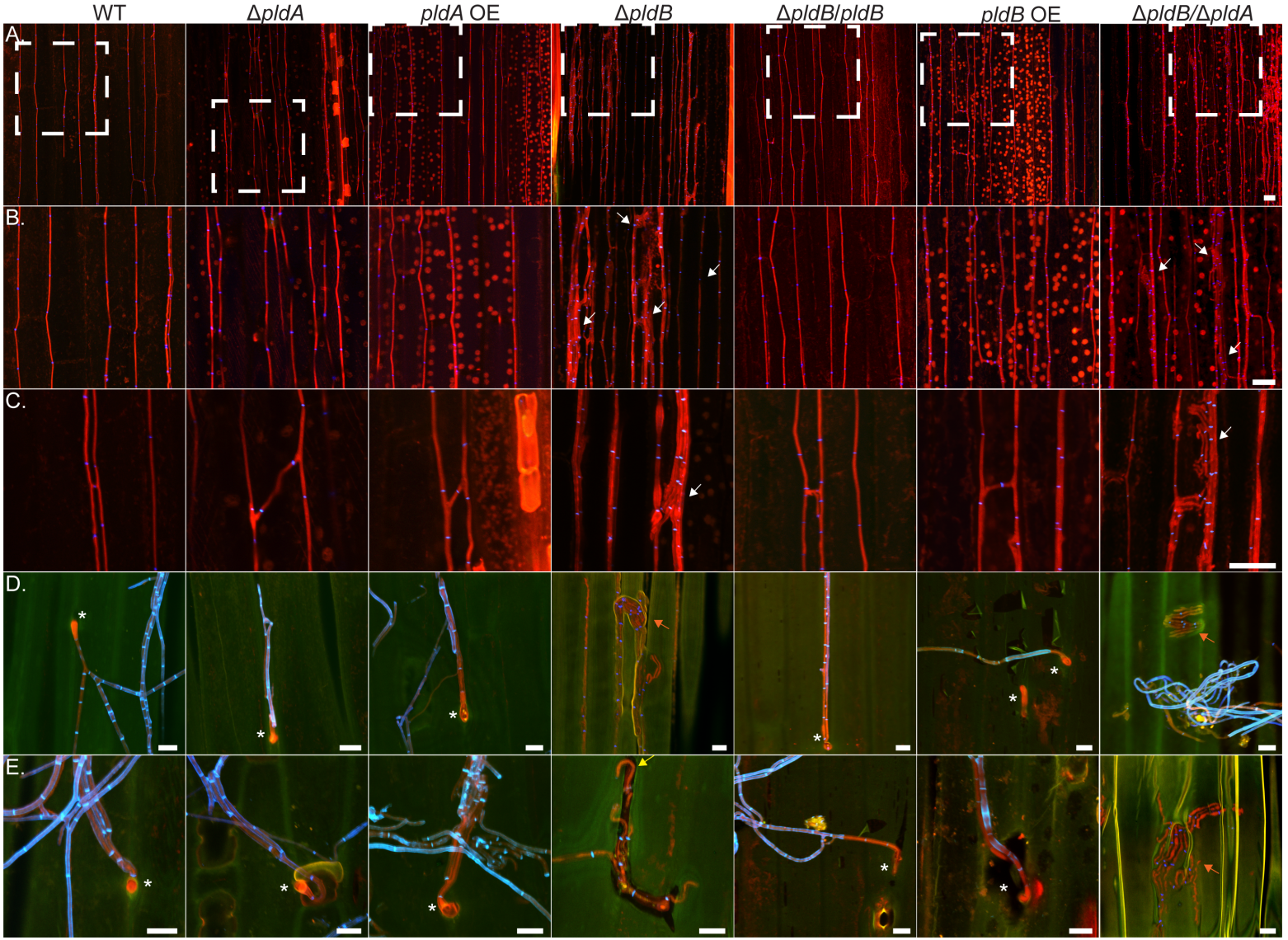
WT
ΔpldA
pldA OE
ΔpldB
ΔpldB/pldB
pldB OE
ΔpldB/ΔpldA
A.
B.
C.
D.
E.

Figure 7: Confocal depth image series of the cellular phenotype of *Lolium perenne* infected with *Epichloë festucae* wild-type, *pldA* and *pldB* mutant strains. Three independent transformants of each described genotype were analysed. Images of only strain are shown, as they are representative of all strains analysed. Strains depicted here are the deletion strains Δ*pldA*#T47, Δ*pldB*#T87 and Δ*pldB*/Δ*pldA*#T5, the complementation strain Δ*pldB*#T87/*pldB*#T4 and the overexpression strains *pldA* OE#T4 and *pldB* OE#T21. Infected *L. perenne* pseudostem samples were stained with WGA-AF488 (chitin-binding, blue pseudocolour) and aniline blue (β-glucan-binding, red pseudocolour) and visualised with confocal laser scanning microscopy. In images showing epiphyllous hyphae (D and E), autofluorescence of the cuticle was captured in green pseudocolour. (A) Representative image (Z = 6 µm) of growth of wild-type (WT), *pldA* (#T47) and *pldB* (#T87) deletion and overexpression strains (#T7/#T21), *pldB* complementation (Δ*pldB*#T87 C4) and *pldB/pldA* double deletion strains (#T5) *in planta*; (B) magnified image of the dashed, white-boxed area in (A); (C) higher magnification image (Z = 4 µm) of representative hyphal branching and fusion *in planta*; (D and E) representative images of an expressorium formed by WT and mutant strains (Z = 4 µm); subcuticular hyphae retained the staining pattern of endophytic hyphae; white arrow: endophytic hyphal bundles in *pldB* deletion and double deletion strains; yellow arrow: hyphae escaping from below the cuticle through rip in cuticle; orange arrow: subcuticular hyphae, note the green hue on hyphae; white star: expressorium. Bar = 10 µm.

Deletion of *pldB*, but not *pldA*, results in decreased localisation of a phosphatidic acid biosensor to the plasma membrane

To analyse the effect of the *pldA* and *pldB* deletions on the localisation of PA in the cell, a PA biosensor was employed. A translational fusion construct was generated from the Spo20 PA-binding domain and GFP, as described by Potocký *et al*. (2014). This construct (henceforth referred to as GFP-PAS, pBH50) was transformed into WT, Δ*pldA* and Δ*pldB* strains, and expression of the fusion protein verified by western blot analysis (Supporting Information Fig. S9).

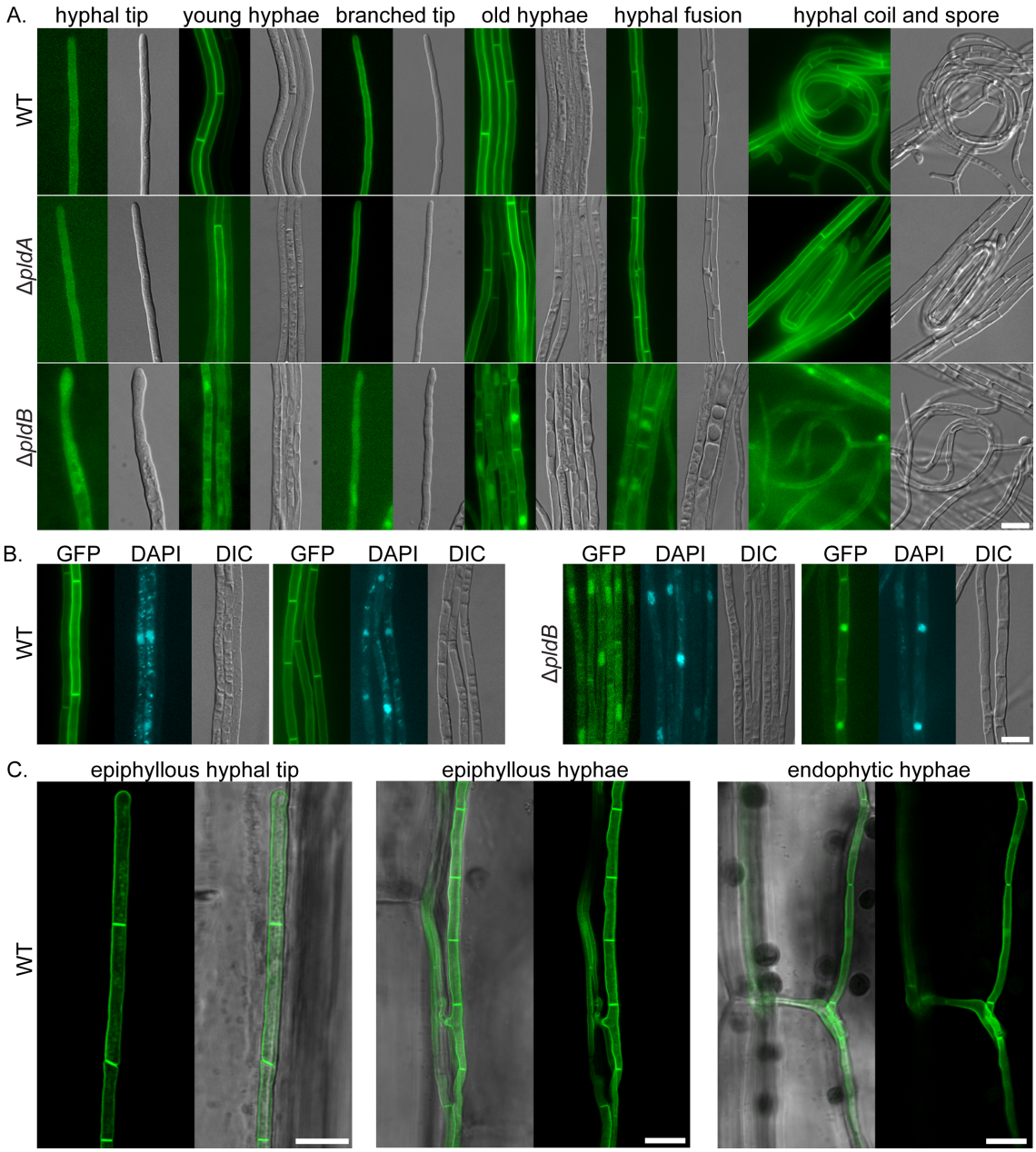

Figure 8: Localisation of the phosphatidic acid biosensor in *Epichloë festucae* wild-type and *pldA* and *pldB* deletion strains growing in axenic culture and *in planta*.

Phosphatidic acid biosensor (PAS, pBH50) constructs were transformed into wild-type (WT) and two different *pldA* (#T47 and #T82) and *pldB* (#T26 and #T87) deletion strains, and multiple transformants analysed. Here, the localisation in WT GFP-PAS #T4, Δ*pldA*#T82 GFP-PAS#T10 and Δ*pldB*#T26 GFP-PAS#T1 are shown as representative of all strains analysed. (A) Strains expressing the PA biosensor were analysed after approx. 5 days of incubation and hyphae of different ages and developmental stages are shown. (B) WT GFP-PAS and Δ*pldB*#T26 GFP-PAS#T1 were incubated as described and stained with 0.071 mM 4',6-diamidino-2-phenylindole

(DAPI) to visualize nuclei. (C) Localisation of the PA biosensor in WT GFP-PAS-infected, mature (>10 weeks) *L. perenne* plants. Representative pictures of the localisation in endophytic and epiphyllous hyphae, as well as n epiphyllous hyphal tips, are shown. Bar = 10 µm.

In the WT strain, the biosensor localised to the PM and septa in young as well as mature hyphae. Interestingly, the signal in recently branched hyphal tips was found to be more intense than in the tips of the colony growth front. PA localisation in the *pldA* deletion strains was indistinguishable from the WT. However, in the *pldB* deletion strains, the signal was largely cytoplasmic, and localisation to the PM and septa was only detected in mature hyphae (Figure 8A). In addition, the PA biosensor accumulated in a circular organelle in the cytoplasm exclusively in the *pldB* deletion strains. Co-staining with the nucleic acid marker DAPI identified these as fungal nuclei (Figure 8B). To examine the localisation of PA in fungal hyphae *in planta*, a WT strain with a PA biosensor construct was inoculated into *L. perenne* seedlings and examined for GFP expression in mature plants. Similar to that described above, the signal was detected evenly along the PM of endophytic as well as epiphyllous hyphal tips and mature hyphae (Figure 8C).

Absence of PldB results in mislocalised ROS production

To investigate the role of PA produced by PldA and PldB in the activation or recruitment of the Nox complex, the production and localisation of superoxide was analysed in culture, making use of NBT and a ROS-ID® Superoxide kit.

When stained with NBT, WT colonies appeared dark blue (Figure 9). Further microscopic analysis revealed that blue formazan precipitate was predominantly localised to hyphal tips. In older hyphae the stain intensity was much reduced. Patches of stain were also identified occasionally throughout the hyphae, and approx. 5% of WT hyphal tips showed an aberrant tip staining pattern, with the stain either localised in patches or completely absent. A similar pattern was observed in the *pldA* deletion strains, as well as the *pldA* and *pldB* overexpression strains. In comparison the aberrant staining of tips was increased to approx. 20% in *noxA* deletion strains, and was even more frequent in *pldB* deletion strains (40%). Normal tip staining was restored in most of the complementation strains (Figure 9).

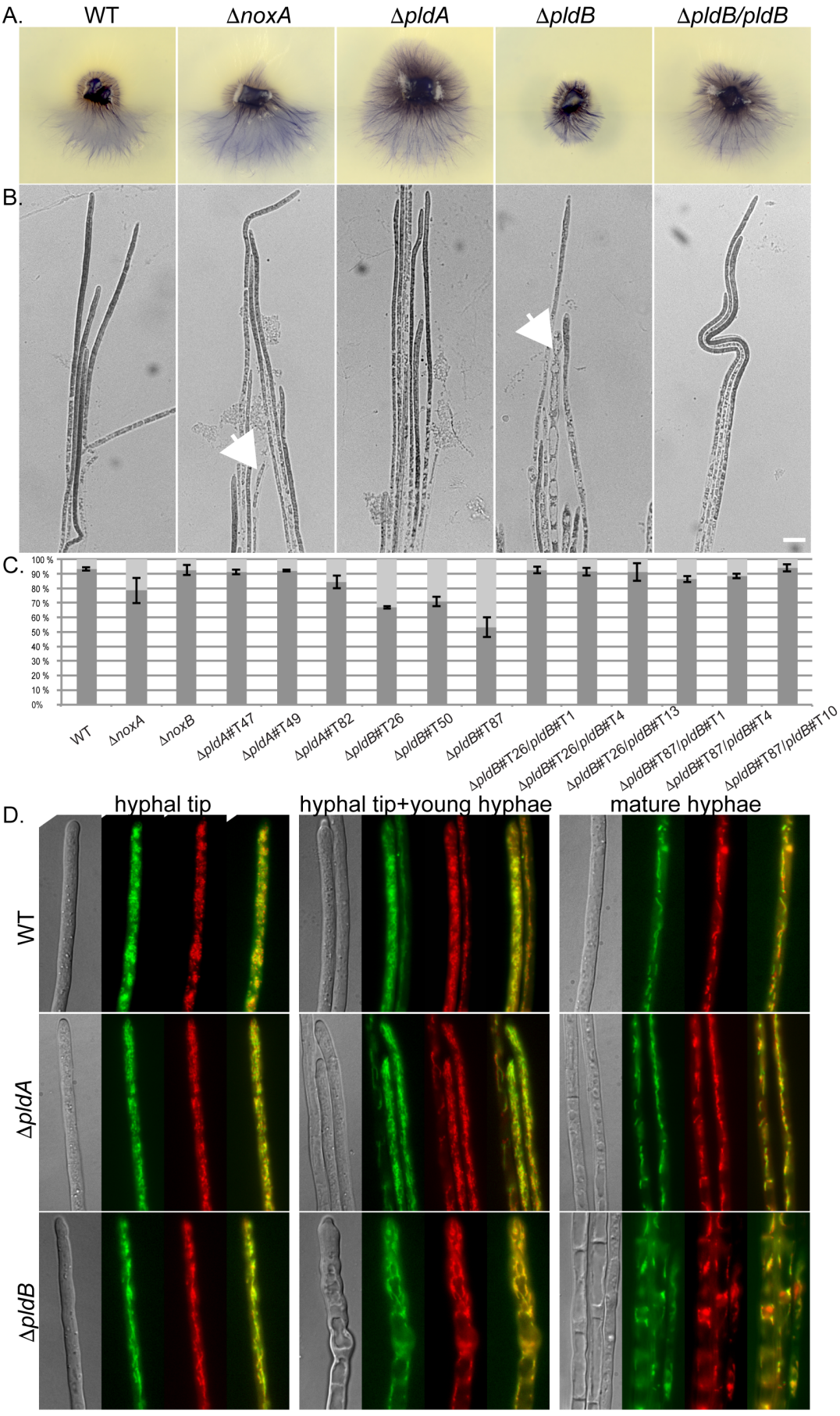
A.
WT
ΔnoxA
ΔpldA
ΔpldB
ΔpldB/pldB
B.
C.
100 %
90 %
80 %
70 %
60 %
50 %
40 %
30 %
20 %
10 %
0%
WT
ΔnoxA
ΔnoxB
ΔpldA#T47
ΔpldA#T49
ΔpldA#T82
ΔpldB#T26
ΔpldB#T50
ΔpldB#T87
ΔpldB#T26/pldB#T1
ΔpldB#T26/pldB#T4
ΔpldB#T26/pldB#T13
ΔpldB#T87/pldB#T1
ΔpldB#T87/pldB#T4
ΔpldB#T87/pldB#T10
D.
hyphal tip
hyphal tip+young hyphae
mature hyphae
WT
ΔpldA
ΔpldB

Figure 9: Analysis of superoxide production in *Epichloë festucae* wild-type, *pldA* and *pldB* deletion stains.

(A) Whole colony image of seven-day old colonies stained with 150 µl of 6.1 mM Nitroblue-Tetrazolium (NBT) solution (Sigma) for five hours. Three independent deletion strains of *pldA* and *pldB* were analysed, and here, representative images of WT, Δ*noxA,* Δ*pldA*#T47, Δ*pldB*#T87, and Δ*pldB*#T87/*pldB*#T4 are shown as representative of all strains analysed. The staining was performed twice. (B) Representative microscopic images of hyphal tips in (A); Bar = 10 µm; (C) Analysis of the occurrence of aberrant hyphal tip staining; 3x50 hypha of two different colonies of the same strain were analysed and the averages plotted (100% = 50 hyphal tips). Statistical significance was calculated using a T-test (Excel) and only *pldB* deletion strains were significantly different from WT (#T26: P = 7.71E-6; #T50: P = 4.22E-4; #T87: P = 5.74E-4). Error bars represent the standard deviation. (D) Localisation of superoxide production by staining with 0.16 mM of ROS-ID® Superoxide probe and co-localisation with mitochondrial staining reagent-Green. The *pldA* deletion strains T47 and T82 and the *pldB* deletion strains T26 and T87 were analysed and images of Δ*pldA*#T47 and Δ*pldB*#T87 shown here are representative of all strains analysed; Bar = 10 µm.

Hyphae were also stained with the ROS-ID® superoxide probe. In WT tips, the probe localised to puncta, which colocalised with a mitochondrial marker. In older hyphae the dye accumulated in long filaments containing more intense puncta, which also colocalised with the mitochondrial marker, indicating that all superoxide detected is generated as a by-product within mitochondria. Similar observations were made with the *pldA* deletion strains. However, in the *pldB* deletion strains the probe localised to long filamentous structures otherwise observed in mature hyphae in tips. These were also found to be mitochondria. In mature hyphae only a few long filamentous, superoxide-containing mitochondria were observed, which might have been caused by the highly vacuolated nature of the *pldB* deletion strains.

While these observations did not demonstrate changes in the superoxide production, potentially due to the higher sensitivity compared to NBT, it did show defects in the organelle organization in the *pldB* deletion strains.

The absence of PldB has no effect on Nox complex component localisations

In mammalian and plant systems, PA produced by PLD has been shown to directly activate gp91^{phox} and promote the recruitment of the Nox complex subunits to the membrane (Karathanassis *et al*., 2002; Taylor *et al*., 2004; Taylor *et al*., 2005; Potocký *et al*., 2012). To test whether the observed mislocalisation of superoxide production in *pldB* deletion strains is caused by the mislocalisation of the Nox components, *pldA* and *pldB* deletions strains were transformed with NoxA, NoxR, BemA, Cdc24 and RacA localisation constructs (Supplemental Figure S10) (Tanaka *et al*., 2011; Eaton, pers. comm.). In transformed WT strains, the NoxA fusion protein was found to localise to the cytoplasm, vesicles and the nuclear envelope. NoxR localised to hyphal tips, mobile vesicles and in puncta to either side of septa. The scaffold protein BemA was observed to localise to the PM of the hyphal tip and to the centre of septa, while Cdc24-GFP was found to localise to puncta at the very tip of the hyphae and at the center of septa as well. The RacA-fusion protein localised to hyphal tips, the PM and internal membranes, as reported previously (Takemoto *et al*., 2011; Siegmund *et al*., 2013; Kayano *et al*., 2018). The localisation of these fusion proteins in both *pldA* and *pldB* deletion strains was comparable to WT strains (Supporting Information Fig. S10).

These results indicate that PA produced by PldA and/or PldB is not required for the correct recruitment of these components of the Nox complex.

Discussion

Multiple studies in plant and mammalian systems highlight the importance of signalling via phospholipase D and its product, PA, in growth, stress response and development and more specifically in actin cytoskeleton rearrangement, vesicle transport, both endo- and exocytosis and Nox complex activation (Selvy *et al*., 2011). In this study an in-depth analysis of two PLD isoforms from *E. festucae* was carried out, which showed that PldB*,* the structurally more complex protein, is required for growth in axenic culture and establishment of a mutualistic interaction with perennial ryegrass. In addition, the deletion of *pldB* resulted in an altered localisation of superoxide production.

A tBLASTn analysis against the Fl1 genome using the *S. cerevisiae* Spo14 sequence as a query resulted in the identification of two Phospholipase D proteins. Although these proteins share 39.8% sequence homology with each other, an analysis with online tools revealed significant structural differences. Only PldB was found to possess both a PH and a PX domain, which are also present in yeast, mammalian and plant Pldζ homologs (Selvy *et al*., 2011). In yeast, the PH domain binds to PtdIns[4,5]P_2 and is involved in the translocation of the protein to membranes. The mammalian PLD1 and PLD2 PX domain bind polyphosphoinositides, with a preference for PtdIns[3,4,5]P_3, and anionic lipids, whereas the PH domain specifically binds PtdIns[3,4]P_2 and PtdIns[4,5]P_2 (Hodgkin *et al*., 2000; Sciorra *et al*., 2002; Stahelin *et al*., 2004). Both domains are involved in localisation of the proteins. The PX domain of PLD2 can additionally be phosphorylated and has been shown to directly bind to interaction partners (Selvy *et al*. 2011). In addition, PldA lacks the polybasic motif required for activation of PLDs in yeast, mammals and plants (Selvy *et al*., 2011). This motif has been reported to bind PtdIns[4,5]P_2 with high affinity and is required for activation of the protein, but not for its localisation (Sciorra *et al*., 1999; Sciorra *et al*., 2000). In *Arabidopsis*, PLDα, a C2-domain containing PLD, has four of the five critical residues substituted, likely abolishing PtdIns[4,5]P_2 binding (Wang, 2000; Selvy *et al*., 2011). Based on these structural differences, the regulation and localisation of the two *E. festucae* PLD isoforms are likely to be very different.

Phosphatidylcholine-metabolizing PLDs in the eukaryotic kingdom have previously been shown to fall into two major groups depending on the presence of a C2 domain or the lipid-binding PH and PK domains. Within the fungal kingdom, we found two clades, one contained homologs of the mammalian and yeast PLDs (containing PH and PX domains), and the other contained PLDs lacking a C2 and a PH/PX domain. PldB, as well as FgPld1, belong to the first clade, and both have a crucial role in axenic growth and virulence/mutualism. The second clade split into PldA-like PLDs and

another similar, but distinct group, which we have called PldA2-like. The PldA-type PLDs contained PldA, as well as FgPld2 and AnPldA, which have previously been shown to have no obvious role in growth or virulence (Hong *et al*., 2003; Ding *et al*. 2017). The PldA2 group contained AfPldA, a secreted PLD with a role in infection (Li *et al*. 2012). This ubiquitous distribution of PldA homologs indicates that these proteins are conserved, despite the lack of an obvious role in axenic culture growth and must thus have a role in different life stages or growth conditions.

To identify the role of these structurally different proteins, and thereby the importance of PA as a lipid signalling molecule in axenic culture, we generated *pldA* and *pldB* deletion and overexpression strains of *E. festucae*. The *pldA* deletion and *pldA* and *pldB* overexpression strains were indistinguishable from WT both in culture as well as *in planta*. Deletion strains of the *pldA* homologs in *A. nidulans* (*AnpldA*) and *F. graminearum* (*Fgpld2*) also exhibit normal phenotypes (Hong *et al*., 2003; Ding *et al*., 2017) suggesting PldA homologs are not required for axenic growth under standard conditions. In comparison, *pldB* deletion strains exhibited reduced colony growth and increased aerial hyphae. Similar phenotypes have been observed in *F. graminearum pld1* deletion strains (Ding *et al*., 2017). Microscopic analysis of *pldB* deletion strains in culture revealed an increase in the diameter of hyphal tips and a high degree of vacuolation, which is uncommon in WT hyphae. In addition, mature hyphae were often variable in diameter, abnormally shaped and frequently swollen, indicating a role of PldB in normal polarized growth. These are similar phenotypes to those previously reported for the *E. festucae racA* deletion mutant (Tanaka *et al*., 2008; Kayano *et al*., 2018). RacA is a small GTPase, which contributes to actin polymerization and Nox complex activation and has been found to act upstream of PLD in mammalian cells (Hess *et al*., 1997; Bishop and Hall, 2000; Cotteret and Chernoff, 2002; Tanaka *et al*., 2008).

IHH have been observed in many *E. festucae* mutants e.g. in strains with a disruption in the STRIPAK complex, the cell wall integrity MAP kinase pathway and the Nox complex (Becker *et al*., 2015; Green *et al*., 2016; Becker *et al*., 2016). In fungi, these structures are formed in response to disruption of hyphal integrity, wounding, changes in cell wall composition and septation defects, and provide a means of protection for the encased hyphae (Bowman *et al*., 2006; Kim and Hyun, 2007). Interestingly, IHH were occasionally observed in the *pldB* deletion strains, suggesting that deletion of *pldB*, and the resulting changes in morphology, result in severe hyphal stress.

In *F. graminearum*, deletion of *pld1* resulted in a severe reduction in conidiation and an abolishment of perithecia formation (Ding *et al*. 2017), whereas many Nox

complex mutants have been found to hyperconidiate (Kayano *et al*., 2013). Formation of coils, phialides and conidia, as well as germination were not affected by deletion of either *pldA* or *pldB*. However, as *E. festucae* generally only generates a low and inconsistent number of conidia in axenic growth, no definitive conclusions could be made regarding alterations to these structures (Becker *et al*., 2015). Sexual development of these strains in culture could not be analysed as *E. festucae* only undergoes sexual reproduction in association with the host plant (Bultman and Leuchtmann, 2009).

Staining of *pldB* deletion strains with the chitin-binding dye CFW frequently revealed small fluorescent puncta in the cytoplasm. This phenotype has previously been connected to defects in the recycling of cell wall components in *A. oryzae* (Higuchi *et al*., 2009). Phospholipase D and PA have both been connected to vesicular trafficking, as well as endo- and exocytosis in yeast and mammalian cells. In *S. cerevisiae*, the deletion of *SPO14* results in a loss of fusion of Golgi-derived vesicles to the prospore membrane during sporulation. This is thought to occur through the failure to recruit the PA-binding SNARE protein Spo20, the loss of lipid fusogenic activity of PA, and the loss of interactions between Spo14 and proteins involved in sporulation (Gavin *et al*., 2002; Riedel *et al*., 2005; Connolly and Engebrecht, 2006; Nakanishi *et al*. 2006). In mammalian cells, PA has been shown to be involved in vesicle transport from the ER to the Golgi apparatus, and in vesicle budding from the Golgi apparatus via ADP ribosylation factor Arf1 signalling (Ktistakis *et al*., 1996; Chen *et al*., 1997). Likewise, PA has been shown to be involved in epidermal-growth factor (EFR)-mediated endocytosis (Shen *et al*., 2001). Furthermore, PA was shown to accumulate at sites of exocytosis, and to be required for the formation of fusion-competent granules in chromaffin cells (Zeniou-Mayer *et al*., 2007). In addition, PLDs in yeast, mammals and plants have also been correlated to actin cytoskeleton organization e.g. *S. cerevisiea* Spo14 acts downstream of Arf-GTPases involved in the regulation of actin polymerization and in mammalian systems both PLDs were found to directly bind to actin (Lee *et al*., 2001; Kusner *et al*., 2002). Interestingly, PLDs in yeasts and mammals were found to act downstream of the small GTPases RacA and Cdc42, which are involved in actin polymerization though the interaction with p21-activated kinases (PAK) and other actin interacting proteins (Cotteret and Chernoff, 2002). In plants, similar observations were made for Pldβ and a recent study found that inhibition of PLD activity disrupts actin filaments (Pleskot *et al*., 2010; Pleskot *et al*., 2012; Pleskot *et al*., 2013).

Deletion of *pldB* in *E. festucae* also resulted in an abolishment of hyphal fusion in axenic culture. This phenotype has been observed for many *E. festucae* single gene

deletion strains (e.g. *noxA*, *noxR*, *racA, mpkA*, *mkkA* and *proA*), as well as deletion strains of their homologs in other related species (e.g. *N. crassa, P. anserina* and *Sordaria macrospora*) (Kayano *et al*., 2013; Tanaka *et al*., 2013; Scott, 2015; Becker *et al*., 2016). Thus, these proteins are likely components of a complex signalling network that regulates cell-to-cell fusion and cell differentiation, e.g. sexual development (Green *et al*., 2016). Interestingly, the deletion of the *pldB* homolog in *N. crassa*, *pla7*, also results in a loss of hyphal fusion (Fleissner, pers. commun.). This demonstrates that PldB is not only required for hyphal fusion in *E. festucae,* but also in other filamentous ascomycetes, highlighting the importance of PLD and PA. Hyphal fusion is required for the formation of interconnected networks and is necessary for the formation of fruiting bodies in fungi belonging to the Ascomycota as well as to the Basidiomycota (Read *et al.*, 2010; Fischer and Glass, 2019). The process of fusion has been especially well studied in *N. crassa*, where both germinating spores (germlings) as well as mature hyphae fuse to other germlings or hyphae, respectively. To date 70 mutants with a fusion defect have been identified, among these are mutants of MAP kinase pathways, the STRIPAK complex, phosphatases, transcription factors, ROS signalling and many more (Fischer and Glass, 2019). This highlights the complexity of this process. Recently the correct membrane composition and actin organization has been shown to be required as well, as an ergosterol deficient mutant and WT treated with the actin-polymerization inhibitor Latranculin B were unable to undergo hyphal fusion (Weichert *et al*., 2016; Roca *et al*., 2016). As discussed above PA is both able to influence membrane curvature and recruit other proteins, and PLD binds actin directly in mammals as well as in plants (Lee *et al*., 2001; Kusner *et al*., 2002: Pleskot *et al*., 2012; Pleskot *et al*., 2013). The question of which of these mechanisms is required for the process of hyphal fusion remains to be elucidated.

Associations between *pldB* deletion strains and *L. perenne* were dramatically different from WT associations. Plants were significantly shorter, and microscopic analysis revealed an increase in hyphal biomass, formation of hyphal bundles and the occasional colonisation of vascular bundles. This phenotype indicates a loss of the mutualistic interaction, and a switch to a more pathogen-like behaviour that has previously been reported for many other deletion mutants (e.g Δ*noxA*, Δ*noxR,* Δ*bemA,* Δ*racA*, Δ*sakA,* Δ*proA,* Δ*hepA,* Δ*mkkA,* Δ*mpkA,* Δ*symB,* Δ*symC and* Δ*mob3)* (Tanaka *et al*., 2006; Takemoto *et al*., 2006; Eaton *et al*. 2010; Tanaka *et al*., 2013; Becker *et al*., 2015; Becker *et al*., 2016; Green *et al*., 2016; Green *et al*., 2017; Chujo *et al*., 2019). A transcriptome analysis of Δ*noxA*, Δ*sakA,* Δ*proA* and Δ*hepA* strains in the interaction with *L. perenne* revealed an upregulation of genes in primary metabolism, degradative enzymes, and transporters, indicative of a starvation

response, potentially resulting from the lack of hyphal fusion, resulting in proliferative growth and the colonisation of vascular bundles (Eaton *et al*., 2015; Chujo *et al*., 2019). However, for the *pldB* deletion strain, infection of vascular bundles was only rarely observed, indicating a somewhat less severe starvation response, despite the increase in hyphal biomass. Recently a role for alkalinization of the apoplast by the endophyte has been suggested as a potential cause for this switch to proliferative growth. This hypothesis was, among others, based on the generation of *E. festucae* mutants defective in pH dependent changes in transcription, that exhibit aberrant growth *in planta* without the lack of hyphal fusion (Lukito *et al*., 2015; Scott *et al*., 2018). Alkalinization of the apoplast has previously been described to be required for virulence of *Fusarium oxysporum* (Masachis *et al*., 2016). The results presented here demonstrate that PldB is required for regulated growth *in planta*, either due to the production of PA and its function as a lipid second messenger, or a direct interaction of PldB with other proteins. This hypothesis could be further tested by providing an exogenous supply of PA or by generating a mutant expressing a PC-hydrolysis negative form of PldB. The *F. graminearum Pld1* mutant was found to be unable to infect wheat heads and corn silks (Ding *et al*., 2017). Therefore, signalling via FgPLD1 and PA, similar to NoxA and NoxB, is required for virulent behaviour of a pathogen and for mutualistic behaviour of a symbiont.

Interestingly, the *pldB* deletion strains were unable to form WT-like expressoria and instead demonstrated a highly reticulate subcuticular growth. Similar observations have been made in *E. festucae* for Δ*noxA*, Δ*noxB*, Δ*noxR*, Δ*symB* and Δ*symC* strains (Becker *et al*., 2016; Green *et al*., 2017). A localised ROS burst, resulting from both Nox1 and Nox2 activity, is crucial for the development of a functional appressorium in *M. oryzae*, and disruption of either disrupts the formation of appressoria. The Nox2 complex is necessary for septin-mediated actin ring reorientation at the septal pore, and Nox1 for the maintenance of the F-actin network during penetration and elongation (Egan *et al*., 2007; Ryder *et al*., 2013). The observation here of a similar phenotype caused by the *pldB* deletion suggests a connection of PldB to NoxA or NoxB, either via direct interaction or complex activation, or a role in regulation of the actin network, as has been shown in other organisms (see above).

Given PldA lacks the lipid binding PX and PH domains it was not surprising that this isoform localised to the cytosol of the cell. Although PldB also localised to the cytoplasm, it was also found associated with septa and the PM. In *S. cerevisiae*, Spo14 is also localised to the cytoplasm, to endosomes, the nucleus, and is recruited to the prospore membrane during sporulation (Rudge *et al*., 1998; Li *et al*., 2000; Garcia-Lopez *et al*., 2011). Similarly, FgPld1 of *F. graminearum* was also observed in the

cytoplasm of young hyphae, but the localisation of FgPld2 or FgPld3 was not analysed. The localisation of mammalian PLD1 and PLD2 is tissue dependent. The mammalian PLD1 is found to associate with perinuclear membranes, the Golgi apparatus and early endosomes, and is recruited to the PM or late endosomes upon activation (Hughes and Parker, 2001; Du *et al*., 2003). Mammalian PLD2, however, is localised at the PM, and is recruited to recycled vesicles, membrane ruffles and β-actin, depending on its phosphorylation status (Colley *et al*., 1997; Selvy *et al*. 2011). The observed cytoplasmic localisation of PldB could be a result of the overexpression of the fusion-protein, which was necessary due to the low expression in culture and *in planta*. Interestingly, however, the localisation constructs were able to rescue the phenotype of the *pldB* deletion strains in culture as well as in *planta*, suggesting that increased PLD activity is either not detrimental to fungal growth or that the protein activity itself is strictly regulated.

In mammals and yeast, PLDs have been found to interact with a multitude of proteins both up- and down-stream in various signalling pathways. However, using yeast two-hybrid assays I was unable to make a connection between PldB and any signalling proteins or the Nox complex. In yeast ScSpo14 is mainly regulated at a transcriptional and translational level, as well as through phosphorylation and by interaction with and availability of PtdIns[4,5]P_2 and PC (Rudge *et al*., 2002; Selvy *et al*., 2011). With the exception of the small GTPase Cdc42, which regulates the Nox complex in filamentous fungi, none of the interaction partners identified in other studies are directly involved in the regulation of Nox activity (Kayano *et al*., 2018). Cdc42 has been reported to be exclusively required for polarized cell growth in *S. cerevisiae*, and to stimulate Spo14 activity during this process. However, the nature of this interaction is unknown (Miller and Johnson, 1994; Harkins *et al*., 2008). In contrast, mammalian PLDs have been found to interact with multiple small GTPases (Arf and Rho family), including, for PLD1, the previously mentioned Rac1 and Cdc42 (Walker *et al*., 2000; Walker and Brown, 2002; Powner *et al*., 2002; Peng and Frohman, 2012).

Besides their role in Nox complex activation, both Rac1 and Cdc42 are required for cell polarity in *N. crassa*. Cdc42 is required for initiating cell polarity while Rac1 is required for maintaining polarized tip growth (Araujo-Palomares *et al*., 2011). Both GTPases are regulated by the GEF Cdc24, required for conidial anastomosis tubes (CAT) formation and fusion of mature hyphae (Araujo-Palomares *et al*., 2011; Lichius *et al*., 2014). Interestingly, in *N. crassa* Cdc42 and Rac1 are required for the opposite chemotropism of the germ and conidial anastomosis tubes (CAT) during conidia germination, where their localised activation results in generation of actin cables (Lichius *et al*., 2014). In contrast, only the deletion of *racA*, but not *cdc42*, results in a

loss of fusion in mature *E. festucae* hyphae (Kayano *et al*. 2018). An interaction between PldB and Rac1 could therefore explain the observed lack of hyphae fusion, stunted growth and changes in ROS production, and should therefore be tested in a future study.

Mammalian PLDs have been found to directly interact with phosphokinase Cα, which phosphorylates $p22^{phox}$ (Regier *et al*., 1999) and the phosphatidylinositol 4-phosphate 5-kinase (fungal homolog: Mss4), which generates PtdIns[4,5]P_2 involved in Nox complex activity in plants (Potocký *et al*., 2012). The lack of interactions of PldB with the proteins tested here could indicate a similar mode of regulation to Spo14 compared to the mammalian homologs. Alternatively, the lack of identified interactions could also be an inherent problem when analysing PldB interactions using yeast two-hybrid, as previously suggested (Riedel *et al*., 2005). To increase the likelihood of identifying PldB interacting proteins and other proteins involved in signalling pathways, a protein-pull down experiment, followed by Mass Spectrometry, should be performed.

To analyse the effect PLD deletion has on PA concentration and distribution, a PA biosensor was generated making use of the characterised PA-binding domain in Spo20 (Nakanishi *et al*., 2004; Potocký *et al*., 2014). Microscopic analysis revealed that the PA biosensor localised to the PM in *E. festucae* WT and *pldA* deletion strains, as has been described in *S. cerevisiae* and in tobacco root hairs (Nakanishi *et al*., 2004; Potocký *et al*., 2014). In *pldB* deletion strains, the presence of the PA biosensor was reduced at the PM in hyphal tips and young hyphae and preferentially located in the cytoplasm and nuclei. Unspecific nuclear localisation of a PA biosensor has been described previously, where treatment with the PLD inhibitor n-butanol decreased PM/nucleus fluorescence intensity ratio (Zeniou-Mayer *et al*., 2007; Potocky et el., 2014). Activation of macrophages has also been observed to shift PA localisation from the nucleus to the PM (Kassas *et al*., 2017). Therefore, an increased nuclear as well as cytoplasmic localisation likely reflects reduced PLD activity. Interestingly in *E. festucae*, the PA biosensor was never observed in nuclei of either the WT or *pldA* deletion strains, but was localised to nuclei in the *pldB* strain. These results indicate that in comparison to PldA, PldB is the main producer of PA in *E. festucae*. Indeed, analysis of the catalytic function of the PldA homolog in *A. nidulans*, AnPldA, showed a substrate preference for phosphatidylethanolamine (PE) instead of PC, which might be required for production of PA in other localisations. To date, several different PA biosensors have been generated and their binding affinities have been studied. In addition to the PA-binding domain of Spo20, the binding domains of the yeast protein Opi1p (103-191 aa) and the mammalian protein PDE4A1 (1-40 aa) have been employed. All three display different localisation profiles, where the Spo20 PABD

localised to the PM and nuclei, the Opi1p PABD to the PM, the ER and the nucleus, and the PDE4A1-PABD to the Golgi (Kassas *et al*. 2017). These differential binding profiles are likely a result of different binding affinities in regard to chemical properties of PA and the membrane target (Kassas *et al*., 2017). To further elucidate the role of PldA, additional PA biosensors could be employed to verify the observed results and a PLD activity test performed on WT and mutant strains.

E. festucae pldB deletion strains showed reduced NBT tip staining, and exhibited long filament like structures instead of dense, more punctate structures as observed in WT when stained with a superoxide probe. Co-staining with a mitochondrial marker revealed that the filaments as well as the punctate structures associated with mitochondria. The differences detected by NBT staining are therefore associated with different WT vs. mutant mitochondrial structures. The deletion of both *noxA* and *racA* in *E. festucae* has previously been shown to reduce the number of stained tips, with the strongest effect observed for the *racA* deletion mutant (Tanaka *et al*, 2006; Kayano *et al*., 2018). Given these findings, whether *noxA* and *racA* NBT changes are also correlated to mitochondrial changes, remains to be determined. Reduced NBT tip staining has been observed for *racA* deletions strains in *A. nidulans*, for *nox1* and *nox2* in *Sclerotinia sclerotium* and for *noxA* and *noxB* in *F. graminearum* (Semighini *et al*., 2008; Kim *et al*., 2011; Wang *et al*. 2014). The reduction of tip staining in the *pldB* mutant, demonstrates a role for PldB in maintaining the normal location and production of superoxide in hyphal tips, even though the current data suggest that this is due to changes in the structure of mitochondria.

Studies in mammalian systems indicate that PA influences the activity of $gp91^{phox}$ and is involved in the recruitment of the cytosolic components. Here we have shown that in *E. festucae,* neither PldA nor PldB are required for NoxA, NoxR, BemA, Cdc24 and RacA localisation at the PM. However, it is worth noting that the GFP-RacA construct used, occurs as both active and inactive RacA. To address this issue, constitutively active or inactive constructs or a suitable reporter as reported previously could be tested (Lichius *et al*., 2014; Kayano *et al*., 2018). Nonetheless, this mode of activation of the Nox complex can likely be excluded. In mammalian cells, however, PA was able to stimulate oxidase activity in a cell-free system and direct interaction between $gp91^{phox}$ and PA, resulting in a conformational change leading to activation of $gp91^{phox}$ (Palicz *et al*., 2001; Qualliotine-Mann *et al*., 1993; Taylor *et al*, 2004; Taylor *et al*., 2012). In addition, a direct interaction between PA and the NADPH oxidase has been described in plant cells (Zhang *et al*., 2009). Therefore, PA might directly activate NoxA (potentially even NoxB), with the lack of PA generated by PldB rendering NoxA

inactive. To date, however, any direct evidence for this hypothesis is still missing and will need to be the focus of a future study.

Here we have identified two *E. festucae* PC-hydrolyzing PLDs, PldA and PldA. Furthermore, we have analysed their role in regulating hyphal growth in axenic culture and in *planta* and their connection to the NADPH oxidase complex. PldB is structurally more complex than PldA and is a homolog of *S. cerevisiae* Spo14 and mammalian PLDs. Unlike PldA, PldB is required for normal hyphal growth, cell-cell fusion, expressoria formation and the maintenance of a mutualistic interaction with *L. perenne*. Furthermore PldB, but not PldA, is required for enhanced recruitment of the PA lipid biosensor to the PM membrane. Although a direct connection between PldB and Nox complex signalling could not be identified within this study, several key observations, such as the similarity between *pldB* and *nox* complex mutant phenotypes and the observation that *pldB* and *nox* complex mutants exhibit reduced superoxide within hyphal tips, supports such a connection. This study highlights the importance of PLD and the lipid second messenger PA in filamentous fungi, not only in relation to superoxide production, but also with regards to hyphal development and differentiation.

Acknowledgements

This research was supported by grants from the Tertiary Education Commission to the Bio-Protection Research Centre, the Royal Society of New Zealand Marsden Fund and by Massey University. We thank Niki Murray, Pani Vijayan and Matthew Savoian (Manawatu Microscopy and Imaging Centre) for support with microscopy, Arvina Ram for technical assistance and Christopher Schardl for provision of *Epichloë* genome sequences.

References

Ago, T., Kuribayashi, F., Hiroaki, H., Takeya, R., Ito, T., Kohda, D., and Sumimoto, H. (2003). Phosphorylation of p47phox directs phox homology domain from SH3 domain toward phosphoinositides, leading to phagocyte NADPH oxidase activation. Proc Natl Acad Sci USA 100, 4474-4479.

Aguirre, J., Rios-Momberg, M., Hewitt, D., and Hansberg, W. (2005). Reactive oxygen species and development in microbial eukaryotes. Trends Microbiol 13, 111-118.

Araujo-Palomares, C. L., Richthammer, C., Seiler, S., and Castro-Longoria, E. (2011). Functional characterization and cellular dynamics of the CDC-42 - RAC - CDC-24 module in *Neurospora crassa*. PloS One 6, e27148.

Becker, M., Becker, Y., Green, K., and Scott, B. (2016). The endophytic symbiont *Epichloë festucae* establishes an epiphyllous net on the surface of *Lolium perenne* leaves by development of an expressorium, an appressorium-like leaf exit structure. New Phytol 211, 240-254.

Becker, Y., Eaton, C. J., Brasell, E., May, K. J., Becker, M., Hassing, B., Cartwright, G. M., Reinhold, L., and Scott, B. (2015). The fungal Cell-Wall Integrity MAPK cascade is crucial for hyphal network formation and maintenance of restrictive growth of *Epichloë festucae* in symbiosis with *Lolium perenne*. Mol Plant-Microbe Interact 28, 69-85.

Becker, Y., Green, K. A., Scott, B., and Becker, M. (2018). Artificial inoculation of *Epichloë festucae* into *Lolium perenne*, and visualisation of endophytic and epiphyllous fungal growth. Bio-protocol 8, e2990.

Bedard, K., and Krause, K. H. (2007). The NOX family of ROS-generating NADPH oxidases: physiology and pathophysiology. Physiol Rev 87, 245-313.

Belambri, S. A., Rolas, L., Raad, H., Hurtado-Nedelec, M., Dang, P. M., and El-Benna, J. (2018). NADPH oxidase activation in neutrophils: Role of the phosphorylation of its subunits. Eur J Clin Invest 48, Suppl 2, e12951.

Bishop, A. L., and Hall, A. (2000). Rho GTPases and their effector proteins. Biochem J 348 Pt 2, 241-255.

Bowman, S. M., Piwowar, A., Al Dabbous, M., Vierula, J., and Free, S. J. (2006). Mutational analysis of the glycosylphosphatidylinositol (GPI) anchor pathway demonstrates that GPI-anchored proteins are required for cell wall biogenesis and normal hyphal growth in *Neurospora crassa*. Eukaryot Cell 5, 587-600.

Bultman, T., and Leuchtmann, A. (2009). Biology of the *Epichloë-Botanophila* interaction: An intriguing association between fungi and insects. Fungal Biol Rev 22, 131-138.

Byrd, A. D., Schardl, C. L., Songlin, P. J., Mogen, K. L., and Siegel, M. R. (1990). The beta-tubulin gene of *Epichloë typhina* from perennial ryegrass (*Lolium perenne*). Curr Gen 18, 347-354.

Candy, A. (2019). Analysis of *Epichloë festucae* membrane lipid composition and its role in Nox complex assembly. In School of Fundamental Science (Palmerston North: Massey University), pp. 196.

Cano-Dominguez, N., Alvarez-Delfin, K., Hansberg, W., and Aguirre, J. (2008). NADPH oxidases NOX-1 and NOX-2 require the regulatory subunit NOR-1 to control cell differentiation and growth in *Neurospora crassa*. Eukaryotic cell 7, 1352-1361.

Chae, Y. C., Kim, J. H., Kim, K. L., Kim, H. W., Lee, H. Y., Heo, W. D., Meyer, T., Suh, P. G., and Ryu, S. H. (2008). Phospholipase D activity regulates integrin-mediated cell spreading and migration by inducing GTP-Rac translocation to the plasma membrane. Mol Biol Cell 19, 3111-3123.

Chen, Y. G., Siddhanta, A., Austin, C. D., Hammond, S. M., Sung, T. C., Frohman, M. A., Morris, A. J., and Shields, D. (1997). Phospholipase D stimulates release of nascent secretory vesicles from the trans-Golgi network. J Cell Biol 138, 495-504.

Christensen, M. J., Bennett, R. J., Ansari, H. A., Koga, H., Johnson, R. D., Bryan, G. T., Simpson, W. R., Koolaard, J. P., Nickless, E. M., and Voisey, C. R. (2008). *Epichloë* endophytes grow by intercalary hyphal extension in elongating grass leaves. Fungal Genet Biol, 45, 84-93.

Chujo, T., Lukito, Y., Eaton, C. J., Dupont, P. Y., Johnson, L. J., Winter, D., Cox, M. P., and Scott, B. (2019). Complex epigenetic regulation of alkaloid biosynthesis and host interaction by heterochromatin protein I in a fungal endophyte-plant symbiosis. Fungal Genet Biol, 125, 71-83.

Chung, K. R., and Schardl, C. L. (1997). Sexual cycle and horizontal transmission of the grass symbiont*, Epichloë typina*. Mycol Res 101: 295–301.

Colley, W. C., Sung, T. C., Roll, R., Jenco, J., Hammond, S. M., Altshuller, Y., Bar-Sagi, D., Morris, A. J., and Frohman, M. A. (1997). Phospholipase D2, a distinct phospholipase D isoform with novel regulatory properties that provokes cytoskeletal reorganization. Curr Biol: CB 7, 191-201.

Connolly, J. E., and Engebrecht, J. (2006). The Arf-GTPase-activating protein Gcs1p is essential for sporulation and regulates the phospholipase D Spo14p. Eukaryot Cell 5, 112-124.

Cotteret, S., and Chernoff, J. (2002). The evolutionary history of effectors downstream of Cdc42 and Rac. Genome Biol 3, REVIEWS0002.

de Jong, C. F., Laxalt, A. M., Bargmann, B. O., de Wit, P. J., Joosten, M. H., and Munnik, T. (2004). Phosphatidic acid accumulation is an early response in the Cf-4/Avr4 interaction. Plant J 39, 1-12.

Ding, M., Zhu, Q., Liang, Y., Li, J., Fan, X., Yu, X., He, F., Xu, H., Liang, Y., and Yu, J. (2017). Differential roles of three FgPLD genes in regulating development and pathogenicity in *Fusarium graminearum*. Fungal Genet Biol 109, 46-52.

Dinno, A. (2017). Dunn's Test of Multiple Comparisons Using Rank Sums. https://cran.r-project.org/web/packages/dunn.test/dunn.test.pdf

Dolan, J. W., Bell, A. C., Hube, B., Schaller, M., Warner, T. F., and Balish, E. (2004). *Candida albicans* PLD I activity is required for full virulence. Med Mycol 42, 439-447.

Du, G., Altshuller, Y. M., Vitale, N., Huang, P., Chasserot-Golaz, S., Morris, A. J., Bader, M. F., and Frohman, M. A. (2003). Regulation of phospholipase D1 subcellular cycling through coordination of multiple membrane association motifs. J Cell Biol 162, 305-315.

Eaton, C. J., Cox, M. P., Ambrose, B., Becker, M., Hesse, U., Schardl, C. L., and Scott, B. (2010). Disruption of signaling in a fungal-grass symbiosis leads to pathogenesis. Plant Physiol 153, 1780-1794.

Eaton, C. J., Dupont, P. Y., Solomon, P., Clayton, W., Scott, B., and Cox, M. P. (2015). A core gene set describes the molecular basis of mutualism and antagonism in *Epichloë* spp. Mol Plant Microbe Interact 28, 218-231.

Eaton, C. J., Jourdain, I., Foster, S. J., Hyams, J. S., and Scott, B. (2008). Functional analysis of a fungal endophyte stress-activated MAP kinase. Curr Genet 53, 163-174.

Edgar, R. C. (2004). MUSCLE: multiple sequence alignment with high accuracy and high throughput. Nucleic Acids Res 32, 1792-1797.

Egan, M. J., Wang, Z.-Y., Jones, M. A., Smirnoff, N., and Talbot, N. J. (2007). Generation of reactive oxygen species by fungal NADPH oxidases is required for rice blast disease. Proc Natl Acad USA 104, 11772-11777.

Faugaret, D., Chouinard, F. C., Harbour, D., El azreq, M. A., and Bourgoin, S. G. (2011). An essential role for phospholipase D in the recruitment of vesicle amine transport protein-1 to membranes in human neutrophils. Biochem Pharmacol 81, 144-156.

Fornstedt, T., Hesselgren, A. M., and Johansson, M. (1997). Chiral assay of atenolol present in microdialysis and plasma samples of rats using chiral CBH as stationary phase. Chirality 9, 329-334.

Garcia-Lopez, M. C., Pelechano, V., Miron-Garcia, M. C., Garrido-Godino, A. I., Garcia, A., Calvo, O., Werner, M., Perez-Ortin, J. E., and Navarro, F. (2011). The conserved foot domain of RNA pol II associates with proteins involved in transcriptional initiation and/or early elongation. Genetics 189, 1235-1248.

Gavin, A. C., Bosche, M., Krause, R., Grandi, P., Marzioch, M., Bauer, A., Schultz, J., Rick, J. M., Michon, A. M., Cruciat, C. M., *et al.* (2002). Functional organization of the yeast proteome by systematic analysis of protein complexes. Nature 415, 141-147.

Gibson, D. G. (2009). Synthesis of DNA fragments in yeast by one-step assembly of overlapping oligonucleotides. Nucleic Acids Res 37, 6984-6990.

Gietz, R. D., and Woods, R. A. (2002). Transformation of yeast by lithium acetate/single-stranded carrier DNA/polyethylene glycol method. Methods Enzymol 350, 87-96.

Green, K. A. (2016). A conserved signalling network regulates *Epichloë festucae* cell-cell fusion and the mutualistic symbiotic interaction between *E. festucae* and *Lolium perenne* (PhD thesis, Massey University, New Zealand).

Green, K. A., Becker, Y., Fitzsimons, H. L., and Scott, B. (2016). An *Epichloë festucae* homologue of MOB3, a component of the STRIPAK complex, is required for

the establishment of a mutualistic symbiotic interaction with *Lolium perenne*. Mol Plant Pathol 17, 1480-1492.

Green, K. A., Becker, Y., Tanaka, A., Takemoto, D., Fitzsimons, H. L., Seiler, S., Lalucque, H., Silar, P., and Scott, B. (2017). SymB and SymC, two membrane associated proteins, are required for *Epichloë festucae* hyphal cell-cell fusion and maintenance of a mutualistic interaction with *Lolium perenne*. Mol Microbiol 103, 657-677.

Green, K. A., Eaton, C. J., Savoian, M. S., and Scott, B. (in press). A homologue of the fungal tetraspanin Pls1 is required for *Epichloë festucae* expressorium formation and establishment of a mutualistic interaction with *Lolium perenne*. Mol Plant Pathol.

Hairfield, M. L., Ayers, A. B., and Dolan, J. W. (2001). Phospholipase D1 is required for efficient mating projection formation in *Saccharomyces cerevisiae*. FEMS Yeast Res 1, 225-232.

Hanahan, D. (1983). Studies on transformation of *Escherichia coli* with plasmids. J Mol Biol 166, 557-580.

Harkins, A. L., London, S. D., and Dolan, J. W. (2008). An upstream regulator and downstream target of phospholipase D1 activity during pheromone response in *Saccharomyces cerevisiae*. FEMS Yeast Res 8, 237-244.

Hassing, B., Winter, D., Becker, Y., Mesarich, C. H., Eaton, C. J., and Scott, B. (2019). Analysis of *Epichloë festucae* small secreted proteins in the interaction with *Lolium perenne*. PloS One 14, e0209463.

Hess, J. A., Ross, A. H., Qiu, R. G., Symons, M., and Exton, J. H. (1997). Role of Rho family proteins in phospholipase D activation by growth factors. J Biol Chem 272, 1615-1620.

Higuchi, Y., Arioka, M., and Kitamoto, K. (2009). Endocytic recycling at the tip region in the filamentous fungus *Aspergillus oryzae*. Commun Integr Biol 2, 327-328.

Hodgkin, M. N., Masson, M. R., Powner, D., Saqib, K. M., Ponting, C. P., and Wakelam, M. J. (2000). Phospholipase D regulation and localisation is dependent upon a phosphatidylinositol 4,5-biphosphate-specific PH domain. Curr Biol 10, 43-46.

Hong, S., Horiuchi, H., and Ohta, A. (2003). Molecular cloning of a phospholipase D gene from *Aspergillus nidulans* and characterization of its deletion mutants. FEMS Microbiol Lett 224, 231-237.

Hong, Y., Devaiah, S. P., Bahn, S. C., Thamasandra, B. N., Li, M., Welti, R., and Wang, X. (2009). Phospholipase D epsilon and phosphatidic acid enhance *Arabidopsis* nitrogen signaling and growth. Plant J 58, 376-387.

Huang, S., Gao, L., Blanchoin, L., and Staiger, C. J. (2006). Heterodimeric capping protein from *Arabidopsis* is regulated by phosphatidic acid. Mol Biol Cell 17, 1946-1958.

Hube, B., and Naglik, J. (2001). *Candida albicans* proteinases: resolving the mystery of a gene family. Microbiology 147, 1997-2005.

Hughes, W. E., and Parker, P. J. (2001). Endosomal localization of phospholipase D 1a and 1b is defined by the C-termini of the proteins, and is independent of activity. Biochem J 356, 727-736.

Itoh, Y., Johnson, R., and Scott, B. (1994). Integrative transformation of the mycotoxin-producing fungus, *Penicillium paxilli*. Curr Genet 25, 508-513.

Jenkins, G. M., and Frohman, M. A. (2005). Phospholipase D: a lipid centric review. Cell Mol Life Sci 62, 2305-2316.

Jiang, C., Zhang, S., Zhang, Q., Tao, Y., Wang, C., and Xu, J. R. (2015). FgSKN7 and FgATF1 have overlapping functions in ascosporogenesis, pathogenesis and stress responses in *Fusarium graminearum*. Environ Microbiol 17, 1245-1260.

Jones, P., Binns, D., Chang, H. Y., Fraser, M., Li, W., McAnulla, C., McWilliam, H., Maslen, J., Mitchell, A., Nuka, G., *et al.* (2014). InterProScan 5: genome-scale protein function classification. Bioinformatics 30, 1236-1240.

Kanai, F., Liu, H., Field, S. J., Akbary, H., Matsuo, T., Brown, G. E., Cantley, L. C., and Yaffe, M. B. (2001). The PX domains of p47phox and p40phox bind to lipid products of PI(3)K. Nat Cell Biol 3, 675-678.

Karathanassis, D., Stahelin, R. V., Bravo, J., Perisic, O., Pacold, C. M., Cho, W., and Williams, R. L. (2002). Binding of the PX domain of p47(phox) to phosphatidylinositol 3,4-bisphosphate and phosphatidic acid is masked by an intramolecular interaction. EMBO J 21, 5057-5068.

Kassas, N., Tanguy, E., Thahouly, T., Fouillen, L., Heintz, D., Chasserot-Golaz, S., Bader, M. F., Grant, N. J., and Vitale, N. (2017). Comparative characterization of phosphatidic acid sensors and their localization during frustrated phagocytosis. J Biol Chem 292, 4266-4279.

Katoh, K., Rozewicki, J., and Yamada, K. D. (2017). MAFFT online service: multiple sequence alignment, interactive sequence choice and visualization. Brief Bioinform, bbx108.

Kaur, G., Sharma, A., Guruprasad, K., and Pati, P. K. (2014). Versatile roles of plant NADPH oxidases and emerging concepts. Biotechnol Adv 32, 551-563.

Kayano, Y., Tanaka, A., Akano, F., Scott, B., and Takemoto, D. (2013). Differential roles of NADPH oxidases and associated regulators in polarized growth, conidiation and hyphal fusion in the symbiotic fungus *Epichloë festucae*. Fungal Genet Biol 56, 87-97.

Kayano, Y., Tanaka, A., and Takemoto, D. (2018). Two closely related Rho GTPases, Cdc42 and RacA, of the endophytic fungus *Epichloë festucae* have contrasting roles for ROS production and symbiotic infection synchronized with the host plant. PLoS Pathog 14, e1006840.

Khang C.H., Berruyer R., Giraldo M.C., Kankanala P., Park S.Y., Czymmek K., *et al.* (2010) Translocation of *Magnaporthe oryzae* effectors into rice cells and their subsequent cell-to-cell movement. Plant Cell. 22(4):1388-403.

Kim, H. J., Chen, C., Kabbage, M., and Dickman, M. B. (2011). Identification and characterization of *Sclerotinia sclerotiorum* NADPH oxidases. Appl Environ Microbiol 77, 7721-7729.

Kim, K. W., and Hyun, J. W. (2007). Nonhost-associated proliferation of intrahyphal hyphae of citrus scab fungus *Elsinoe fawcettii*: refining the perception of cell-within-a-cell organization. Micron 38, 565-571.

Koonin, E. V. (1996). A duplicated catalytic motif in a new superfamily of phosphohydrolases and phospholipid synthases that includes poxvirus envelope proteins. Trends Biochem Sci 21, 242-243.

Ktistakis, N. T., Brown, H. A., Waters, M. G., Sternweis, P. C., and Roth, M. G. (1996). Evidence that phospholipase D mediates ADP ribosylation factor-dependent formation of Golgi coated vesicles. J Cell Biol 134, 295-306.

Kusner, D. J., Barton, J. A., Wen, K. K., Wang, X., Rubenstein, P. A., and Iyer, S. S. (2002). Regulation of phospholipase D activity by actin. Actin exerts bidirectional modulation of Mammalian phospholipase D activity in a polymerization-dependent, isoform-specific manner. J Biol Chem 277, 50683-50692.

Lacaze, I., Lalucque, H., Siegmund, U., Silar, P., and Brun, S. (2015). Identification of NoxD/Pro41 as the homologue of the p22phox NADPH oxidase subunit in fungi. Mol Microbiol 95, 1006-1024.

Lambeth, J. D., Cheng, G., Arnold, R. S., and Edens, W. A. (2000). Novel homologs of gp91phox. Trends Biochem Sci 25, 459-461.

Lambeth, J. D., and Neish, A. S. (2014). Nox enzymes and new thinking on reactive oxygen: a double-edged sword revisited. Annu Rev Pathol 9, 119-145.

Lara-Ortiz, T., Riveros-Rosas, H., and Aguirre, J. (2003). Reactive oxygen species generated by microbial NADPH oxidase NoxA regulate sexual development in *Aspergillus nidulans*. Mol Microbiol 50, 1241-1255.

Latch, G. C. M., and Christensen, M. J. (1985). Artificial infection of grasses with endophytes. Ann Appl Biol 107, 17-24.

Lee, S., Park, J., and Lee, Y. (2003). Phosphatidic acid induces actin polymerization by activating protein kinases in soybean cells. Molecules Cells 15, 313-319.

Lee, S., Park, J. B., Kim, J. H., Kim, Y., Kim, J. H., Shin, K. J., Lee, J. S., Ha, S. H., Suh, P. G., and Ryu, S. H. (2001). Actin directly interacts with phospholipase D, inhibiting its activity. J Biol Chem 276, 28252-28260.

Letunic, I., Doerks, T., and Bork, P. (2015). SMART: recent updates, new developments and status in 2015. Nucleic Acids Res 43, D257-260.

Li, X., Gao, M., Han, X., Tao, S., Zheng, D., Cheng, Y., Yu, R., Han, G., Schmidt, M., and Han, L. (2012). Disruption of the phospholipase D gene attenuates the virulence of *Aspergillus fumigatus*. Infect Immun 80, 429-440.

Li, X., Routt, S. M., Xie, Z., Cui, X., Fang, M., Kearns, M. A., Bard, M., Kirsch, D. R., and Bankaitis, V. A. (2000). Identification of a novel family of nonclassic yeast phosphatidylinositol transfer proteins whose function modulates phospholipase D activity and Sec14p-independent cell growth. Mol Biol Cell 11, 1989-2005.

Lichius, A., Goryachev, A. B., Fricker, M. D., Obara, B., Castro-Longoria, E., and Read, N. D. (2014). CDC-42 and RAC-1 regulate opposite chemotropisms in *Neurospora crassa*. J Cell Sci 127, 1953-1965.

Liscovitch, M., Czarny, M., Fiucci, G., Lavie, Y., and Tang, X. (1999). Localization and possible functions of phospholipase D isozymes. Biochem Biophys Acta 1439, 245-263.

Liscovitch, M., Czarny, M., Fiucci, G., and Tang, X. (2000). Phospholipase D: molecular and cell biology of a novel gene family. Biochem J 345 Pt 3, 401-415.

Lukito, Y., Chujo, T., and Scott, B. (2015). Molecular and cellular analysis of the pH response transcription factor PacC in the fungal symbiont *Epichloë festucae*. Fungal Genet Biol 85, 25-37.

Malagnac, F., Lalucque, H., Lepere, G., and Silar, P. (2004). Two NADPH oxidase isoforms are required for sexual reproduction and ascospore germination in the filamentous fungus *Podospora anserina*. Fungal Genet Biol, 41, 982-997.

Marino, D., Dunand, C., Puppo, A., and Pauly, N. (2012). A burst of plant NADPH oxidases. Trends Plant Sci 17, 9-15.

Marschall, R., Siegmund, U., Burbank, J., and Tudzynski, P. (2016). Update on Nox function, site of action and regulation in *Botrytis cinerea*. Fungal Biol Biotechnol 3, article number 8.

Masachis, S., Segorbe, D., Turra, D., Leon-Ruiz, M., Furst, U., El Ghalid, M., Leonard, G., Lopez-Berges, M. S., Richards, T. A., Felix, G., *et al.* (2016). A fungal pathogen secretes plant alkalinizing peptides to increase infection. Nat Microbiol 1, article number 16043.

McLain, N., and Dolan, J. W. (1997). Phospholipase D activity is required for dimorphic transition in *Candida albicans*. Microbiology 143 (Pt 11), 3521-3526.

McPhail, L. C., Qualliotine-Mann, D., and Waite, K. A. (1995). Cell-free activation of neutrophil NADPH oxidase by a phosphatidic acid-regulated protein kinase. Proc Natl Acad USA 92, 7931-7935.

Miller, J. H. (1972). Experiments in molecular genetics (Cold Spring Harbor, N. Y.: Cold Spring Harbor Laboratory).

Miller, P. J., and Johnson, D. I. (1994). Cdc42p GTPase is involved in controlling polarized cell growth in *Schizosaccharomyces pombe*. Mol Cell Biol 14, 1075-1083.

Morris, A. J. (2007). Regulation of phospholipase D activity, membrane targeting and intracellular trafficking by phosphoinositides. Biochem Soc Symp, 247-257.

Nakanishi, H., de los Santos, P., and Neiman, A. M. (2004). Positive and negative regulation of a SNARE protein by control of intracellular localization. Mol Biol Cell 15, 1802-1815.

Nakanishi, H., Morishita, M., Schwartz, C. L., Coluccio, A., Engebrecht, J., and Neiman, A. M. (2006). Phospholipase D and the SNARE Sso1p are necessary for vesicle fusion during sporulation in yeast. J Cell Sci 119, 1406-1415.

Palicz, A., Foubert, T. R., Jesaitis, A. J., Marodi, L., and McPhail, L. C. (2001). Phosphatidic acid and diacylglycerol directly activate NADPH oxidase by interacting with enzyme components. J Biol Chem 276, 3090-3097.

Park, J. W. (1996). Phosphatidic acid-induced translocation of cytosolic components in a cell-free system of NADPH oxidase: mechanism of activation and effect of diacylglycerol. Biochem Biophys Res Commun 229, 758-763.

Peng, X., and Frohman, M. A. (2012). Mammalian phospholipase D physiological and pathological roles. Acta Physiol 204, 219-226.

Pleskot, R., Li, J., Zarsky, V., Potocky, M., and Staiger, C. J. (2013). Regulation of cytoskeletal dynamics by phospholipase D and phosphatidic acid. Trends Plant Sci 18, 496-504.

Pleskot, R., Pejchar, P., Bezvoda, R., Lichtscheidl, I. K., Wolters-Arts, M., Marc, J., Zarsky, V., and Potocky, M. (2012). Turnover of phosphatidic acid through distinct signaling pathways affects multiple aspects of pollen tube growth in tobacco. Front Plant Sci 3, article number 54.

Pleskot, R., Potocky, M., Pejchar, P., Linek, J., Bezvoda, R., Martinec, J., Valentova, O., Novotna, Z., and Zarsky, V. (2010). Mutual regulation of plant phospholipase D and the actin cytoskeleton. J Plant 62, 494-507.

Ponting, C. P., and Kerr, I. D. (1996). A novel family of phospholipase D homologues that includes phospholipid synthases and putative endonucleases: identification of duplicated repeats and potential active site residues. Protein Sci 5, 914-922.

Potocký, M., Pejchar, P., Gutkowska, M., Jimenez-Quesada, M. J., Potocka, A., Alche Jde, D., Kost, B., and Zarsky, V. (2012). NADPH oxidase activity in pollen tubes is affected by calcium ions, signaling phospholipids and Rac/Rop GTPases. J Plant Physiol 169, 1654-1663.

Potocký, M., Pleskot, R., Pejchar, P., Vitale, N., Kost, B., and Zarsky, V. (2014). Live-cell imaging of phosphatidic acid dynamics in pollen tubes visualized by Spo20p-derived biosensor. New Phytol 203, 483-494.

Powner, D. J., Hodgkin, M. N., and Wakelam, M. J. (2002). Antigen-stimulated activation of phospholipase D1b by Rac1, ARF6, and PKCalpha in RBL-2H3 cells. Mol Biol Cell 13, 1252-1262.

Powner, D. J., and Wakelam, M. J. (2002). The regulation of phospholipase D by inositol phospholipids and small GTPases. FEBS Lett 531, 62-64.

Qualliotine-Mann, D., Agwu, D. E., Ellenburg, M. D., McCall, C. E., and McPhail, L. C. (1993). Phosphatidic acid and diacylglycerol synergize in a cell-free system for activation of NADPH oxidase from human neutrophils. J Biol Cem 268, 23843-23849.

Rahnama, M., Forester, N., Ariyawansa, K. G. S. U., Voisey, C. R., Johnson, L. J., Johnson, R. D., and Fleetwood, D. J. (2017). Efficient targeted mutagenesis in *Epichloë festucae* using a split marker system. J Microbiol Methods 134, 62-65.

Read, N.D., Fleißner, A., Roca, M. G., and Glass, N. L. (2010). Hyphal Fusion. In Borkovich, K. A. and Ebbole, D.J.(ed), Cellular and molecular biology of filamentous fungi, chapter 19, p 260-273.

Regier, D. S., Greene, D. G., Sergeant, S., Jesaitis, A. J., and McPhail, L. C. (2000). Phosphorylation of p22phox is mediated by phospholipase D-dependent and -independent mechanisms. Correlation of NADPH oxidase activity and p22phox phosphorylation. J Biol Chem 275, 28406-28412.

Regier, D. S., Waite, K. A., Wallin, R., and McPhail, L. C. (1999). A phosphatidic acid-activated protein kinase and conventional protein kinase C isoforms phosphorylate p22(phox), an NADPH oxidase component. J Biol Chem 274, 36601-36608.

Riedel, C. G., Mazza, M., Maier, P., Korner, R., and Knop, M. (2005). Differential requirement for phospholipase D/Spo14 and its novel interactor Sma1 for regulation of exocytotic vesicle fusion in yeast meiosis. J Biol Chem 280, 37846-37852.

Roca, M. G., Kuo, H. C., Lichius, A., Freitag, M., & Read, N. D. (2010). Nuclear dynamics, mitosis, and the cytoskeleton during the early stages of colony initiation in *Neurospora crassa*. Eukaryotic Cell, *9*(8), 1171–1183.

Roca, M. G., Weichert, M., Siegmund, U., Tudzynski, P., and Fleissner, A. (2012). Germling fusion via conidial anastomosis tubes in the grey mould *Botrytis cinerea* requires NADPH oxidase activity. Fungal Biol 116, 379-387.

Rudge, S. A., Cavenagh, M. M., Kamath, R., Sciorra, V. A., Morris, A. J., Kahn, R. A., and Engebrecht, J. (1998). ADP-Ribosylation factors do not activate yeast phospholipase Ds but are required for sporulation. Mol Biol Cell 9, 2025-2036.

Rudge, S. A., Zhou, C., and Engebrecht, J. (2002). Differential regulation of Saccharomyces cerevisiae phospholipase D in sporulation and Sec14-independent secretion. Genetics 160, 1353-1361.

Ryder, L. S., Dagdas, Y. F., Mentlak, T. A., Kershaw, M. J., Thornton, C. R., Schuster, M., Chen, J., Wang, Z., and Talbot, N. J. (2013). NADPH oxidases regulate septin-mediated cytoskeletal remodeling during plant infection by the rice blast fungus. Proc Natl Acad USA 110, 3179-3184.

Sang, Y., Cui, D., and Wang, X. (2001). Phospholipase D and phosphatidic acid-mediated generation of superoxide in *Arabidopsis*. Plant Physiol 126, 1449-1458.

Schardl, C. L., Leuchtmann, A., and Spiering, M. J. (2004). Symbioses of grasses with seedborne fungal endophytes. Annu Rev Plant Biol 55, 315-340.

Schardl, C. L., Young, C. A., Hesse, U., Amyotte, S. G., Andreeva, K., Calie, P. J., Fleetwood, D. J., Haws, D. C., Moore, N., Oeser, B., *et al*. (2013). Plant-symbiotic fungi as chemical engineers: multi-genome analysis of the Clavicipitaceae reveals dynamics of alkaloid loci. PLoS Genet 9, e1003323.

Sciorra, V. A., Rudge, S. A., Prestwich, G. D., Frohman, M. A., Engebrecht, J., and Morris, A. J. (1999). Identification of a phosphoinositide binding motif that mediates activation of mammalian and yeast phospholipase D isoenzymes. EMBO J 18, 5911-5921.

Sciorra, V. A., Rudge, S. A., Wang, J., McLaughlin, S., Engebrecht, J., and Morris, A. J. (2002). Dual role for phosphoinositides in regulation of yeast and mammalian phospholipase D enzymes. J Cell Biol 159, 1039-1049.

Scott, B., Green, K., and Berry, D. (2018). The fine balance between mutualism and antagonism in the *Epichloë festucae*-grass symbiotic interaction. Curr Opin Plant Biol 44, 32-38.

Scott, B., and Schardl, C. L. (1993). Fungal symbionts of grasses: evolutionary insights and agricultural potential. Trends Microbiol 1, 196-200.

Segmüller, N., Kokkelink, L., Giesbert, S., Odinius, D., van Kan, J., and Tudzynski, P. (2008). NADPH oxidases are involved in differentiation and pathogenicity in *Botrytis cinerea.* Mol Plant-Microbe Interact 21, 808-819.

Selvy, P. E., Lavieri, R. R., Lindsley, C. W., and Brown, H. A. (2011). Phospholipase D: enzymology, functionality, and chemical modulation. Chem Rev 111, 6064-6119.

Semighini, C. P., and Harris, S. D. (2008). Regulation of apical dominance *in Aspergillus nidulans* hyphae by reactive oxygen species. Genetics 179, 1919-1932.

Shen, Y., Xu, L., and Foster, D. A. (2001). Role for phospholipase D in receptor-mediated endocytosis. Mol Cell Biol 21, 595-602.

Siegmund, U., Heller, J., van Kan, J. A., and Tudzynski, P. (2013). The NADPH oxidase complexes in *Botrytis cinerea*: evidence for a close association with the ER and the tetraspanin Pls1. PloS One 8, e55879.

Spiers, A. G., and Hopcroft, D. H. (1993). Black canker and leaf spot of Salix in New Zealand caused by *Glomerella miyabeana* (*Colletotrichum gloeosporioides*). Eur J Forest Pathol 23, 92-102.

Stahelin, R. V., Ananthanarayanan, B., Blatner, N.R., Singh, S., Bruzik, K. S., Murray, D., and Cho, W. (2004). Mechanism of membrane binding of the phospholipase D1 PX domain. J Biol Chem 279, 54918-54926.

Stamatakis, A. (2014). RAxML version 8: a tool for phylogenetic analysis and post-analysis of large phylogenies. Bioinformatics 30, 1312-1313.

Sung, T. C., Roper, R. L., Zhang, Y., Rudge, S. A., Temel, R., Hammond, S. M., Morris, A. J., Moss, B., Engebrecht, J., and Frohman, M. A. (1997). Mutagenesis of phospholipase D defines a superfamily including a trans-Golgi viral protein required for poxvirus pathogenicity. EMBO J 16, 4519-4530.

Takemoto, D., Kamakura, S., Saikia, S., Becker, Y., Wrenn, R., Tanaka, A., Sumimoto, H., and Scott, B. (2011). Polarity proteins Bem1 and Cdc24 are components of the filamentous fungal NADPH oxidase complex. Proc Natl Acad USA 108, 2861-2866.

Takemoto, D., Tanaka, A., and Scott, B. (2006). A p67Phox-like regulator is recruited to control hyphal branching in a fungal-grass mutualistic symbiosis. Plant Cell 18, 2807-2821.

Tanaka, A., Cartwright, G. M., Saikia, S., Kayano, Y., Takemoto, D., Kato, M., Tsuge, T., and Scott, B. (2013). ProA, a transcriptional regulator of fungal fruiting body development, regulates leaf hyphal network development in the *Epichloë festucae-Lolium perenne* symbiosis. Mol Microbiol 90, 551-568.

Tanaka, A., Christensen, M. J., Takemoto, D., Park, P., and Scott, B. (2006). Reactive oxygen species play a role in regulating a fungus-perennial ryegrass mutualistic interaction. Plant Cell 18, 1052-1066.

Tanaka, A., Takemoto, D., Hyon, G. S., Park, P., and Scott, B. (2008). NoxA activation by the small GTPase RacA is required to maintain a mutualistic symbiotic association between *Epichloë festucae* and perennial ryegrass. Mol Microbiol 68, 1165-1178.

Taylor, R. M., Foubert, T. R., Burritt, J. B., Baniulis, D., McPhail, L. C., and Jesaitis, A. J. (2004). Anionic amphiphile and phospholipid-induced conformational changes in human neutrophil flavocytochrome b observed by fluorescence resonance energy transfer. Biochim Biophys Acta 1663, 201-213.

Taylor, R. M., Riesselman, M. H., Lord, C. I., Gripentrog, J. M., and Jesaitis, A. J. (2012). Anionic lipid-induced conformational changes in human phagocyte flavocytochrome b precede assembly and activation of the NADPH oxidase complex. Arch Biochem Biophys 521, 24-31.

Tong, L. C., Silar, P., and Lalucque, H. (2014). Genetic control of anastomosis in *Podospora anserin*a. Fungal Genet Biol 70, 94-103.

Tudzynski, P., Heller, J., and Siegmund, U. (2012). Reactive oxygen species generation in fungal development and pathogenesis. Curr Opin Microbiol 15, 653-659.

Waite, K. A., Wallin, R., Qualliotine-Mann, D., and McPhail, L. C. (1997). Phosphatidic acid-mediated phosphorylation of the NADPH oxidase component p47-phox. Evidence that phosphatidic acid may activate a novel protein kinase. J Biol Chem 272, 15569-15578.

Walker, S. J., and Brown, H. A. (2002). Specificity of Rho insert-mediated activation of phospholipase D1. J Biol Chem 277, 26260-26267.

Walker, S. J., Wu, W. J., Cerione, R. A., and Brown, H. A. (2000). Activation of phospholipase D1 by Cdc42 requires the Rho insert region. J Biol Chem 275, 15665-15668.

Wang, L., Mogg, C., Walkowiak, S., Joshi, M., and Subramaniam, R. (2014). Characterization of NADPH oxidase genes NoxA and NoxB in *Fusarium graminearum*. Can J Plant Pathol 36, 12-21.

Wang, X. (2000). Multiple forms of phospholipase D in plants: the gene family, catalytic and regulatory properties, and cellular functions. Progress Lipid Res 39, 109-149.

Weichert, M., Lichius, A., Priegnitz, B. E., Brandt, U., Gottschalk, J., Nawrath, T., Groenhagen, U., Read, N. D., Schulz, S. and Fleißner, A. (2016). Accumulation of specific sterol precursors targets a MAP kinase cascade mediating cell-cell recognition and fusion. Proc Natl Acad Sci USA, 113(42), 11877–11882.

Young, C. A., Bryant, M. K., Christensen, M. J., Tapper, B. A., Bryan, G. T., and Scott, B. (2005). Molecular cloning and genetic analysis of a symbiosis-expressed gene cluster for lolitrem biosynthesis from a mutualistic endophyte of perennial ryegrass. Mol Genet Genomics 274, 13-29.

Zeniou-Meyer, M., Zabari, N., Ashery, U., Chasserot-Golaz, S., Haeberle, A. M., Demais, V., Bailly, Y., Gottfried, I., Nakanishi, H., Neiman, A. M., *et al*. (2007). Phospholipase D1 production of phosphatidic acid at the plasma membrane promotes exocytosis of large dense-core granules at a late stage. J Biol Chem 282, 21746-21757.

Zerbino, D. R., Achuthan, P., Akanni, W., Amode, M. R., Barrell, D., Bhai, J., Billis, K., Cummins, C., Gall, A., Girón, C. G., *et al*. (2018). Ensembl 2018. Nucleic Acids Res 46, D754-D761.

Zhang, Y., Zhu, H., Zhang, Q., Li, M., Yan, M., Wang, R., Wang, L., Welti, R., Zhang, W., and Wang, X. (2009). Phospholipase dalpha1 and phosphatidic acid regulate NADPH oxidase activity and production of reactive oxygen species in ABA-mediated stomatal closure in *Arabidopsis*. Plant Cell 21, 2357-2377.

Zhao, Y. L., Zhou, T. T., and Guo, H. S. (2016). Hyphopodium-specific VdNoxB/VdPls1-dependent ROS-Ca2+ signaling is required for plant infection by *Verticillium dahliae*. PLoS Pathog 12, e1005793.

Supporting Information

Supporting Information Table S1: Biological material.

Organism/Strain	Characteristics	Reference
E. coli		
DH5α	F⁻, φ80*lacZ*, ΔM15, Δ(*lacZYA-argF*), U169, *recA1*, *endA1*, *hsdR17* (r_k^-, m_k^-), *phoA*, *supE44*, *λ*⁻, *thi-1*, *gyrA96*, *relA1*	Invitrogen
S. cerevisiae		
AH109	MATa, trp1-901, leu2-3, 112, ura3-52, his3-200, gal4Δ, gal80Δ, LYS2::GAL1UAS-GAL1TATAHIS3, GAL2UAS-GAL2TATA-ADE2, URA3::MEL1 UASMEL1TATA-lacZ, MEL1	Clontech
AH109 (AB, BD)	AH109/pGADT7 & pGBKT7; *LEU2, TRP1*	This study
AH109 (AB-T7, BD-p53)	AH109/pGADT7-T7 & pGBKT7-p53; *LEU2, TRP1*	This study
AH109 (AD-PldB, BD)	AH109/pBH60 & pGBKT7; *LEU2, TRP1*	This study
AH (AD, BD-PldB)	AH109/pGADT7 & pBH61; *LEU2, TRP1*	This study
AH109 (AD-MssD, BD)	AH109/pBH63 & pGBKT7; *LEU2, TRP1*	This study
AH (AD, BD-MssD)	AH109/pGADT7 & pBH62; *LEU2, TRP1*	This study
AH109 (AD-PkcA, BD)	AH109/pBH64 & pGBKT7; *LEU2, TRP1*	This study
AH (AD, BD-PkcA)	AH109/pGADT7 & pBH65; *LEU2, TRP1*	This study
AH109 (AD-PldB, BD-NoxR)	AH109/pBH60 & pPN113; *LEU2, TRP1*	This study
AH109 (AD-PldB, BD-Cdc24)	AH109/pBH60 & pPN173; *LEU2, TRP1*	This study
AH109 (AD-PldB, BD-Cdc42)	AH109/pBH60 & pYR9; *LEU2, TRP1*	This study
AH109 (AD-PldB, BD-RacA)	AH109/pBH60 & pYR7; *LEU2, TRP1*	This study
AH109 (AD-PldB, BD-BemA)	AH109/pBH60 & pPN172; *LEU2, TRP1*	This study
AH109 (AD-PldB, BD-MssD)	AH109/pBH60 & pBH62; *LEU2, TRP1*	This study
AH109 (AD-PldB, BD-PkcA)	AH109/pBH60 & pBH65; *LEU2, TRP1*	This study
AH109 (AD-NoxR, BD-PldB)	AH109/ pPN112 & pBH61; *LEU2, TRP1*	This study
AH109 (AD-Cdc24, BD-PldB)	AH109/ pPN160 & pBH61; *LEU2, TRP1*	This study
AH109 (AD-Cdc42, BD-PldB)	AH109/pYR8 & pBH61; *LEU2, TRP1*	This study
AH109 (AD-RacA, BD-PldB)	AH109/pYR6 & pBH61; *LEU2, TRP1*	This study
AH109 (AD-Mss4, BD-PldB)	AH109/pBH63 & pBH61; *LEU2, TRP1*	This study
AH109 (AD-PkcA, BD-PldB)	AH109/pBH64 & pBH61; *LEU2, TRP1*	This study
E. festucae		
PN2278 (Fl1)	Wild-type isolated from *Festuca longifolia*	Young *et al*. 2005
PN2326 (Δ*noxA)*	WT/Δ*noxA*::P*trpC-hph;* Hyg^R	Tanaka *et al*., 2006
PN2469 (Δ*noxB)*	WT/Δ*noxB*::P*trpC-nptII*-T*trpC;* Gen^R	Tanaka *et al*., 2006
PN3272 (Δ*pldA*#T47)	WT/Δ*pldA*::P*trpC-hph;* Hyg^R	This study
PN3273 (Δ*pldA*#T49)	WT/Δ*pldA*::P*trpC-hph;* Hyg^R	This study
PN3274 (Δ*pldA*#T82)	WT/Δ*pldA*::P*trpC-hph;* Hyg^R	This study
pldA overexpression #T3	WT/pCE129/pII99, Gen^R	This study
pldA overexpression #T4	WT/pCE129/pII99, Gen^R	This study
pldA overexpression #T9	WT/pCE129/pII99, Gen^R	This study
PN3275 (Δ*pldB*#T26)	WT/Δ*pldB*::P*trpC-nptII*-P*trpC;* Gen^R	This study
PN3276 (Δ*pldB*#T50)	WT/Δ*pldB*::P*trpC-nptII*-P*trpC;* Gen^R	This study
PN3277(Δ*pldB*#T87)	WT/Δ*pldB*::P*trpC-nptII*-P*trpC;* Gen^R	This study
pldB overexpression #T6	WT/pBH48/pII99, Gen^R	This study
pldB overexpression #T21	WT/pBH48/pII99, Gen^R	This study
pldB overexpression #T22	WT/pBH48/pII99, Gen^R	This study
Δ*pldB*/Δ*pldA*#T3	Δ*pldB* T87/Δ*pldA*::P*trpC-hph;* Gen^R; Hyg^R	This study

Organism/Strain	Characteristics	Reference
Δ*pldB*/Δ*pldA*#T5	Δ*pldB* T26/Δ*pldA*::P*trpC-hph;* Gen^R; Hyg^R	This study
WT GFP-NoxA#T1	WT/pNoxA-GFP/pBH12, Hyg^R	This study
WT GFP-NoxA#T4	WT/pNoxA-GFP/pBH12, Hyg^R	This study
WT GFP-NoxA#T5	WT/pNoxA-GFP/pBH12, Hyg^R	This study
WT GFP-NoxA#T7	WT/pNoxA-GFP/pBH12, Hyg^R	This study
WT NoxR-GFP#T1	WT/pNPP9, Hyg^R	Green pers. comm.
WT Cdc24-GFP#T9	WT/pNPP6, Hyg^R	Green pers. comm.
WT Cdc24-GFP#T33	WT/pNPP6, Hyg^R	Green pers. comm.
WT BemA-GFP#T20	WT/pCE139, pII99, Gen^R	Green pers. comm.
WT BemA-GFP#T23	WT/pCE139, pII99, Gen^R	Green pers. comm.
WT BemA-GFP#T24	WT/pCE139, pII99, Gen^R	Green pers. comm.
WT RacA-GFP#T1	WT/pPN154, Hyg^R	This study
WT RacA-GFP#T6	WT/pPN154, Hyg^R	This study
WT RacA-GFP#T7	WT/pPN154, Hyg^R	This study
WT RacA-GFP#T8	WT/pPN154, Hyg^R	This study
WT PA-biosensor #T4	WT/pBH50, HygR	This study
WT PA-biosensor #T7	WT/pBH50, Hyg^R	This study
WT PA-biosensor #T8	WT/pBH50, Hyg^R	This study
WT PA-biosensor #T9	WT/pBH50, Hyg^R	This study
WT PA-biosensor #T11	WT/pBH50, Hyg^R	This study
WT GFP-PldA#T3	WT/pBH37, Gen^R	This study
WT GFP-PldA#T4	WT/pBH37, Gen^R	This study
WT GFP-PldA#T5	WT/pBH37, Gen^R	This study
WT GFP-PldA#T9	WT/pBH37, Gen^R	This study
WT GFP-PldA#T14	WT/pBH37, Gen^R	This study
WT PldA-mCherry#T1	WT/pBH38, Hyg^R	This study
WT PldA-mCherry#T4	WT/pBH38, Hyg^R	This study
WT PldA-mCherry#T5	WT/pBH38, Hyg^R	This study
WT PldA-mCherry#T6	WT/pBH38, Hyg^R	This study
WT GFP-PldB#T13	WT/pBH54 Gen^R	This study
WT GFP-PldB#T14	WT/pBH54 Gen^R	This study
WT GFP-PldB#T15	WT/pBH54 Gen^R	This study
WT GFP-PldB#T16	WT/pBH54 Gen^R	This study
WT PldB-mCherry#T4	WT/pBH52, Hyg^R	This study
WT PldB-mCherry#T8	WT/pBH52, Hyg^R	This study
WT GFP#T1	WT/pBH28, Gen^R	This study
WT GFP#T6	WT/pBH28, Gen^R	This study
WT mCherry#T1	WT/pCE126, pBH12, Hyg^R	This study
WT mCherry#T2	WT/pCE126, pBH12, Hyg^R	This study
Δ*pldA*#T47 NoxR-GFP	Δ*pldA*#T47/pNPP9/pII99, Hyg^R, Gen^R	This study
Δ*pldA*#T47 Cdc24-GFP#T1	Δ*pldA*#T47/pNPP6/pII99, Hyg^R, Gen^R	This study
Δ*pldA*#T47 Cdc24-GFP#T2	Δ*pldA*#T47/pNPP6/pII99, Hyg^R, Gen^R	This study
Δ*pldA*#T47 Cdc24-GFP#T4	Δ*pldA*#T47/pNPP6/pII99, Hyg^R, Gen^R	This study
Δ*pldA*#T47 BemA-GFP#T17	Δ*pldA*#T47/pCE139/pII99, Hyg^R, Gen^R	This study
Δ*pldA*#T47 BemA-GFP#T23	Δ*pldA*#T47/pCE139/pII99, Hyg^R, Gen^R	This study
Δ*pldA*#T47 RacA-GFP#T3	Δ*pldA*#T47/pPN154/pII99, Hyg^R, Gen^R	This study
Δ*pldA*#T47 RacA-GFP#T4	Δ*pldA*#T47/pPN154/pII99, Hyg^R, Gen^R	This study
Δ*pldA*#T47 RacA-GFP#T15	Δ*pldA*#T47/pPN154/pII99, Hyg^R, Gen^R	This study
Δ*pldA*#T47 PA biosensor#T10	Δ*pldA*#T47/pBH50/pII99, Hyg^R, Gen^R	This study
Δ*pldA*#T82 GFP-NoxA#T2	Δ*pldA*#T82/pGFP-NoxA/pII99, Hyg^R, Gen^R	This study
Δ*pldA*#T82 GFP-NoxA#T3	Δ*pldA*#T82/pGFP-NoxA/pII99, Hyg^R, Gen^R	This study
Δ*pldA*#T82 GFP-NoxA#T5	Δ*pldA*#T82/pGFP-NoxA /pII99, Hyg^R, Gen^R	This study
Δ*pldA*#T82 NoxR-GFP#T29	Δ*pldA*#T82/pNPP9/pII99, Hyg^R, Gen^R	This study
Δ*pldA*#T82 Cdc24-GFP#T1	Δ*pldA*#T82/pNPP6/pII99, Hyg^R, Gen^R	This study
Δ*pldA*#T82 Cdc24-GFP#T25	Δ*pldA*#T82/pNPP6/pII99, Hyg^R, Gen^R	This study
Δ*pldA*#T82 BemA-GFP#T3	Δ*pldA*#T82/pCE139/pII99, Hyg^R, Gen^R	This study

Organism/Strain	Characteristics	Reference
Δ*pldA*#T82 BemA-GFP#T9	Δ*pldA*#T82/pCE139/pII99, Hyg^R, Gen^R	This study
Δ*pldA*#T82 BemA-GFP#T14	Δ*pldA*#T82/pCE139/pII99, Hyg^R, Gen^R	This study
Δ*pldA*#T82 RacA-GFP#T1	Δ*pldA*#T82/pPN154/pII99, Hyg^R, Gen^R	This study
Δ*pldA*#T82 RacA-GFP#T12	Δ*pldA*#T82/pPN154/pII99, Hyg^R, Gen^R	This study
Δ*pldA*#T82 PA biosensor#T10	Δ*pldA*#T82/pBH50/pII99, Hyg^R, Gen^R	This study
Δ*pldB*#T26 complementation #T1	Δ*pldB*#T26/pBH53 Hyg^R, Gen^R	This study
Δ*pldB*#T26 complementation #T4	Δ*pldB*#T26/pBH53 Hyg^R, Gen^R	This study
Δ*pldB*#T26 complementation #T13	Δ*pldB*#T26/pBH53 Hyg^R, Gen^R	This study
Δ*pldB*#T26 GFP-NoxA#T1	Δ*pldB*#T26/pGFP-NoxA/pBH12, Hyg^R, Gen^R	This study
Δ*pldB*#T26 GFP-NoxA#T2	Δ*pldB*#T26/pGFP-NoxA/pBH12, Hyg^R, Gen^R	This study
Δ*pldB*#T26 GFP-NoxA#T3	Δ*pldB*#T26/pGFP-NoxA/pBH12, Hyg^R, Gen^R	This study
Δ*pldB* T26 NoxR-GFP#T1	Δ*pldB*#T26/pNPP9, Hyg^R, Gen^R	This study
Δ*pldB*#T26 Cdc24-GFP#T1	Δ*pldB*#T26/pNPP6, Hyg^R, Gen^R	This study
Δ*pldB*#T26 Cdc24-GFP#T2	Δ*pldB*#T26/pNPP6, Hyg^R, Gen^R	This study
Δ*pldB*#T26 BemA-GFP#T1	Δ*pldB*#T26/pCE139, Hyg^R, Gen^R	This study
Δ*pldB*#T26 BemA-GFP#T3	Δ*pldB*#T26/pCE139/pBH12, Hyg^R, Gen^R	This study
Δ*pldB*#T26 BemA-GFP#T5	Δ*pldB*#T26/pCE139/pBH12, Hyg^R, Gen^R	This study
Δ*pldB*#T26 RacA-GFP#T1	Δ*pldB*#T26/pPN154, Hyg^R, Gen^R	This study
Δ*pldB*#T26 RacA-GFP#T2	Δ*pldB*#T26/pPN154, Hyg^R, Gen^R	This study
Δ*pldB*#T26 PA biosensor#T1	Δ*pldB*#T26/pBH50, Hyg^R, Gen^R	This study
Δ*pldB*#T26 PA biosensor#T2	Δ*pldB*#T26/pBH50, Hyg^R, Gen^R	This study
Δ*pldB*#T26 PA biosensor#T3	Δ*pldB*#T26/pBH50, Hyg^R, Gen^R	This study
Δ*pldB*#T26 GFP-PldB#T5	Δ*pldB*#T26/pBH54/pBH12, Hyg^R, Gen^R	This study
Δ*pldB*#T26 GFP-PldB#T6	Δ*pldB*#T26/pBH54/pBH12, Hyg^R, Gen^R	This study
Δ*pldB*#T26 GFP-PldB#T9	Δ*pldB*#T26/pBH54/pBH12, Hyg^R, Gen^R	This study
Δ*pldB*#T26 PldB-mCherry#T1	Δ*pldB*#T26/pBH52, Hyg^R, Gen^R	This study
Δ*pldB*#T26 PldB-mCherry#T2	Δ*pldB*#T26/pBH52, Hyg^R, Gen^R	This study
Δ*pldB*#T26 PldB-mCherry#T3	Δ*pldB*#T26/pBH52, Hyg^R, Gen^R	This study
Δ*pldB*#T26 GFP#T1	Δ*pldB*#T26/pBH28, pBH12, Hyg^R, Gen^R	This study
Δ*pldB*#T26 mCherry#T2	Δ*pldB*#T26/pCE126, pBH12, Hyg^R, Gen^R	This study
Δ*pldB*#T26 mCherry#T3	Δ*pldB*#T26/pCE126, pBH12, Hyg^R, Gen^R	This study
Δ*pldB*#T87 complementation#T1	Δ*pldB*#T87/pBH53, Hyg^R, Gen^R	This study
Δ*pldB*#T87 complementation#T4	Δ*pldB*#T87/pBH53, Hyg^R, Gen^R	This study
Δ*pldB*#T87 complementation#T10	Δ*pldB*#T87/pBH53, Hyg^R, Gen^R	This study
Δ*pldB*#T87 GFP-NoxA#T1	Δ*pldB*#T87/pGFP-NoxA/pBH12, Hyg^R, Gen^R	This study
Δ*pldB*#T87 NoxR-GFP#T4	Δ*pldB*#T87/pNPP9/pBH12, Hyg^R, Gen^R	This study
Δ*pldB*#T87 Cdc24-GFP#T1	Δ*pldB*#T87/pNPP6/pBH12, Hyg^R, Gen^R	This study
Δ*pldB*#T87 Cdc24-GFP#T2	Δ*pldB*#T87/pNPP6/pBH12, Hyg^R, Gen^R	This study
Δ*pldB*#T87 Cdc24-GFP#T3	Δ*pldB*#T87/pNPP6/pBH12, Hyg^R, Gen^R	This study
Δ*pldB*#T87 BemA-GFP#T2	Δ*pldB*#T87/pCE139/pBH12, Hyg^R, Gen^R	This study
Δ*pldB*#T87 RacA-GFP#T1	Δ*pldB*#T87/pPN154/pBH12, Hyg^R, Gen^R	This study
Δ*pldB*#T87 RacA-GFP#T2	Δ*pldB*#T87/pPN154/pBH12, Hyg^R, Gen^R	This study
Δ*pldB*#T87 RacA-GFP#T3	Δ*pldB*#T87/pPN154/pBH12, Hyg^R, Gen^R	This study
Δ*pldB*#T87 PA biosensor#T1	Δ*pldB*#T87/pBH50, Hyg^R, Gen^R	This study
Δ*pldB*#T87 PA biosensor#T2	Δ*pldB*#T87/pBH50, Hyg^R, Gen^R	This study

Organism/Strain	Characteristics	Reference
Δ*pldB*#T87 PA biosensor#T3	Δ*pldB*#T87/pBH50, Hyg^R, Gen^R	This study
Δ*pldB*#T87 GFP-PldB#T1	Δ*pldB*#T87/pBH54/pBH12, Hyg^R, Gen^R	This study
Δ*pldB*#T87 GFP-PldB#T2	Δ*pldB*#T87/pBH54/pBH12, Hyg^R, Gen^R	This study
L. perenne		
L. perenne cv. Samson	-	AgResearch
Plasmid	**Characteristics**	**Reference**
PN1862 (pSF15.15)	pSP72 containing 1.4-kb *Hind*III P*trpC-hph* from pCB1004 cloned into *Sma*I site. Amp^R; Hyg^R; *Nco*I-free P*trpC-hph*	S. Foster
PN4111 (pPN94)	pSF14.14 containing 0.8-kb *Sal*I/*Xba*I *tef* promoter in *Xho*I/*Xba*I site and 0.6-kb *EcoR*I/*Bgl*II T*trpC* in *Eco*RI/*Bgl*II site	Takemoto *et al*. 2006
PN4183 (pRS426)	*ori*(f1)-l*acZ*-T7 promoter-MCS (*Kpn*I-*Sac*I)-T3 promoter-*lacI*-*ori*(pMB1)-amp^R-*ori* (2 micron), *URA3;* Amp^R	Christianson *et al*. 1992
PN 1687 (pII99)	P*trpC-nptII*-T*trpC*, Amp^R/Gen^R	Lara-Ortíz *et al*. 2003
PN4241 (pBV579)	pAN583 containing a 0.1 kb *Bsr*GI/*Bam*HI fragment containing NLS (three tandem repeats of the nuclear localisation signal from simian virus large T-antigen) from pEBFP2-Nuc	Khang *et al*. 2010
pUC57	5' *pldA* flank	This study
pPN82	pBlueScriptII® KS(+) containing 1.4-kb HindIII PtrpC-hph and Pgpd-EGFP-T*trpC*; Amp^R /Hyg^R	Tanaka *et al*. 2006
pGADT7	GAL4-AD, SV40-NLS, LEU2, Amp^R	Takara Bio USA Inc.
pGBKT7	GAL4-BD, SV40-NLS, TRP1, Kan^R	Takara Bio USA Inc.
pGADT7-7	pGBKT& containing SV40large T-antigen$_{aa86-708}$ cDNA, Amp^R	Takara Bio USA Inc.
pGBKT7-p53	pGBKT7 containing murine p53$_{aa72-390}$ cDNA, $Kana^R$	Takara Bio USA Inc.
pPN112	pGAD-T7containing a *noxR* insert, Amp^R	Takemoto *et al*., 2011
pPN113	pGBK-T7 containing a *noxR* insert, Kan^R	Takemoto *et al*., 2011
pYR6	pGAD-T7containing a *racA* insert, Amp^R	Becker *et al*., (in preparation)
pYR7	pGBK-T7 containing a *racA* insert, Kan^R	Becker *et al*., (in preparation)
pPN160	pGAD-T7containing a *cdc24* insert, Amp^R	Takemoto *et al*., 2011
pPN173	pGBK-T7 containing a *cdc24* insert, Kan^R	Takemoto *et al*., 2011
pYR8	pGAD-T7containing a *cdc42* insert, Amp^R	Becker *et al*., (in preparation)
pYR9	pGBK-T7 containing a *cdc42* insert, Kan^R	Becker *et al*., (in preparation)
pPN172	pGBK-T7 containing a *bemA* insert, Kan^R	Takemoto *et al*., 2011
pPN154	pPN94 containing 0.7-kb *Xba*I/*Xho*I *egfp* and 0.6-kb *Xho*I/*Not*I *racA* in XbaI/NotI site	Takemoto *et al*., 2011
pNPP6	pPN94 containing 3.0-kb *Xba*I/*Cla*I *cdc*24 and 0.7-kb *Cla*I/*Not*I 3GA-*egfp* in *Xba*I/*Not*I site.	Takemoto *et al*., 2011
pNPP9	pPN94 containing 1.6-kb *Eco*RI/*Cla*I *noxR* and 0.7-kb ClaI/NotI 3GA-*egfp* in *EcoR*I/*Not*I site.	Takemoto *et al*., 2011
pCE139	pRS425 containing *bemA-egfp*	Eaton, pers. comm.
pGFP-NoxA	pRS425 containing *egfp-noxA*	Eaton, pers. comm.
pCE131	pRS426 containing *pldA* deletion construct, Hyg^R	This study
pCE121	pRS426 containing *pldB* deletion construct, Gen^R	This study
pCE129	pRS426 containing a P*gdp-pldA*-T*trpC* overexpression construct	This study
pCE126	pRS426 containing P*gpd*-mCherry-T*trpC* insert	Candy, 2019
pBH12	pPN94 containing 723 bp *B. cinerea tub* terminator insert amplified from pNR1 downstream of *hph*; Hyg^R	Hassing *et al*., 2019

Organism/Strain	Characteristics	Reference
pBH16	pBH12 containing mCherry-NLS amplified from pBV579, Hyg^R	This study
pBH28	pBH12 containing *nptII* replacing *hph* and *gfp;* Gen^R	Hassing *et al*., 2019
pBH37	pBH28 containing P*gpd-gfp-pldA*-T*trpC*, Gen^R	This study
pBH38	pBH12 containing P*gpd-pldA-mCherry*-T*trpC*, Hyg^R	This study
pBH48	pRS426 containing a P*gdp-pldB*-T*trpC* overexpression construct	This study
pBH50	pBH12 containing the PA-localisation construct (*gfp*, bp 151-273 of *S. cerevisiae SPO20*), Hyg^R	This study
pBH52	pBH12 containing P*gpd-pldB-mCherry*-T*trpC*, Hyg^R	This study
pBH53	pBH12 containing a *pldB* complementation construct	This study
pBH54	pBH28 containing P*gpd-gfp-pldB*-T*trpC*, Gen^R	This study
pBH60	pGADT7 containing a *pldB* insert, Amp^R	This study
pBH61	pGBK-T7 containing a *pldB* insert, Kan^R	This study
pBH62	pGBK-T7 containing a *mssD* insert, Kan^R	This study
pBH63	pGAD-T7 containing a *mssD* insert, Amp^R	This study
pBH64	pGAD-T7 containing a *pkcA* insert, Amp^R	This study
pBH65	pGBK-T7 containing a *pkcA* insert, Kan^R	This study

Supporting Information Table S2: Primer sequences.

Name	Sequence (5'-3')	Purpose
PldA1	GCGGATAACAATTTCACACAGGAAACAGCCCCTAGACCTGACGGAAGG	*pldA* deletion, 3' fragment
PldA2	AAATGCTCCTTCAATATCAGTTCCAAGCTCCCTCTGAGTTGGTGACGAC	*pldA* deletion, 3' fragment
PldA5	CCAGCACTCGTCCGAGGGCAAAGGAATAGAAGTCATGTTAGCCGTTGCTG	*pldA* deletion, 5' fragment
PldA6	GTAACGCCAGGGTTTTCCCAGTCACGACATGTTTTCGGATTCGGCG	*pldA* deletion, 5' fragment
PldA7	ACAGCTACCCCGCTTGAGCAGACATCACCATGTCCAAGACTGGGGAAGTTTC	*pldA* overexpression
PldA8	AGATTCGTCAAGCTGTTTGATGATTTCAGTTAGGTGTACACACTTTCTGTCC	*pldA* overexpression
PldA9	TTTGGTCGTTGGGACGCTCGC	*pldA* sequencing
PldA10	TCAGCAGCCTTCCTTTGTGAG	*pldA* sequencing
PldA11	ACAAGTTGAGCGAATCTAAGC	Verification of *pldA* deletion
PldA12	AAGTCGTCACCAACTCAGAGG	Verification of *pldA* deletion
PldA13	CCCATTTTACCACTTGGCGTC	Verification of *pldA* deletion
PldA14	CTCAAAGTAGCACACTCCTCG	Verification of *pldA* deletion
PldB1	GCGGATAACAATTTCACACAGGAAACAGCAGTTTGGCCCTGTTTGTTGC	*pldB* deletion, 3' fragment
PldB2	CCAAGCCCAAAAAGTGCTCCTTCAATATCCCAGCATGGAAGGCAAATCG	*pldB* deletion, 3' fragment
PldB3	CTCGAAAATCATTCCTACTAAGATGGGTACTTGTAGGCAGTGGTGAGCT	*pldB* deletion, 5' fragment
PldB4	GGTAACGCCAGGGTTTTCCCAGTCACGACCATAGACGCTGTATCCGCCA	*pldB* deletion, 5' fragment
PldB5	ACAGCTACCCCGCTTGAGCAGACATCACCATGCCTTTTGATTTCAGCATG	*pldB* overexpression, 5' fragement
PldB6	AGATTCGTCAAGCTGTTTGATGATTTCAGCTAGTTGCTGTGGAACGATC	*pldB* overexpression, 3' fragement

Name	Sequence (5'-3')	Purpose
PldB7	CTGCTATCAGTCAGAAGTGGCGTCTTGACAGACTGTTGC	*pldB* overexpression, 3' fragement
PldB8	ACGCCACTTCTGACTGATAGCAGCCGGCCGGCGCATGTAAAG TTCAGG	*pldB* overexpression, 5' fragement
PldB9	CTTCCGCTCGTTTTGGTAGTC	*pldB* sequencing
PldB10	ACTCCGCTTGCCATACCATCC	*pldB* sequencing
PldB11	GACTCCATAAATGAAATGCTC	*pldB* sequencing
PldB12	CACTGGTTGAGCGTATCATTC	*pldB* sequencing
PldB13	CCTTGGACACATCGGCAGGTC	*pldB* sequencing
PldB14	ACAACCACTTGACCGTCCAGC	Verification of *pldB* deletion
PldB15	TTGAGTTGCCAGAACCCAGAG	Verification of *pldB* deletion
PldB16	GCAACGTGTATCTTTAGCTCC	Verification of *pldB* deletion
PldB17	ATAAGTGTGCTGAGATTGCAC	Verification of *pldB* deletion
BH59	TATCCACGCCCTCCTACATC	Verification of *pldA* deletion
BH60	GTTGACGGCAATTTCGATG	Verification of *pldA* deletion
BH75	CAGTGAGCGAGGAAGCGGAAGGCTTGCTTAGCTTGATATCTG	pBH12 amplification
BH76	CTGAAATCATCAAACAGCTTG	pBH12 amplification
BH78	GTGTCACCTAAATCGTATGTG	*pldB* complementation construct
BH79	GGAGGTGGAGGTTCTGGTGGAGGTGGATCTATGGTGAGCAA GGGCGAGGA	*mCherry* with linker forward
BH114	GTGACACTATAGAACTCGACGAATTCCCTTGTATCTCTACA	Amplification of P*gdp+gfp* forward
BH191	CATAGATCCACCTCCACCAGAACCTCCACCTCCCTTGTACAGC TCGTCCATGC	Amplification of P*gdp+gfp* with linker reverse
BH192	GGAGGTGGAGGTTCTGGTGGAGGTGGATCTATGTCCAAGACT GGGGAAGTTTC	*pldA* with linker forward
BH193	GTCGAGTTCTATAGTGTCACC	Amplification of vector backbone
BH196	GGTGATGTCTGCTCAAGCGG	Amplification of vector backbone
BH197	CTTCCGCTTCCTCGCTCACTG	Amplification of vector backbone
BH198	CCGCTTGAGCAGACATCACCATGTCCAAGACTGGGGAAGTTT C	*pldA* forward with overhang to P*gdp*
BH199	CAAGCTGTTTGATGATTTCAGTTAAGATCTGTACAGCTCGTCC ATGCCG	*mCherry* reverse overhang to pBH12
BH200	CATAGATCCACCTCCACCAGAACCTCCACCTCCGGTGTACACA CTTTCTGTCCA	*pldA* reverse with overhang to linker
BH202	CATAGATCCACCTCCACCAGAACCTCCACCTCCGTTGCTGTGGA ACGATCAGTTG	*pldB* reverse with linker
BH206	CATAGATCCACCTCCACCAGAACCTCCACCTCCGGTGTACACA CTTTCTGTCCA	*npt2* reverse for split marker deletion
BH207	CATAGATCCACCTCCACCAGAACCTCCACCTCCGGTGTACACA CTTTCTGTCCA	*npt2* forward for split marker deletion
BH220	CACATACGATTTAGGTGACACTAGCAACGTGTATCTTTAGCTC	*pldB* forward for complementation
BH222	GACGCCACTAAGACTAGTTGACTGAAATCATCAAACAGCTTG	amplification of pBH50 backbone
BH223	CACCTGCTCCGGCACCAGCGCCCTTGTACAGCTCGTCCATGC C	amplification of pBH50 backbone
BH224	CCGCTTGAGCAGACATCACCATGTCACCGGCAGAACATGG	*pldB* reverse with overhang to P*gdp*
BH235	GACCGGCAGATCTATTGTATACCCCTTCTGCTTTTGCTGGAA	*pldB* reverse for complementation

Name	Sequence (5'-3')	Purpose
BH236	GTATACAATAGATCTGCCGGTC	backbone amplification forward without terminator
BH239	TTCTGGTGGAGGTGGATCTATGTCACCGGCAGAACATGGTAA	*pldB* forward overhang to linker
BH241	ATGGCCATGGAGGCCAGTGAATTCATGTCACCGGCAGAACATGG	*pldB* forward for pGAD-T7
BH242	CATCTGCAGCTCGAGCTCGATGGATCCCTAGTTGTAGATTGACAGCGG	*pldB* reverse for pGAD-T7
BH243	GCATATGGCCATGGAGGCCGAATTCATGTCACCGGCAGAACATGG	*pldB* forward for pGBK-T7
BH244	TGCTAGTTATGCGGCCGCTGCAGGCTAGTTGTAGATTGACAGCGG	*pldB* reverse for pGBK-T7
BH245	GCATATGGCCATGGAGGCCGAATTCATGCCCTCGTTTCTCAACGAC	*mssD* forward for pGAD-T7
BH246	TGCTAGTTATGCGGCCGCTGCAGGCTAAACCATGCGTACGCCGCTG	*mssD* reverse for pGAD-T7
BH247	ATGGCCATGGAGGCCAGTGAATTCATGCCCTCGTTTCTCAACGAC	*mssD* forward for pGBK-T7
BH248	CATCTGCAGCTCGAGCTCGATGGATCCCTAAACCATGCGTACGCCGCTG	*mssD* reverse for pGBK-T7
BH249	ATGGCCATGGAGGCCAGTGAATTCATGAGCGAAGACGAAAAAAAG	*pkcA* forward for pGAD-T7
BH250	CATCTGCAGCTCGAGCTCGATGGATCCTCATTCAAAATCCGCGGTGTAC	*pkcA* reverse for pGAD-T7
BH251	GCATATGGCCATGGAGGCCGAATTCATGAGCGAAGACGAAAAAAAG	*pkcA* forward for pGBK-T7
BH252	TGCTAGTTATGCGGCCGCTGCAGGTCATTCAAAATCCGCGGTGTAC	*pkcA* reverse for pGBK-T7
TtrpC-F	CTGAAATCATCAAACAGCTTGACG	backbone for overexpression construct
pRS426-TtrpC-R	GCGGATAACAATTTCACACAGGAAACAGCCCATCTTAGTAGGAATGATTTTCG	backbone for overexpression construct
pRS426-Pgdp-F	GTAACGCCAGGGTTTTCCCAGTCACGACGAATTCCCTTGTATCTCTACA	backbone for overexpression construct
pRS426-Pgdp-R	GGTGATGTCTGCTCAAGCGGGGTAG	backbone for overexpression construct
pRS426_F	GCTGTTTCCTGTGTGAAATTG	*pRS426* backbone
pRS426_R	GGGTTTTCCCAGTCACGAC	*pRS426* backbone
hph_F	AGCTTGGAACTGATATTGAAGG	P*trpC-hph* for deletion constructs
hph_R	CGTCCGAGGGCAAAGGAATAG	P*trpC-hph* for deletion constructs
nptIIF	GATATTGAAGGAGCACTTTTTG	P*trpC-npt2*-T*trpC* for deletion constructs
nptIIR	CTACCCATCTTAGTAGGAATG	P*trpC-npt2*-T*trpC* for deletion constructs
Primers used for RT-qPCR.		
BH185	CGTCAAAGCTGGCCACATTT	*pldA* for
BH186	TGCAAGAACTCCATGGGCAT	*pldA* rev
BH187	CGGCTTTCCTATCGACGACA	*pldB* for
BH188	ACCATTTTGCTCCTCCGTGA	*pldB* rev

Supporting Information Methods S1: Construct design.

For generation of the *pldA* replacement construct (pCE131) a 1,439 bp PCR fragment 5' of *pldA* and a 1292 bp PCR fragment 3' of *pldA* were amplified using Phusion polymerase with the primer combination PldA6/PldA5 and PldA1/PldA2. The 5' fragment was unable to be amplified directly from *E. festucae* genomic DNA so was synthesized by GenScript as an insert in pUC57. For the generation of the *pldB* replacement construct, pCE121, a 1,133 bp PCR fragment 5' of *pldB* and a 943 bp PCR fragment 3' of *pldB* were amplified as described making use of the primer combinations PldB4/PldB3 and PldB1/PldB2. P*trpC-hph* (1394 bp) cassette for the *pldA* replacement construct was amplified from pSF15.15 with the primer combination hph_F/hph_R and P*trpC-npt2*-T*trpC* (1,741 bp) for the *pldB* replacement construct from pII99 with the primers nptIIF/nptIIR. The backbone pRS426 was amplified with the primers pRS426_F/pRS426_R.

The *pldB* complementation construct (pBH53) was generated from three PCR fragments: the backbone was amplified from pBH12 with BH236/BH78 (4,540 bp) and the two *pldB* fragments were amplified with BH220/PldB8 (3,843 bp) and PldB7/BH235 (3,335 bp) from genomic DNA. The first of the *pldB* fragments included 1548 bp of the promoter region and the latter 357 bp of the terminator region.

For the generation of the *pldA* overexpression construct (pCE129), *pldA* (2,906 bp) was amplified from WT genomic DNA with the primers PldA7/PldA8. For the *pldB* overexpression construct pBH48, *pldB* was amplified in two fragments with the following combinations: PldB5/PldB8 (2,774 bp) and PldB6/PldB7 (2,985 bp). The pRS426 backbone was amplified as described above and P*gpd* and T*trpC* with pRS426-Pgdp-F/pRS426-Pgdp-R (2,310 bp) and TtrpC-F/ pRS426-TtrpC-R (569 bp), from pPN82 and pII99 respectively.

The mCherry fusion protein encoding constructs were assembled from three backbone fragments and the *pldA* (pBH38) or *pldB* (pBH52) coding region. These included: a 2,817 bp fragment amplified from pBH16 with BH76/BH75, containing T*trpC* and a *hph* cassette, from a 4,608 bp fragment amplified from pBH28 with BH197/196 containing genes for replication in *E. coli* and P*gpd* from a 765 bp fragment amplified from pBV579 with BH79/BH199 encoding *mCherry*. *pldA* was amplified from gDNA with BH198/BH200 (2,956 bp) and *pldB* in two fragments with BH224/PldB8 and PldB7/BH202 (2,986 bp). For the N-terminal GFP fusion protein constructs the backbone was amplified in two fragments from pBH28. One fragment was 4,810 bp in length and was amplified with BH76/BH193 and the other one was 3,080 bp in length and was amplified with BH114/BH191. Genomic DNA was used to amplify *pldA* (2,965 bp) with BH192/PldA8 and *pldB* (5,198 bp) in two fragments with BH239/PldB8 and

PldB7/PldB6. Gibson assembly resulted in the plasmids pBH37 (GFP-PldA) and pBH54 (GFP-PldB). All designed fusion protein constructs encode a $(GGGS)_2$ linker between the protein of interest and the fluorophore.

The Y2H vectors were generated as follows: *mssD* (EfM3.031950) was amplified from cDNA with the primers BH247/BH248 (2,940 bp) for insertion into pGADT7 (pBH63) and with BH245/BH246 (2,938 bp) for insertion into pGBKT7 (pBH62); *pkcA* (EfM3.006500), was amplified from cDNA with the primers BH249/BH250 (3,474 bp) for insertion into pGADT7 (pBH64) and with BH251/BH252 (3,472 bp) for insertion into pGBKT7 (pBH65); *pldB* was amplified from genomic DNA as amplifications from cDNA were unsuccessful, however the position of introns had previously been confirmed via PCR on short fragment cDNA. The gene was amplified in two fragments with the primers BH241/PldB8 (2,292 bp) and PldB7/BH242 (2,924 bp) for insertion into pGADT7 (pBH60) and with BH243/PldB8 (2,268 bp) and PldB7/BH244 (2,921 bp) for insertion into pGBKT7 (pBH61). The backbone vectors were amplified in *E. coli* and subsequently pGADT7 was restriction enzyme digested with *Eco*RI and *Bam*HI and pGBKT7 with *Eco*RI and *Pst*I. The Gibson-assembly reaction was performed following the gel extraction and purification of all fragments.

For the generation of the PA biosensor (pBH50) the genetic sequence of PA binding region of Spo20 (aa 51-91) including a 5xGA linker and a stop codon (total 156 bp) was ordered from GenScript. The backbone was amplified in two fragments from pBH28 with the primers BH222/BH75 (2,838 bp) and BH197/BH223 (5,326 bp).

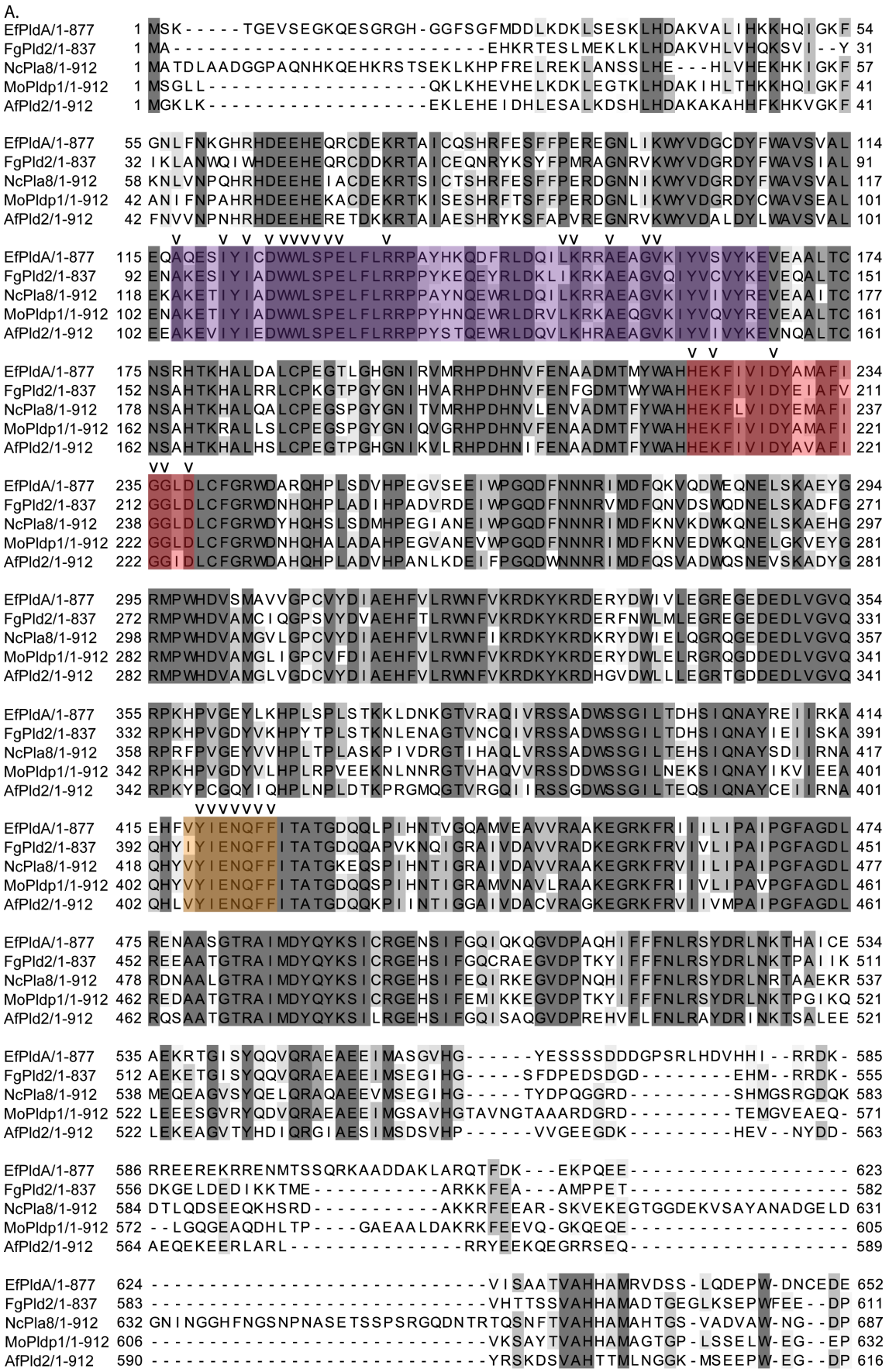
A.
EfPldA/1-877
FgPld2/1-837
NcPla8/1-912
MoPldp1/1-912
AfPld2/1-912

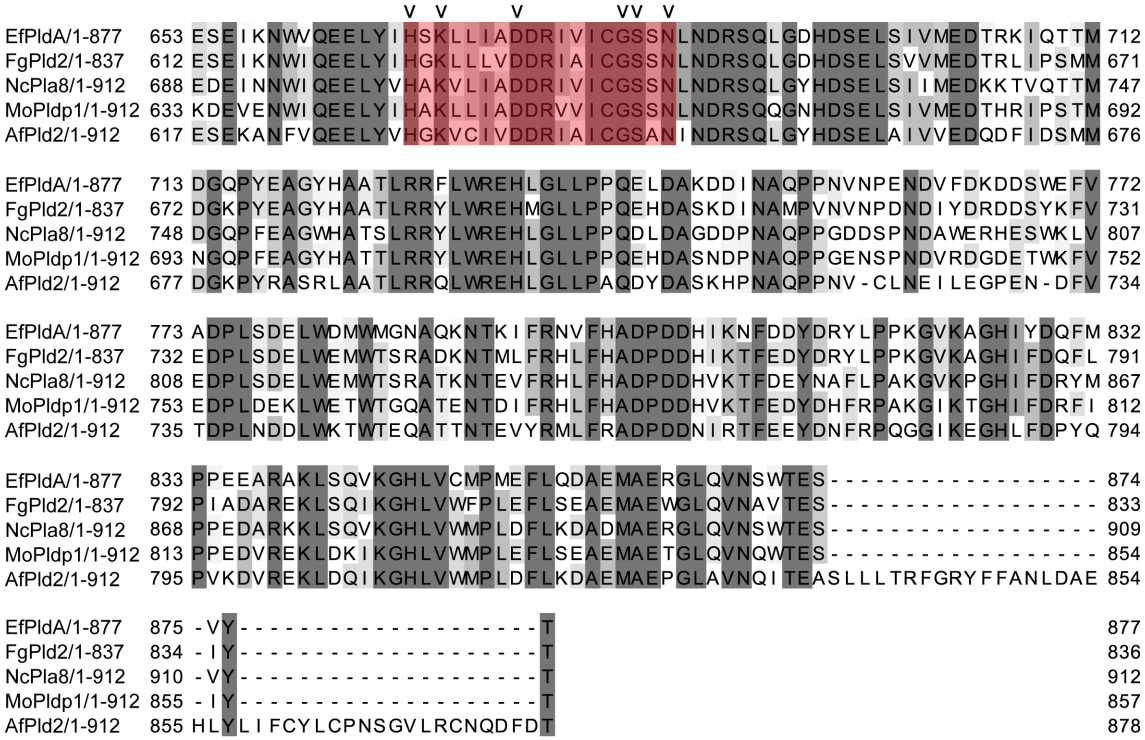

B.

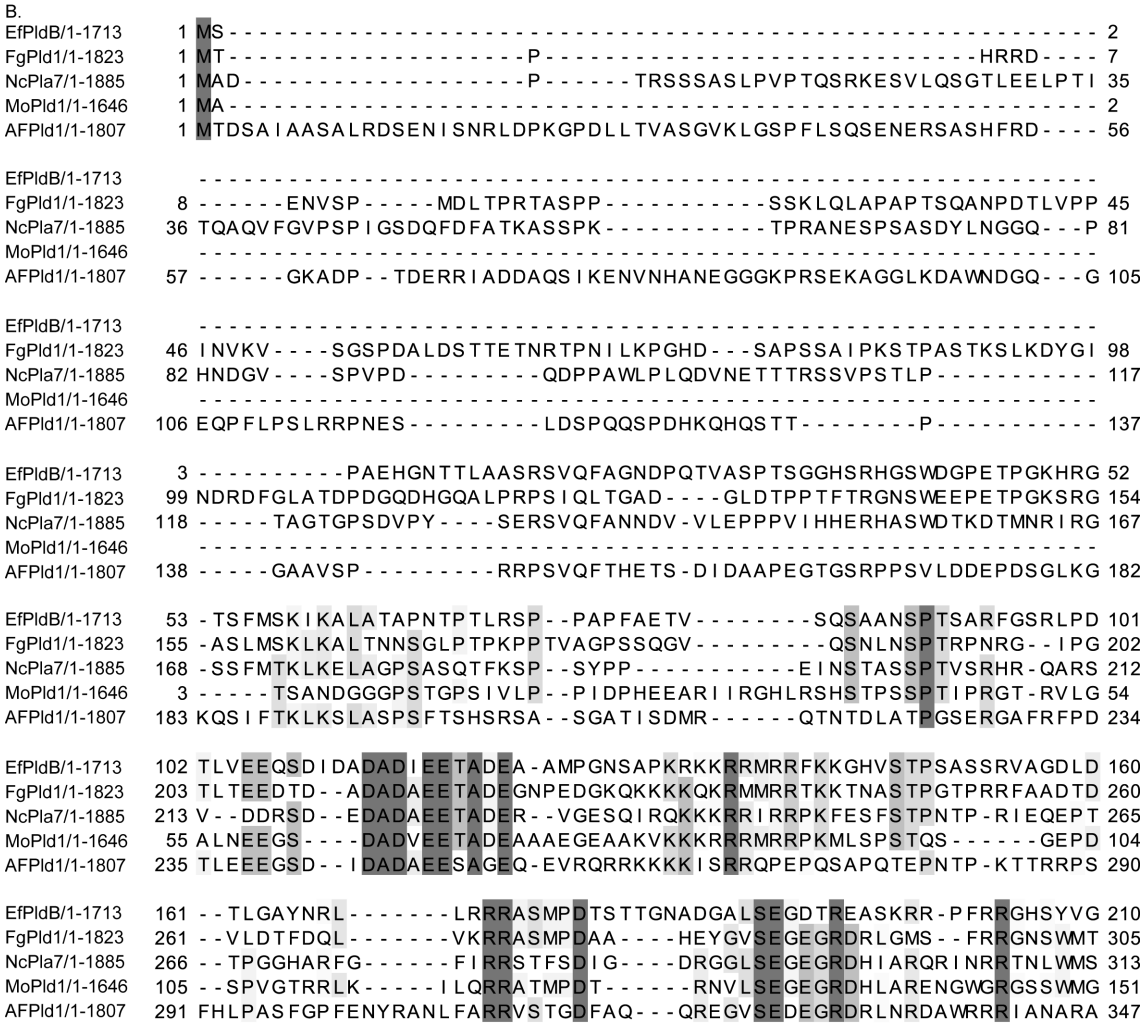

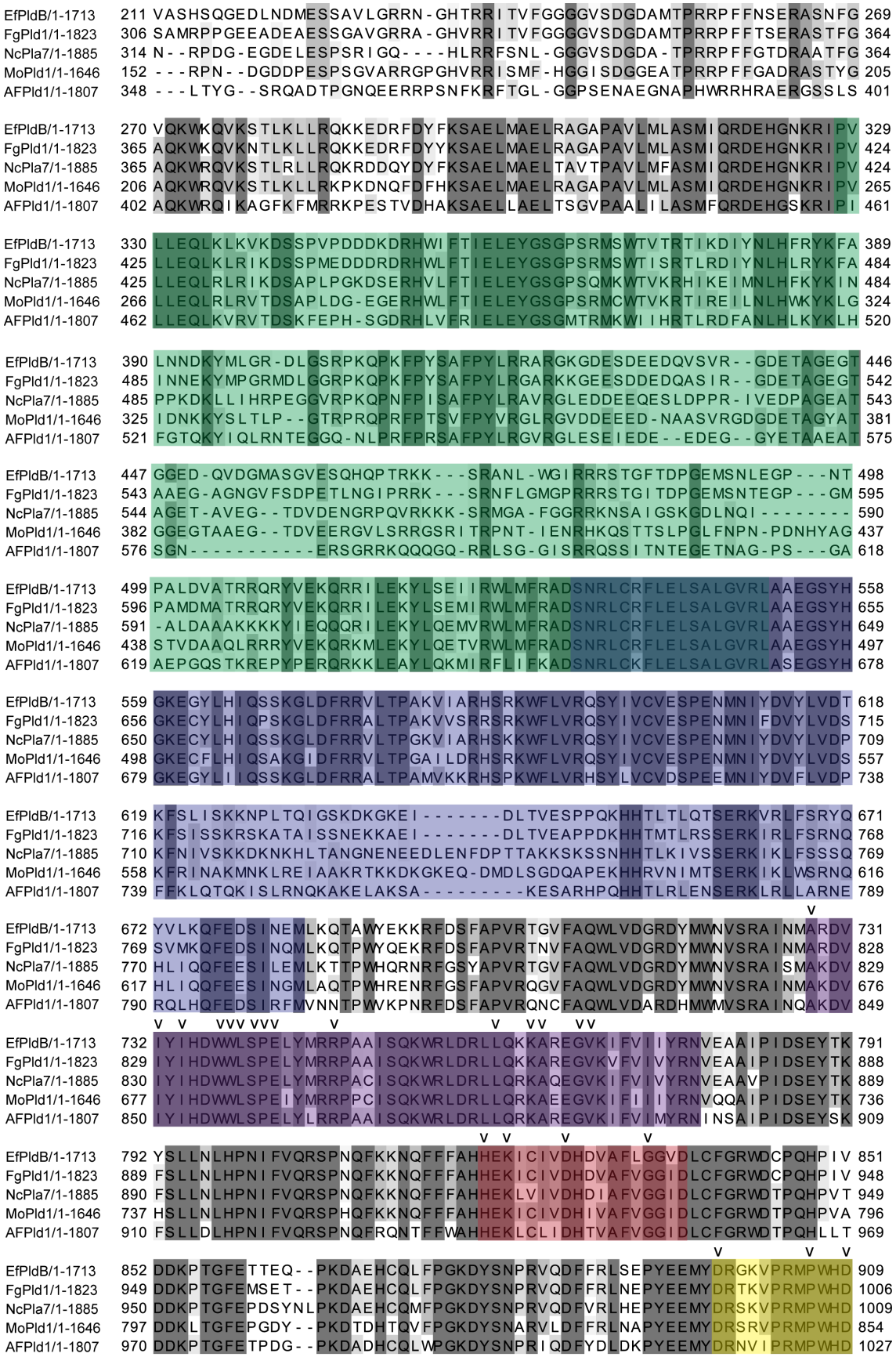
EfPldB/1-1713 211 VASHSQGEDLNDMESSAVLGRRN-GHTRRITVFGGGGVSDGDAMTPRRPFFNSERASNFG 269
FgPld1/1-1823 306 SAMRPPGEEADEAESSGAVGRRA-GHVRRITVFGGGGVSDGDAMTPRRPFFTSERASTFG 364
NcPla7/1-1885 314 N--RPDG-EGDELESPSRIGQ----HLRRFSNL-GGGVSDGDA-TPRRPFFGTDRAATFG 364
MoPld1/1-1646 152 ---RPN--DGDDPESPSGVARRGPGHVRRISMF-HGGISDGGEATPRRPFFGADRASTYG 205
AFPld1/1-1807 348 ---LTYG--SRQADTPGNQEERRPSNFKRFTGL-GGPSENAEGNAPHWRRHRAERGSSLS 401
EfPldB/1-1713 270 VQKWKQVKSTLKLLRQKKEDRFDYFFKSAELMAELRAGAPAVLMLASMIQRDEHGNKRIPV 329
FgPld1/1-1823 365 AQKWKQVKNTLKLLRQKKEDRFDYYKSAELMAELRAGAPAVLMLASMIQRDEHGNKRIPV 424
NcPla7/1-1885 365 AQKWRQVKSTLRLLRQKRDDQYDYFKSAELMAELTAVTPAVLMFASMIQRDEHGNKRIPV 424
MoPld1/1-1646 206 AQKWRQVKSTLKLLRKPKDNQFDFHKSAELMAELRAGAPAVLMLASMIQRDEHGNKRIPV 265
AFPld1/1-1807 402 AQKWRQIKAGFKFMRRKPESTVDHAKSAELLAELTSGVPAALILASMFQRDEHGSKRIPI 461
EfPldB/1-1713 330 LLEQLKLKVKDSSPVPDDDKDRHWIFTIELEYGSGPSRMSWTVTRTIKDIYNLHFRYKFA 389
FgPld1/1-1823 425 LLEQLKLRIKDSSPMEDDDRDRHWLFTIELEYGSGPSRMSWTISRTLRDIYNLHLRYKFA 484
NcPla7/1-1885 425 LLEQLRLRIKDSAPLPGKDSERHVLFTIELEYGSGPSQMKWTVKRHIKEIMNLHFKYKIN 484
MoPld1/1-1646 266 LLEQLRLRVTDSAPLDG-EGERHWLFTIELEYGSGPSRMCWTVKRTIREILNLHWKYKLG 324
AFPld1/1-1807 462 LLEQLKVRVTDSKFEPH-SGDRHLVFRIELEYGSGMTRMKWIIHRTLRDFANLHLKYKLH 520
EfPldB/1-1713 390 LNNDKYMLGR-DLGSRPKQPKFPYSAFPYLRRARGKGDESDEEDQVSVR--GDETAGEGT 446
FgPld1/1-1823 485 INNEKYMPGRMDLGGRPKQPKFPYSAFPYLRGARKKGEESDDEDQASIR--GDETAGEGT 542
NcPla7/1-1885 485 PPKDKLLIHRPEGGVRPKQPNFPISAFPYLRAVRGLEDDEEQESLDPPR-IVEDPAGEAT 543
MoPld1/1-1646 325 IDNKKYSLTLP--GTRPRQPRFPTSVFPYVRGLRGVDDEEED-NAASVRGDGDETAGYAT 381
AFPld1/1-1807 521 FGTQKYIQLRNTEGGQ-NLPRFPRSAFPYLRGVRGLESEIEDE--EDEG--GYETAAEAT 575
EfPldB/1-1713 447 GGED-QVDGMASGVESQHQPTRKK---SRANL-WGIRRRSTGFTDPGEMSNLEGP---NT 498
FgPld1/1-1823 543 AAEG-AGNGVFSDPETLNGIPRRK---SRNFLGMGPRRRSTGITDPGEMSNTEGP---GM 595
NcPla7/1-1885 544 AGET-AVEG--TDVDENGRPQVRKKK-SRMGA-FGGRRKNSAIGSKGDLNQI-------- 590
MoPld1/1-1646 382 GGEGTAAEG--TDVEERGVLSRRGSRITRPNT-IENRHKQSTTSLPGLFNPN-PDNHYAG 437
AFPld1/1-1807 576 SGN-----------ERSGRRKQQQGQ-RRLSG-GISRRQSSITNTEGETNAG-PS---GA 618
EfPldB/1-1713 499 PALDVATRRQRYVEKQRRILEKYLSEIIRWLMFRADSNRLCRFLELSALGVRLAAEGSYH 558
FgPld1/1-1823 596 PAMDMATRRQRYVEKQRRILEKYLSEMIRWLMFRADSNRLCRFLELSALGVRLAAEGSYH 655
NcPla7/1-1885 591 -ALDAAAKKKKYIEQQQRILEKYLQEMVRWLMFRADSNRLCRFLELSALGVRLAAEGSYH 649
MoPld1/1-1646 438 STVDAAQLRRRYVEKQRKMLEKYLQETVRWLMFRADSNRLCRFLELSALGVRLAAEGSYH 497
AFPld1/1-1807 619 AEPGQSTKREPYPERQRKKLEAYLQKMIRFLIFKADSNRLCKFLELSALGVRLASEGSYH 678
EfPldB/1-1713 559 GKEGYLHIQSSKGLDFRRVLTPAKVIARHSRKWFLVRQSYIVCVESPENMNIYDVYLVDT 618
FgPld1/1-1823 656 GKECYLHIQPSKGLDFRRALTPAKVVSRRSRKWFLVRQSYIVCVESPENMNIFDVYLVDS 715
NcPla7/1-1885 650 GKECYLHIQSSKGLDFRRVLTPGKVIARHSKKWFLVRQSYIVCVESPENMNIYDVYLVDP 709
MoPld1/1-1646 498 GKECFLHIQSAKGIDFRRVLTPGAILDRHSRKWFLVRQSYIVCVESPENMNIYDVYLVDS 557
AFPld1/1-1807 679 GKEGYLIIQSSKGLDFRRALTPAMVKKRHSPKWFLVRHSYLVCVDSPEEMNIYDVFLVDP 738
EfPldB/1-1713 619 KFSLISKKNPLTQIGSKDKGKEI-------DLTVESPPQKHHTLTLQTSERKVRLFSRYQ 671
FgPld1/1-1823 716 KFSISSKRSKATAISSNEKKAEI-------DLTVEAPPDKHHTMTLRSSERKIRLFSRNQ 768
NcPla7/1-1885 710 KFNIVSKKDKNKHLTANGNENEEDLENFDPTTAKKSKSSNHHTLKIVSSERKIKLFSSSQ 769
MoPld1/1-1646 558 KFRINAKMNKLREIAAKRTKKDKGKEQ-DMDLSGDQAPEKHHRVNIMTSERKIKLWSRNQ 616
AFPld1/1-1807 739 FFKLQTQKISLRNQKAKELAKSA---------KESARHPQHHTLRLENSERKLRLLARNE 789
EfPldB/1-1713 672 YVLKQFEDSINEMLKQTAWYEKKRFDSFAPVRTGVFAQWLVDGRDYMWNVSRAINMARDV 731
FgPld1/1-1823 769 SVMKQFEDSINQMLKQTPWYQEKRFDSFAPVRTNVFAQWLVDGRDYMWNVSRAINMARDV 828
NcPla7/1-1885 770 HLIQQFEESILEMLKTTPWHQRNRFGSYAPVRTGVFAQWLVDGRDYMWNVSRAISMAKDV 829
MoPld1/1-1646 617 HLIQQFEESINGMLAQTPWHRENRFGSFAPVRQGVFAQWLVDGRDYMWNVSRAINMAKDV 676
AFPld1/1-1807 790 RQLHQFEDSIRFMVNNTPWVKPNRFDSFAPVRQNCFAQWLVDARDHMWMVSRAINQAKDV 849
EfPldB/1-1713 732 IYIHDWWLSPELYMRRPAAISQKWRLDRLLQKKAREGVKIFVIIYRNVEAAIPIDSEYTK 791
FgPld1/1-1823 829 IYIHDWWLSPELYMRRPAAISQKWRLDRLLQKKAREGVKVFVIVYRNVEAAIPIDSEYTK 888
NcPla7/1-1885 830 IYIHDWWLSPELYMRRPACISQKWRLDRLLQRKAQEGVKIFVIVYRNVEAAVPIDSEYTK 889
MoPld1/1-1646 677 IYIHDWWLSPEIYMRRPPCISQKWRLDRLLQRKAEEGVKIFIIIYRNVQQAIPIDSEYTK 736
AFPld1/1-1807 850 IYIHDWWLSPELYLRRPAAISQKWRLDRLLQRKAREGVKIFVIMYRNINSAIPIDSEYSK 909
EfPldB/1-1713 792 YSLLNLHPNIFVQRSPNQFKKNQFFFAHHEKICIVDHDVAFLGGVDLCFGRWDCPQHPIV 851
FgPld1/1-1823 889 FSLLNLHPNIFVQRSPNQFKKNQFFFAHHEKICIVDHDVAFVGGIDLCFGRWDCPQHPIV 948
NcPla7/1-1885 890 FSLLNLHPNIFVQRSPNQFKKNQFFFAHHEKLVIVDHDIAFVGGIDLCFGRWDTPQHPVT 949
MoPld1/1-1646 737 HSLLNLHPNIFVQRSPHQFKKNQFFFAHHEKICIVDHIVAFVGGIDLCFGRWDTPQHPVA 796
AFPld1/1-1807 910 FSLLDLHPNIFVQRSPNQFRQNTFFWAHHEKLCLIDHTVAFVGGIDLCFGRWDTPQHLLT 969
EfPldB/1-1713 852 DDKPTGFETTEQ--PKDAEHCQLFPGKDYSNPRVQDFFRLSEPYEEMYDRGKVPRMPWHD 909
FgPld1/1-1823 949 DDKPTGFEMSET--PKDAEHCQLFPGKDYSNPRVQDFFRLNEPYEEMYDRTKVPRMPWHD 1006
NcPla7/1-1885 950 DDKPTGFEPDSYNLPKDAEHCQMFPGKDYSNPRVQDFVRLHEPYEEMYDRSKVPRMPWHD 1009
MoPld1/1-1646 797 DDKLTGFEPGDY--PKDTDHTQVFPGKDYSNARVLDFFRLNAPYEEMYDRSRVPRMPWHD 854
AFPld1/1-1807 970 DDKPTGFETPDG--PKDADHCQLWPGKDYSNPRIQDFYDLDKPYEEMYDRNVIPRMPWHD 1027

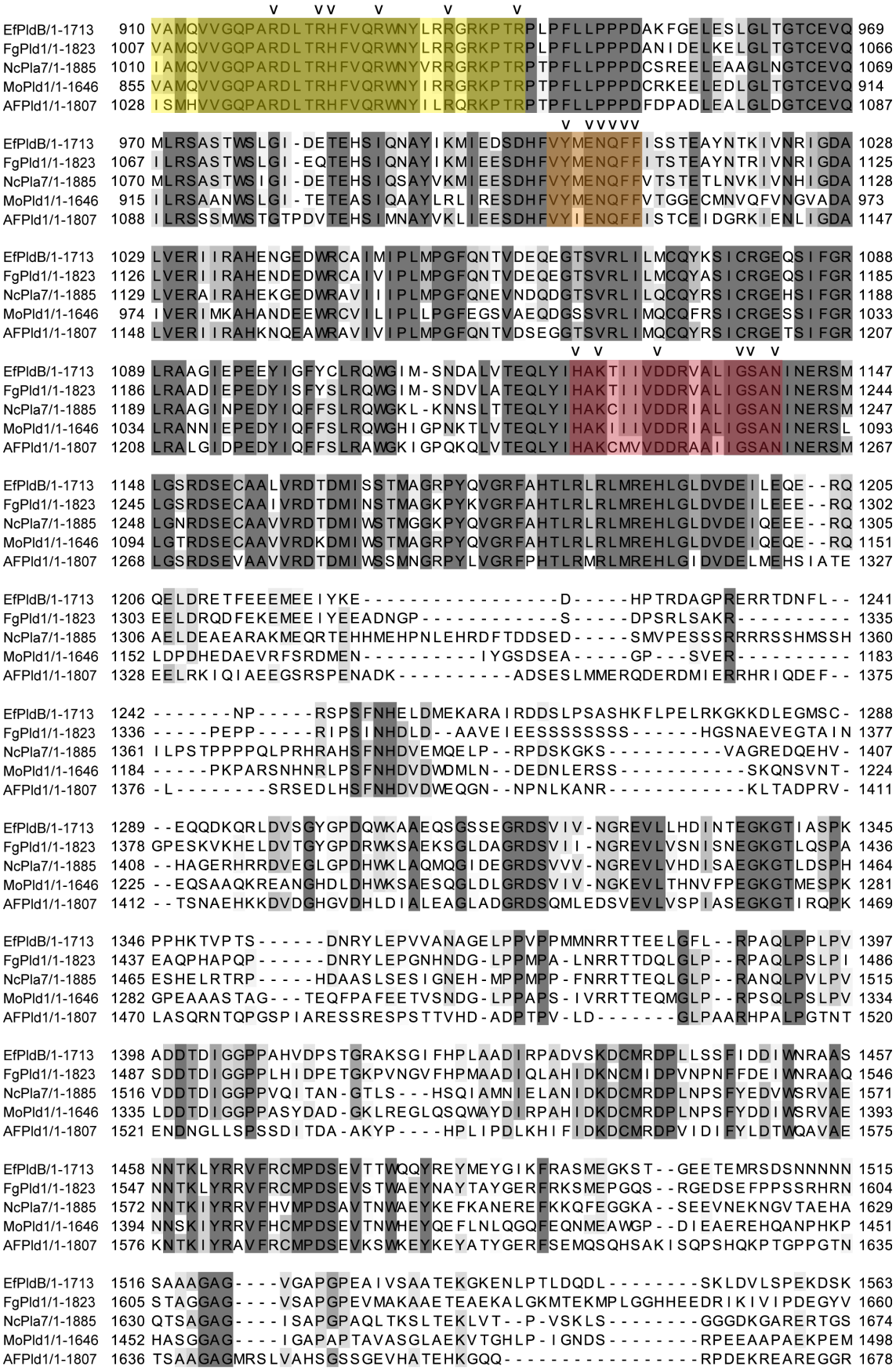

Supporting Information Fig. S1: Amino acid sequence alignment of *Epichloë festucae* PldA and PldB with homologs from other Ascomycete fungi.

(A) PldA amino acid sequence alignment; (B) PldB amino-acid sequence alignment. Grey shading according to percentage identity, dark grey: high identity, light grey: low identity. Green box: PH (phox homology) domain; blue box: PX (pleckstrin homology) domain; purple box: motif I; red box: motif II and IV; orange box: motif III; yellow box: polybasic motif; *Ef*: *Epichloë festucae* (EfPldB: EfM3.032570, EfPldA: EfM3.055250); *Fg*: *Fusarium graminearum (*FgPld1: XP_011318823.1, FgPld2: XP_011317835.1); *Mo*: *Magnaporthe oryzae* (MoPld1: XP_003717990.1, MoPldp1 XP_003712119.1); *Nc*: *Neurospora crassa* (NcPla7: XP_957594.3*,* NcPla8: XP_001728077.1); *Af*: *Aspergillus fumigatus* (AfPld1: KEY78740.1, AfPldA; XP_748951.1). Amino acids marked with “v” are conserved according to Sung *et al*. (1997) and Sciorra *et al*. 1999; Sciorra *et al*. 2002).

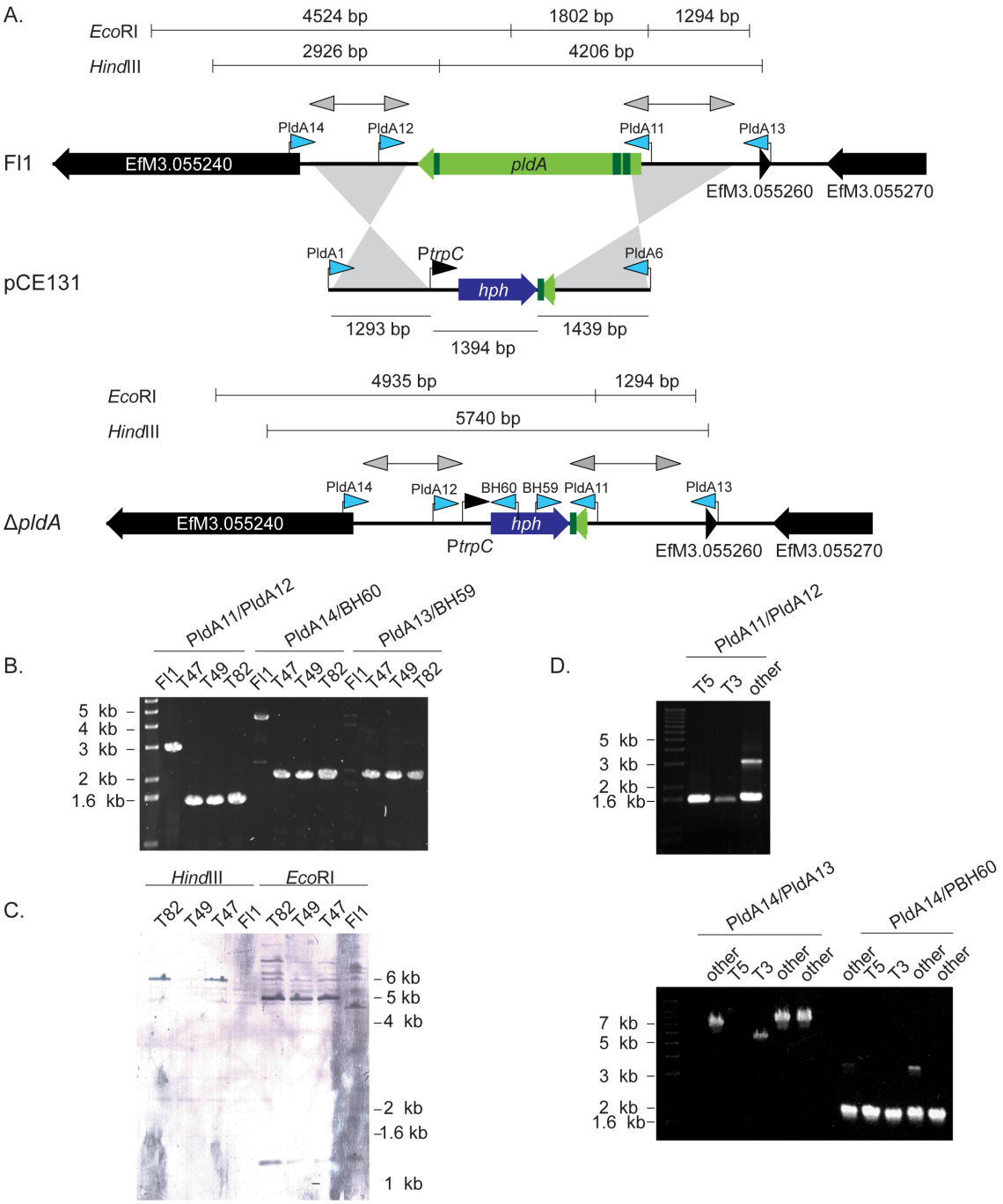
A.
EcoRI
4524 bp
1802 bp
1294 bp
HindIII
2926 bp
4206 bp
PldA14
PldA12
PldA11
PldA13
Fl1
EfM3.055240
pldA
EfM3.055260
EfM3.055270
PldA1
PtrpC
PldA6
pCE131
hph
1293 bp
1394 bp
1439 bp
EcoRI
4935 bp
1294 bp
HindIII
5740 bp
PldA14
PldA12
BH60
BH59
PldA11
PldA13
ΔpldA
EfM3.055240
hph
PtrpC
EfM3.055260
EfM3.055270
B.
PldA11/PldA12
PldA14/BH60
PldA13/BH59
Fl1 T47 T49 T82 Fl1 T47 T49 T82 Fl1 T47 T49 T82
5 kb
4 kb
3 kb
2 kb
1.6 kb
C.
HindIII
EcoRI
T82 T49 T47 Fl1 T82 T49 T47 Fl1
6 kb
5 kb
4 kb
2 kb
1.6 kb
1 kb
D.
PldA11/PldA12
T5 T3 other
5 kb
3 kb
2 kb
1.6 kb
PldA14/PldA13
PldA14/PBH60
other T5 T3 other other other T5 T3 other other
7 kb
5 kb
3 kb
2 kb
1.6 kb

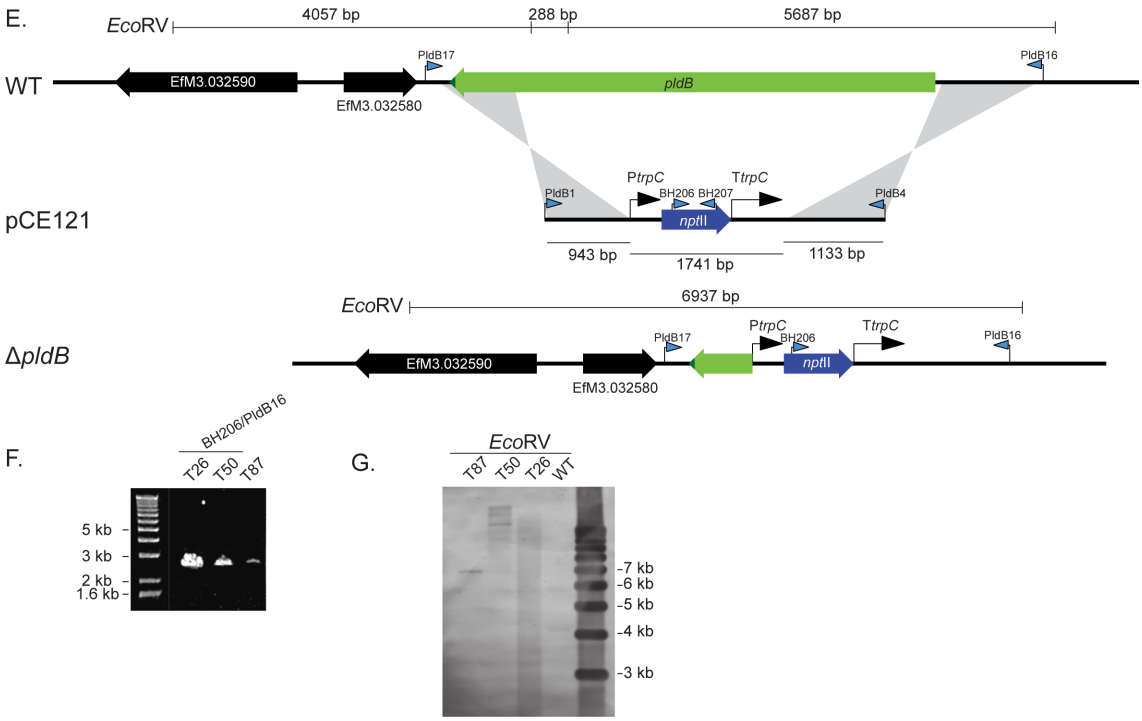

Supporting Information Fig. S2: Strategy for the deletion of *Epichloë festucae pldA* and *pldB* and verification of deletion by Southern blot analysis.

(A) Physical map of the *pldA* wild-type (WT) genomic locus, linear insert of the *pldA* replacement construct, pCE131, and the recombinant locus showing restriction enzyme sites for *Eco*RI and *Hind*III. Grey shading indicates regions of recombination. Numbers indicate the PCR primer pairs used for Gibson assembly (PldA1/PldA6) and deletion mutant screening (BH59/BH60/PldA11/PldA12/PldA13/PldB14). (B) PCR screening of deletion candidates with the PCR primer pair PldA11/PldA12, generated expected bands of 2,947 bp in WT, and 1555 bp in deletion mutants, the pair PldA14/BH60 generated expected band of 2,058 bp in deletion mutants and the pair BH59/PldA13 generated expected band of 2,114 bp in deletion mutants. Unspecific bands were generated in the WT for the PldA14/BH60 and BH59/PldA13 PCRs due to the lack of the *hph* gene. (C) NBT/BCIP-stained Southern blot of digests (approx. 1 µg) from *E. festucae* WT, Δ*pldA*#T47 (PN3272), *ΔpldA*#T49 (PN3273) and Δ*pldA*#T82 (PN3274) strains probed with digoxigenin (DIG)-11-dUTP-labeled linear pCE131. Expected bands for *Eco*RI digest: 4,524 bp, 1,802 bp and 1,294 bp in WT, and 4,935 bp and 1,294 bp in the deletion mutants. Expected bands for *Hind*III digest: 2,926 bp and 4,206 bp in WT, and 5,704 bp in the deletion mutants. (D) PCR screening of *pldA*/*pldB* double deletion strains. Strains were generated by deletion of *pldA* in the Δ*pldB*#T87 background. PCR screening with the primer combination PldA11/PldA12 resulted in the expected band of 1,555 bp in deletion mutants T5 and T3, whereas other transformants had the additional WT band of 2,947 bp. Screening with the primer

combination PldA14/PldA13 resulted in the expected band of 4,869 bp in T3 and of 6,261 bp in negative transformants. Due to overloading of the gel, bands were generally observed higher than expected. PCR screening with the primers PldA14/BH60 resulted in the expected single band at 2,058 bp in T5 and T3, whereas other, negative transformants had an additional unspecific band. (E) Physical map of the *pldB* WT genomic locus, linear insert of the *pldB* replacement construct, pCE121, and the recombinant locus showing restriction enzyme sites for *Eco*RV. Grey shading indicates regions of recombination. Numbers indicate the PCR primer pairs used for Gibson assembly (PldB1/PldB4), deletion mutant screening (PldB16/PldB17/BH206) and amplification of the deletion cassette PldB1/BH207 and BH206/PldB4. (F) PCR screening of deletion candidates with the PCR primer pair BH206/PldB16, generated expected band of 2,465 bp in deletion mutants. As expected no band was observed in WT due to the lack of the *nptII* gene (G) NBT/BCIP-stained Southern blot of digests (approx. 1 µg) of *E. festucae* WT, Δ*pldB*#T26 (PN3275), Δ*pldB*#T50 (PN3276) and Δ*pldB*#T87 (PN3277) strains probed with digoxigenin (DIG)-11-dUTP-labeled linear pCE121. Expected bands of 4,057 bp and 5,687 bp in WT and 6,937 bp in the deletion mutants. Only the digest of Δ*pldB*#T87 genomic DNA resulted in the expected band whereas T50 and T26 exhibited bands of a larger size, indicating multiple integrations.

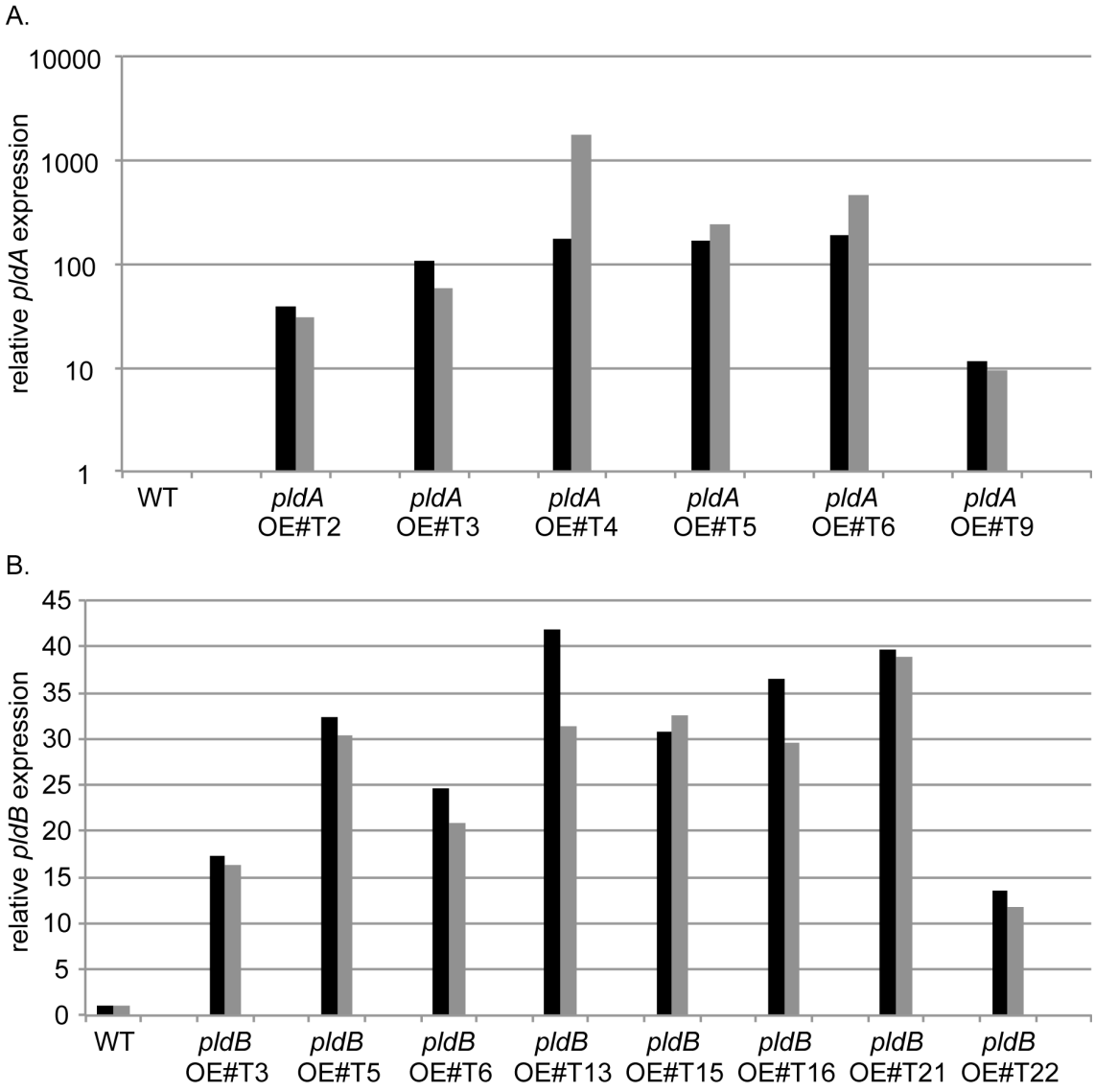

Supporting Information Fig. S3: qRT-PCR analysis of *Epichloë festucae pldA* and *pldB* overexpression strains.

Relative expression of *pldA* (A) and *pldB* (B) was determined relative to wild-type (WT) gene expression. The analysis was performed with two technical replicates. Reference genes coding for elongation factor 2 (*EF-2*, black bar) and 40S ribosomal protein S22 (*S22*, grey bar) were used for normalization and the relative expression was calculated as described by Lukito *et al*. (2015). Notice the different scales in (A) compared to (B). The *pldA* overexpression strains T3, T4 and T9 and *pldB* overexpression strains T6, T21 and T22 were chosen for further analysis. For the qRT-PCR the primer combinations BH185/BH186 and BH187/BH188 were used for *pldA* and *pldB*, respectively.

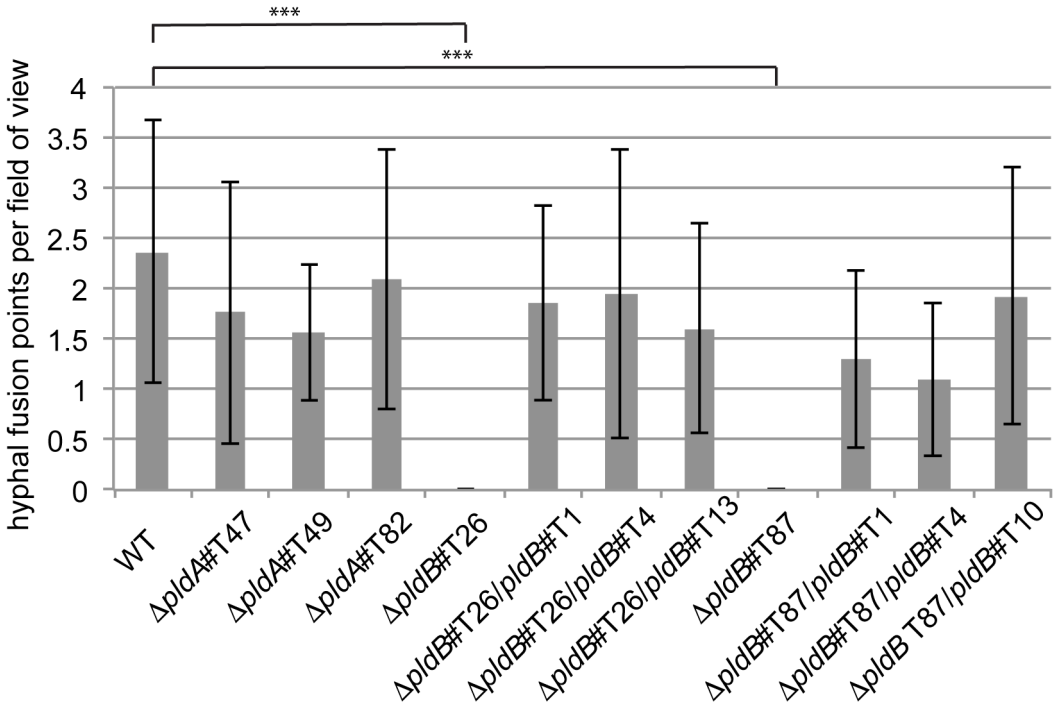

Supporting Information Fig. S4: Quantification of hyphal fusion events in *Epichloë festucae* wild-type and *pldA* and *pldB* deletion strains.

Wild-type (WT), deletion and complementation strains were grown on 3% H_2O agar for 14 days and hyphal fusion events in 3 x 10 fields of view were counted per strain. The average of 30 counts, including the standard deviation, is plotted. To identify significant differences between strains, a *t*-test was performed (Excel). Only *pldB* deletion strains #T26 and #T87 were significantly different from WT (P = 3.4e-10 repectively).

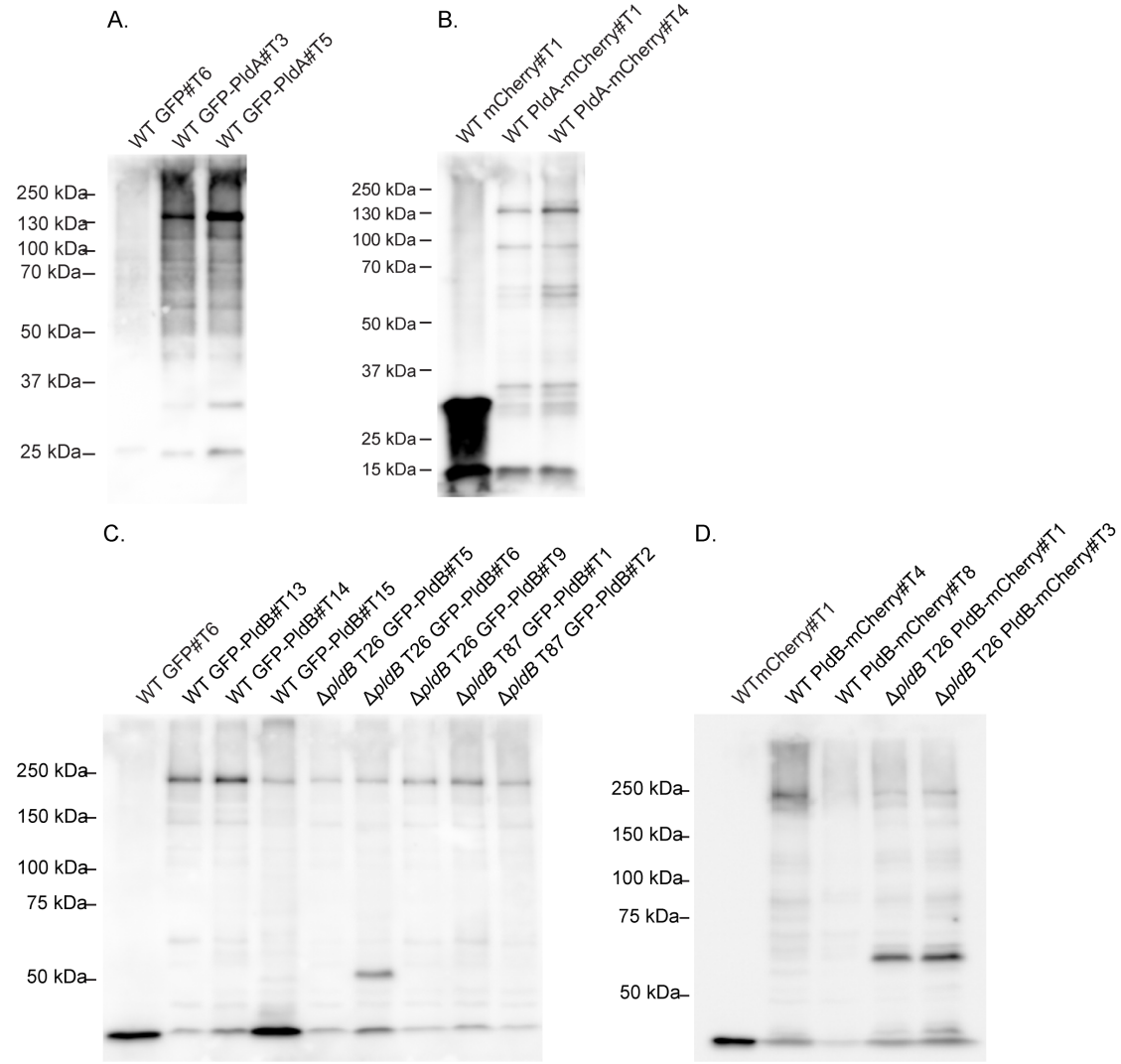

Supporting Information Fig. S5: Verification of the expression of GFP-PldA, GFP-PldB, PldA-mCherry and PldB-mCherry fusion proteins in *Epichloë festucae* by western blot.

Strains expressing the fusion proteins were grown in potato-dextrose liquid media for 3 days, and total protein extracted. Proteins were resolved on a 10% (PldA fusions) or 7% (PldB fusions) acrylamide gel, transferred onto a PVDF membrane and probed with an α-GFP or α-mCherry antibody respectively. Subsequently a secondary α-rabbit antibody conjugated to horseradish peroxidase was applied and the western blot was developed via a chemiluminescence reaction. (A) Wild-type (WT) GFP-PldA (pBH37, #T3/#T5); (B) WT PldA-mCherry (pBH38, #T1/#T4); (C) WT GFP-PldB (pBH54, #T13/#T14/#T15), Δ*pldB*#T26 GFP-PldB (#T5/#T6/#T9) and Δ*pldB*#T87 GFP-PldB (#T1/#T2); (D) WT pldB-mCherry (pBH52, #T4/#T8), Δ*pldB* T26 PldB-mCherry (#T1/#T3). Expected protein sizes: GFP: 27 kDa; mCherry: 28.8 kDa; PldA-GFP: 128.3 kDa; PldA-mCherry: 130.1 kDa; PldB-GFP: 220.4 kDa; PldB-mCherry: 222.2 kDa.

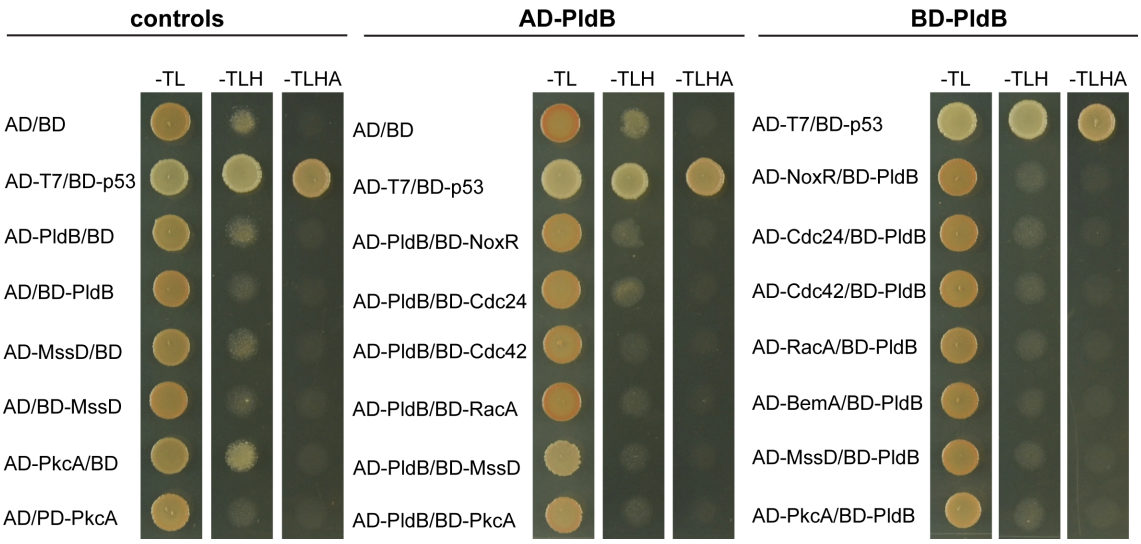

Supporting Information Fig. S6: PldB of *Epichloë festucae* does not interact with components of the Nox complex or regulators identified in mammalian cells.

Yeast two-hybrid analysis of the interactions of PldB with *E. festucae* NoxR, Cdc24, Cdc42, RacA, BemA, PkcA (EfM3.006500), MssD (EfM3.031950). Yeast strain AH109 was transformed with bait and prey vectors and plated on CMD plates lacking leucine and tryptophan (-L/T), leucine, tryptophan and histidine (-L/T/H) or leucine, tryptophan, histidine and adenine (-L/T/H/A). Empty pGADT7/pGBKT7 (AD/BD) were used as negative controls and the vectors pGADT7-T7/pGBKT7-p53 (AD-T7/BH-p53) as a positive control.

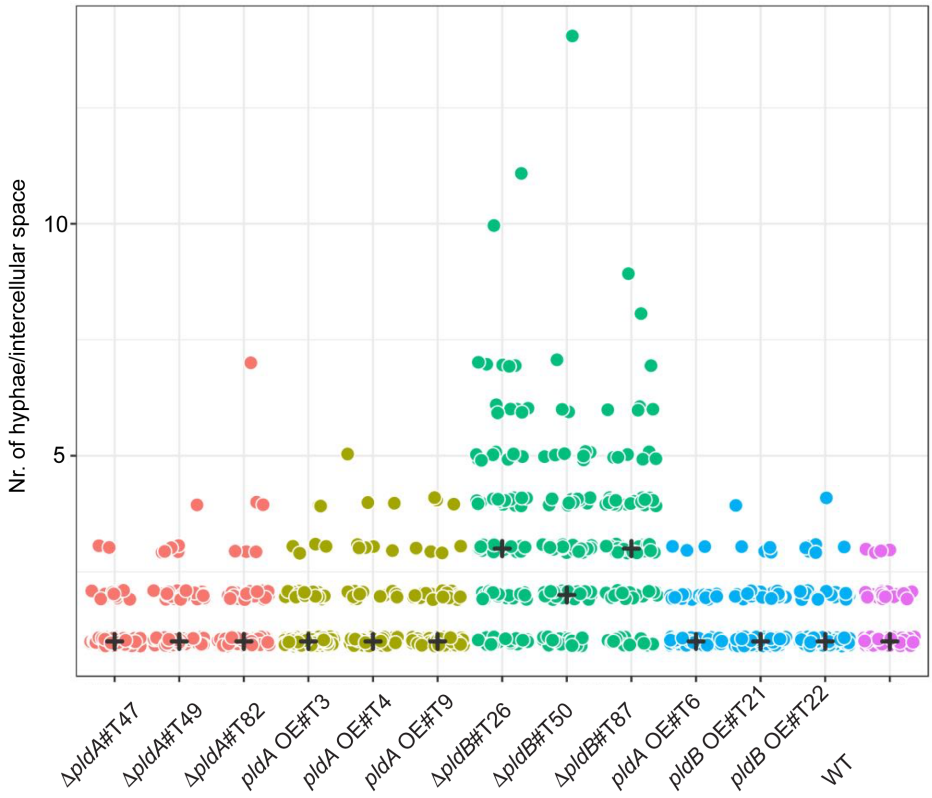

Supporting Information Fig. S7: Number of hyphae per intercellular space in *Epichloë festucae* WT and *pldA* and *pldB* mutant strain-infected *Lolium perenne* plants.

Number of hyphae per intercellular space were counted in fixed, toluidine blue-stained pseudostem cross sections. For each strain, 100 infected intercellular spaces were evaluated, with counting started at the outermost leaf. The data was analysed with the Dunn test, and only data obtained from plants infected with *pldB* deletion strains were significantly different from data of WT-infected plants (P = 0.0000).

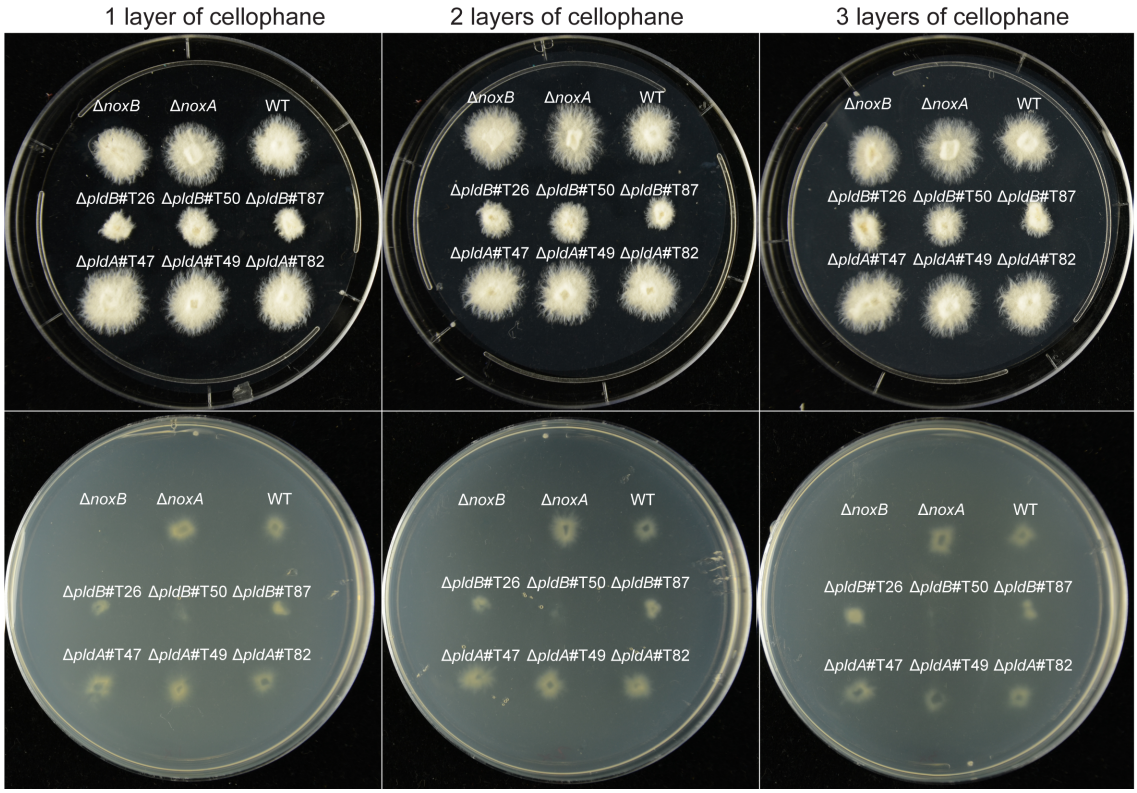

Supporting Information Fig. S8: Cellophane membrane penetration by *Epichloë festucae* wild-type, *pldB*, *noxA* and *noxB* deletion strains.

Wild-type (WT) and mutant strains were inoculated onto potato-dextrose agar plates covered with one, two or three cellophane membranes. Penetration of the cellophane membranes strains was evaluated after one week of incubation. The test was performed twice with a representative image of those results shown here.

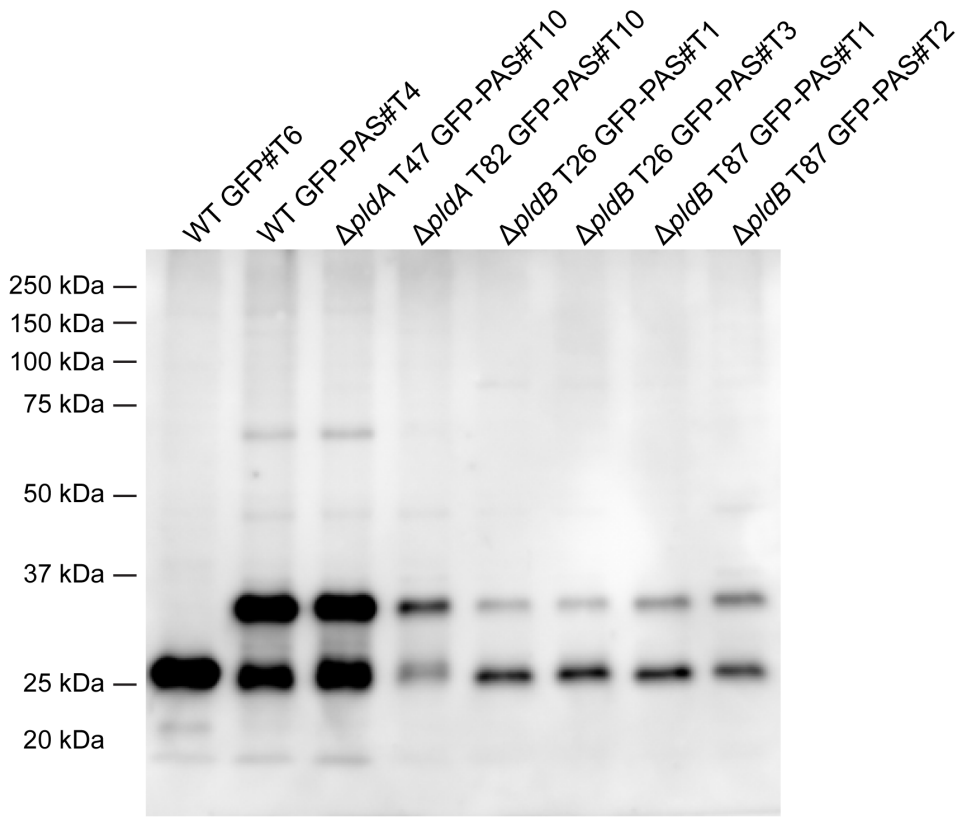

Supporting Information Fig. S9: Verification of the expression of the phosphatidic acid biosensor in the *Epichloë festucae* wild-type and *pldA* and *pldB* deletion strains by western analysis.

Phosphatidic acid biosensor (PAS)-expressing strains were grown in potato-dextrose liquid culture for three days and total protein was extracted. The western analysis was performed with the following strains: wild-type (WT) GFP-PAS#T4, Δ*pldA*#T47 GFP-PAS#T10, Δ*pldA*#T82 GFP-PAS#T10, Δ*pldB*#T26 GFP-PAS#T1 and #T3, Δ*pldB*#T87 GFP-PAS#T1 and #T2. From each extract, 15 µl were resolved on a 10% acrylamide gel. Proteins were then transferred onto PVDF membranes and probed with an α-GFP antibody. Subsequently a secondary α-rabbit antibody conjugated to horseradish peroxidase was applied and the western blot was developed via a chemiluminescence reaction. Expected protein sizes: GFP: 27 kDa; GFP-PAS: 32 kDa.

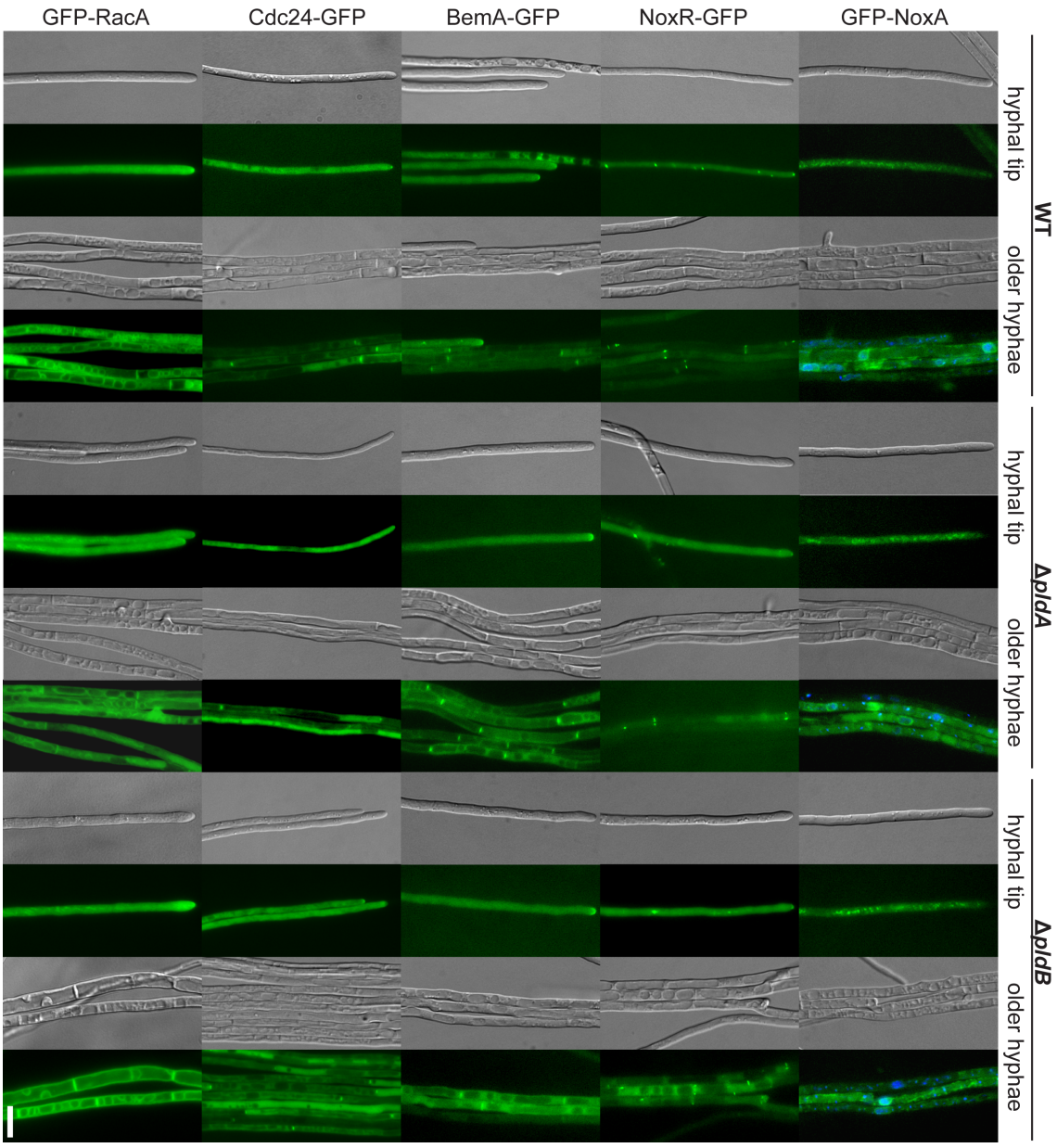
GFP-RacA
Cdc24-GFP
BemA-GFP
NoxR-GFP
GFP-NoxA
hyphal tip
older hyphae
WT
hyphal tip
older hyphae
ΔpldA
hyphal tip
older hyphae
ΔpldB

Supporting Information Fig. S10: Localisation of Nox complex components in *Epichloë festucae* wild-type and *pldA* and *pldB* deletion strains.

The localisation of NoxA, NoxR, BemA, Cdc24 and RacA GFP fusion constructs was analysed after approx. five days of incubation. Constructs were transformed into wild-type (WT) and two different *pldA* (T47 and T82) or *pldB* (T26 and T87) deletion strains, and multiple transformants analysed. As not all localization constructs encode a resistance gene, strains were co-transformed with pBH12 (Hyg^R) or pII99 (Gen^R) when appropriate. Here the localisation in the Δ*pldA*#T82 and Δ*pldB*#T26 strains are shown as representative of all the strains analysed. (A) Localisation of GFP-NoxA (pGFP-NoxA) in WT (T4), Δ*pldA*#T82 (T3) and Δ*pldB*#T26 (T1), nuclei were visualized using 0.071 mM DAPI stain; (B) Localisation of NoxR-GFP (pNPP9) in WT (T1), Δ*pldA*#T82 (T29) and Δ*pldB*#T26 (T1); (C) Localisation of BemA-GFP (pCE139) in WT (T23), Δ*pldA*#T82 (T3) and Δ*pldB*#T26 (T3); (D) Localisation of Cdc24-GFP (pNPP6) in WT (T33), Δ*pldA*#T82 (T1) and Δ*pldB*#T26 (T1); (E) Localisation of GFP-RacA (pPN154) in WT (T6), Δ*pldA*#T82 (T1) and Δ*pldB*#T26 (T1); Bar = 10 µm.

Chapter 4: A fungal homolog of the mammalian tumour suppressor protein PTEN is required for the mutualistic interaction between the filamentous ascomycete *Epichloë festucae* and perennial ryegrass

A fungal homolog of the mammalian tumour suppressor protein PTEN is required for the mutualistic interaction between the filamentous ascomycete *Epichloë festucae* and perennial ryegrass

Berit Hassing[1,2], Carl H. Mesarich[2,3], Carla Eaton[1,2], Barry Scott[1,2]

[1]School of Fundamental Sciences, Massey University, Palmerston North, NZ,

[2]Bio-Protection Research Centre, NZ,

[3]School of Agriculture and Environment, Massey University, Palmerston North, NZ.

Abstract

The filamentous fungus *Epichloë festucae* is an endophyte of the agriculturally important pasture grass, *Lolium perenne* (perennial ryegrass). This interaction is defined as being mutually beneficial, with both partners receiving a net benefit from the association. During host colonization, the growth and transmission of *E. festucae* is highly regulated. Signalling via reactive oxygen species (ROS) generated by the fungus is of great importance to the interaction and disruption of single genes in the ROS-generating NADPH oxidase (Nox) complex results in the break-down of the interaction, accompanied by a switch to proliferative growth of the fungus. In mammalian cells, lipid signalling has been shown to be involved in the recruitment of the cytosolic subunits of the Nox complex. Here, the role of the fungal homolog of the mammalian tumour suppressor protein PTEN, a phosphoinositide 3,4,5-trisphosphate 3-phosphatase, was analysed. This protein, named TepA, localised to the cytoplasm as well as to septa. However, no differences in the localisation of specific phosphoinositide biosensors or in superoxide production of mutant strains was observed. Neither deletion, nor overexpression influenced growth of *E. festucae* in axenic culture; however, inoculation of deletion strains resulted in a mild stunting of host plants, indicating that the PTEN homolog is required for the mutualistic interaction between *E. festucae* and perennial ryegrass.

Introduction

The fungal endophyte *Epichloë festucae* forms a mutually beneficial interaction with perennial ryegrass, *Lolium perenne* (Schardl *et al*., 2001). In this interaction, the fungus forms an intercellular hyphal network throughout the aerial tissues of the plant. This hyphal network is highly regulated and synchronized with growth of the plant host. Indeed, intercellular hyphae predominantly extend by intercalary growth, a process that involves hyphal stretching followed by cell wall material deposition, with regular tip growth only observed in meristematic tissues (Christensen *et al*., 2008). In addition to forming an intercellular hyphal network, the fungus can exit the plant by the formation of expressoria to build a hyphal network on the plant surface (Becker *et al*., 2016). This epiphyllous network is crucial for the sexual stage of the life cycle, in which hyphae engulf the host inflorescence with a dense hyphal structure, called a stroma, which produces spores that are transferred to a stroma of the opposite mating type to initiate sexual development (Scott and Schardl, 1993; Chung *et al*., 1997).

Many characterized signalling pathways have been shown to play important roles in the mutualistic interaction between *E. festucae* and *L. perenne*, e.g. the cell wall integrity (CWI) MAP kinase pathway, the high-osmolarity glycerol (HOG) MAP kinase pathway, the striatin-interacting phosphatase and kinase (STRIPAK) complex, and signalling via reactive oxygen species (ROS) (Tanaka *et al*., 2006; Eaton *et al*., 2008; Becker *et al*., 2015; Green *et al*., 2016). Disruption of single genes encoding components of these signalling complexes can result in a breakdown of the symbiotic interaction, which is characterized by the loss of restrictive growth, an increase of hyphal biomass, and the stunting or premature death of the plant (Tanaka *et al*., 2006; Eaton *et al*., 2008; Becker *et al*., 2015). ROS signalling is important in many fungal developmental processes, e.g. sexual development in *Aspergillus nidulans*, *Magnaporthe oryzae* and *Neurospora crassa*, virulence in *M. oryzae, Claviceps purpurea* and *Botrytis cinerea*, and hyphal fusion in *E. festucae, N. crassa* and *B. cinere*a (Tanaka *et al*., 2006; Egan *et al*., 2007; Giesbert *et al*., 2008; Segmüller *et al*., 2008; Semighii and Harris, 2008; Cano-Domingues *et al*., 2008; Becker *et al*., 2015; Ryder *et al*., 2013; Tudzynski *et al*., 2012). ROS is generated by membrane-integrated NADPH oxidases (Nox) that rely on multiple membrane-bound and cytosolic components for activity. Filamentous fungi contain multiple Nox proteins, which fall into three distinct families. The most well described is the NoxA (Nox1) complex consisting of the catalytic subunit NoxA, the membrane-integrated protein NoxD, the adaptor protein NoxR, the scaffolding protein BemA, and the small GTPase RacA (Tanaka *et al*., 2006; Takemoto *et al*., 2006; Tanaka *et al*., 2008; Takemoto *et al*., 2011; Lacaze *et*

al., 2015; Tudzynski *et al*., 2012). In addition, signalling via the guanidine exchange factor Cdc24 and the small GTPase Cdc42 affects Nox complex activity (Kayano *et al*., 2018). The NoxB (Nox2) complex is less well characterized and consists of the catalytic subunit NoxB, the tetraspannin Psl1, NoxR, and other subunits (Sigmund *et al*., 2013; Marschall *et al*., 2016; Green *et al*., 2019 (in press)).

Fungal Nox complexes are homologs of mammalian oxidase complexes, with which they share some, but not all of the cytosolic subunits. Mammals contain five Nox subfamilies and two dual oxidase (DUOX) subfamilies. The most well-known Nox complex is the Nox2 complex (fungal NoxA and NoxB), which is required for the oxidative bust response of macrophages to pathogen attack (Babior *et al*., 1999). The complex consists of gp91phox (Nox2, fungal NoxA), p22phox (fungal NoxD), p67phox (fungal NoxR), the small GTPase Rac2, p40phox and p47phox. No fungal homologs of p40phox and p47phox have been described to date. In addition to their role in defence against pathogens, Nox complexes are also required for developmental and signalling processes (Lambeth *et al*., 2000; Brown and Griendling, 2009). Plants encode NADPH oxidases as well, the so called respiratory burst homologs (RBHOs), which contain a calcium-binding EF-hand motive, similar to fungal NoxC and mammalian Nox5. These RBHOs are involved in stress responses, responses to pathogens, and in pollen tube and root hair growth (Marino *et al*., 2012).

While the components of the Nox complex have been well described in fungi and mammals, many open questions still remain with regard to how this complex is activated. Many subunits of the Nox complex contain lipid-binding domains and several studies in mammalian and plant cells suggest a role for phosphoinositides in the activation of the Nox complex, among these phosphaditylinositol 4,5-bisphosphate (PtdIns[4,5]P_2). Phosphoinositides consist of a glycerol backbone with two fatty acid chains attached via an ester bond, and a headgroup in position one consisting of phosphate esterified to an inositol ring. This inositol ring can be phosphorylated and dephosphorylated in three positions by multiple kinases and phosphatases, theoretically resulting in seven different types of phosphorylated phosphatidylinositol (Balla, 2013; de Craene *et al*., 2017). Phosphoinositides have been shown to affect cellular functions by interacting with proteins that reside in membranes or by recruiting proteins to the membrane through a multitude of different characterized PtdIns-binding domains or polybasic amino acid (aa) stretches (Balla, 2013; de Craene *et al*., 2017). The asymmetric distribution of phospholipids, their kinases and phosphatases within the cellular membranes is a way to define and maintain membrane identity (Falkenburger *et al*., 2010; de Craene *et al*., 2017). The bisphosphorylated PtdInd[4,5]P_2 is the most abundant of the phosphoinositides (30% of phosphoinositides

in yeast, 45% in humans) and is largely localised at the inner leaflet of the plasma membrane (PM) (di Paolo and de Camilli, 2006; de Craene *et al*., 2017). Collectively, in yeast, plants and humans, it is required for endocytosis, exocytosis, actin cytoskeleton rearrangement, activity of iron channels, and the establishment of cell polarity (Balla, 2013; de Craene *et al*., 2017).

In mammalian cells, it has been shown to be required for phospholipase D (PLD) activity, which is involved in the activation of the Nox complex (Qualliotine-Mann *et al*., 1993; Sciorra *et al*., 1999; Karathanassis *et al*., 2002; Taylor *et al*., 2004). In addition, cleavage of PtdIns[4,5]P_2 by phospholipase C (PLC) results in the activation of the protein kinase C protein family, which activates the Nox complex through phosphorylation of the subunits (Horowitz *et al*.,1999; Belambri *et al*., 2018). An early study by Kanai and associates (2001) suggested that p47phox weakly binds to PtdIns[4,5]P_2 and in tobacco pollen tube and tobacco By-2 cell line PM extracts, the addition of exogenous PtdIns[4,5]P_2 resulted in an increased NADPH oxidase activity (Potocký *et al*., 2012). In mammalian cells, PtdIns[4,5]P_2 can be generated via the phosphorylation of PtdIns[4]P by a phosphatidylinositol 4-phosphate 5-kinase (type I PtdIns4P5K) or the phosphorylation of PtdIns[5]P by a phosphatidylinositol 5-phosphate 4-kinase (type II PtdIns5P4K). In addition, it can be produced through the dephosphorylation of PtdIns[3,4,5]P_3 by the phosphatidylinositol 3,4,5-trisphosphate 3-phosphatase PTEN (Phosphatase and TENsin homolog). PTEN is a lipid phosphatase as well as a dual specificity protein phosphatase, able to dephosphorylate tyrosine-, serine- and threonine-phosphorylated proteins. In mammals the lipid phosphatase activity is essential in its role as a tumour suppressor protein, as the dephosphorylation of PtdIns[3,4,5]P_3 inhibits the activation of proteins downstream of the phosphatidylinositol 3-kinase and serine/threonine kinase AKT pathway (PI3K/AKT pathway) that regulates cell growth and survival (Manning and Cantley, 2007). Disruption of PTEN results in unregulated cell proliferation and the onset of cancer (Liaw *et al*., 1999; Chen *et al*., 2018). Recent studies, however, suggest that the protein phosphatase function of PTEN is also required for its function (Wozniak *et al*., 2017). The *Arabidopsis thaliana* PTEN homolog is required for pollen development (Gupta *et al*., 2002).

In fungi, PtdIns[3,4,5]P_3 was considered to be absent due to the lack of a class I phosphatidylinositol 3-kinase, despite the presence of a PTEN homolog. Only the measurable increase of PtdIns[3,4,5]P_3 in response to the deletion of the PTEN-encoding homolog in *Schizosaccharomyces pombe*, *Spptn1*, supports the hypothesis that fungi are able to generate PtdIns[3,4,5]P_3 and that the PTEN homolog has lipid phosphatase activity (Mitra *et al*., 2004). This observation resulted in the identification

of an alternative pathway for the generation of PtdIns[3,4,5]P_3 by making use of a class III phosphatidylinositol 3-kinase, Vps34p, and the phosphatidylinositol 4-phosphate 5-kinase, Its3p (Mitra *et al*., 2004). As filamentous fungi encode homologs of these proteins, a similar pathway for the production of these phosphoinositides is expected to be present in filamentous fungi, despite the lack of biochemical evidence to date.

Deletion of *Spptn1* resulted in misshapen vacuoles and osmotic fragility, whereas deletion of the *PTEN* homolog in *Saccharomyces cerevisiae*, *ScTEP1*, resulted in a mislocalisation of dityrosine during sporulation and increased resistance to the phosphoinositide-3 kinase inhibitor, wortmannin (Heymont *et al*., 2000; Mitra *et al*., 2004). In filamentous fungi, the role of the PTEN homologs has to date only been investigated in *Fusarium graminearum* and *Ustilago maydis*. Deletion of the PTEN-encoding homolog in *F. graminearum*, *Fgtep1*, resulted in an increased sensitivity to lithium, reduced production of conidia and decreased germination in the presence of wortmannin. In addition, the deletion resulted in reduced virulence on wheat coleoptiles (Zhang *et al*., 2010). In *U. maydis,* deletion of the *PTEN*-encoding homolog *Umptn1* reduced virulence on maize, teliospore production and germination (Vijayakrishnapillai *et al*., 2019).

This study focusses on the role of the *E. festucae* PTEN homolog TepA and its influence on the distribution of PtdIns[4,5]P_2 and PtdIns[3,4,5]P_3. The effect of the deletion and the overexpression of *tepA* is analysed during axenic growth as well as in the mutualistic interaction with *L. perenne*. In addition, the question of whether the mutation of *tepA* influences the activation of the Nox complex or the localisation of its subunits is investigated.

Materials and Methods

Bioinformatic analyses

A tBLASTn analysis against the *E. festucae* Fl1 genome was performed on the Kentucky Endophyte database using the protein sequence of ScTep1 (endophyte.uky.edu, Schardl *et al*., 2013) and the genomic and protein sequence of EfM3.013870 was obtained from the same site. Expression analysis of *tepA* made use of transcriptome datasets generated by Chujo *et al*. (2019) and Eaton *et al*. (2015). The protein sequence of TepA was analysed with InterProScan (Jones *et al*., 2014) and protein alignments were generated using MAFFT (Katoh *et al*., 2017) and JalView (version 1.0). Boxplots were generated online with BoxPlotR (available on http://shiny.chemgrid.org/boxplotr/). Dunn's test for multiple comparisons, as implemented in the R package dunn.test v 1.3.5 (Dinno, 2017) was used to identify significant differences in the number of hyphae per intercellular space between all deletion and over-expression strains. One-way ANOVAs were used to test for differences in plant phenotypes between WT and overexpression strains. In each case, the ANOVA was fitted with R, and a Bonferroni correction was applied to all p-values to account for multiple testing.

Strains and growth conditions

Escherichia coli strains were grown at 37°C in lysogeny broth (LB; 1% tryptone, 0.5% yeast extract, 1% NaCl). When necessary, 1.5% agar was added to solidify the growth medium. The LB medium was supplemented with 100 µg/mL ampicillin for selection of transformed cells.

E. festucae strains were grown at 22°C on 2.4% Potato Dextrose (PD) supplemented with 1.5% agar or in 2.4% liquid PD medium for up to 7 d. If required, the medium was supplemented with 150 µg/mL hygromycin B or 200 µg/mL geneticin. All strains are listed in Supplemental Table S1.

Plant growth and inoculation

E. festucae strains were inoculated into *L. perenne* seedlings (cv. Samson) as described by Latch and Christensen (1989). Inoculated plants were grown in root trainers with a photoperiod of 16 h light and 8 h dark, with artificial lighting (approximately 100 µE/m2/s) at 22°C.

DNA analysis, PCR and sequencing

E. festucae genomic DNA was isolated from freeze-dried mycelium, as previously described by Byrd *et al*. (1990). Plasmid DNA was isolated from *E. coli* liquid cultures using the High Pure plasmid isolation kit (Roche).

PCR amplification of short fragments for screening purposes (<3 kbp) was conducted using One-Taq (NEB) polymerase and of long fragments (>3 kbp) for subsequent cloning procedures using Phusion Polymerase (NEB). PCRs were performed as described in the provided manufacturer's instructions. PCRs with very long primers (>40 bp) required for Gibson assembly (Gibson *et al*., 2009) were performed according to a modified 2-step/3-step protocol in which only the first five cycles were performed as per manufacturer's instructions. The last 25 cycles were performed as follows: 10 s at 98°C (denaturation), 30 s/kbp at 72°C (elongation), followed by a final extension for 5 min at 72°C. PCR fragments were separated by agarose-gel electrophoresis on a 0.8% gel and gel extractions were performed with the Wizard SV Gel and PCR clean-up kit (Promega) as per manufacturer's instructions. Sequencing of plasmids was performed at the Massey Genome Centre with the Big-DyeTM Terminator Version 3.1 Ready Reaction Cycle Sequencing Kit (Applied BioSystems, Carlsbad, California, USA). For separation, an ABI3730 genetic analyser (Applied Bio Systems) was utilized. Sequence data was analysed and assembled using MacVector (version 14.5.2).

Preparation of constructs

All constructs were designed in MacVector (v14.5.2) and assembled via Gibson assembly (Gibson, 2009). All primers and generated plasmids can be found in Supplemental Table S2.

For generation of the *tepA* replacement construct (pBH43) a 1,269 bp PCR fragment 5' of *tepA* and a 1291 bp PCR fragment 3' of *tepA* were amplified using Phusion polymerase with the primer combination BH210/BH211 and BH208/BH209. The P*trpC*-*hph* (1394 bp) cassette was amplified from pSF15.15 with the primer combination hph_F/hph_R and the backbone pRS426 was amplified with the primers pRS426_F/pRS426_R. The overexpression construct, pCE122, *tepA* (1,798 bp) was amplified from WT genomic DNA with the primers tep5/tep6. The pRS426 backbone was amplified as described above and P*gpd* and T*trpC* with pRS426-Pgdp-F/pRS426-Pgdp-R (2310 bp) and TtrpC-F/ pRS426-TtrpC-R (569 bp), from pPN82 and pII99 respectively. The C-terminal mCherry fusion protein encoding constructs were assembled from three backbone fragments and the *tepA* (pBH42) coding region. The *tepA* coding region was amplified from WT genomic DNA with the primers

BH203/BH204. The backbone fragments included: a 2,817 bp fragment amplified from pBH16 with BH76/BH75, containing T*trpC* and a *hph* cassette, a 4,608 bp fragment amplified from pBH28 with BH197/196 containing genes for replication in *E. coli* and P*gpd* and a 765 bp fragment amplified from pBV579 with BH79/BH199 encoding *mCherry*. For the N-terminal GFP fusion protein construct, pBH41, the backbone was amplified in two fragments from pBH28. One fragment was 4,810 bp in length and was amplified with BH76/BH193 and the other one was 3,080 bp in length and was amplified with pBH114/BH191. The *tepA* coding region was amplified with BH195/tep6. Both fusion protein constructs encode a $(GGGS)_2$ linker between the protein of interest and the fluorophore.

Transformation of organisms

E. coli DH5α cells were made chemically competent and transformed as described by Hanahan *et al*. (1983). *E. festucae* strains were transformed by PEG-mediated protoplast transformation (Young *et al*., 2005) Protoplasts were generated as described by Itoh *et al*. (1994) and transformed with up to 5 µg of the construct of interest. Following an overnight recovery step on regeneration (RG) medium (Young *et al*., 2005), protoplasts were overlaid with 0.8% RG agar containing hygromycin B or geneticin to a final concentration of 150 µg/mL or 200 µg/mL, respectively.

Southern blot analysis

For Southern blots, high quality genomic DNA was extracted as described, and approx. 1.2 µg was digested with the chosen enzyme. The Southern blot was conducted and developed as described in the Dig Easy Hyb (Roche) instruction manual.

Western blot

E. festucae strains were grown in liquid PD medium for 3 d and then harvested by filtering through a nappy liner. Following multiple washing steps, the mycelium was snap-frozen and ground to a fine powder. Approx. 500 µl of lysis buffer (50 mM Tris-HCL, 100 mM NaCl, 10 mM EDTA, 0.2 mM PMFS, 0.1 mM DTT, 1 µl/mL NP40, 1 µl/mL Protease inhibitor cocktail (Roche)) were added to each sample and the solution was vortexed repeatedly. Subsequently, the samples were centrifuged at 14,000 g at 4°C for 15 min and the pellet was discarded.

Approx. 15-20 µL of protein solution was loaded onto a 10% SDS acrylamide gel and separated for about 2 h at 100 V. The transfer onto PVDF membranes was conducted at approx. 100 V for 1.10 h. Membranes were blocked with 5% trim milk powder in TBS-T and probed with a primary rabbit anti-GFP antibody (Abcam, ab290,

1:3000 dilution) or a primary rabbit anti-mCherry antibody (Abcam, ab167453, 1:2000 dilution). A secondary goat anti-rabbit HRP antibody (Abcam, ab6721, 1:10000 dilution) was used for the final antibody incubation, and the blots were developed using Amersham ECL Western blotting solution (GE Healthcare Life Sciences).

qRT-PCR

RNA was isolated from snap-frozen fungal mycelia using TRIzol reagent (Invitrogen). Synthesis of cDNA was performed with the QuantiTect Reverse Transcriptase kit (Qiagen) as per manufacturer's instructions. The qRT-PCRs were performed with the SYBR Green (Invitrogen) reagent as described in the manual, and the reactions run on a LightCycler 480 System (Roche). Genes coding for translation elongation factor 2 (*EF-2*, M3 model number on the database http://www.endophyte.uky.edu (Schardl *et al*., 2013): EfM3.021210EfM3.021210) and 40S ribosomal protein S22 (*S22*, EfM3.016650) were chosen as reference genes (Lukito *et al*., 2015). The gene expression was calculated relative to the WT gene expression as previously described (Lukito *et al*., 2015). The qRT-PCR on tepA was performed with the primer combination BH189/BH190. Sequences can be found in Supplemental Table S2.

Microscopy

For analysis of hyphal growth, strains were inoculated in the following way: a square petri dish was filled with about 70 mL of 3% H_2O agar, and following its solidification, a sterilized microscopic slide was placed on top. Subsequently, the slide was covered with 1.5% H_2O agar and after it had set, a small amount of mycelium was inoculated at the edge of the microscopic slide. These plates were incubated at 22°C for 5–7 d. For analysis, an Olympus IX83 inverted fluorescence microscope was used. To visualize the cell wall, mycelia were stained with 3 µl of a 3 mg/mL Calcofluor white (CFW) solution.

For transmission electron microscopy (TEM), infected pseudostem tissue was fixed and embedded in resin as described by Spiers and Hopcroft (1993). Samples were cut, and a subset of sections were stained with 0.05% toluidine blue in phosphate buffer and heat-fixed at approx. 100°C for 10 s. These sections were examined with a Zeiss Axiophot Microscope with differential interference contrast (DIC) Optics and Colour CCD camera. Other sections were stained with lead citrate and analysed with a FEI Tecnai G2 Biotwin TEM.

For confocal laser microscopy, pseudostem samples were prepared as previously described (Becker *et al*., 2016, 2018). Samples were fixed and destained in 100% EtOH, permeabilized with 10% KOH and infiltrated with wheat germ-agglutinin

conjugated to AlexaFluor 488 (WGA-AF488, Molecular Probes/Invitrogen) and aniline blue diammonium salt (Sigma). Samples were analysed with a Leica SP5DM6000B confocal microscope (488 nm argon and 561 nm DPSS laser, 40× oil immersion objective, NA= 1.3) (Leica Microsystems).

Analysis of superoxide production

To analyse superoxide production in *E. festucae*, two methods were employed: staining of whole colonies with Nitroblue-tetrazolium (NBT) and staining with the ROS-ID ® Superoxide probe (ENZO LifeSciences). The NBT staining was performed as described by Tanaka *et al*., (2006). In brief, 7-d-old colonies were covered with approx. 150 µl of NBT solution (Sigma) and incubated for 5 h before analysis. For staining with the superoxide probe, 3 µl of a 1:30 dilution (0.16 mM) in H_2O were added to an approx. 5-d-old colony section. It was then covered with a coverslip and incubated in the dark for 10 min before analysis.

Results

Epichloë festucae encodes a homolog of the mammalian tumour suppressor protein PTEN

To identify the gene encoding the *E. festucae PTEN* homolog, a tBLASTn analysis was performed against the Fl1 genome using *S. cerevisiae* Tep1 as a query. This search returned one putative homolog, EfM3.013870, with an E-value of 5e-13. This gene, designated as *tepA*, encodes a protein of 547 aa. Analysis of gene expression, making use of available transcriptome datasets, revealed a moderate level of expression in culture (20.76 RPMK) and no differential expression *in planta* or in any of the symbiotic mutants analysed to date (Δ*sakA*, Δ*noxA*, Δ*proA*, or Δ*hepA*) (Eaton *et al*., 2015; Chujo *et al*., 2019; Hassing *et al*., 2019; Chujo *et al*., 2019). Submission of the protein sequence to InterProScan (Jones *et al*., 20014) revealed the presence of a dual specificity phosphatase activity domain (153–202 aa) embedded in the tensin-type phosphatase domain, which is typical of PTEN-type proteins from humans and fungi. Furthermore, all conserved aa of the catalytic P-, WPD- and TI-loops were found to be present (Figure 1). The P-loop (H-C-X_2-G-X_2-R) provides the required residues for catalytic activity, whereas the WDP- and TI-loop form the walls of the catalytic cavity. The TI-loop is of special importance, as it increases the width of the cavity compared to other dual specificity phosphatases to accommodate PtdIns[3,4,5]P_3 (Lee *et al*., 1999). The anionic lipid-binding C2 domain and the PDZ (PSD-95, Discs-large, ZO-1)-binding motif (binds proteins with a PDZ motif), however, were found to be missing in TepA, as has been described for all fungal homologs analysed to date (Cid *et al*., 2008). Interestingly, two of the four conserved aa of the N-terminal PtdIns[4,5]P_2-binding domain (PBD; K/R-X_4-K/R-X-K/R-K/R) were found to be absent in TepA as well as in *Fg*Tep1. This motif has previously been described as being required for activity and localisation of PTEN (Campbell *et al*., 2003; Walker *et al*., 2004). Protein sequence alignment of the tensin-type phosphatase domain of PTEN, *Fg*Tep1, TepA, *Sp*Ptn1 and *Sc*Tep1 demonstrated an *S. cerevisiae*-specific insertion in *Sc*Tep1, as well as an apparent filamentous fungus-specific insertion in TepA and *Fg*Tep1 (Cid *et al*., 2008).

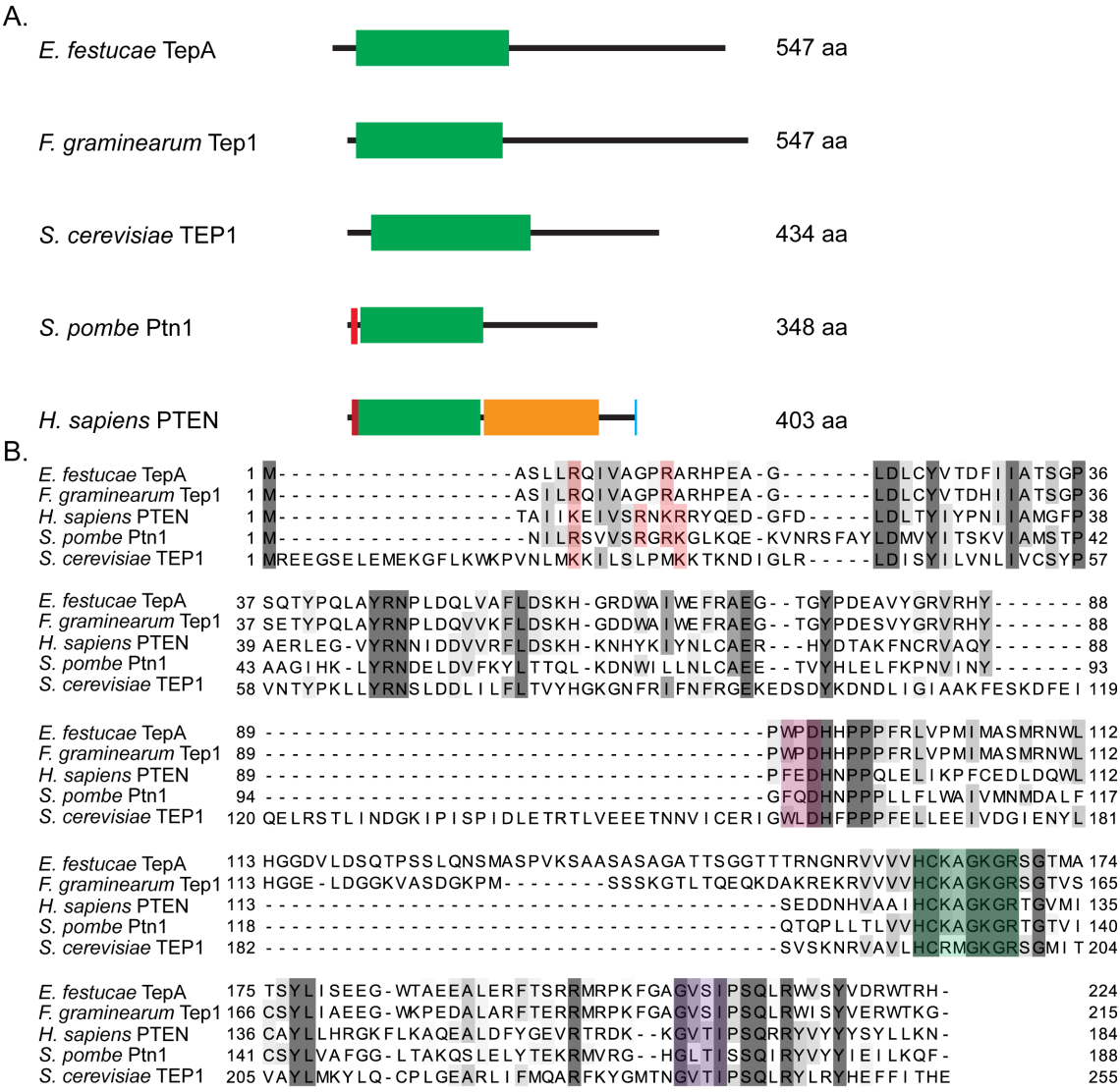

Figure 1: Domain structure and protein sequence alignment of *Epichloë festucae* TepA with *H. sapiens* PTEN and its homologs from other fungi.

E. festucae TepA was compared to *S. pombe* Ptn1 (CAA22831.1), *S. cerevisiae* Tep1 (P53916.1), *F. graminearum* Tep1 (XP_011323458.1) and human PTEN (AAD13528.1). (A) Schematic representation of *Ef*TepA, *Sp*Ptn1, *Sc*Tep1, *Fg*Tep1 and *Hs*PTEN protein domain structure. Green box: tensin-type phosphatase domain, red box: PtdIns[4,5]P_2-binding domain, orange box: C2 domain. Size of the protein indicated in number of aa. (B) Amino acid sequence alignment of the tensin-type phosphatase domain of TepA, *Sp*Ptn1, *Sc*TEP1, *Fg*Tep1 and *Hs*PTEN; red highlights: conserved aa of the PtdIns[4,5]P_2-binding domain; light purple box: WPD-loop; green box: P-loop (active site); dark purple box: Ti-loop. Sequences were annotated according to InterProScan (Jones *et al.*, 2014) and by comparison of the domains identified by Lee *et al.*, (1999). Sequences are shaded in a grey scale based on their percentage identity.

Epichloë festucae TepA localises to the cytoplasm and to septa

Mammalian PTEN has been described to bind to the membrane for a few hundred milliseconds to dephosphorylate several PtdIns[3,4,5]P_3 molecules before dissociating to the cytoplasm (Vazquez *et al*., 2006). To analyse the localisation of TepA during axenic growth, TepA localisation constructs were generated and transformed into wild-type (WT) protoplasts. To avoid the possibility of the fluorescent protein influencing the observed localisation, N-terminal mCherry and C-terminal GFP fusion constructs were designed based on the genomic DNA sequence of *tepA* (pBH41, pBH42). The successful integration of the fusion protein was verified by PCR and the expression of the complete fusion protein via western blot (Supplemental Figure S1). Interestingly, slight differences in the localisation of the mCherry and the GFP fusion protein were observed. While the GFP-TepA fusion protein localised to the cytoplasm in hyphal tips and young hyphae, comparable to the localisation of GFP and mCherry under the regulation of a constitutive promoter, the TepA-mCherry fusion protein was found to localise to the cytoplasm as well as septa in young hyphae (Figure 2). Localisation to septa in mature hyphae that underwent hyphal fusion was observed for both fusion proteins. These observations provide support for the presence of a lipid-binding domain in TepA, despite differences in the PtdIns[4,5]P_2-binding domain that change the consensus sequence and the lack of a C2 domain. The improved localisation of the TepA-mCherry construct compared to the GFP-TepA construct suggests that the addition of an N-terminal tag reduces binding affinity.

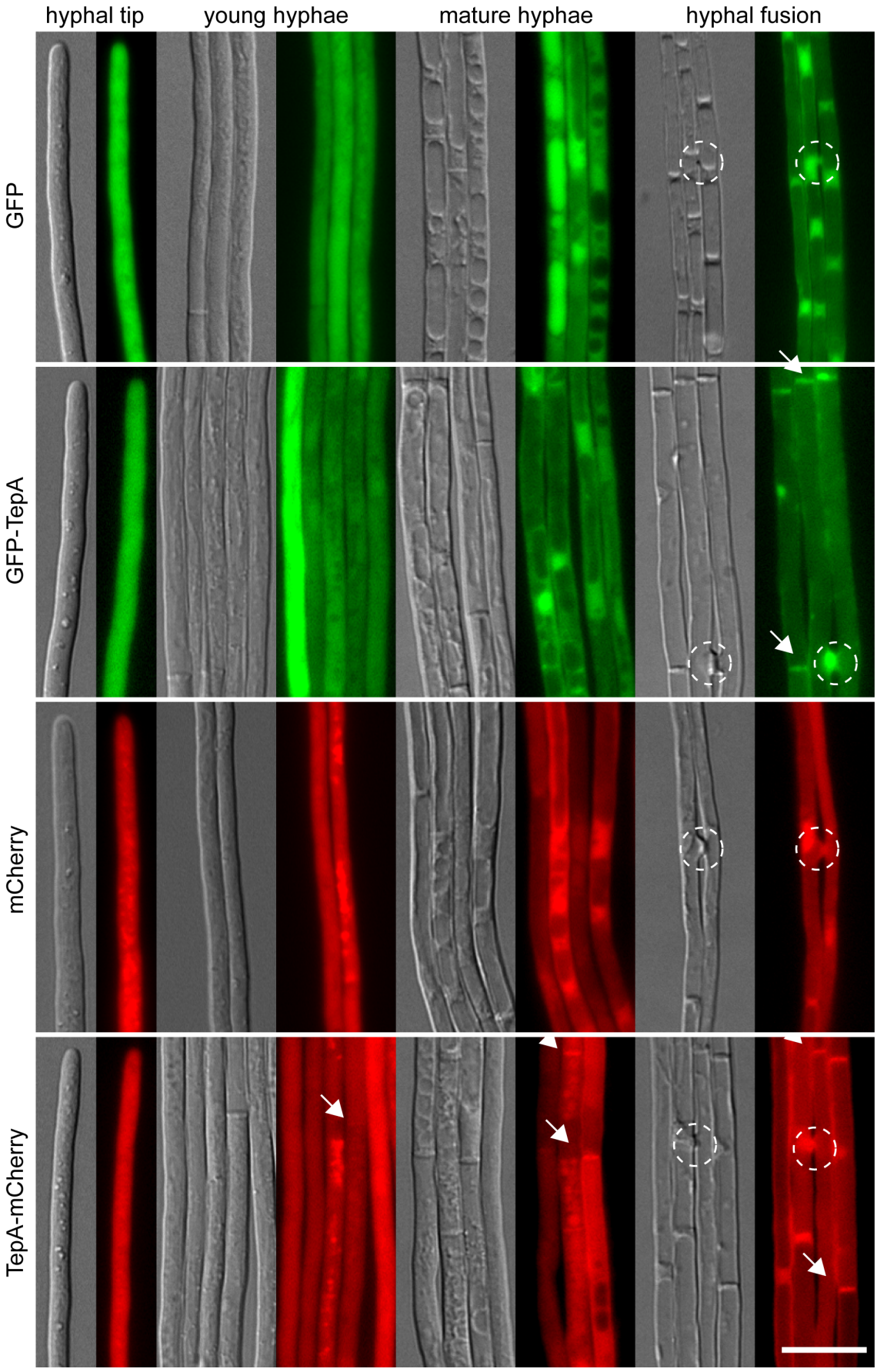
hyphal tip
young hyphae
mature hyphae
hyphal fusion
GFP
GFP-TepA
mCherry
TepA-mCherry

Figure 2: Localisation of TepA during axenic growth of *Epichloë festucae*.
Strains were grown on 1.5% H_2O agar for 5 d before examination using a fluorescence microscope. The images shown of wild-type (WT) expressing GFP (pBH28, #T6), GFP-TepA (pBH41, #T4), mCherry (pCE126, #T2) and TepA-mCherry (pBH42, #T2) are representative of all strains analysed. As indicated, hyphae of different ages were analysed. White circles: hyphal fusion, white arrows: localisation at septa. Bar = 10 µm.

Generation of *Epichloë festucae tepA* deletion and overexpression strains

To analyse the role of TepA, and thereby the role of PtdIns[3,4,5]P_3 and PtdIns[4,5]P_2, in the growth of *E. festucae*, *tepA* deletion and overexpression strains were generated. Gene deletion was achieved by employing a gene replacement approach making use of the homologous recombination machinery of *E. festucae*. A linear insert of the gene replacement construct (pBH43) was transformed into Fl1 protoplasts and protoplasts overlaid with selection medium. Approx. 200 Hyg^R transformants were screened by PCR for replacement of the gene, resulting in the identification of three deletion strains (#T80, #T87, #T102). Analysis of these strains revealed that all strains contained tandem integrations of the deletion cassette (Supplemental Figure S2).

Overexpression strains were generated by transformation of WT protoplasts with a circular construct, pCE122, containing the genomic sequence of *tepA* under the control of the *A. nidulans gpd* promoter. Overexpression constructs were co-transformed with pII99, a plasmid encoding a geneticin resistance marker. Resistant strains were selected and screened for the integration of the overexpression construct by PCR. Subsequently, *tepA* expression levels were analysed via qRT-PCR and strains (#T4, #T7, #T20) with different levels of expression compared to the WT were used for the following studies (Supplemental Figure S3).

Deletion and overexpression of *Epichloë festucae tepA* does not influence growth in culture

The growth rate and morphology of the deletion and overexpression strains of *tepA* were indistinguishable from WT (Figure 3). Microscopic analysis of WT revealed smooth hyphae with a consistent diameter, formation of hyphal bundles, hyphal coils and hyphal cell-to-cell fusion. Similar structures were observed in both the deletion and the overexpression strains (Figure 3). Staining of hyphae with the chitin stain Calcofluor white (CFW) resulted in an even staining of the fungal cell wall in WT as well as the mutant strains (Figure 3).

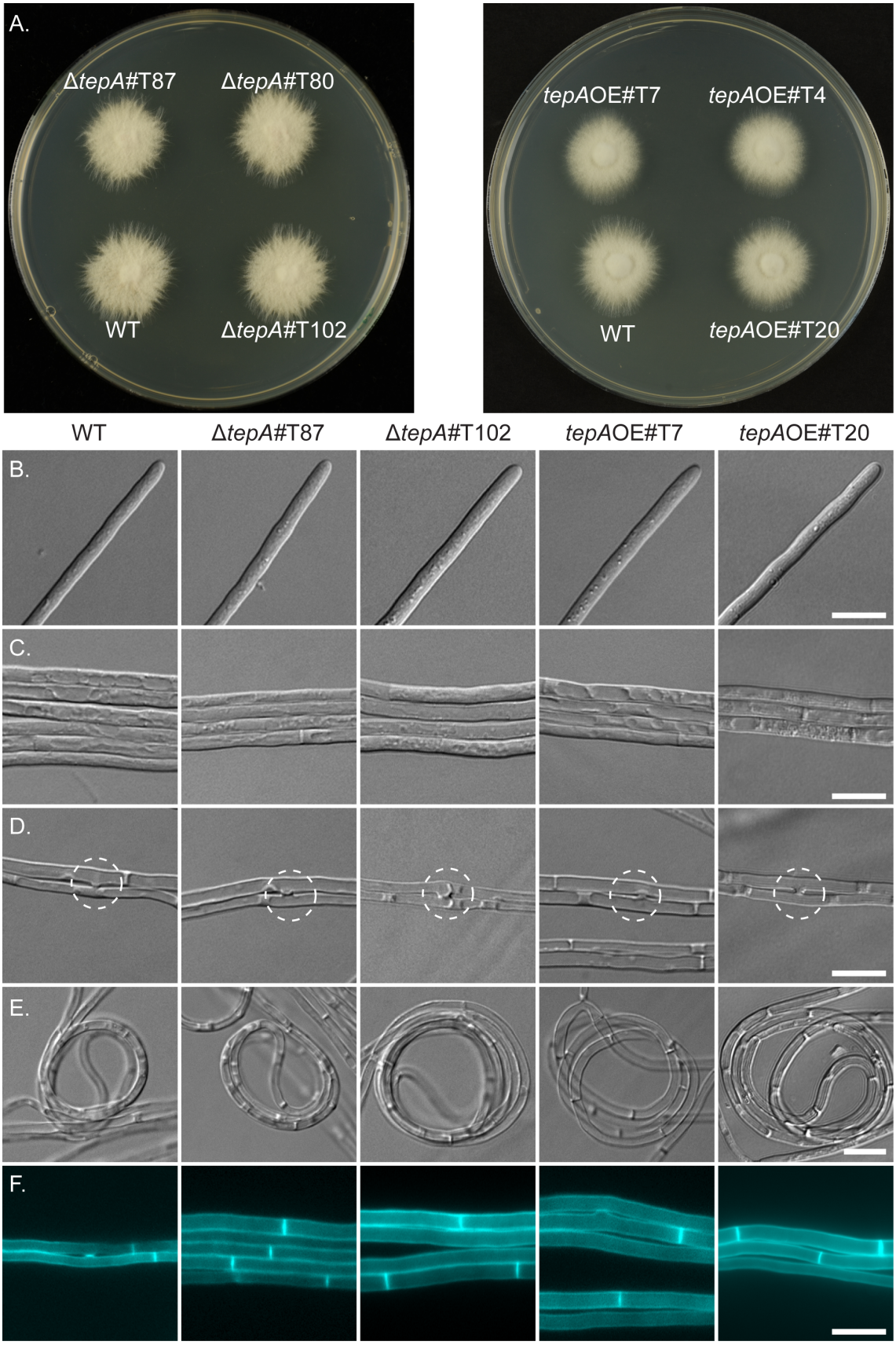
A.
ΔtepA#T87
ΔtepA#T80
WT
ΔtepA#T102
tepAOE#T7
tepAOE#T4
WT
tepAOE#T20
WT
ΔtepA#T87
ΔtepA#T102
tepAOE#T7
tepAOE#T20
B.
C.
D.
E.
F.

Figure 3: Culture phenotype of *Epichloë festucae* wild-type and *tepA* mutants. Wild-type (WT) as well as deletion strains (#T80, #T87, #T102) and overexpression strains (#T4, #T7, #T20) were analysed multiple times. The images shown are representative of all strains analysed. (A) Whole colony morphology of WT and mutant strains grown on 2.4% PA agar for seven days before examination; (B-F) strains were grown for seven days on 1.5% H_2O agar before analysis; (B) Hyphal tip morphology in WT and mutant strains; (C) Formation of hyphal bundles in WT and mutant strains; (D) Hyphal fusion in WT and mutant strains; (E) Hyphal coil formation in WT and mutant strains; (F) Typical staining of hyphal bundle with Calcofluor white (CFW). White circle: hyphal fusion; Bar = 10 µm.

Thus, the deletion or overexpression of *tepA*, and thereby the hypothesized changes in the PI concentrations, do not influence the growth of *E. festucae* in axenic culture.

Deletion of *Epichloë festucae tepA* influences fungal growth *in planta*

As described previously, deletion of *tep1* in *F. graminearum* and *ptn1* in *U. maydis* resulted in a decreased virulence on wheat and maize, respectively (Zhang *et al*., 2010; Vijayakrishnapillai *et al*., 2018). To investigate whether the deletion or overexpression of *tepA* in *E. festucae* has any effect on the host interaction, mutant strains were inoculated into *L. perenne* seedlings and the whole plant phenotype analysed 10 weeks post-inoculation. Plants infected with the overexpression strains were indistinguishable from WT-infected plants with regard to the length of the tillers as well as the number of tillers (Figure 4, Supplemental Figure S4). Only three plants infected with *tepA* deletion strains survived (2x #T80 and 1x #T87), but all of these plants had a reduced tiller length compared to WT-infected plants (Figure 4).

WT
ΔtepA#T80
WT
ΔtepA#T87
WT
tepAOE#T4
WT
tepAOE#T7
WT
tepAOE#T20

Figure 4: Whole-plant interaction phenotype of *Lolium perenne* plants infected with *Epichloë festucae* WT and *tepA* mutant strains.

Wild-type (WT) and *tepA* mutant strain-infected plants were harvested 10 weeks post-inoculation. Number of infected plants: WT (9,5), *tepA* deletion strains #T80, #T87 (2/1), *tepA* overexpression strains #T4, #T7, #T20: (5/3/2),

To examine the growth of hyphae *in planta*, pseudostem-cross sections were fixed, embedded in resin and thin sections stained with toluidine blue (Figure 5). The number of mutant hyphae per intercellular space (average of 1.7 hyphae/intercellular space) was significantly increased (P = 1.11E-6) compared to plants infected with WT (1.2 hyphae/intercellular space), whereas the number of hyphae/intercellular space in the overexpression strains remained unchanged (average of 1.3, P = 0.15). In contrast to other symbiotic mutants of *E. festucae* examined to date, no vascular bundle colonization was observed for the *tepA* deletion or *tepA* overexpression strains. Analysis of sections of plant tissue infected with WT and the deletion mutants using transmission electron microscopy (TEM) also demonstrated an increase of hyphal biomass in plant tissue infected with the deletion mutant, whereas the ultrastructure of the hyphae themselves was indistinguishable from WT hyphae (Figure 5).

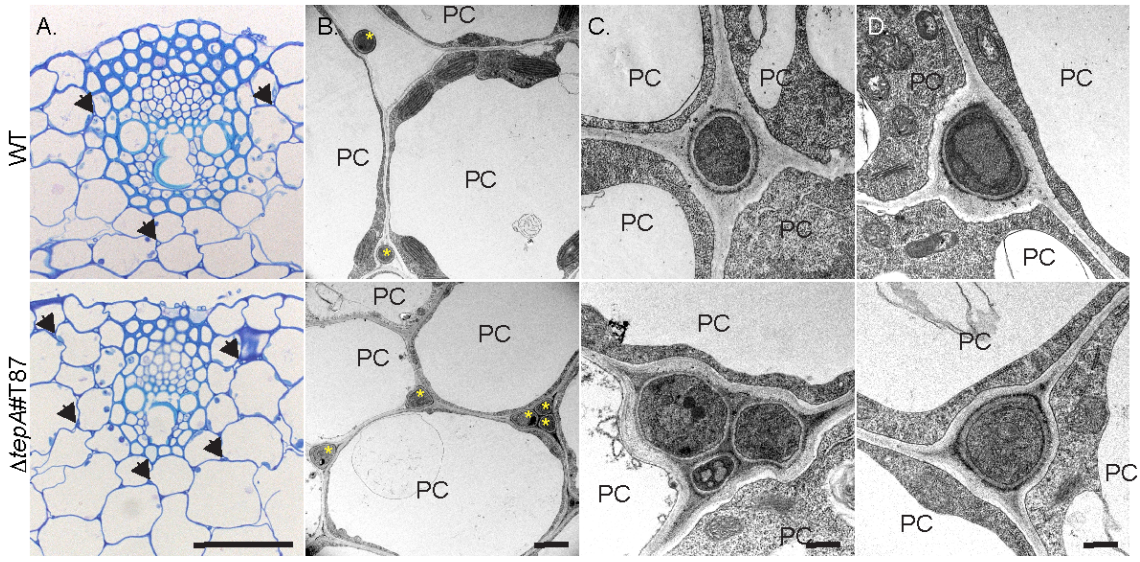

Figure 5: Examination of pseudostem sections of *Lolium perenne* plants infected with *Epichloë festucae* wild-type and *tepA* deletion strains by light- and transmission electron microscopy.

Infected *L. perenne* pseudostem samples were prepared for light- and transmission electron microscopy (TEM) as described in Materials and Methods. Because of the low number of infected plants obtained, only representative images of wild-type (WT) and

Δ*tepA*#T87 are shown. As the phenotype of plants infected with overexpression strains was comparable to WT-infected plants, no TEM analysis was performed. (A) Vascular bundle of WT and Δ*tepA*#T87-infected plants stained with toluidine blue and imaged with a light microscope; Bar = 50 µm; (B) Representative TEM micrographs of growth of WT and Δ*tepA*#T87 in infected plants; Bar = 10 µm. (C and D) Representative TEM micrographs of the hyphal structure of WT and Δ*tepA*#T87 in infected plants; Bar = 0.5 µm. Black arrow/yellow star: hyphae, PC: plant cell.

In addition, longitudinal sections of the pseudostem of infected plants were infiltrated with WGA-AF488 (blue pseudocolour), a chitin-binding stain, and aniline blue (red pseudocolour), a β-glucan-binding dye. In WT-infected plants, usually only one or two hyphae can be detected between neighbouring plant cells, which branch and fuse with neighbouring hyphae to give rise to a hyphal network throughout the whole plant (Figure 6). The pattern of growth by the overexpression strains was indistinguishable from WT; however, in plants infected with the deletion mutants, large bundles of hyphae were occasionally observed, a result consistent with an increase in hyphal biomass (Figure 6).

These results indicate that *tepA* is required for WT-like growth in the *E. festucae–L. perenne* interaction.

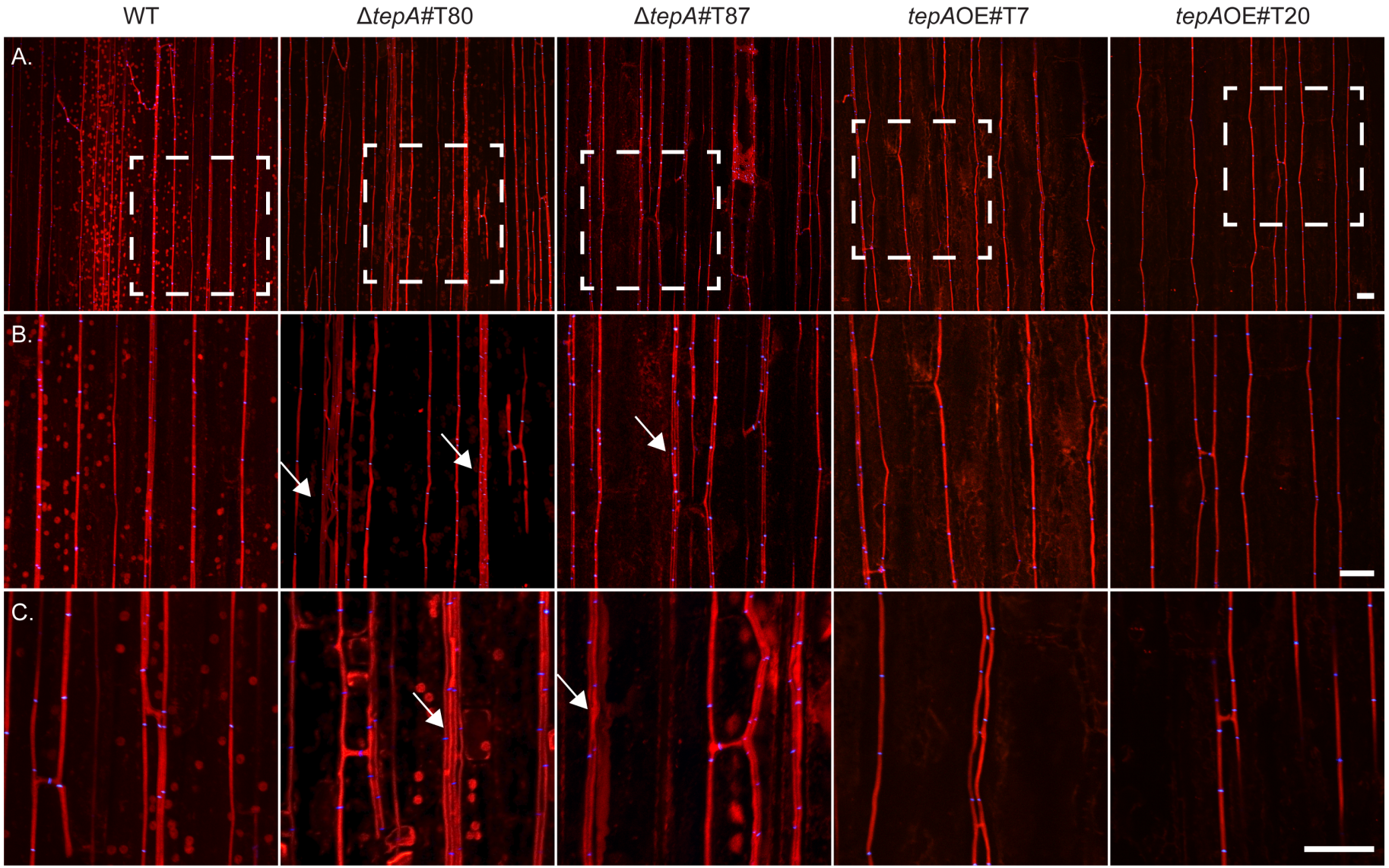
WT
ΔtepA#T80
ΔtepA#T87
tepAOE#T7
tepAOE#T20
A.
B.
C.

Figure 6: Confocal depth series of longitudinal sections of *Lolium perenne* infected with *Epichloë festucae* wild-type and *tepA* mutant strains.

Infected *L. perenne* pseudostem samples were stained with WGA-AF488 (chitin-binding, blue pseudocolour) and aniline blue (β-glucan-binding, red pseudocolour) and visualized with CLSM. Representative images of plant material infected with wild-type (WT), Δ*tepA*#T80 and Δ*tepA* #T87 and *tepA* overexpression (OE) strains #T7 and #T20 are shown. As no plants infected with Δ*tepA*#T102 were obtained, no images are shown. (A) Representative image (Z = 6 µm) of WT and *tepA* deletion and overexpression strains *in planta;* Bar = 10 µm; (B) Magnified images of white boxed region in (A); Bar = 10 µm. (C) Higher magnification images (Z = 4 µm) of hyphal branching and fusion of WT, *tepA*-deletion and overexpression strains *in planta*; White arrows: hyphal bundles; Bar = 10 µm.

Deletion or overexpression of *Epichloë festucae tepA* does not change localisation of lipid biosensors

To investigate whether the deletion or overexpression of *tepA* changes the concentration or localisation of specific lipid molecules, different lipid biosensors were transformed into the mutant strains. The *Mus musculus* Bruton's tyrosine kinase (BTK, NP_038510) PH domain has previously been described to specifically bind to PtdIns[3,4,5]P_3, the substrate of TepA. Therefore, a construct consisting of the DNA sequence coding for aa 3-169 fused to *gfp* under the regulation of the *A. nidulans gpd* promoter was used for the detection of PtdIns[3,4,5]P_3 (pCE105, Candy 2019). The PH domain of PLC δ1 (NP_112346) from *M. musculus* was found to specifically bind to PtdIns[4,5]P_2, and a construct encoding aa 13-139 fused to GFP was used to selectively detect the product of TepA, PtdIns[4,5,]P_2 (pCE107, Candy 2019). Several studies suggest a link between the production of PtdIns[4,5,]P_2 and the generation of phosphatidic acid (PA), as the PA-generating phospholipase D requires PtdIns[4,5,]P_2 for activity (Sciorra *et al*., 1999; Sciorra *et al*., 2002). Therefore, a PA biosensor, consisting of the PA-binding domain of *S. cereviseae* Spo20 (aa 51-95) fused to eGFP, was used as well (pBH50, Hassing *et al*., in preparation). All biosensor constructs were transformed into protoplasts of WT, the *tepA* deletion strain #T87, and the overexpression strain with the highest level of *tepA* expression in culture, #T7.

WT
tepAOE
ΔtepA
hyphal tip
mature hyphae
hyphal tip
mature hyphae
hyphal tip
mature hyphae
PA biosensor
PtdIns[4,5]P2 biosensor
PtdIns[3,4,5]P3 biosensor
n.a.

Figure 7: Localisation of PA, PtdIns[4,5]P_2 and PtdIns[3,4,5]P_3 in *Epichloë festucae* wild-type and *tepA* mutant strains.

Strains were incubated on 1.5% H_2O agar for approx. five days before analysis by fluorescence microscopy. Constructs were transformed into WT, the *tepA* deletion strain #T87, and the *tepA* overexpression strain #T7. As not all biosensor constructs encode a resistance gene, strains were co-transformed with pBH12 (Hyg^R) or pII99 (Gen^R) when appropriate. Multiple transformants were analysed and images of the indicated transformants are shown as representative of all transformants analysed. (A) Localisation of the phosphatidic-acid (PA) biosensor (pBH50) in WT (#T4), *tepA* overexpression (#T2) and *tepA* deletion (#T3) strains; (B) Localisation of the PtdIns[4,5]P_2 biosensor (pCE107) in WT (#T3), *tepA* overexpression (#T6) and *tepA* deletion (#TN2) strains; White arrows indicate regions with increased signal intensity. (C) Localisation of the PtdIns[3,4,5]P_3 biosensor (pCE105) in WT (#T9), and *tepA* overexpression strains (#T3). No *tepA* deletion strains expressing the PtdIns[3,4,5]P_3 biosensor were obtained. Bar = 10 µm.

In WT cells, the PA biosensor was found to localise evenly to the PM and septa of hyphae of all ages, and the same observations were made for the *tepA* deletion and overexpression strains (Figure 7). The PtdIns[3,4,5]P_3 biosensor localised to the cytoplasm in young and mature WT cells, indicating a lack or very low concentration of PtdIns[3,4,5]P_3 in hyphae during axenic growth. Similar results were obtained for the *tepA* overexpression strains. Initial transformants of the *tepA* deletion strains demonstrated a weak localisation to mobile vesicles, but this result has to date not been reproduced, despite multiple transformations and screening of approx. 50 transformants (Figure 7). The biosensor for detection of PtdIns[4,5]P_2 was observed to evenly line the cell wall, in a fashion comparable to the PA biosensor in WT hyphae. However, as previously described, accumulation of the PtdIns[4,5]P_2 biosensor was increased at a subapical collar-like structure, indicating a role in endocytosis (Candy 2019). Similar observations were made for both mutant strains, indicating that the effect of the loss or the overexpression of *tepA* on the lipid distribution is not sufficient to influence the localisation of a PtdIns[4,5]P_2 biosensor.

Deletion or overexpression of *Epichloë festucae tepA* does not change localisation of the Nox complex components

Both BemA and Cdc24 have lipid-binding domains, corresponding to PX and PH domain, respectively, which are proposed to be required for the localisation of NoxR to the hyphal tip (Takemoto *et al.*, 2011). Other components of the Nox complex have

also been shown to interact with phospholipids directly or indirectly. To identify whether possible changes in the lipid composition resulting from the deletion or overexpression of *tepA* would result in a changed localisation of the Nox complex components, the localisation of NoxA, NoxR, BemA, Cdc24 and RacA was analysed in *tepA* deletion and overexpression strains and compared to the localisation in WT. To this end, the previously generated protein-GFP fusion constructs of Nox complex components were transformed into WT, *tepA* deletion #T87 and *tepA* overexpression #T7 protoplasts (Takemoto *et al*., 2011; Eaton, pers. comm). In WT, GFP-NoxA was found to localise to perinuclear membranes and patches at the PM, similar to the pattern described for NoxA in *B. cinerea* (Figure 8) (Marschall *et al*., 2016). NoxR-GFP localised to a punctate structure at the hyphal tip, to mobile vesicles, and to puncta on either side of the septa. BemA-GFP was observed as an arch at the hyphal tip and in the centre of septa, potentially the septal pore. GFP-Cdc24 localised to a punctum at the hyphal tip and to the centre of septa, in a manner similar to BemA. GFP-RacA was identified at intracellular membranes, the PM and hyphal tips; therefore, all proteins localised as described previously (Figure 8) (Takemoto *et al*., 2011; Kayano *et al*., 2018). All fusion proteins were found to localise in the same way in the *tepA* deletion and overexpression strains, indicating that the effect of the modification of *tepA* on the lipid composition is not sufficient to mislocalise any of the Nox complex components.

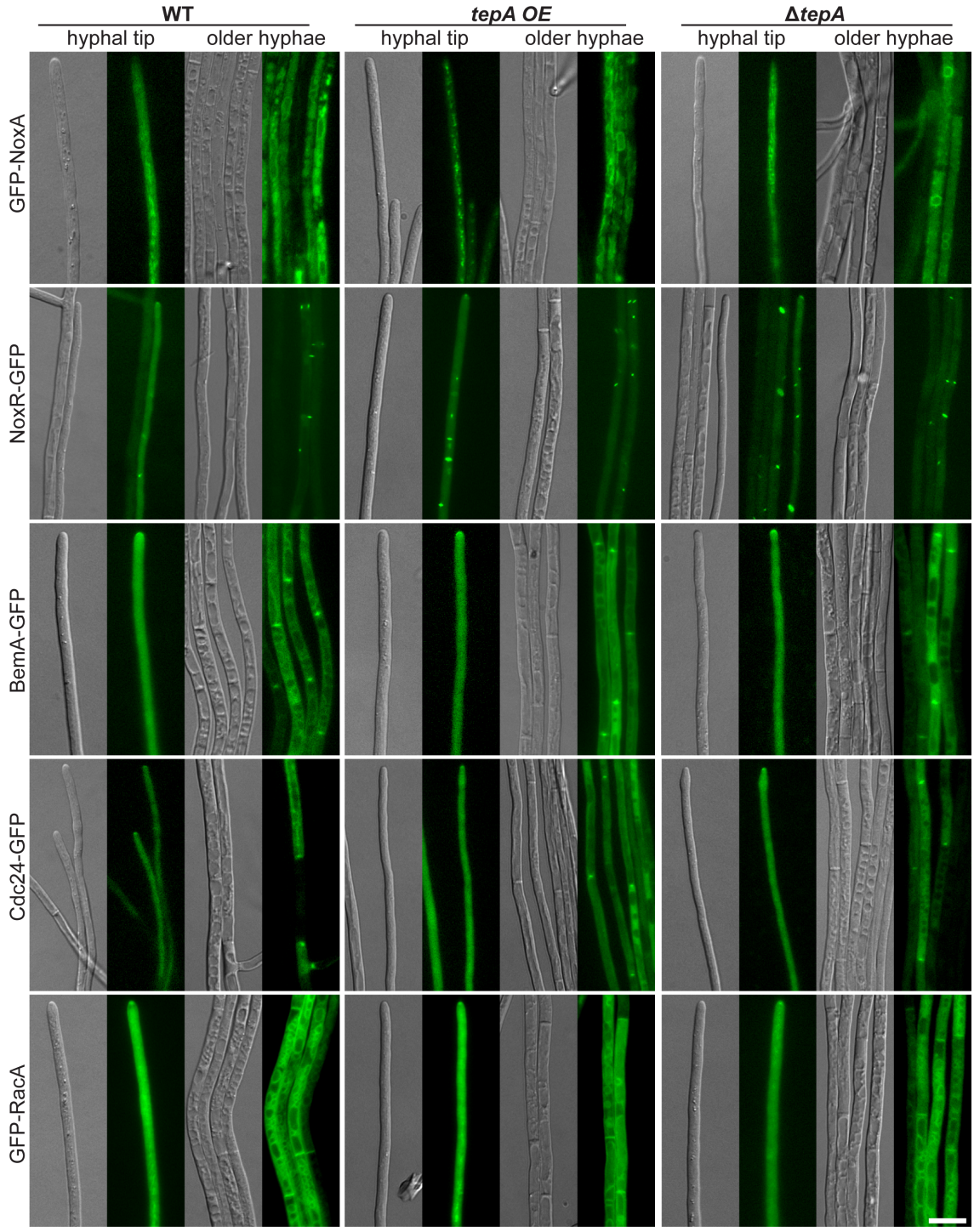

Figure 8: Localisation of Nox complex components in *Epichloë festucae* wild-type and *tepA* mutant strains.

Strains were grown for approx. five days on 1.5% H_2O agar before examination with a fluorescence microscope. Multiple strains were analysed and the images shown are representative of all strains analysed. As not all localization constructs encode a resistance gene, strains were co-transformed with pBH12 (Hyg^R) or pII99 (Gen^R) when appropriate. (A) Localisation of GFP-NoxA (pGFP-NoxA) in WT (#T4), Δ*tepA*#T102 (#T1), *tepA* OE#T7 (#T2); (B) Localisation of NoxR-GFP (pNPP9) in WT (#T1),

Δ*tepA*#T87 (#T1), *tepA* OE#T7 (#T1);(C) Localisation of BemA-GFP (pCE139) in WT (#T23), Δ*tepA*#T87 (#T1), *tepA* OE#T7 (#T6); (D) Localisation of Cdc24-GFP (pNPP6) in WT (#T33), Δ*tepA*#T87 (#T1), *tepA* OE#T7 (#T4); (E) Localisation of GFP-Rac (pPN154) in WT (#T6), Δ*tepA*#T87 (#T2), *tepA* OE#T7 (#T1); Bar = 10 µm.

Deletion or overexpression of *Epichloë festucae tepA* might increase ROS production

PtdIns[4,5]P_2 has previously been shown to increase the activity of the Nox complex (Potocký *et al*., 2012). Therefore, ROS production was analysed in deletion and overexpression strains. ROS was detected using nitroblue-tetrazolium (NBT), which precipitates as a blue formazan product when reduced by superoxide, and the fluorescent ROS-ID® superoxide probe.

Staining of WT colonies with NBT resulted in formation of a blue precipitate throughout the colony, but especially towards the growth front. This was comparable to that observed for *tepA* overexpression strains. The *tepA* deletion strains, however were generally stained more intensely, suggesting there is an increase of ROS production in this background (Figure 9A). Staining of WT hyphae with the fluorescent ROS-ID® superoxide probe revealed a localised production of superoxide in punctate structures in the hyphal tip and in elongated filaments in mature hyphae, that have previously been suggested to be mitochondria (Marschall and Tudzynski, 2014; Hassing *et al*., in preparation). Similar observations were made for hyphae of the *tepA* deletion and overexpression strains treated with this probe (Figure 9B).

These results suggest that deletion or overexpression of *tepA* does not result in measurable differences in superoxide production.

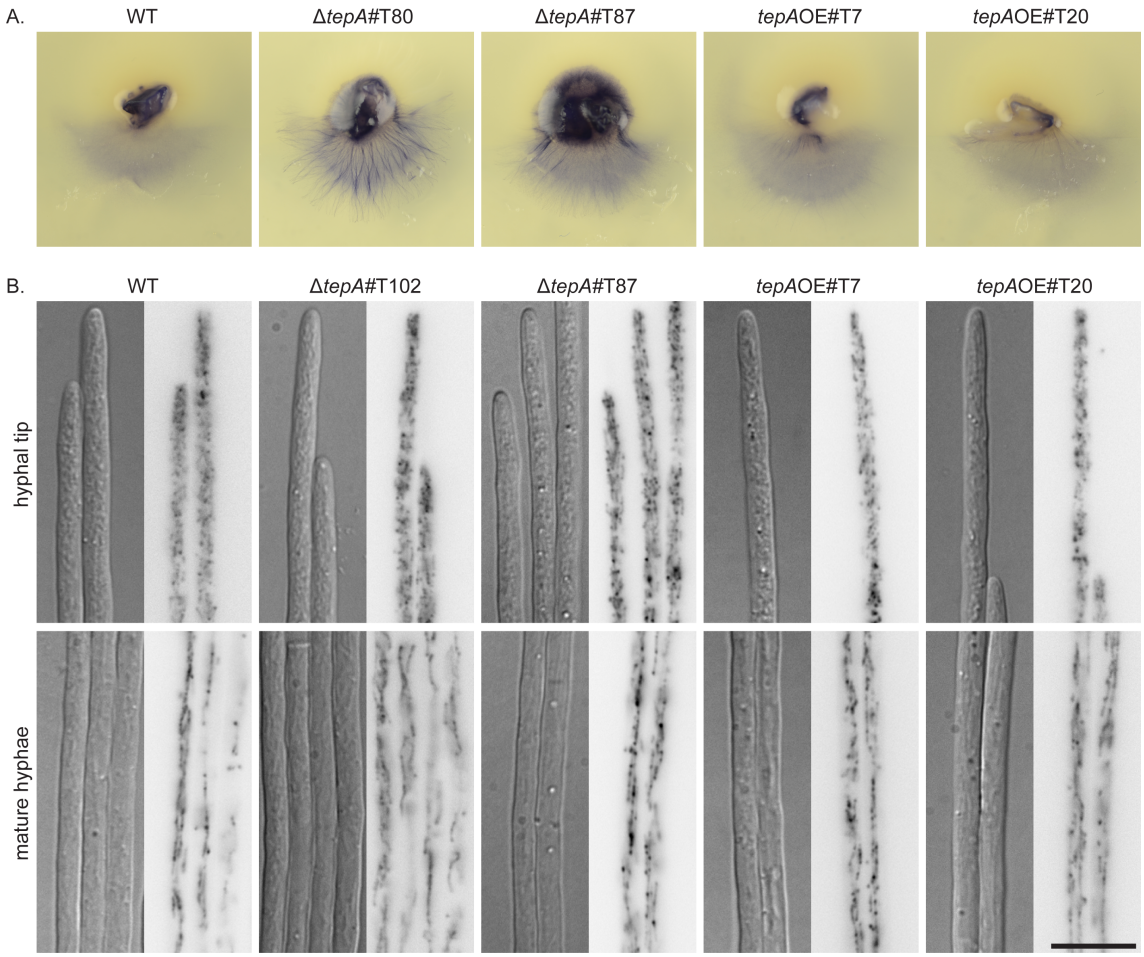

Figure 9: Detection of superoxide in *Epichloë festucae* wild-type and *tepA* mutant strains.

(A) Seven-day old colonies of wild-type (WT), *tepA* deletion strains #T80 and #T87 and *tepA* overexpression strains #T7 and #T20 were stained with nitroblue tetrazolium (NBT) and representative images of that analysis are shown. Strains were grown on 2.4% PD agar as described above. The experiment was performed twice. (B and C) Fluorescence microscopy of hyphal tips (B) and young hyphal bundles (C) stained with ROS-ID® superoxide probe. WT, *tepA* deletion strains #T87 and #T102 and *tepA* overexpression strains #T7 and #T20 were grown for approx. five days on 2.4% PD agar before staining. Bar = 10 µm.

Discussion

Phosphoinositides are minor components of cellular plasma membranes. Yet, they have been implicated in many major cellular processes that include, for example, cytoskeleton rearrangement, the regulation of ion channels, the establishment of cell polarity and the regulation of cellular proliferation and cancer (De Craene *et al*., 2017). A multitude of kinases and phosphatases regulate the local production of phosphoinositides, and their disruption often results in cellular defects. One of these enzymes is the mammalian phosphatidylinositol 3,4,5-trisphosphate 3-phosphatase PTEN, a major tumour suppressor protein (Milella *et al*., 2015, Balla, 2013). This study analysed the role of the PTEN homolog from *E. festucae* (TepA) in both hyphal growth and the mutualistic interaction with perennial ryegrass. These results showed that a functional TepA is required for the mutualistic symbiotic interaction, but not for hyphal growth in axenic culture. In addition, the influence of the mutation of TepA and possible resulting changes in lipid concentration on the activity of the Nox complex was analysed as this complex is partially regulated by lipid signalling and has important roles in mammals, plants and fungi (Babior *et al*., 1999; Kanai *et al*., 2001; Karthanassis *et al*., 2002; Ago *et al*., 2003; Marino *et al*., 2012; Tudzynski *et al*., 2012; Scott, 2015). While the deletion or overexpression of *tepA* did not result in detectable changes in the membrane lipid composition and the localisation of the Nox complex components was not altered, a small increase in ROS production was detected by NBT staining in *tepA* deletion strains.

The structural analysis of *E. festucae* TepA revealed similarities as well as significant differences to human PTEN. All structural motifs important for the binding of PtdIns[3,4,5]P_3 in the active site cavity were present in TepA. However, several residues of the N-terminal PtdIns[4,5]P_2-binding motif, the C2 anionic lipid-binding domain, and the PZD motif were absent. Several studies suggest that the PtdIns[4,5]P_2-binding domain, the catalytic site, as well as the CRB3 loop and the cα2 helix loop within the C2 domain, are required for lipid binding of PTEN, and together form a membrane-binding interface (Lee *et al*., 1999; Walker *et al*., 2004; Vazquez *et al*., 2006; Nguyen *et al*., 2014). The localisation to the membrane, and thereby the activity of PTEN, is regulated by different kinases through phosphorylation of the C-terminal tail, which results in formation of a closed conformation of the protein, where the C-terminal tail associates with the membrane-binding interface and inhibits membrane binding (Vazquez *et al*., 2000; Odriozola *et al*., 2007; Nguyen *et al*., 2014; Chen *et al*., 2018). Dephosphorylation of PTEN by the intrinsic protein phosphatase activity of PTEN leads to a conversion from a closed to an open structure and

recruitment of the protein to the membrane (Vazquez *et al*., 2000; Naderali *et al*., 2018). In addition, PTEN is regulated by a multitude of other secondary modifications such as oxidation, acetylation and SUMOylation (Naderali *et al*., 2018). The apparent differences in the protein structure of human PTEN and *E. festucae* TepA suggests that there are differences in the ability of the *E. festucae* protein to bind, and to be recruited, to membranes.

Interestingly, TepA was found to localise to the cytosol as well as to septa of hyphae grown in axenic culture. These results were similar to the observed localisation of the PTEN homolog in *S. pombe*, which was found to localise to septa and cytoplasmic puncta (Mitra *et al*., 2004). This might suggest the presence of unidentified lipid-binding domains in the fungal PTEN homologs. In contrast to the C-terminal fusion protein, the N-terminal fusion protein of TepA in *E. festucae* showed reduced septa binding, suggesting that fusion of the fluorophore to this end of the protein results in steric inhibition of the binding domain. Although there are few studies on the localisation of PTEN homologs in fungi, the localisation of this protein in mammalian cells has been extensively studied. In the original studies, PTEN was found to localise to the cytosol but more recent studies have shown that it also localises to membranes, nuclei, mitochondria and the ER. Also, PTEN is able to exit the cell and be taken up by recipient cells, resulting in the deactivation of the P3K/AKT pathway (Putz *et al*., 2012; Hopkins *et al*., 2013; Naderali *et al*., 2018). Localisation in the nucleus was found to be mediated by an internal functional nuclear localisation signal, which is required for tumour suppression in a phosphatase-independent manner (Bononi and Pinton *et al*., 2015; Naderali *et al*., 2018). Mitochondrial PTEN was found to contribute to apoptosis by sustaining ROS production, and PTEN in the ER was reported to regulate Ca^{2+} release (Zhu *et al*., 2008; Bononi *et al*., 2013; Naderali *et al*., 2018). In *E. festucae,* none of these additional localisations were observed for TepA, potentially because the high-level expression of this protein masked a more intricate localisation pattern. However, the *S. pombe* PTEN homolog has also been found to localise to septa, which might indicate different localisation patterns and different roles for this protein in fungi.

Both the deletion and the overexpression strains were found to be indistinguishable from the WT in their hyphal growth rate and colony morphology. Similar observations have been made for deletion strains of the PTEN homolog from *F. graminearum* and *U. maydis* (Zhang *et al*.,2010; Vijayakrishnapillai *et al*., 2018). The *S. pombe tep1* deletion mutant was also indistinguishable from the WT when examined by light microscopy. However, TEM analysis revealed an abnormal vacuolar morphology, highlighting the subtlety of some of these culture phenotypes (Mitra *et al*., 2004). Because *E. festucae* strain FI1 sporulates rather poorly in culture, it is quite

difficult to test for changes in this developmental phenotype unless there is a major effect, which was not the case for the Δ*tepA* mutant. It is also difficult to assess any defect in the sexual cycle as this developmental stage only occurs on the host when it undergoes reproductive development (Scott and Schardl, 1993; Chung and Schardl, 1997). Deletion strains of *Fgtep1*, *Umtp1* and *Sptep1*, however, have all been shown to have sporulation defects. *FgtepA* deletion resulted in a decreased germination rate of conidia in response to the phosphatidylinositol 3-kinase inhibitor wortmannin, and deletion of *Umtp1* resulted in decreased teliospore production (Zhang *et al*., 2010; Vijayakrishnapillai *et al*., 2018). In *S. cerevisiae*, deletion of *tep1* resulted in a defect of dityrosine deposition in the spore cell wall, which, however, did not influence viability or growth (Heymont *et al*., 2000). Furthermore, *ptn1* deletion strains in *S. pombe* were found to be more sensitive to osmotic stress, and *ptn1* deletion strains in *U. maydis* were more sensitive to cell wall stress induced by addition of Congo Red or CFW (Mitra *et al*., 2004; Vijayakrishnapillai *et al*., 2018). While these stress agents have not yet been tested, growth on H_2O agar, which also results in osmotic stress on fungal hyphae, did not influence growth of the *E. festucae tepA* deletion mutant.

Inoculation of the *E. festucae tepA* deletion mutants into *L. perenne* resulted in a slight stunting of the host plant 10 weeks post-inoculation, and microscopic analysis revealed an increase of hyphal biomass and formation of hyphal bundles *in planta*. Despite the lack of a significant number of infected plants to perform a statistical analysis, the observation that the same plant phenotype was observed for two independent transformants provides strong evidence that deletion of *tepA* impacts on development of a mutualistic symbiotic interaction. Plants infected with the overexpression strains had no obvious whole-plant or cellular phenotype. These results suggest that TepA is required for establishment and maintenance of a mutualistic symbiotic interaction between *E. festucae* and *L. perenne*, potentially due to its function in the regulation of the PtdIns[3,4,5]P_3 concentration in the cell. To date, many *E. festucae* single gene deletion mutants have been identified that cause dramatic stunting of the plant, e.g. deletion of components of the Nox complex (*noxA*, *noxB*, *noxR*, *psl1*), components of the high-osmolarity glycerol (HOG) and cell wall integrity (CWI) MAP kinase signalling pathways (*sakA*, *mpkA*, *mpkB*), and the STRIPAK signalling complex (*mob3*) (Tanaka *et al*., 2006; Tanaka *et al*., 2008; Eaton *et al*., 2008; Becker *et al*., 2015; Green *et al*., 2016; Green *et al*., 2019 (in press)). The severe phenotype observed for these mutants is perhaps not surprising given the central role these pathways play in signal sensing and transduction in *E. festucae*. Although the host interaction phenotype for the *tepA* mutant is much less severe, this result does highlight the importance of lipid signalling for the symbiotic interaction. Single deletion

of many of the components of the Nox complex results in a dramatic host interaction phenotype, highlighting the importance of ROS signalling for regulation of growth *in planta*. However, other mutants such as Δ*bemA,* which is a component of the Nox complex, and is known to interact with NoxR and Cdc24, also results in WT-like growth in culture and mild stunting *in planta* (Takemoto *et al*., 2011). Similar to the *tepA* deletion strains, growth of the *bemA* deletion strain *in planta* is characterized by an increase in hyphal biomass; however, *bemA* mutant hyphae were often swollen, which was not observed for the *tepA* deletion mutants. Interestingly, the *bemA* deletion mutant was shown to be sensitive towards SDS, indicating a defect in cell wall integrity, a phenotype similar to that described for the deletion of the *U. maydis ptn1* homolog (Takemoto *et al*., 2011; Vijayakrishnapillai *et al*., 2018). In *N. crassa*, deletion of *bemA* results in the production of inviable ascospores, and deletion of *ptn1* in *U. maydis* results in a reduction in teliospore formation (Cano-Dominguez *et al*., 2008; Vijayakrishnapillai *et al*., 2018). However, analysis of the *S. cerevisiae* Bem1 PX domain revealed a preferential binding to PtdIns[4]P, and genetic analysis of BemA in *N. crassa* showed that the PX domain is not required for membrane binding (Argo *et al*., 2003; Schürg *et al*., 2013). Nonetheless, it is important to keep in mind that the binding specificity of BemA in filamentous fungi has not been analysed to date and might be different to what has been described in yeast, given fungal BemA also interacts with proteins that do not have homologs in yeast, for example RacA (Kayano *et al*., 2018).

The corresponding TepA homologs in *F. graminearum* and *U. maydis* have been shown to be required for WT-like virulence on wheat and maize, respectively. The *F. graminearum tep1* deletion strain produces significantly shorter brown lesions on infected wheat coleoptiles, and the *U. maydis ptn1* deletion strains resulted in fewer and smaller tumours and increased survival rate of the host (Zhang *et al*., 2010; Vijayakrishnapillai *et al*., 2018). Therefore, PTEN is an important protein for fungi that have either mutualistic or pathogenic interactions with their hosts.

To analyse whether the deletion of *tepA* or its overexpression could affect the localisation and concentration of lipids in the fungal hyphae, PA, PtdIns[4,5]P_2 and PtdIns[3,4,5]P_3 lipid biosensors were introduced into these different genetic backgrounds (Candy, 2019). The PA biosensor was found to localise to the PM and septa of hyphae of all ages in both mutant and wild-type strains, similar to observation in mammals, yeast and plants (Nakashini *et al*., 2004; Potocký *et al*., 2014; Kassas *et al*., 2017). While it was anticipated that deletion of *tepA* would increase the pool of PtdIns[4,5]P_2, and therefore impact on the activity of enzymes such as phospholipase

D, which require this lipid for activation, this was not reflected by the localisation of the PA biosensor (Sciorra *et al*., 1999; Sciorra *et al*., 2002).

The localisation of the PtdIns[4,5]P_2 biosensors was comparable to the PA biosensor in that it localised to the PM and septa. However, the signal was increased in the subapical region, as has been described previously by Candy (2019). In contrast to the previous study, a lack of signal at the apex of the hyphae was not observed here, potentially due to the use of different magnifications during microscopy. The PM localisation of PtdIns[4,5]P_2 has previously been described in mammalian cells, yeast and plants. Indeed, PtdIns[4,5]P_2 was found to be the major phosphoinositide at the PM, where it serves as a precursor for other signalling molecules, as well as serves a role in cell polarity, endo- and exocytosis, actin cytoskeleton rearrangement and activation of transporters (di Paolo and de Camilli, 2006; Balla, 2013; De Creane *et al*., 2017). An asymmetric distribution of PtdIns[4,5]P_2 at sites of polar growth has been observed in multiple organisms and is required for the yeast to hyphal transition of *C. albicans* (Vernay *et al*., 2012). Interestingly, the subapical concentration of the biosensor coincided with the so-called endocytic collar, a region with increased endocytic activity (Taheri-Talesh *et al*., 2008; Echauri-Espinosa *et al*., 2012). Observations for the localisation of the PtdIns[4,5]P_2 biosensor in the *tepA* deletion and overexpression strain were comparable to the WT strains, indicating that the contribution of TepA to the PtdIns[4,5]P_2 pool is negligible (Gericke *et al*., 2013).

The biosensor that detects PtdIns[3,4,5]P_3 was found to localise to the cytosol in WT as well as the *tepA* overexpression strains. This result suggests that PtdIns[3,4,5]P_3 is either absent or present in very low amounts in the cell. This is not surprising, as PtdIns[3,4,5]P_3 in mammalian cells are present in very low concentrations, although still sufficient to support their key role in cell proliferation. In *S. pombe*, measurable levels of PtdIns[3,4,5]P_3 are only detected upon deletion of *tep1* (Mitra *et al*., 2004; Balla, 2013; De Creane *et al*., 2017). Besides a role in the PI3K/Akt pathway, PtdIns[3,4,5]P_3 together with PtdIns[4,5]P_2, are involved in establishing cell polarity in mammalian cells and the slime mould *Dictyostelium* (Servant *et al*., 2000; Iijima and Devreotes, 2002; Iijima *et al*., 2004; Balla, 2013). Interestingly, the localisation of PtdIns[3,4,5]P_3 at the leading edge of the *Dictyostelium* cell and localisation of the PTEN homolog at the opposite edge is required for chemotaxis. Deletion of either the phosphoinositide 3-kinases or PTEN reduces the efficiency of chemotaxis and their activity at opposite ends of the cell is required to maintain the PtdIns[3,4,5]P_3 gradient necessary for chemotaxis (Iijima and Devreotes, 2002; Iijima *et al*., 2004). While chemotaxis of mammalian cells also requires a PtdIns[3,4,5]P_3 gradient, it is largely regulated in a PTEN-independent way (Balla, 2013). These

observations raise interesting biological questions about the function of PtdIns[3,4,5]P_3 in fungal polarized growth and a potential role of *tepA* in preventing the diffusion of PtdIns[3,4,5]P_3 to maintain polarization. However, no deletion strains with a sufficiently strong fluorescent signal were obtained in this study. In addition to the analysis of the membrane composition using biosensors, a biochemical analysis should be performed in the future.

To investigate whether TepA and the levels of PtdIns[4,5]P_2 have a role in localisation of the Nox complex, individual components of the Nox complex were localised in the *tepA* deletion and overexpression strains. However, no mislocalisation could be observed, a result that correlates with the lack of a quantifiable effect on superoxide production. While some studies suggest a role of PtdIns[4,5]P_2 in the activation of the Nox complex, e.g. increased oxidase activity due to exogenous addition of PtdIns[4,5]P_2 or the weak binding of PtdIns[4,5]P_2 by p47phox, many suggest otherwise (Kanai *et al*., 2001; Potocký *et al*., 2012). p47phox has been reported to contain two lipid binding sites, of which binds to PtdIns[3,4]P_2 or PtdIns[4]P and the other to acidic phospholipids like PA (Argo *et al*., 2003; Stahelin *et al*., 2003; Karathanassis *et al*., 2002). p40phox on the other hand has been found to bind to PtdIns[3]P, and fungal BemA, potentially the functional equivalent of these proteins, has been reported to bind PtdIns[4]P (Kanai *et al*., 2001; Stahelin *et al*., 2003). However, to date the lipid binding of the subunits of the Nox complex have only been analysed in mammalian cells and therefore might be different in filamentous fungi. Indeed, the slight increase in NBT staining intensity observed in the *tepA* deletion mutants might indicate a previously unexplored role of PtdIns[3,4,5]P_3 in Nox complex activity. Furthermore, TepA might be indirectly involved in Nox complex activation through a role in regulating cell polarity and motility, a role which has long been established in mammalian cells and *Dictyostelium* (Liliental *et al*., 2000; Heit *et al*., 2008). In these organisms, PtdIns[3,4,5]P_3 has been shown to recruit and activate Rho-GEFs, which in turn activate Rac GTPases, like Rac and Cdc42, as well as lipid kinases (Raftopoulo and Hall, 2004; Kost, 2008). This polarized location of PtdIns[3,4,5]P_3 is as least partially dependent on PTEN activity (Iijima and Devreotes, 2002; Funamoto *et al*., 2002). To further analyse the role of lipid signalling in the activation and localisation of the Nox complex, the elucidation of the binding affinities of the lipid domains in the Nox complex components will be important to know.

In this study, the role of the homolog of the mammalian tumour suppressor protein PTEN was analysed during axenic growth, as well as in the mutualistic interaction between *E. festucae* and *L. perenne*. Neither deletion nor overexpression of the protein resulted in a change in the levels of PtdIns[4,5]P_2 or PtdIns[3,4,5]P_3,

respectively, or altered growth of the fungus in axenic culture. However, inoculation of the deletion strains into *L. perenne* plants resulted in a mild stunting of the plant host. This phenotype was accompanied by an increase of hyphal biomass and the formation of hyphal bundles *in planta*, which might indicate a defect in polarized growth *in planta.* This result, together with previously published work, establishes that PTEN homologs are required for both mutualistic and pathogenic host interactions.

Acknowledgements

This research was supported by grants from the Tertiary Education Commission to the Bio-Protection Research Centre, the Royal Society of New Zealand Marsden Fund and by Massey University. The authors thank Niki Murray, Pani Vijayan and Matthew Savoian (Manawatu Microscopy and Imaging Centre) for support with microscopy and imaging, Arvina Ram for technical support, Aleysha Candy for providing strains and plasmids, and Chris Schardl for providing *Epichloë* spp. sequence data.

References

Ago, T., Kuribayashi, F., Hiroaki, H., Takeya, R., Ito, T., Kohda, D., and Sumimoto, H. (2003). Phosphorylation of p47phox directs phox homology domain from SH3 domain toward phosphoinositides, leading to phagocyte NADPH oxidase activation. Proc Natl Acad Sci U S A 100, 4474-4479.

Ago, T., Takeya, R., Hiroaki, H., Kuribayashi, F., Ito, T., Kohda, D., and Sumimoto, H. (2001). The PX domain as a novel phosphoinositide- binding module. Biochem Biophys Res Commun 287, 733-738.

Babior, B.M. (1999). NADPH Oxidase: An Update. Blood 93, 1464-1476.

Balla, T. (2013). Phosphoinositides: Tiny lipids with giant impact on cell regulation. Physiol Rev 93, 1019-1137.

Becker, M., Becker, Y., Green, K., and Scott, B. (2016). The endophytic symbiont *Epichloë festucae* establishes an epiphyllous net on the surface of *Lolium perenne* leaves by development of an expressorium, an appressorium-like leaf exit structure. New Phytol 211, 240-254.

Becker, Y., Eaton, C.J., Brasell, E., May, K.J., Becker, M., Hassing, B., Cartwright, G.M., Reinhold, L., and Scott, B. (2015). The fungal Cell-Wall Integrity MAPK cascade is crucial for hyphal network formation and maintenance of restrictive growth of *Epichloë festucae* in symbiosis with *Lolium perenne*. Mol Plant-Microbe Interact 28, 69-85.

Becker, Y., Green, K.A., Scott, B., and Becker, M. (2018). Artificial inoculation of *Epichloë festucae* into *Lolium perenne*, and visualisation of endophytic and epiphyllous fungal growth. Bio-protocol 8, e2990.

Belambri, S.A., Rolas, L., Raad, H., Hurtado-Nedelec, M., Dang, P.M., and El-Benna, J. (2018). NADPH oxidase activation in neutrophils: Role of the phosphorylation of its subunits. Eur J Clin Invest 48 Suppl 2, e12951.

Bononi, A., Bonora, M., Marchi, S., Missiroli, S., Poletti, F., Giorgi, C., Pandolfi, P.P., and Pinton, P. (2013). Identification of PTEN at the ER and MAMs and its regulation of Ca^{2+} signaling and apoptosis in a protein phosphatase-dependent manner. Cell Death Differ 20, 1631-1643.

Bononi, A., and Pinton, P. (2015). Study of PTEN subcellular localization. Methods 77-78, 92-103.

Brown, D.I., and Griendling, K.K. (2009). Nox proteins in signal transduction. Free Radic Biol Med 47, 1239-1253.

Byrd, A.D., Schardl, C.L., Songlin, P.J., Mogen, K.L., and Siegel, M.R. (1990). The beta-tubulin gene of *Epichloë typhina* from perennial ryegrass (*Lolium perenne*). Curr Genet 18, 347-354.

Campbell, R.B., Liu, F., and Ross, A.H. (2003). Allosteric activation of PTEN phosphatase by phosphatidylinositol 4,5-bisphosphate. J Biol Chem 278, 33617-33620.

Candy, A. (2019). Analysis of *Epichloë festucae* membrane lipid composition and its role in Nox complex assembly. A thesis presented in fulfilment of the requirement for the degree of Master of Science, School of Fundamental Science (Palmerston North: Massey University), pp. 196.

Cano-Dominguez, N., Alvarez-Delfin, K., Hansberg, W., and Aguirre, J. (2008). NADPH oxidases NOX-1 and NOX-2 require the regulatory subunit NOR-1 to control cell differentiation and growth in *Neurospora crassa*. Eukaryot Cell 7, 1352-1361.

Chen, C.Y., Chen, J., He, L., and Stiles, B.L. (2018). PTEN: tumor suppressor and metabolic regulator. Front Endocrinol 9, 338.

Christensen, M.J., Bennett, R.J., Ansari, H.A., Koga, H., Johnson, R.D., Bryan, G.T., Simpson, W.R., Koolaard, J.P., Nickless, E.M., and Voisey, C.R. (2008). *Epichloë* endophytes grow by intercalary hyphal extension in elongating grass leaves. Fungal Genet Biol 45, 84-93.

Chujo, T., Lukito, Y., Eaton, C.J., Dupont, P.Y., Johnson, L.J., Winter, D., Cox, M.P., and Scott, B. (2019). Complex epigenetic regulation of alkaloid biosynthesis and host interaction by heterochromatin protein I in a fungal endophyte-plant symbiosis. Fungal Genet Biol 125, 71-83.

Chung, K.R., and Schardl, C.L. (1997). Sexual cycle and horizontal transmission of the grass symbiont, Epichloë typina. Mycol Res 101.

Cid, V.J., Rodriguez-Escudero, I., Andres-Pons, A., Roma-Mateo, C., Gil, A., den Hertog, J., Molina, M., and Pulido, R. (2008). Assessment of PTEN tumor suppressor activity in nonmammalian models: the year of the yeast. Oncogene 27, 5431-5442.

De Craene, J.O., Bertazzi, D.L., Bar, S., and Friant, S. (2017). Phosphoinositides, major actors in membrane trafficking and lipid signaling pathways. Int J Mol Sci 18, article number 632.

Di Paolo, G., and De Camilli, P. (2006). Phosphoinositides in cell regulation and membrane dynamics. Nature 443, 651-657.

Dinno, A. (2017). Dunn's Test of Multiple Comparisons Using Rank Sums. https://cran.r-project.org/web/packages/dunn.test/dunn.test.pdf

Eaton, C.J., Cox, M.P., Ambrose, B., Becker, M., Hesse, U., Schardl, C.L., and Scott, B. (2010). Disruption of signaling in a fungal-grass symbiosis leads to pathogenesis. Plant Physiol 153, 1780-1794.

Eaton, C.J., Dupont, P.Y., Solomon, P., Clayton, W., Scott, B., and Cox, M.P. (2015). A core gene set describes the molecular basis of mutualism and antagonism in *Epichloë* spp. Mol Plant-Microbe Interact 28, 218-231.

Eaton, C.J., Jourdain, I., Foster, S.J., Hyams, J.S., and Scott, B. (2008). Functional analysis of a fungal endophyte stress-activated MAP kinase. Curr Genet 53, 163-174.

Echauri-Espinosa, R.O., Callejas-Negrete, O.A., Roberson, R.W., Bartnicki-Garcia, S., and Mourino-Perez, R.R. (2012). Coronin is a component of the endocytic collar of hyphae of *Neurospora crassa* and is necessary for normal growth and morphogenesis. PLoS One 7, e38237.

Egan, M.J., Wang, Z.Y., Jones, M.A., Smirnoff, N., and Talbot, N.J. (2007). Generation of reactive oxygen species by fungal NADPH oxidases is required for rice blast disease. Proc Natl Acad Sci U S A 104, 11772-11777.

Falkenburger, B.H., Jensen, J.B., Dickson, E.J., Suh, B.C., and Hille, B. (2010). Phosphoinositides: lipid regulators of membrane proteins. J Physiol 588, 3179-3185.

Funamoto, S., Meili, R., Lee, S., Parry, L., and Firtel, R.A. (2002). Spatial and temporal regulation of 3-phosphoinositides by PI 3-kinase and PTEN mediates chemotaxis. Cell 109, 611-623.

Gericke, A., Leslie, N.R., Lösche, M., and Ross, A.H. (2013). PtdIns(4,5)P2-mediated cell signaling: emerging principles and PTEN as a paradigm for regulatory mechanism. Adv Exp Med Biol 991, 85-104.

Gibson, D.G. (2009). Synthesis of DNA fragments in yeast by one-step assembly of overlapping oligonucleotides. Nucleic Acids Res 37, 6984-6990.

Giesbert, S., Schurg, T., Scheele, S., and Tudzynski, P. (2008). The NADPH oxidase Cpnox1 is required for full pathogenicity of the ergot fungus *Claviceps purpurea*. Mol Plant Pathol 9, 317-327.

Green, K.A., Becker, Y., Fitzsimons, H.L., and Scott, B. (2016). An *Epichloë festucae* homologue of MOB3, a component of the STRIPAK complex, is required for the establishment of a mutualistic symbiotic interaction with *Lolium perenne*. Mol Plant Pathol 17, 1480-1492.

Green, K.A., Becker, Y., Tanaka, A., Takemoto, D., Fitzsimons, H.L., Seiler, S., Lalucque, H., Silar, P., and Scott, B. (2017). SymB and SymC, two membrane associated proteins, are required for *Epichloë festucae* hyphal cell-cell fusion and maintenance of a mutualistic interaction with *Lolium perenne*. Mol Microbiol 103, 657-677.

Gupta, R., Ting, J.T., Sokolov, L.N., Johnson, S.A., and Luan, S. (2002). A tumor suppressor homolog, AtPTEN1, is essential for pollen development in *Arabidopsis*. Plant Cell 14, 2495-2507.

Hanahan, D. (1983). Studies on transformation of *Escherichia coli* with plasmids. J Mol Biol 166, 557-580.

Heit, B., Robbins, S.M., Downey, C.M., Guan, Z., Colarusso, P., Miller, B.J., Jirik, F.R., and Kubes, P. (2008). PTEN functions to 'prioritize' chemotactic cues and prevent 'distraction' in migrating neutrophils. Nat Immun 9, 743.

Heymont, J., Berenfeld, L., Collins, J., Kaganovich, A., Maynes, B., Moulin, A., Ratskovskaya, I., Poon, P.P., Johnston, G.C., Kamenetsky, M., *et al*. (2000). TEP1, the yeast homolog of the human tumor suppressor gene PTEN/MMAC1/TEP1, is linked to the phosphatidylinositol pathway and plays a role in the developmental process of sporulation. Proc Natl Acad Sci U S A 97, 12672-12677.

Hopkins, B.D., Fine, B., Steinbach, N., Dendy, M., Rapp, Z., Shaw, J., Pappas, K., Yu, J.S., Hodakoski, C., Mense, S., *et al*. (2013). A secreted PTEN phosphatase that enters cells to alter signaling and survival. Science 341, 399-402.

Horowitz, A., Murakami, M., Gao, Y., and Simons, M. (1999). Phosphatidylinositol-4,5-bisphosphate mediates the interaction of syndecan-4 with protein kinase C. Biochemistry 38, 15871-15877.

Iijima, M., and Devreotes, P. (2002). Tumor suppressor PTEN mediates sensing of chemoattractant gradients. Cell 109, 599-610.

Iijima, M., Huang, Y.E., Luo, H.R., Vazquez, F., and Devreotes, P.N. (2004). Novel mechanism of PTEN regulation by its phosphatidylinositol 4,5-bisphosphate binding motif is critical for chemotaxis. J Biol Chem 279, 16606-16613.

Itoh, Y., Johnson, R., and Scott, B. (1994). Integrative transformation of the mycotoxin-producing fungus, *Penicillium paxilli*. Curr Genet 25, 508-513.

Jones, P., Binns, D., Chang, H.Y., Fraser, M., Li, W., McAnulla, C., McWilliam, H., Maslen, J., Mitchell, A., Nuka, G., *et al.* (2014). InterProScan 5: genome-scale protein function classification. Bioinformatics 30, 1236-1240.

Karathanassis, D., Stahelin, R.V., Bravo, J., Perisic, O., Pacold, C.M., Cho, W., and Williams, R.L. (2002). Binding of the PX domain of p47(phox) to phosphatidylinositol 3,4-bisphosphate and phosphatidic acid is masked by an intramolecular interaction. EMBO J 21, 5057-5068.

Kassas, N., Tanguy, E., Thahouly, T., Fouillen, L., Heintz, D., Chasserot-Golaz, S., Bader, M.F., Grant, N.J., and Vitale, N. (2017). Comparative characterization of phosphatidic acid sensors and their localization during frustrated phagocytosis. J Biol Chem 292, 4266-4279.

Katoh, K., Rozewicki, J., and Yamada, K.D. (2017). MAFFT online service: multiple sequence alignment, interactive sequence choice and visualization. Brief Bioinform. bbx108.

Kayano, Y., Tanaka, A., Akano, F., Scott, B., and Takemoto, D. (2013). Differential roles of NADPH oxidases and associated regulators in polarized growth, conidiation and hyphal fusion in the symbiotic fungus *Epichloë festucae*. Fungal Genet Biol 56, 87-97.

Kayano, Y., Tanaka, A., and Takemoto, D. (2018). Two closely related Rho GTPases, Cdc42 and RacA, of the endophytic fungus *Epichloë festucae* have contrasting roles for ROS production and symbiotic infection synchronized with the host plant. PLoS Pathog 14, e1006840.

Khang C.H., Berruyer R., Giraldo M.C., Kankanala P., Park S.Y., Czymmek K., *et al.* (2010) Translocation of *Magnaporthe oryzae* effectors into rice cells and their subsequent cell-to-cell movement. Plant Cell. 22(4):1388-403.

Kost, B. (2008). Spatial control of Rho (Rac-Rop) signaling in tip-growing plant cells. Trends Cell Biol 18, 119-127.

Lacaze, I., Lalucque, H., Siegmund, U., Silar, P., and Brun, S. (2015). Identification of NoxD/Pro41 as the homologue of the p22phox NADPH oxidase subunit in fungi. Mol Microbiol 95, 1006-1024.

Lara-Ortiz, T., Riveros-Rosas, H., and Aguirre, J. (2003). Reactive oxygen species generated by microbial NADPH oxidase NoxA regulate sexual development in *Aspergillus nidulans*. Mol Microbiol 50, 1241-1255.

Lambeth, J.D., Cheng, G., Arnold, R.S., and Edens, W.A. (2000). Novel homologs of gp91phox. Trends Biochem Sci 25, 459-461.

Latch, G.C.M., and Cristensen, M.J. (1985). Artificial infection of grasses with endophytes. Ann Appl Biol 107, 17-24.

Lee, J.O., Yang, H., Georgescu, M.M., Di Cristofano, A., Maehama, T., Shi, Y., Dixon, J.E., Pandolfi, P., and Pavletich, N.P. (1999). Crystal structure of the PTEN tumor suppressor: implications for its phosphoinositide phosphatase activity and membrane association. Cell 99, 323-334.

Letunic, I., Doerks, T., and Bork, P. (2015). SMART: recent updates, new developments and status in 2015. Nucleic Acids Res 43, D257-260.

Li, J., Yen, C., Liaw, D., Podsypanina, K., Bose, S., Wang, S.I., Puc, J., Miliaresis, C., Rodgers, L., McCombie, R., *et al.* (1997). PTEN, a putative protein tyrosine phosphatase gene mutated in human brain, breast, and prostate cancer. Science 275, 1943-1947.

Liaw, D., Marsh, D.J., Li, J., Dahia, P.L., Wang, S.I., Zheng, Z., Bose, S., Call, K.M., Tsou, H.C., Peacocke, M., *et al*. (1997). Germline mutations of the PTEN gene in Cowden disease, an inherited breast and thyroid cancer syndrome. Nat Genet 16, 64-67.

Liliental, J., Moon, S.Y., Lesche, R., Mamillapalli, R., Li, D., Zheng, Y., Sun, H., and Wu, H. (2000). Genetic deletion of the Pten tumor suppressor gene promotes cell motility by activation of Rac1 and Cdc42 GTPases. Curr Biol 10, 401-404.

Lukito, Y., Chujo, T., and Scott, B. (2015). Molecular and cellular analysis of the pH response transcription factor PacC in the fungal symbiont *Epichloë festucae*. Fungal Genet Biol 85, 25-37.

Manning, B.D., and Cantley, L.C. (2007). AKT/PKB signaling: navigating downstream. Cell 129, 1261-1274.

Marino, D., Dunand, C., Puppo, A., and Pauly, N. (2012). A burst of plant NADPH oxidases. Trends Plant Sci 17, 9-15.

Marschall, R., Siegmund, U., Burbank, J., and Tudzynski, P. (2016). Update on Nox function, site of action and regulation in *Botrytis cinerea*. Fungal Biol Biotechnol 3, article number 8.

Marschall, R., and Tudzynski, P. (2014). A new and reliable method for live imaging and quantification of reactive oxygen species in *Botrytis cinerea*: technological advancement. Fungal Genet Biol 71, 68-75.

Milella, M., Falcone, I., Conciatori, F., Cesta Incani, U., Del Curatolo, A., Inzerilli, N., Nuzzo, C.M., Vaccaro, V., Vari, S., Cognetti, F., *et al*. (2015). PTEN: multiple functions in human malignant tumors. Front Oncol 5, article number 24.

Mitra, P., Zhang, Y., Rameh, L.E., Ivshina, M.P., McCollum, D., Nunnari, J.J., Hendricks, G.M., Kerr, M.L., Field, S.J., Cantley, L.C., *et al*. (2004). A novel phosphatidylinositol(3,4,5)P3 pathway in fission yeast. J Cell Biol 166, 205-211.

Naderali, E., Khaki, A.A., Rad, J.S., Ali-Hemmati, A., Rahmati, M., and Charoudeh, H.N. (2018). Regulation and modulation of PTEN activity. Mol Biol Rep 45, 2869-2881.

Nakanishi, H., de los Santos, P., and Neiman, A.M. (2004). Positive and negative regulation of a SNARE protein by control of intracellular localization. Mol Biol Cell 15, 1802-1815.

Nguyen, H.N., Afkari, Y., Senoo, H., Sesaki, H., Devreotes, P.N., and Iijima, M. (2014). Mechanism of human PTEN localization revealed by heterologous expression in *Dictyostelium*. Oncogene 33, 5688-5696.

Odriozola, L., Singh, G., Hoang, T., and Chan, A.M. (2007). Regulation of PTEN activity by its carboxyl-terminal autoinhibitory domain. J Biol Chem 282, 23306-23315.

Potocký, M., Pejchar, P., Gutkowska, M., Jimenez-Quesada, M.J., Potocka, A., Alche Jde, D., Kost, B., and Zarsky, V. (2012). NADPH oxidase activity in pollen tubes is affected by calcium ions, signaling phospholipids and Rac/Rop GTPases. J Plant Physiol 169, 1654-1663.

Potocký, M., Pleskot, R., Pejchar, P., Vitale, N., Kost, B., and Zarsky, V. (2014). Live-cell imaging of phosphatidic acid dynamics in pollen tubes visualized by Spo20p-derived biosensor. New Phytol 203, 483-494.

Putz, U., Howitt, J., Doan, A., Goh, C.P., Low, L.H., Silke, J., and Tan, S.S. (2012). The tumor suppressor PTEN is exported in exosomes and has phosphatase activity in recipient cells. Sci Signal 5, issue 243, article number 70.

Qualliotine-Mann, D., Agwu, D.E., Ellenburg, M.D., McCall, C.E., and McPhail, L.C. (1993). Phosphatidic acid and diacylglycerol synergize in a cell-free system for activation of NADPH oxidase from human neutrophils. J Biol Chem 268, 23843-23849.

Raftopoulou, M., and Hall, A. (2004). Cell migration: Rho GTPases lead the way. Dev Biol 265, 23-32.

Ryder, L.S., Dagdas, Y.F., Mentlak, T.A., Kershaw, M.J., Thornton, C.R., Schuster, M., Chen, J., Wang, Z., and Talbot, N.J. (2013). NADPH oxidases regulate septin-mediated cytoskeletal remodeling during plant infection by the rice blast fungus. Proc Natl Acad Sci U S A 110, 3179-3184.

Schardl, C.L. (2001). *Epichloë festucae* and related mutualistic symbionts of grasses. Fungal Genet Biol 33, 69-82.

Schardl, C.L., Young, C.A., Hesse, U., Amyotte, S.G., Andreeva, K., Calie, P.J., Fleetwood, D.J., Haws, D.C., Moore, N., Oeser, B., *et al*. (2013). Plant-symbiotic fungi as chemical engineers: multi-genome analysis of the Clavicipitaceae reveals dynamics of alkaloid loci. PLoS Genet 9, e1003323.

Schürg, T., Brandt, U., Adis, C., and Fleißner, A. (2012). The *Saccharomyces cerevisiae* BEM1 homologue in *Neurospora crassa* promotes co-ordinated cell behaviour resulting in cell fusion. Mol Microbiol 86, 349-366.

Sciorra, V.A., Rudge, S.A., Prestwich, G.D., Frohman, M.A., Engebrecht, J., and Morris, A.J. (1999). Identification of a phosphoinositide binding motif that mediates activation of mammalian and yeast phospholipase D isoenzymes. EMBO J 18, 5911-5921.

Sciorra, V.A., Rudge, S.A., Wang, J., McLaughlin, S., Engebrecht, J., and Morris, A.J. (2002). Dual role for phosphoinositides in regulation of yeast and mammalian phospholipase D enzymes. J Cell Biol 159, 1039-1049.

Scott, B., and Schardl, C.L. (1993). Fungal symbionts of grasses: evolutionary insights and agricultural potential. Trends Microbiol 1, 196-200.

Segmüller, N., Kokkelink, L., Giesbert, S., Odinius, D., van Kan, J., and Tudzynski, P. (2008). NADPH oxidases are involved in differentiation and pathogenicity in *Botrytis cinerea*. Mol Plant-Microbe Interact 21, 808-819.

Semighini, C.P., and Harris, S.D. (2008). Regulation of apical dominance in *Aspergillus nidulans* hyphae by reactive oxygen species. Genetics 179, 1919-1932.

Servant, G., Weiner, O.D., Herzmark, P., Balla, T., Sedat, J.W., and Bourne, H.R. (2000). Polarization of chemoattractant receptor signaling during neutrophil chemotaxis. Science 287, 1037-1040.

Siegmund, U., Heller, J., van Kan, J.A., and Tudzynski, P. (2013). The NADPH oxidase complexes in *Botrytis cinerea*: evidence for a close association with the ER and the tetraspanin Pls1. PLoS One 8, e55879.

Spiers, A.G., and Hopcroft, D.H. (1993). Black canker and leaf spot of Salix in New Zealand caused by *Glomerella miyabeana* (*Colletotrichum gloeosporioides*). Eur J Plant Pathol 23, 92-102.

Stahelin, R.V., Burian, A., Bruzik, K.S., Murray, D., and Cho, W. (2003). Membrane binding mechanisms of the PX domains of NADPH oxidase p40phox and p47phox. J Biol Chem 278, 14469-14479.

Taheri-Talesh, N., Horio, T., Araujo-Bazan, L., Dou, X., Espeso, E.A., Penalva, M.A., Osmani, S.A., and Oakley, B.R. (2008). The tip growth apparatus of *Aspergillus nidulans*. Mol Biol Cell 19, 1439-1449.

Takemoto, D., Kamakura, S., Saikia, S., Becker, Y., Wrenn, R., Tanaka, A., Sumimoto, H., and Scott, B. (2011). Polarity proteins Bem1 and Cdc24 are components of the filamentous fungal NADPH oxidase complex. Proc Natl Acad Sci U S A 108, 2861-2866.

Takemoto, D., Tanaka, A., and Scott, B. (2006). A p67Phox-like regulator is recruited to control hyphal branching in a fungal-grass mutualistic symbiosis. Plant Cell 18, 2807-2821.

Tanaka, A., Christensen, M.J., Takemoto, D., Park, P., and Scott, B. (2006). Reactive oxygen species play a role in regulating a fungus-perennial ryegrass mutualistic interaction. Plant Cell 18, 1052-1066.

Tanaka, A., Takemoto, D., Hyon, G.S., Park, P., and Scott, B. (2008). NoxA activation by the small GTPase RacA is required to maintain a mutualistic symbiotic association between *Epichloë festucae* and perennial ryegrass. Mol Microbiol 68, 1165-1178.

Taylor, R.M., Foubert, T.R., Burritt, J.B., Baniulis, D., McPhail, L.C., and Jesaitis, A.J. (2004). Anionic amphiphile and phospholipid-induced conformational changes in human neutrophil flavocytochrome b observed by fluorescence resonance energy transfer. Biochim Biophys Acta 1663, 201-213.

Tudzynski, P., Heller, J., and Siegmund, U. (2012). Reactive oxygen species generation in fungal development and pathogenesis. Curr Opin Microbiol 15, 653-659.

Vazquez, F., Matsuoka, S., Sellers, W.R., Yanagida, T., Ueda, M., and Devreotes, P.N. (2006). Tumor suppressor PTEN acts through dynamic interaction with the plasma membrane. Proc Natl Acad Sci U S A 103, 3633-3638.

Vazquez, F., Ramaswamy, S., Nakamura, N., and Sellers, W.R. (2000). Phosphorylation of the PTEN tail regulates protein stability and function. Mol Cell Biol 20, 5010-5018.

Vernay, A., Schaub, S., Guillas, I., Bassilana, M., and Arkowitz, R.A. (2012). A steep phosphoinositide bis-phosphate gradient forms during fungal filamentous growth. J Cell Biol 198, 711-730.

Vijayakrishnapillai, L.M.K., Desmarais, J.S., Groeschen, M.N., and Perlin, M.H. (2018). Deletion of ptn1, a PTEN/TEP1 orthologue, in *Ustilago maydis* reduces pathogenicity and teliospore development. J Fungi (Basel) vol. 5, issue 1, article number 1.

Walker, S.M., Leslie, N.R., Perera, N.M., Batty, I.H., and Downes, C.P. (2004). The tumour-suppressor function of PTEN requires an N-terminal lipid-binding motif. Biochem J 379, 301-307.

Wang, X. (2000). Multiple forms of phospholipase D in plants: the gene family, catalytic and regulatory properties, and cellular functions. Prog Lipid Res 39, 109-149.

Wozniak, D.J., Kajdacsy-Balla, A., Macias, V., Ball-Kell, S., Zenner, M.L., Bie, W., and Tyner, A.L. (2017). PTEN is a protein phosphatase that targets active PTK6 and inhibits PTK6 oncogenic signaling in prostate cancer. Nat Commun 8, 1508.

Young, C.A., Bryant, M.K., Christensen, M.J., Tapper, B.A., Bryan, G.T., and Scott, B. (2005). Molecular cloning and genetic analysis of a symbiosis-expressed gene cluster for lolitrem biosynthesis from a mutualistic endophyte of perennial ryegrass. Mol Genet Genomics 274, 13-29.

Zhang, D., Fan, F., Yang, J., Wang, X., Qiu, D., and Jiang, L. (2010). FgTep1p is linked to the phosphatidylinositol-3 kinase signalling pathway and plays a role in the virulence of *Fusarium graminearum* on wheat. Mol Plant Pathol 11, 495-502.

Zhu, Y., Wloch, A., Wu, Q., Peters, C., Pagenstecher, A., Bertalanffy, H., and Sure, U. (2009). Involvement of PTEN promoter methylation in cerebral cavernous malformations. Stroke 40, 820-826.

Supplemental Information

Supplemental Table S1: Biological material.

Organism/Strain	Characteristics	Reference
E. coli		
DH5α	F$^-$, φ80*lacZ*, ΔM15, Δ(*lacZYA-argF*), U169, *recA1*, *endA1*, *hsdR17* (r_k^-, m_k^-), *phoA*, *supE44*, λ$^-$, *thi-1*, *gyrA96*, *relA1*	Invitrogen
E. festucae		
PN2278 (Fl1)	Wild-type isolated from *Festuca longifolia*	Young *et al*., 2005
Δ*tepA* T80	WT/Δ*tepA*::P*trpC-hph;* Hyg^R	This study
PN3278 (Δ*tepA*T87)	WT/Δ*tepA*::P*trpC-hph;* Hyg^R	This study
PN3279 (Δ*tep*AT102)	WT/Δ*epA*::P*trpC-hph;* Hyg^R	This study
tepA overexpression T4	WT/pCE122/ES30, Gen^R	This study
tepA overexpression T7	WT/pCE122/ES30, Gen^R	This study
tepA overexpression T20	WT/pCE122/ES30, Gen^R	This study
WT GFP-NoxA#T1	WT/pGFP-NoxA/pBH12, Hyg^R	Hassing *et al*., (in preparation)
WT GFP-NoxA#T4	WT/pGFP-NoxA/pBH12, Hyg^R	Hassing *et al*., (in preparation)
WT GFP-NoxA#T5	WT/pGFP-NoxA/pBH12, Hyg^R	Hassing *et al*., (in preparation)
WT GFP-NoxA#T7	WT/pGFP-NoxA/pBH12, Hyg^R	Hassing *et al*., (in preparation)
WT NoxR-GFP#T1	WT/pNPP9, Hyg^R	Green pers. comm.
WT Cdc24-GFP#T9	WT/pNPP6, Hyg^R	Green pers. comm.
WT Cdc24-GFP#T33	WT/pNPP6, Hyg^R	Green pers. comm.
WT BemA-GFP#T20	WT/pCE139, pII99, Gen^R	Green pers. comm.
WT BemA-GFP#T23	WT/pCE139, pII99, Gen^R	Green pers. comm.
WT BemA-GFP#T24	WT/pCE139, pII99, Gen^R	Green pers. comm.
WT GFP-RacA#T1	WT/pPN154, Hyg^R	Hassing *et al*., (in preparation)
WT GFP-RacA#T6	WT/pPN154, Hyg^R	Hassing *et al*., (in preparation)
WT GFP-RacA#T7	WT/pPN154, Hyg^R	Hassing *et al*., (in preparation)
WT GFP-RacA#T8	WT/pPN154, Hyg^R	Hassing *et al*., (in preparation)
WT GFP-TepA#T4	WT/pBH41, Gen^R	This study
WT GFP-TepA#T5	WT/pBH41, Gen^R	This study
WT GFP-TepA#T9	WT/pBH41, Gen^R	This study
WT GFP-TepA#T15	WT/pBH41, Gen^R	This study
WT TepA-mCherry#T1	WT/pBH42, Hyg^R	This study

WT TepA-mCherry#T2	WT/pBH42, Hyg^R	This study
WT TepA-mCherry#T3	WT/pBH42, Hyg^R	This study
WT TepA-mCherry#T10	WT/pBH42, Hyg^R	This study
WT GFP#T6	WT/pBH28, Gen^R	Hassing *et al*., (in preparation)
WT mCherry#T1	WT/pCE126, pSF16.17, Gen^R	Hassing *et al*., (in preparation)
WT mCherry#T2	WT/pCE126, pSF16.17, Gen^R	Hassing *et al*., (in preparation)
WT PA-biosensor#T4	WT/pBH50, Hyg^R	Hassing *et al*., (in preparation)
WT PA-biosensor#T7	WT/pBH50, Hyg^R	Hassing *et al*., (in preparation)
WT PA-biosensor#T8	WT/pBH50, Hyg^R	Hassing *et al*., (in preparation)
WT PA-biosensor#T9	WT/pBH50, Hyg^R	Hassing *et al*., (in preparation)
WT PA-biosensor#T11	WT/pBH50, Hyg^R	Hassing *et al*., (in preparation)
WT PLC-GFP#T2	WT/pCE105/pBH12, Hyg^R	This study
WT PLC-GFP#T3	WT/pCE105/pBH12, Hyg^R	This study
WT PLC-GFP#T7	WT/pCE105/pBH12, Hyg^R	This study
WT BTK-GFP#T9	WT/pCE107/pII99, Gen^R	Candy, 2019
WT BTK-GFP#T20	WT/pCE107/pII99, Gen^R	Candy, 2019
Δ*tepA*#T87 NoxR-GFP#T1	Δ*tepA*#T87/pNPP9/pII99, Hyg^R, Gen^R	This study
Δ*tepA*#T87 NoxR-GFP#T2	Δ*tepA*#T87/pNPP9/pII99, Hyg^R, Gen^R	This study
Δ*tepA*#T87 Cdc24-GFP#T1	Δ*tepA*#T87/pNPP6/pII99, Hyg^R, Gen^R	This study
Δ*tepA*#T87 Cdc24-GFP#T3	Δ*tepA*#T87/pNPP6/pII99, Hyg^R, Gen^R	This study
Δ*tepA*#T87 Cdc24-GFP#T5	Δ*tepA*#T87/pNPP6/pII99, Hyg^R, Gen^R	This study
Δ*tepA*#T87 BemA-GFP#T1	Δ*tepA*#T87/pCE139/pII99, Hyg^R, Gen^R	This study
Δ*tepA*#T87 BemA-GFP#T3	Δ*tepA*#T87/pCE139/pII99, Hyg^R, Gen^R	This study
Δ*tepA*#T87 BemA-GFP#T5	Δ*tepA*#T87/pCE139/pII99, Hyg^R, Gen^R	This study
Δ*tepA*#T87 GFP-RacA#T2	Δ*tepA*#T87/pPN154/pII99, Hyg^R, Gen^R	This study
Δ*tepA*#T87 GFP-RacA#T3	Δ*tepA*#T87/pPN154/pII99, Hyg^R, Gen^R	This study
Δ*tepA*#T87 PA-biosensor#T3	Δ*tepA*#T87/pBH50/pII99, Hyg^R, Gen^R	This study
Δ*tepA*#T87 PA-biosensor#T4	Δ*tepA*#T87/pBH50/pII99, Hyg^R, Gen^R	This study
Δ*tepA*#T87 PLC-GFP#TN1	Δ*tepA*#T87/pCE105/pII99, Hyg^R, Gen^R	This study
Δ*tepA*#T87 PLC-GFP#TN2	Δ*tepA*#T87/pCE105/pII99, Hyg^R, Gen^R	This study
Δ*tepA*#T102 GFP-NoxA#T1	Δ*tepA*#T87/pGFP-NoxA /pII99, Hyg^R, Gen^R	This study

Δ*tepA*#T102 GFP-NoxA#T2	Δ*tepA*#T87/pGFP-NoxA/pII99, Hyg^R, Gen^R	This study
tepA overexpression#T7 GFP-NoxA#T1	Δ*tepA*#T87/pGFP-NoxA/pBH12, Hyg^R, Gen^R	This study
tepA overexpression#T7 GFP-NoxA#T2	Δ*tepA* T87/pGFP-NoxA /pBH12, Hyg^R, Gen^R	This study
tepA overexpression#T7 NoxR-GFP#T1	*tepA* overexpression#T7/pNPP9, Hyg^R, Gen^R	This study
tepA overexpression#T7 NoxR-GFP#T4	*tepA* overexpression#T7/pNPP9, Hyg^R, Gen^R	This study
tepA overexpression#T7 NoxR-GFP#T6	*tepA* overexpression#T7/pNPP9, Hyg^R, Gen^R	This study
tepA overexpression#T7 Cdc24-GFP#T1	*tepA* overexpression#T7/pNPP6, Hyg^R, Gen^R	This study
tepA overexpression#T7 Cdc24-GFP#T4	*tepA* overexpression#T7/pNPP6, Hyg^R, Gen^R	This study
tepA overexpression#T7 Cdc24-GFP#T12	*tepA* overexpression#T7/pNPP6, Hyg^R, Gen^R	This study
tepA overexpression#T7 BemA-GFP#T6	*tepA* overexpression#T7/pCE139/pBH12, Hyg^R, Gen^R	This study
tepA overexpression#T7 BemA-GFP#T9	*tepA* overexpression#T7/pCE139/pBH12, Hyg^R, Gen^R	This study
tepA overexpression#T7 BemA-GFP#T11	*tepA* overexpression#T7/pCE139/pBH12, Hyg^R, Gen^R	This study
tepA overexpression#T7 GFP-RacA#T1	*tepA* overexpression#T7/pPN154, Hyg^R, Gen^R	This study
tepA overexpression#T7 GFP-RacA#T3	*tepA* overexpression#T7/pPN154, Hyg^R, Gen^R	This study
tepA overexpression#T7 GFP-RacA#T4	*tepA* overexpression#T7/pPN154, Hyg^R, Gen^R	This study
tepA overexpression#T7 GFP-RacA#T5	*tepA* overexpression#T7/pPN154, Hyg^R, Gen^R	This study
tepA overexpression#T7 PA-biosensor#T1	*tepA* overexpression#T7/pBH50, Hyg^R, Gen^R	This study
tepA overexpression#T7 PA-biosensor#T2	*tepA* overexpression#T7/pBH50, Hyg^R, Gen^R	This study
tepA overexpression#T7 PLC-GFP#T6	*tepA* overexpression#T7/pCE105/pBH12, Hyg^R, Gen^R	This study
tepA overexpression#T7 PLC-GFP#T11	*tepA* overexpression#T7/pCE105/pBH12, Hyg^R, Gen^R	This study
tepA overexpression#T7 BTK-GFP#T1	*tepA* overexpression#T7/pCE107/pBH12, Hyg^R, Gen^R	This study
tepA overexpression#T7 BTK-GFP#T2	*tepA* overexpression#T7/pCE107/pBH12, Hyg^R, Gen^R	This study

L. perenne		
L. perenne cv. Samson	-	AgResearch
Plasmid	**Characteristics**	**Reference**
PN1862 (pSF15.15)	pSP72 containing 1.4-kb *Hind*III P*trpC-hph* from pCB1004 cloned into *Sma*I site. Amp^R; Hyg^R; *Nco*I-free P*trpC-hph*	S. Foster
PN4183 (pRS426)	*ori*(f1)-l*acZ*-T7 promoter-MCS (*Kpn*I-*Sac*I)-T3 promoter-*lacI*-*ori*(pMB1)-amp^R-*ori* (2 micron), *URA3;* Amp^R	Christianson *et al*. 1992
PN1687 (pII99)	P*trpC-nptII*-T*trpC*, Amp^R/Gen^R	Lara-Ortíz *et al*., 2003
PN4241 (pBV579)	pAN583 containing a 0.1 kb *Bsr*GI/*Bam*HI fragment containing NLS (three tandem repeats of the nuclear localisation signal from simian virus large T-antigen) from pEBFP2-Nuc	Khang *et al*., 2010
pPN82	pBlueScriptII® KS(+) containing 1.4-kb HindIII PtrpC-hph and Pgpd-EGFP-TtrpC; Amp^R /Hyg^R	Tanaka *et al*., 2006
pPN154	pPN94 containing 0.7-kb *Xba*I/*Xho*I *egfp* and 0.6-kb *Xho*I/*Not*I *racA* in *Xba*I/*Not*I site, Hyg^R	Takemoto *et al*., 2011
pNPP6	pPN94 containing 3.0-kb *Xba*I/*Cla*I *cdc*24 and 0.7-kb *Cla*I/*Not*I 3GA-*egfp* in *Xba*I/*Not*I site. Hyg^R	Takemoto *et al*., 2011
pNPP9	pPN94 containing 1.6-kb *Eco*RI/*Cla*I *noxR* and 0.7-kb *Cla*I/*Not*I 3GA-*egfp* in *Eco*RI/NotI site, Hyg^R	Takemoto *et al*., 2011
pCE126	pRS426 containing P*gpd*-mCherry-T*trpC* insert	Candy, 2019
pCE139	pRS425 containing *bemA-gfp*	Eaton, pers. comm.
pGFP-NoxA	pRS425 containing *noxA-gfp*	Eaton, pers. comm.
pCE122	pRS426 containing a P*gdp-tepA*-T*trpC* overexpression construct	This study
pCE105	pRS426 containing a P*gpdA*-$PH_{PLC\text{-}d1}$-5Gly-eGFP-T*trpC* insert	Candy, 2019
pCE107	pRS426 containing a P*gpdA*-PH_{BTK}-5Gly-eGFP-T*trpC* insert	Candy, 2019
pCE126	pRS426 containing a P*gpd*-mCherry-T*trpC* insert	Candy, 2019
pBH16	pBH12 containing mCherry-NLS amplified from pBV579	This study
pBH12	pPN94 containing 723 bp *B. cinerea tub* terminator insert amplified from pNR1 downstream of *hph*; Hyg^R	Hassing *et al*., 2019
pBH28	pBH12 containing *nptII* replacing *hph* and *gfp*; Gen^R	Hassing *et al*., 2019
pBH41	pBH28 containing P*gpd-gfp-tepA*-T*trpC*, Gen^R	This study
pBH42	pBH12 containing P*gpd-tepA-mCherry*-T*trpC*, Hyg^R	This study
pBH43	pRS426 containing the *tepA* deletion construct, Hyg^R	This study
pBH50	pBH12 containing the 0.87 kbp PA-localization construct (*gfp*, bp 151-273 of *S. cerevisiae SPO20*), Hyg^R	Hassing *et al*., (in preparation)

Supplemental Table S2: Primers used in this study.

Name	**Sequence (5'-3')**	**Purpose**
tep5	ACAGCTACCCCGCTTGAGCAGACATCACCATGGCCTCGTTGTTGCGGCAG	*tepA* for overexpression construct
tep6	AGATTCGTCAAGCTGTTTGATGATTTCAGTTATTTCTGGCCATTCCCAAC	*tepA* for overexpression construct
BH60	GTTGACGGCAATTTCGATG	verification of deletion
BH75	CAGTGAGCGAGGAAGCGGAAGGCTTGCTTAGCTTGATATCTG	pBH12 amplification
BH76	CTGAAATCATCAAACAGCTTG	pBH12 amplification
BH79	GGAGGTGGAGGTTCTGGTGGAGGTGGATCTATGGTGAGCAAGGGCGAGGA	*mCherry* with linker forward

BH114	GTGACACTATAGAACTCGACGAATTCCCTTGTATCTCTACA	Amplification of P*gdp+gfp* forward
BH191	CATAGATCCACCTCCACCAGAACCTCCACCTCCCTTGTACAGCTCGTCCATGC	Amplification of P*gdp+gfp* with linker reverse
BH193	GTCGAGTTCTATAGTGTCACC	Amplification of vector backbone
BH195	GGAGGTGGAGGTTCTGGTGGAGGTGGATCTATGGCCTCGTTGTTGCGGCAG	Forward amplification of *tepA* with linker
BH196	GGTGATGTCTGCTCAAGCGG	Amplification of vector backbone
BH197	CTTCCGCTTCCTCGCTCACTG	Amplification of vector backbone
BH199	CAAGCTGTTTGATGATTTCAGTTAAGATCTGTACAGCTCGTCCATGCCG	*mCherry* reverse overhang to pBH12
BH203	CCGCTTGAGCAGACATCACCATGGCCTCGTTGTTGCGGCAG	*tepA* forward, overhang to P*gpd*
BH204	CATAGATCCACCTCCACCAGAACCTCCACCTCCTTTCTGGCCATTCCCAACCAAG	*tepA* reverse, overhang to *mCherry*
BH208	GGGTTTTCCCAGTCACGACATCGATCTTCCGCGACGCAGAGTACAACT	*tepA* 3'flank for deletion
BH209	CCTTCAATATCAGTTCCAAGCTGTAGATTTTCTCATTGTTTC	*tepA* 3'flank for deletion
BH210	CGTCCGAGGGCAAAGGAATAGGCCTGCGTAGGAAAAGCGAGATTATG	*tepA* 5'flank for deletion
BH211	CAATTTCACACAGGAAACAGCATCGATGTCAACAAGTCAAGACACGCA	*tepA* 5'flank for deletion
BH212	TTACAGAGACCGAGGCGATC	verification of deletion
BH213	CGAGAGAAATCATTGCCCGG	verification of deletion
BH214	GAGAGAGAGAGAGAGAGAGAG	verification of deletion
BH215	CTTTGCTCTCCCCGTTGTC	verification of deletion
TtrpC-F	CTGAAATCATCAAACAGCTTGACG	backbone for overexpression construct
pRS426-TtrpC-R	GCGGATAACAATTTCACACAGGAAACAGCCCATCTTAGTAGGAATGATTTTCG	backbone for overexpression construct
pRS426-Pgdp-F	GTAACGCCAGGGTTTTCCCAGTCACGACGAATTCCCTTGTATCTCTACA	backbone for overexpression construct
pRS426-Pgdp-R	GGTGATGTCTGCTCAAGCGGGGTAG	backbone for overexpression construct
pRS426_F	GCTGTTTCCTGTGTGAAATTG	pRS426 backbone
pRS426_R	GGGTTTTCCCAGTCACGAC	pRS426 backbone
hph_F	AGCTTGGAACTGATATTGAAGG	*hph* for deletion constructs

hph_R	CGTCCGAGGGCAAAGGAATAG	*hph* for deletion constructs
Primers used for RT-qPCR.		
BH189	GAGGAGATTCTGGAACCGGC	*tepA* forward
BH190	CCTCGGCATCATCGTCATCA	*tepA* reverse

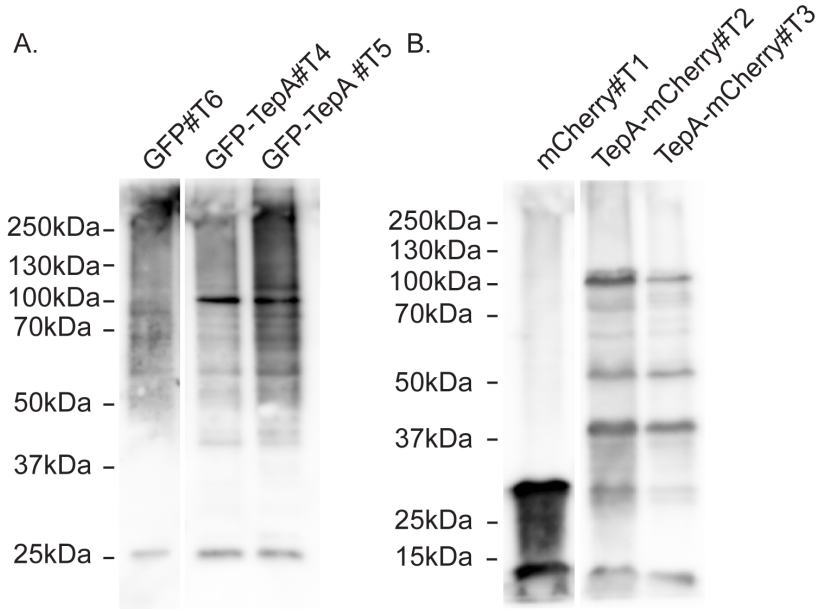

Supplemental Figure S1: Verification of the expression of GFP-TepA and TepA-mCherry fusion proteins in *Epichloë festucae* by western blot analysis.

Strains expressing the fusion proteins were incubated in liquid media for three days and total protein extracted. Approx. 15 µl of protein extract was loaded onto a 10% SDS acrylamide gel, separated and transferred onto PVDF membrane. Following transfer, membranes were probed with α-GFP or α-mCherry antibodies (Abcam), respectively. Following the incubation with a secondary α-rabbit antibody (Abcam) conjugated to horseradish peroxidase (HRP), western blots were developed using a chemiluminescence reaction. All controls and fusion-protein constructs were expressed in the WT background, and the detection of GFP (GFP#T6), GFP-fusion proteins (GFP-TepA#T4 and GFP-TepA#T5), mCherry (mCherry#T1) and mCherry-fusion proteins (TepA-mCherry#T2 and #T3) is shown. The GFP and mCherry expression controls are the same as previously described in Hassing *et al*. (in preparation) as they were run on the same gel. Expected protein sizes: GFP: 27 kDa; mCherry: 28.8 kDa; GFP-TepA: 86.18 kDa; TepA-mCherry: 87.98 kDa.

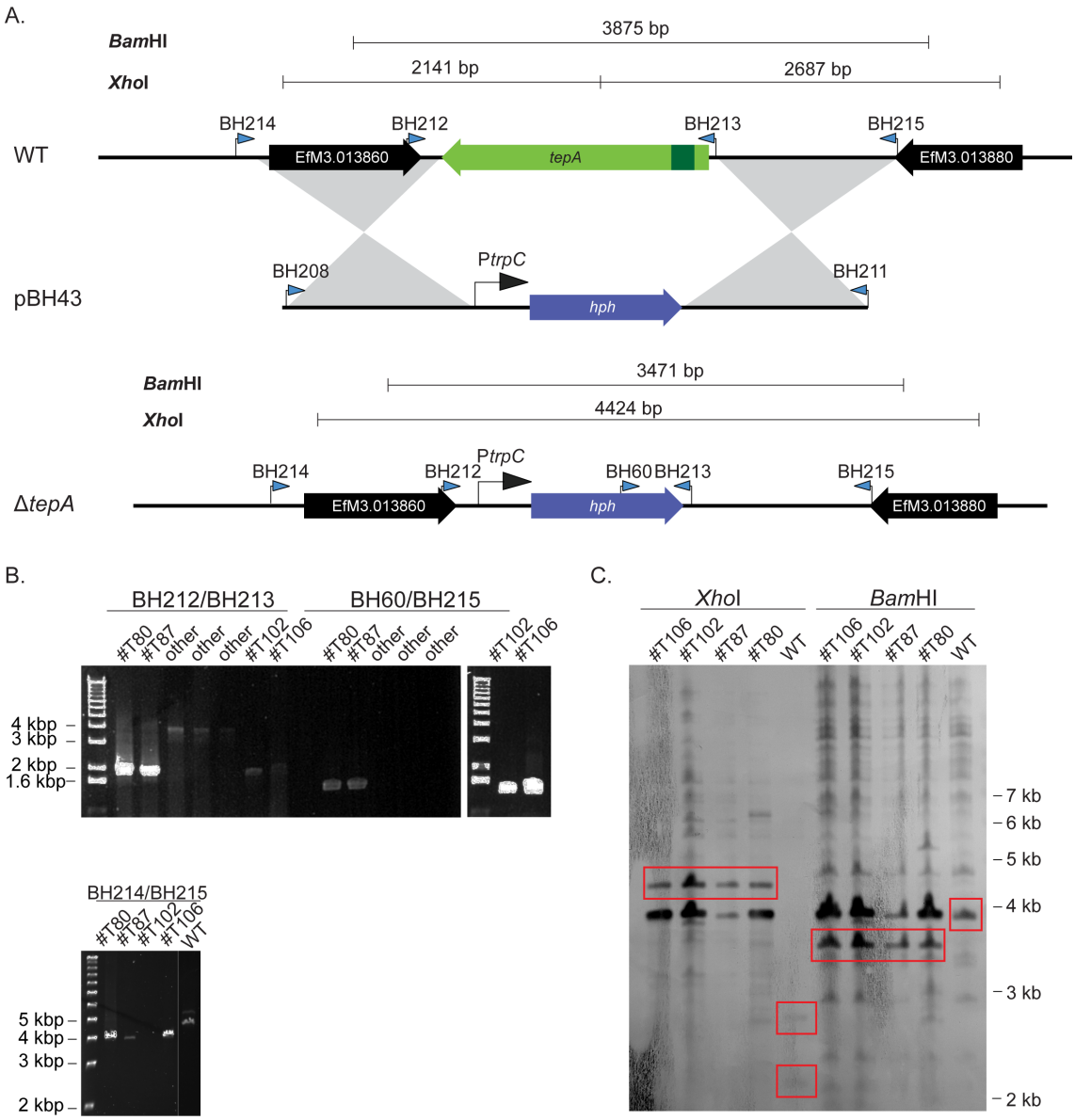

Supplemental Figure S2: Strategy for the deletion of *Epichloë festucae tepA* and Southern blot analysis.

(A) Physical map of the *tepA* wild-type (WT) genomic locus, linear insert of the *tepA* replacement construct, pBH43, and the mutant locus showing restriction enzyme sites for *Bam*HI and *Xho*I. Grey shading indicates regions of recombination. Numbers indicate the PCR primer pairs used for Gibson assembly (BH208/BH211) and deletion mutant screening (BH214/BH215/BH212/BH213/BH60). (B) PCR screening of deletion candidates with the PCR primer pair BH212/BH213, generated expected bands of 1,687 bp for the deletion mutants #T80, #T87, #T102 and #T106. Ectopic transformants had a non-specific band of approx. 3,500 bp. The primer pair BH60/BH215 generated a band of 1,455 bp for the deletion mutants #T80, #T87, #T102 and #T106, but as expected no band for the ectopic transformants. The primer pair BH214/BH215 generated expected bands of 4,040 bp for the deletion mutants

#T80, #T87 and #T106, and 4,444 bp for WT. (C) NBT/BCIP-stained Southern blot of digests (approx. 1 µg) from *E. festucae* WT, Δ*tepA*#T80, Δ*tepA*#T87(PN3278), Δ*tepA*#T102 (PN3279) and Δ*tepA*#T106 strains probed with digoxigenin (DIG)-11-dUTP-labeled linear PCR fragment of pBH43. Expected bands for *Bam*HI digest: 3,875 bp in WT, and 3,471 bp in the deletion mutants. Expected bands for *Xho*I digest: 2,141 bp and 2,687 bp in WT, and 4,424 bp in the deletion mutants. The presence of a smaller and a larger band in the *Xho*I and *Bam*HI digests respectively, indicates tandem integrations of the deletion cassette.

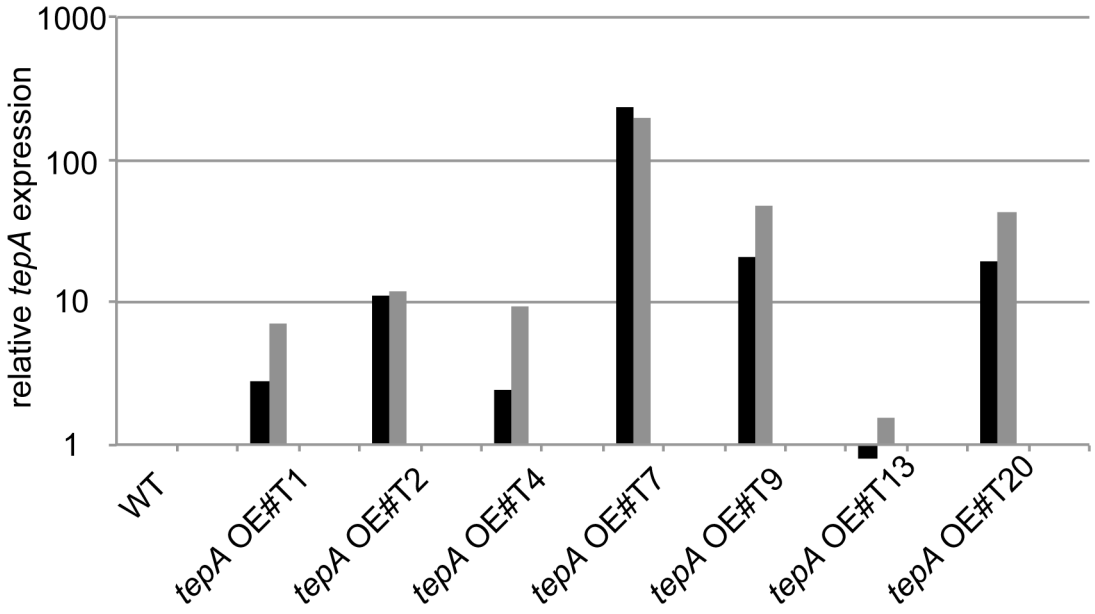

Supplemental Figure S3: Expression analysis of *Epichloë festucae tepA* overexpression strains by qRT-PCR.

Expression of *tepA* was determined relative to the wild-type (WT) expression using genes coding for elongation factor 2 (*EF-2*, black bar) and 40S ribosomal protein S22 (*S22*, grey bar) for normalization. For the amplification of *tepA* the primer pair BH189/199 was used. The relative expression was calculated as previously described (Lukito et. 2015). Strains #T4, #T7 and #T20 were chosen for further analysis.

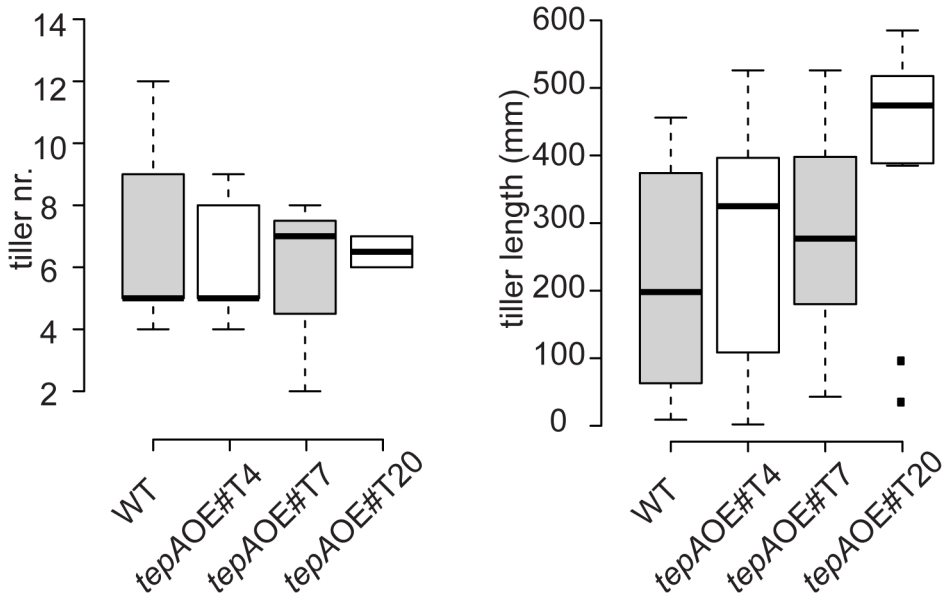

Supplemental Figure S4: Growth analysis of *Lolium perenne* plants infected with *Epichloë festucae* wild-type and *tepA* overexpression strains.

Number of plants infected with *tepA* overexpression strains #T4, #T7, #T20 (5/3/2). Box plots were generated using BoxPlotR (available on http://shiny.chemgrid.org/boxplotr/). One-way ANOVAs were used to test for differences in plant phenotypes between wild-type (WT) and mutant strains. In each case, the ANOVA was fitted with R and a Bonferroni correction was applied to all p-values to account for multiple testing. No analyses were performed with the *tepA* deletion mutant-infected plants due to the lack of a statistically significant number of infected plants. Only plants infected with the *tepA* overexpression strain #T20 have a significantly increased tiller length (P = 6.5E-4).

Chapter 5: Conclusions and Future Work

While the second and the third Results chapters both focused on the larger topic of lipid signalling and communication within the hyphal network, the first chapter of Results focused on the communication with the host *Lolium perenne* through small secreted proteins, which is a very distinct topic by itself. Therefore, the conclusion and future work chapter will be separated into two sections. The first will focus on the suite of putative effectors generated by *Epichloë festucae,* and the second on the role of lipid signalling via phosphatidic acid (PA) and phosphatidylinositol 4,5-phosphate (PtdIns[4,5]P_2) produced from phosphatidylinositol 3,4,5-trisphosphate (PtdIns[3,4,5]P_3) by phospholipase D (PLD) and the fungal phosphatase and tensin homolog (PTEN), respectively.

E. festucae small secreted proteins

Conclusions

This study is one of just a few focusing on the role of small secreted proteins (Ssps) in *E. festucae,* and the first to perform a genome-wide analysis of putative effectors in the first fully assembled genome of an *Epichloë* species. Several key findings emerged from this research, which will be highlighted in the following section.

1.) *E. festucae* genes coding for putative effectors are evenly distributed throughout the genome

I found 141 genes encoding Ssps in *E. festucae.* This is at the lower end of the range, as many other plant symbionts were found to encode several hundred (Lo Presti *et al*., 2015). *E. festucae* genes encoding for Ssps were not found in close association with AT-rich regions, putative 'birthplaces' of effector genes or telomeres, nor were they found to be clustered. This is unlike the organisation of similar genes described for many plant-pathogenic fungi. Therefore, there was no indication for an increased mutation rate or selection pressure on these genes based on the analysis of their location in the genome alone.

2.) *E. festucae* genes coding for putative effectors are associated with miniature inverted repeat transposable elements (MITEs) and are only mildly affected by heterochromatin silencing

Ssp-encoding genes were found to be more likely to contain a MITE in their promoter sequence. MITEs have previously been suggested to influence gene expression in *E. festucae* during growth *in planta* and indeed genes in the effector candidate category

were significantly more highly expressed *in planta* than genes in other categories (Fleetwood *et al*., 2011; Winter *et al*., 2018). However, whether they are involved in silencing during axenic growth or enhancing expression during growth *in planta* remains to be seen. Interestingly, proximity to AT-rich regions has been shown to influence gene expression in *E. festucae* as well; however, this does not seem to be the case for Ssp-encoding genes (Winter *et al*., 2018).

Deletion of the gene coding for the heterochromatin protein HepA only resulted in a small upregulation of putative effector gene expression in axenic culture, indicating that they are only slightly affected by heterochromatin silencing. This is consistent with the observed distance from AT-rich regions, which are in a highly heterochromatic state in culture and again highlights the possibility of MITEs as regulators of *ssp* gene expression (Chujo *et al*., 2014).

3.) GpiB, SspM, SspN and SspO are not required for growth in axenic culture or in the interaction with *L. perenne* under the conditions analysed

GpiB, SspM, SspN and SspO were chosen for functional analysis based on their high expression *in planta* and their expression profile in four different symbiotic mutants. They were found to be secreted; however, their deletion or overexpression did not result in changes in hyphal growth in culture, nor in the mutualistic interaction with *L. perenne.* This suggests that they are not required for the mutualistic interaction in ways that have been described for Ssps in other interactions. These Ssps might be functionally redundant with each other, or with other secreted *E. festucae* Ssps or have minor contributions that are not detectable by single gene deletion.

Interestingly, however, *sspO* deletion strains were unable to colonize *E. festucae* ovules and seeds, which indicates that SspO might be a protein necessary for the horizontal transfer of this endophyte into seeds by a yet unidentified mechanism.

Future work

While all aims of this study have been addressed, many observations raised new questions:

1.) Is the expression of Ssp-encoding genes regulated by MITEs?

While MITEs were observed in the promoter region of Ssp-encoding genes in *F. oxysporum,* in this organism, they were found to not influence gene expression (Schmidt *et al*., 2013). In *E. festucae*, however, MITEs have been found to be significantly more frequent both in genes coding for Ssps as well as in genes coding for other secreted proteins. Genes in both categories are significantly upregulated during

growth *in planta.* To address this question, constructs with and without the MITEs from the promoter region of the gene of interest could be fused to a reporter gene such as *egfp* and their expression examined during growth *in planta*. The design of constructs containing MITEs of different families would also allow the analysis of the effect of different MITE families on gene expression.

2.) Are small secreted proteins required for the interaction between *E. festucae* and *L. perenne*?

The bioinformatic analysis conducted in this study generated a suite of 141 putative effectors that are potentially involved in regulating the mutualistic interaction, including potential cell wall binding proteins and putative toxins. A future study could analyse different candidates using new methods of gene deletion, such as CRISPR-Cas9, which would enable multiple genes to be deleted at the same time, allowing a less time-consuming analysis of candidates. The complete assembly of further genomes of *Epichloë* species would allow a more global analysis of the repertoire of Ssps and might answer questions in regard to host specificity. The increasing number of characterised effectors produced by fungi with varying lifestyles will facilitate future studies on this field e.g. through the identification of homologs and conserved motifs. Indeed, since the completion of this study, the gene downstream of the gene coding for repeat-containing protein SspN has been found to encode a DUF3328 domain (Ye *et al*., 2019). Proteins containing this domain have been shown to be required for oxidative macrocyclization of the ribosomally synthesized and post-translationally modified peptides asperipin-2a and ustilotoxin B produced by *Aspergillus* species (Nagano *et al*., 2015; Je at al., 2019). Thus, SspN is likely to be processed into cyclic peptides.

3.) Is SspO required for the colonization of *L. perenne* ovules and seeds?

A preliminary analysis revealed that *sspO* deletion strains were unable to infect ovules or seeds of the host plant which opens up interesting new possibilities for the role of SspO in this interaction. First, however, this analysis should be repeated with a larger numbers of infected plants and analysed ovules and seeds. This observation highlights that many proteins might only be required for specific stages of the lifecycle of the interaction, as has been observed during the infection of many plant pathogenic fungi such as *Ustilago* species (Skibbe *et al*., 2010; Ökmen *et al*., 2018). As, however, we are often unable to observe all life stages in the laboratory, truly important regulators might not be identified. Given the potential role of SspO in seed infection, other stages

of the lifecycle of plants infected with *ssp* deletion mutants, such as the sexual cycle, should be examined as well.

The role of lipid signalling in the mutualistic interaction between *E. festucae* and *L. perenne*

Conclusions

To date, the role of lipid signalling in filamentous fungi has not been analysed in detail. Here three lipid species and the proteins involved in their production were analysed regarding their role in *E. festucae* axenic growth as well as in the interaction with *L. perenne*. In addition, their impact on superoxide production via the Nox complex was analysed. In these studies, a number of novel findings were obtained:

1.) Lipid signalling is required for growth of *E. festucae* in culture and *in planta*

Deletion of *pldB* and *tepA* disrupted the interaction between *E. festucae* and *L. perenne*, but only deletion of *pldB* influenced growth in culture. This indicates that, while lipid signalling generally is crucial for growth in *planta* not every lipid species and protein is equally important. This likely reflects the importance of the protein chosen for analysis. Disruption of *pldB* had a pronounced effect on the PA concentration, while deletion of *tepA* did not significantly decrease the concentration of PtdIns[4,5]P_2, as observed through the localisation of biosensors. Deletion of the gene encoding the phosphatidylinositol 4-phosphate 5-kinase Mss4, which is likely the main producer of PtdIns[4,5]P_2, however, is lethal in yeast (Strahl and Thorner, 2007). To date I was unable to identify whether the observed phenotype in *tepA* deletion strains was caused by defects due to accumulation of PtdIns[3,4,5]P_3, or due to the phosphatase activity of the protein. Both PA and PLD, as well as PTEN and its metabolites are involved with actin organization, endocytosis and exocytosis in mammals (Selvy *et al*., 2011; de Craene *et al*., 2017). Analysis of their role in these processes in fungi could aid in identification of the cause of the growth defect *in planta*.

2.) Lipid signalling though PldB and PA is required for hyphal fusion

This is the first study to demonstrate the importance of PA and PLD, in particular PldB, for hyphal fusion. This lack of hyphal fusion could be caused by: A) a general reduction of fusogenic PA in the membrane, influencing membrane structure, B) the loss of localized PA accumulation through PldB activity necessary for membrane fusion, C) the recruitment of other proteins to the fusion points through the localized activity of

PldB, D) the loss of PldB as a signalling protein. Interestingly, many strains defective in signalling pathways such as ROS or MAP kinase signalling have also been shown to be unable to undergo hyphal fusion, and additionally, are disrupted in the mutualistic interaction with the host. These observations indicate the presence of a larger network that regulates hyphal fusion and mutualism. PldB and PA could be key players in these pathways through the recruitment of downstream proteins, or could be required for the local production of a fusogenic lipid as the last step required in the fusion process. Multiple studies demonstrate that changes in the actin cytoskeleton and secretion are necessary during hyphal fusion and PLD and PA have both been shown to interact with many actin-interacting proteins as well as to be involved in exocytosis in mammals (Jang *et al*., 2012; Fischer and Glass, 2019).

3.) Lipid signalling might influence superoxide production via the Nox complex

Deletion of *pldB* resulted in a drop in the number of tips stained by NBT, which however might be attributed to a change in mitochondria organization, and deletion of *tepA* resulted in an increased staining by NBT. While these results to date are only suggestive of a role for lipid signalling in the regulation of the Nox complex in fungi, there is abundant evidence for such a role in mammals and plants. Whether PA might be able to directly activate Nox, as has been reported in plants, remains to be investigated (Taylor *et al*., 2015; Potocký *et al*., 2012). An interesting question is whether deletion of *tepA*, resulted in an increase in PtdIns[3,4,5]P_3, and in turn an increase in NBT staining intensity. In mammalian cells Rac was found to be stimulated via a PtdIns[3,4,5]P_3-responsive GEF, and in neutrophils, deletion of PTEN resulted in increased ROS production (Han *et al*., 1998; Luo and Hondal; 2015). These results indicate a role for PtdIns[3,4,5]P_3 in Nox complex activation.

Future work

While the analysis of the effect of the deletion of *E. festucae pld* isoforms and *tepA* delivered novel and interesting results, many questions remain to be answered and should be the focus of further studies:

1.) How are PA and PLD regulating hyphal fusion and morphology?

Many proteins have been shown to regulate hyphal fusion; however, lipid signalling has not been addressed until now (Fischer and Glass, 2019). PA produced by PLD activity might act by targeted protein recruitment, such as actin cytoskeleton regulating- or other signalling proteins (e.g. the Nox complex), or by influencing membrane curvature. This question could be addressed in many ways such as through the identification of

interaction partners by pull-down assays followed by mass spectrometry, analysis of actin distribution in *pldB* deletion mutants, or analysis of the oscillation of the components of the cell wall integrity (CWI) and MAK-2 MAP kinase signal response pathways prior to fusion in *N. crassa* (Fischer and Glass 2019). Answering these questions would significantly contribute to the understanding of the process of hyphal fusion.

Equally important would be to understand the reason for the hyphal morphology defects, and whether this is directly due to the reduction of PA or the loss of PLD, which itself is acting upstream of other proteins (Jang *et al*., 2012). This could be addressed by exogenous addition of PA to *pldB* deletion strains or complementation with a *pldB* construct in which active sites are mutated.

2.) Do filamentous fungi produce PtdIns[3,4,5]P_3 and is it involved in establishing polarity?

To date, only one study has demonstrated production of PtdIns[3,4,5]P_3 in a fungal species (Mitra *et al*. 2004). In order to further investigate the role of PTEN homologs in filamentous fungi, first the question of whether fungi are able to generate PtdIns[3,4,5]P_3 should be addressed. While biosensors are a useful tool in identifying the location of a particular lipid, an in depth analysis of the composition of fungal membranes should be conducted including the analysis of several mutants, including PTEN homolog deletion mutants. In addition, the lipid phosphatase activity of this protein should be confirmed in filamentous fungi. This would subsequently allow a more informed analysis of the role of the PTEN homologs during interaction with plants and whether observed defects can be attributed to a role of the PTEN homologs in establishing polarity and chemotaxis, as has been observed in the slime mould and mammalian cells (Ijima *et al*., 2004; Heit *et al*., 2008). An influence on chemotropic behaviour could easily be studied in *N. crassa* where spore germ tubes show specific chemotropic behaviour towards germ tubes emerging from spores with a genetically identical or different genotype (Wright *et al*., 2007; Heller *et al*., 2016).

3.) Is lipid signalling involved in the regulation of the Nox complex?

While some of the results provided here indicate a link between lipid signalling and the Nox complex, definitive evidence is still missing. The first step into analysing a role for specific lipid species should be the determination of the lipid-binding specificity of the subunits of the Nox complex specifically with proteins from filamentous fungi. Both BemA and Cdc24 have obvious lipid-binding domains, and both Rac1 and Cdc42 contain polybasic motifs involved in lipid binding. This could be studied though

liposome pull-down assays, where liposomes with different lipid composition could be generated and the ability of the proteins of interest to bind to them could be assessed or through the use of PIP strips (Huang *et al*., 2006; Sharma *et al*., 2008). These strips are designed for the identification of the lipid binding specificity of purified proteins and are available from commercial sources. Many studies in mammalian cells suggest a role of phosphoinositides phosphorylated in the third position to be involved with Nox complex activation; therefore, these lipid species might be good candidates for a future study (Kanai *et al*., 2001; Ago *et al*., 2001).

Bibliography

Ambrose, K.V., Koppenhöfer, A.M., and Belanger, F.C. (2014). Horizontal gene transfer of a bacterial insect toxin gene into the *Epichloë* fungal symbionts of grasses. Scientific Reports 4, article number 5562.

Arbiser, J.L., Petros, J., Klafter, R., Govindajaran, B., McLaughlin, E.R., Brown, L.F., Cohen, C., Moses, M., Kilroy, S., Arnold, R.S., *et al*. (2002). Reactive oxygen generated by Nox1 triggers the angiogenic switch. Proc Natl Acad Sci USA 99, 715-720.

Babior, B.M. (1999). NADPH Oxidase: An Update. Blood 93, 1464-1476.

Balla, T. (2013). Phosphoinositides: Tiny lipids with giant impact on cell regulation. Physiol Rev 93, 1019-1137.

Bastias, D.A., Martínez-Ghersa, M.A., Ballaré, C.L., and Gundel, P.E. (2017). *Epichloë* fungal endophytes and plant defenses: not just alkaloids. Trends Plant Sci 22, 939-948.

Becker, M., Becker, Y., Green, K., and Scott, B. (2016). The endophytic symbiont *Epichloë festucae* establishes an epiphyllous net on the surface of *Lolium perenne* leaves by development of an expressorium, an appressorium-like leaf exit structure. New Phytol 211, 240-254.

Becker, Y., Eaton, C. J., Brasell, E., May, K. J., Becker, M., Hassing, B., Cartwright, G. M., Reinhold, L., and Scott, B. (2015). The fungal Cell-Wall Integrity MAPK cascade is crucial for hyphal network formation and maintenance of restrictive growth of *Epichloë festucae* in symbiosis with *Lolium perenne*. Mol Plant-Microbe Interact 28, 69-85.

Becker, Y., Green, K.A., Scott, B., and Becker, M. (2018). Artificial inoculation of *Epichloë festucae* into *Lolium perenne*, and visualisation of endophytic and epiphyllous fungal growth. Bio-protocol 8, e2990.

Bedard, K., and Krause, K.H. (2007). The NOX family of ROS-generating NADPH oxidases: physiology and pathophysiology. Physiol Rev 87, 245-313.

Belambri, S.A., Rolas, L., Raad, H., Hurtado-Nedelec, M., Dang, P.M., and El-Benna, J. (2018). NADPH oxidase activation in neutrophils: Role of the phosphorylation of its subunits. Eur J Clin Investig 48 Suppl 2, e12951.

Bermúdez-Brito, M., Goulielmaki, E., and Papakonstanti, E.A. (2015). Focus on PTEN Regulation. Front Oncol 5, 166-166.

Bernoux, M., Ellis, J.G., and Dodds, P.N. (2011). New insights in plant immunity signaling activation. Curr Opin Plant Biol 14, 512-518.

Bhattacharjee, S. (2005). Reactive oxygen species and oxidative burst: Roles in stress, senescence and signal transduction in plants. Current Science 89, 1113-1121.

Bieberich, E. (2018). Sphingolipids and lipid rafts: Novel concepts and methods of analysis. Chem Phys Lipids 216, 114-131.

Boller, T., and Felix, G. (2009). A renaissance of elicitors: Perception of microbe-associated molecular patterns and danger signals by pattern-recognition receptors. Annu Rev Plant Biol 60, 379-406.

Boller, T., and He, S.Y. (2009). Innate immunity in plants: an arms race between pattern recognition receptors in plants and effectors in microbial pathogens. Science 324, 742-744.

Bolton, M.D., van Esse, H.P., Vossen, J.H., de Jonge, R., Stergiopoulos, I., Stulemeijer, I.J., van den Berg, G.C., Borras-Hidalgo, O., Dekker, H.L., de Koster, C.G., *et al*. (2008). The novel *Cladosporium fulvum* lysin motif effector Ecp6 is a virulence factor with orthologues in other fungal species. Mol Microbiol 69, 119-136.

Bonangelino, C.J., Nau, J.J., Duex, J.E., Brinkman, M., Wurmser, A.E., Gary, J.D., Emr, S.D., and Weisman, L.S. (2002). Osmotic stress-induced increase of phosphatidylinositol 3,5-bisphosphate requires Vac14p, an activator of the lipid kinase Fab1p. J Cell Biol156, 1015-1028.

Botelho, R.J., Teruel, M., Dierckman, R., Anderson, R., Wells, A., York, J.D., Meyer, T., and Grinstein, S. (2000). Localized biphasic changes in phosphatidylinositol-4,5-bisphosphate at sites of phagocytosis. J Cell Biol 151, 1353-1368.

Bouton, J.H., Gates, R.N., Belesky, D.P., and Owsley, M. (1993). Yield and persistence of tall fescue in the southeastern coastal plain after removal of its endophyte. Agron J 85, 52-55.

Breitenbach, M., Weber, M., Rinnerthaler, M., Karl, T., and Breitenbach-Koller, L. (2015). Oxidative stress in fungi: its function in signal transduction, interaction with plant hosts, and lignocellulose degradation. Biomolecules 5, 318-342.

Bultman, T.L., and Leuchtmann, A. (2008). Biology of the *Epichloë–Botanophila* interaction: an intriguing association between fungi and insects. Fungal Biol Rev 22, 131-138.

Cano-Dominguez, N., Alvarez-Delfin, K., Hansberg, W., and Aguirre, J. (2008). NADPH oxidases NOX-1 and NOX-2 require the regulatory subunit NOR-1 to control cell differentiation and growth in *Neurospora crassa*. Eukaryot Cell 7, 1352-1361.

Carman, G.M., and Henry, S.A. (2007). Phosphatidic acid plays a central role in the transcriptional regulation of glycerophospholipid synthesis in *Saccharomyces cerevisiae*. J Biol Chem 282, 37293-37297.

Cesari, S., Bernoux, M., Moncuquet, P., Kroj, T., and Dodds, P.N. (2014). A novel conserved mechanism for plant NLR protein pairs: the "integrated decoy" hypothesis. Front Plant Sci 5, 606-606.

Chauhan, A., Chauhan, V.P., and Brockerhoff, H. (1991). Activation of protein kinase C by phosphatidylinositol 4,5-bisphosphate: possible involvement in Na+/H+ antiport down-regulation and cell proliferation. Biochem Biophys Res Commun 175, 852-857.

Chen, C.Y., Chen, J., He, L., and Stiles, B.L. (2018). PTEN: Tumor Suppressor and Metabolic Regulator. Front Endocrinol 9, article number 338.

Chiarugi, P., Pani, G., Giannoni, E., Taddei, L., Colavitti, R., Raugei, G., Symons, M., Borrello, S., Galeotti, T., and Ramponi, G. (2003). Reactive oxygen species as essential mediators of cell adhesion. J Cell Biol161, 933-944.

Choi, H.W., and Klessig, D.F. (2016). DAMPs, MAMPs, and NAMPs in plant innate immunity. BMC Plant Biol 16, article number 232.

Choi, J., Tanaka, K., Cao, Y., Qi, Y., Qiu, J., Liang, Y., Lee, S.Y., and Stacey, G. (2014). Identification of a plant receptor for extracellular ATP. Science 343, 290-294.

Christensen, M.J., Bennett, R.J., Ansari, H.A., Koga, H., Johnson, R.D., Bryan, G.T., Simpson, W.R., Koolaard, J.P., Nickless, E.M., and Voisey, C.R. (2008). *Epichloë* endophytes grow by intercalary hyphal extension in elongating grass leaves. Fungal Genet Biol 45, 84-93.

Christensen, M.J., Bennett, R.J., and Schmid, J. (2002). Growth of *Epichloë*/*Neotyphodium* and p-endophytes in leaves of *Lolium* and *Festuca* grasses. Mycol Res 106, 93-106.

Chujo, T., Lukito, Y., Eaton, C.J., Dupont, P.Y., Johnson, L.J., Winter, D., Cox, M.P., and Scott, B. (2019). Complex epigenetic regulation of alkaloid biosynthesis and host interaction by heterochromatin protein I in a fungal endophyte-plant symbiosis. Fungal Genet Biol 125, 71-83.

Chujo, T., and Scott, B. (2014). Histone H3K9 and H3K27 methylation regulates fungal alkaloid biosynthesis in a fungal endophyte-plant symbiosis. Mol Microbiol 92, 413-434.

Chung, K.R., and Schardl, C.L. (1997). Sexual cycle and horizontal transmission of the grass symbiont, *Epichloë typhina*. Mycol Res 101, 295-301.

Clay, K., and Schardl, C. (2002). Evolutionary origins and ecological consequences of endophyte symbiosis with grasses. Am Nat 160 Suppl 4, S99-S127.

Constabel, C.P., Yip, L., and Ryan, C.A. (1998). Prosystemin from potato, black nightshade, and bell pepper: primary structure and biological activity of predicted systemin polypeptides. Plant Mol Biol 36, 55-62.

Cook, D.E., Mesarich, C.H., and Thomma, B.P.H.J. (2015). Understanding plant immunity as a surveillance system to detect invasion. Annu Rev Phytopathol 53, 541-563.

Couto, D., and Zipfel, C. (2016). Regulation of pattern recognition receptor signalling in plants. Nat Rev Immunol 16, 537.

Dangl, J.L., and Jones, J.D. (2001). Plant pathogens and integrated defence responses to infection. Nature 411, 826-833.

de Jonge, R., van Esse, H.P., Kombrink, A., Shinya, T., Desaki, Y., Bours, R., van der Krol, S., Shibuya, N., Joosten, M.H., and Thomma, B.P. (2010). Conserved fungal LysM effector Ecp6 prevents chitin-triggered immunity in plants. Science 329, 953-955.

Denoux, C., Galletti, R., Mammarella, N., Gopalan, S., Werck, D., De Lorenzo, G., Ferrari, S., Ausubel, F.M., and Dewdney, J. (2008). Activation of defense response pathways by OGs and Flg22 elicitors in *Arabidopsis* seedlings. Molecular Plant 1, 423-445.

Desrivières, S., Cooke, F.T., Parker, P.J., and Hall, M.N. (1998). MSS4, a phosphatidylinositol-4-phosphate 5-kinase required for organization of the actin cytoskeleton in *Saccharomyces cerevisiae*. J Biol Chem 273, 15787-15793.

Ding, M., Zhu, Q., Liang, Y., Li, J., Fan, X., Yu, X., He, F., Xu, H., Liang, Y., and Yu, J. (2017). Differential roles of three FgPLD genes in regulating development and pathogenicity in *Fusarium graminearum*. Fungal Genet Biol 109, 46-52.

Dirschnabel, D.E., Nowrousian, M., Cano-Domínguez, N., Aguirre, J., Teichert, I., and Kück, U. (2014). New insights into the roles of NADPH oxidases in sexual development and ascospore germination in *Sordaria macrospora*. Genetics 196, 729-744.

Djamei, A., Schipper, K., Rabe, F., Ghosh, A., Vincon, V., Kahnt, J., Osorio, S., Tohge, T., Fernie, A.R., Feussner, I., *et al.* (2011). Metabolic priming by a secreted fungal effector. Nature 478, 395-398.

Dodds, P.N., and Rathjen, J.P. (2010). Plant immunity: towards an integrated view of plant-pathogen interactions. Nat Rev Genet 11, 539-548.

Doherty, M.K., Pealing, S.L., Miles, C.S., Moysey, R., Taylor, P., Walkinshaw, M.D., Reid, G.A., and Chapman, S.K. (2000). Identification of the active site acid/base catalyst in a bacterial fumarate reductase: a kinetic and crystallographic study. Biochemistry 39, 10695-10701.

Döhlemann, G., and Hemetsberger, C. (2013). Apoplastic immunity and its suppression by filamentous plant pathogens. New Phytol 198, 1001-1016.

Döhlemann, G., Reissmann, S., Assmann, D., Fleckenstein, M., and Kahmann, R. (2011). Two linked genes encoding a secreted effector and a membrane protein are essential for *Ustilago maydis*-induced tumour formation. Mol Microbiol 81, 751-766.

Döhlemann, G., van der Linde, K., Assmann, D., Schwammbach, D., Hof, A., Mohanty, A., Jackson, D., and Kahmann, R. (2009). Pep1, a secreted effector protein of *Ustilago maydis*, is required for successful invasion of plant cells. PloS Pathog 5, e1000290.

Dong, S., Raffaele, S., and Kamoun, S. (2015). The two-speed genomes of filamentous pathogens: waltz with plants. Curr Opin Genet Dev 35, 57-65.

Dufourc, E.J. (2008). Sterols and membrane dynamics. J Chem Biol 1, 63-77.

Dupont, P.Y., Eaton, C.J., Wargent, J.J., Fechtner, S., Solomon, P., Schmid, J., Day, R.C., Scott, B., and Cox, M.P. (2015). Fungal endophyte infection of ryegrass reprograms host metabolism and alters development. New Phytol 208, 1227-1240.

Eaton, C.J., Cox, M.P., Ambrose, B., Becker, M., Hesse, U., Schardl, C.L., and Scott, B. (2010). Disruption of signaling in a fungal-grass symbiosis leads to pathogenesis. Plant Physiol 153, 1780-1794.

Eaton, C.J., Dupont, P.Y., Solomon, P., Clayton, W., Scott, B., and Cox, M.P. (2015). A core gene set describes the molecular basis of mutualism and antagonism in *Epichloë* spp. Mol Plant Microbe Interact 28, 218-231.

Eaton, C.J., Jourdain, I., Foster, S.J., Hyams, J.S., and Scott, B. (2008). Functional analysis of a fungal endophyte stress-activated MAP kinase. Current Genetics 53, 163-174.

Eaton, C.J., Stärkel, C., and Scott, B. (2013). Role of the cell fusion gene *idcA* in fungal mutualism. In 27th Fungal Genetics Conference (Pacific Grove, CA, USA).

Egan, M.J., Wang, Z.-Y., Jones, M.A., Smirnoff, N., and Talbot, N.J. (2007). Generation of reactive oxygen species by fungal NADPH oxidases is required for rice blast disease. Proc Natl Acad Sci USA 104, 11772-11777.

Eyster, K.M. (2007). The membrane and lipids as integral participants in signal transduction: lipid signal transduction for the non-lipid biochemist. Adv Physiol Educ 31, 5-16.

Falkenburger, B.H., Jensen, J.B., Dickson, E.J., Suh, B.-C., and Hille, B. (2010). Phosphoinositides: lipid regulators of membrane proteins. J Physiol 588, 3179-3185.

Fischer, M.S., and Glass, N.L. (2019). Communicate and fuse: How filamentous fungi establish and maintain an interconnected mycelial network. Front Microbiol 10, article number 619.

Fleetwood, D.J., Khan, A.K., Johnson, R.D., Young, C.A., Mittal, S., Wrenn, R.E., Hesse, U., Foster, S.J., Schardl, C.L., and Scott, B. (2011). Abundant degenerate miniature inverted-repeat transposable elements in genomes of epichloid fungal endophytes of grasses. Genome Biol Evol 3, 1253-1264.

Franceschetti, M., Maqbool, A., Jiménez-Dalmaroni, M.J., Pennington, H.G., Kamoun, S., and Banfield, M.J. (2017). Effectors of filamentous plant pathogens: Commonalities amid diversity. Microbiol Mol Biol Rev 81, e00066-00016.

Friesen, T.L., Stukenbrock, E.H., Liu, Z., Meinhardt, S., Ling, H., Faris, J.D., Rasmussen, J.B., Solomon, P.S., McDonald, B.A., and Oliver, R.P. (2006). Emergence of a new disease as a result of interspecific virulence gene transfer. Nature Genetics 38, 953-956.

Fuchs, B., Krischke, M., Mueller, M.J., and Krauss, J. (2017). Herbivore-specific induction of defence metabolites in a grass–endophyte association. Funct Ecol 31, 318-324.

Gibellini, F., and Smith, T.K. (2010). The Kennedy pathway—De novo synthesis of phosphatidylethanolamine and phosphatidylcholine. IUBMB Life 62, 414-428.

Godi, A., Di Campli, A., Konstantakopoulos, A., Di Tullio, G., Alessi, D.R., Kular, G.S., Daniele, T., Marra, P., Lucocq, J.M., and De Matteis, M.A. (2004). FAPPs control Golgi-to-cell-surface membrane traffic by binding to ARF and PtdIns(4)P. Nat Cell Biol 6, 393-404.

Gourgues, M., Brunet-Simon, A., Lebrun, M.H., and Levis, C. (2004). The tetraspanin BcPls1 is required for appressorium-mediated penetration of *Botrytis cinerea* into host plant leaves. Mol Microbiol 51, 619-629.

Graham, K.A., Kulawiec, M., Owens, K.M., Li, X., Desouki, M.M., Chandra, D., and Singh, K.K. (2010). NADPH oxidase 4 is an oncoprotein localized to mitochondria. Cancer Biol Ther 10, 223-231.

Granado, J., Felix, G., and Boller, T. (1995). Perception of fungal sterols in plants (subnanomolar concentrations of ergosterol elicit extracellular alkalinization in tomato cells). Plant Physiol 107, 485-490.

Green, K.A., Becker, Y., Fitzsimons, H.L., and Scott, B. (2016). An *Epichloë festucae* homologue of MOB3, a component of the STRIPAK complex, is required for

the establishment of a mutualistic symbiotic interaction with *Lolium perenne*. Mol Plant Pathol 17, 1480-1492.

Green, K.A., Becker, Y., Tanaka, A., Takemoto, D., Fitzsimons, H.L., Seiler, S., Lalucque, H., Silar, P., and Scott, B. (2017). SymB and SymC, two membrane associated proteins, are required for *Epichloë festucae* hyphal cell-cell fusion and maintenance of a mutualistic interaction with *Lolium perenne*. Mol Microbiol 103, 657-677.

Green, K.A., Eaton, C.J., Savoian, M.S., and Scott, B. (in press). A homologue of the fungal tetraspanin Pls1 is required for *Epichloë festucae* expressorium formation and establishment of a mutualistic interaction with *Lolium perenne*. Mol Plant Pathol.

Guo, Y.-L., Fitz, J., Schneeberger, K., Ossowski, S., Cao, J., and Weigel, D. (2011). Genome-wide comparison of nucleotide-binding site-leucine-rich repeat-encoding genes in Arabidopsis. Plant Physiol 157, 757-769.

Guttman, D.S., McHardy, A.C., and Schulze-Lefert, P. (2014). Microbial genome-enabled insights into plant–microorganism interactions. Nat Rev Genet 15, 797-813.

Hahn, H., McManus, M.T., Warnstorff, K., Monahan, B.-., Young, C.A., Davies, E., Tapper, B., and Scott, B. (2008). *Neotyphodium* fungal endophytes confer physiological protection to perennial ryegrass (*Lolium perenne* L.) subjected to a water deficit. Environ Exp Bot 63, 183–199.

Hamel, L.-P., Nicole, M.-C., Duplessis, S., and Ellis, B.E. (2012). Mitogen-activated protein kinase signaling in plant-interacting fungi: distinct messages from conserved messengers. Plant Cell 24, 1327-1351.

Hammond, S.M., Altshuller, Y.M., Sung, T.C., Rudge, S.A., Rose, K., Engebrecht, J., Morris, A.J., and Frohman, M.A. (1995). Human ADP-ribosylation factor-activated phosphatidylcholine-specific phospholipase D defines a new and highly conserved gene family. J Biol Chem 270, 29640-29643.

Han, J., Luby-Phelps, K., Das, B., Shu, X., Xia, Y., Mosteller, R.D., Krishna, U.M., Falck, J.R., White, M.A., and Broek, D. (1998). Role of substrates and products of PI 3-kinase in regulating activation of Rac-related guanosine triphosphatases by vav. Science 279, 558-560.

Hassing, B., Winter, D., Becker, Y., Mesarich, C.H., Eaton, C.J., and Scott, B. (2019). Analysis of *Epichloë festucae* small secreted proteins in the interaction with *Lolium perenne*. PloS One 14, e0209463.

Heath, M.C. (2000). Hypersensitive response-related death. In Programmed cell death in higher plants, E. Lam, H. Fukuda, and J.T. Greenberg, eds. (Dordrecht: Springer), pp. 77-90.

Heit, B., Robbins, S.M., Downey, C.M., Guan, Z., Colarusso, P., Miller, B.J., Jirik, F.R., and Kubes, P. (2008). PTEN functions to "prioritize" chemotactic cues and prevent "distraction" in migrating neutrophils. Nat Immunol 9, 743-752.

Heller, J., Zhao, J., Rosenfield, G., Kowbel, D.J., Gladieux, P., and Glass, N.L. (2016). Characterization of greenbeard genes involved in long-distance kind discrimination in a microbial eukaryote. PLoS Biol 14, e1002431-e1002431.

Henneberry, A.L., Wright, M.M., and McMaster, C.R. (2002). The major sites of cellular phospholipid synthesis and molecular determinants of fatty acid and lipid head group specificity. Mol Biol Cell 13, 3148-3161.

Hennessy, L.M., Popay, A.J., Finch, S.C., Clearwater, M.J., and Cave, V.M. (2016). Temperature and plant genotype alter alkaloid concentrations in ryegrass infected with an *Epichloë* endophyte and this affects an insect herbivore. Front Plant Sci 7, 1097-1097.

Herman, P.K., and Emr, S.D. (1990). Characterization of VPS34, a gene required for vacuolar protein sorting and vacuole segregation in *Saccharomyces cerevisiae*. Mol Cell Biol 10, 6742-6754.

Heymont, J., Berenfeld, L., Collins, J., Kaganovich, A., Maynes, B., Moulin, A., Ratskovskaya, I., Poon, P.P., Johnston, G.C., Kamenetsky, M., *et al*. (2000). TEP1, the yeast homolog of the human tumor suppressor gene PTEN/MMAC1/TEP1, is linked to the phosphatidylinositol pathway and plays a role in the developmental process of sporulation. Proc Natl Acad Sci USA 97, 12672-12677.

Holz, R.W., Hlubek, M.D., Sorensen, S.D., Fisher, S.K., Balla, T., Ozaki, S., Prestwich, G.D., Stuenkel, E.L., and Bittner, M.A. (2000). A pleckstrin homology domain specific for phosphatidylinositol 4,5-bisphosphate (PtdIns-4,5-P2) and fused to green fluorescent protein identifies plasma membrane PtdIns-4,5-P2 as being important in exocytosis. J Biol Chem 275, 17878-17885.

Hong, S., Horiuchi, H., and Ohta, A. (2003). Molecular cloning of a phospholipase D gene from *Aspergillus nidulans* and characterization of its deletion mutants. FEMS microbiology letters 224, 231-237.

Huang, S., Gao, L., Blanchoin, L., and Staiger, C.J. (2006). Heterodimeric capping protein from Arabidopsis is regulated by phosphatidic acid. Mol Biol Cell 17, 1946-1958.

Iijima, M., and Devreotes, P. (2002). Tumor suppressor PTEN mediates sensing of chemoattractant gradients. Cell 109, 599-610.

Iijima, M., Huang, Y.E., Luo, H.R., Vazquez, F., and Devreotes, P.N. (2004). Novel mechanism of PTEN regulation by its phosphatidylinositol 4,5-bisphosphate binding motif is critical for chemotaxis. J Biol Chem 279, 16606-16613.

Ischebeck, T., Seiler, S., and Heilmann, I. (2010). At the poles across kingdoms: phosphoinositides and polar tip growth. Protoplasma 240, 13-31.

Jang, J.H., Lee, C.S., Hwang, D., and Ryu, S.H. (2012). Understanding of the roles of phospholipase D and phosphatidic acid through their binding partners. Prog Lipid Res 51, 71-81.

Jashni, M.K., Dols, I.H.M., Iida, Y., Boeren, S., Beenen, H.G., Mehrabi, R., Collemare, J., and de Wit, P.J.G.M. (2015). Synergistic action of a metalloprotease and a serine srotease from *Fusarium oxysporum* f. sp. *lycopersici* cleaves chitin-binding tomato chitinases, reduces their antifungal activity, and enhances fungal virulence. Mol Plant Microbe Interact 28, 996-1008.

Jia, Y., McAdams, S.A., Bryan, G.T., Hershey, H.P., and Valent, B. (2000). Direct interaction of resistance gene and avirulence gene products confers rice blast resistance. EMBO J 19, 4004-4014.

Johnson, L.J., Koulman, A., Christensen, M., Lane, G.A., Fraser, K., Forester, N., Johnson, R.D., Bryan, G.T., and Rasmussen, S. (2013). An extracellular siderophore is required to maintain the mutualistic interaction of *Epichloë festucae* with *Lolium perenne*. PloS Pathog 9, e1003332.

Johnson, R.D., Lane, G.A., Koulman, A., Cao, M., Fraser, K., Fleetwood, D.J., Voisey, C.R., Dyer, J.M., Pratt, J., Christensen, M.J., *et al*. (2015). A novel family of cyclic oligopeptides derived from ribosomal peptide synthesis of an in planta-induced gene, *gigA*, in *Epichloë* endophytes of grasses. Fungal Genet Biol 85, 14-24.

Jones, J.D.G., and Dangl, J.L. (2006). The plant immune system. Nature 444, 323-329.

Kanai, F., Liu, H., Field, S.J., Akbary, H., Matsuo, T., Brown, G.E., Cantley, L.C., and Yaffe, M.B. (2001). The PX domains of p47phox and p40phox bind to lipid products of PI(3)K. Nat Cell Biol 3, 675-678.

Kassas, N., Tanguy, E., Thahouly, T., Fouillen, L., Heintz, D., Chasserot-Golaz, S., Bader, M.F., Grant, N.J., and Vitale, N. (2017). Comparative characterization of phosphatidic acid sensors and their localization during frustrated phagocytosis. J Biol Chem 292, 4266-4279.

Kaur, G., Sharma, A., Guruprasad, K., and Pati, P.K. (2014). Versatile roles of plant NADPH oxidases and emerging concepts. Biotechnol Adv 32, 551-563.

Kayano, Y., Tanaka, A., Akano, F., Scott, B., and Takemoto, D. (2013). Differential roles of NADPH oxidases and associated regulators in polarized growth, conidiation and hyphal fusion in the symbiotic fungus *Epichloë festucae*. Fungal Genet Biol 56, 87-97.

Kayano, Y., Tanaka, A., and Takemoto, D. (2018). Two closely related Rho GTPases, Cdc42 and RacA, of the endophytic fungus *Epichloë festucae* have contrasting roles for ROS production and symbiotic infection synchronized with the host plant. PloS Pathog 14, e1006840.

Kazan, K., and Lyons, R. (2014). Intervention of phytohormone pathways by pathogen effectors. Plant Cell 26, 2285-2309.

Kihara, A., Noda, T., Ishihara, N., and Ohsumi, Y. (2001). Two distinct Vps34 phosphatidylinositol 3-kinase complexes function in autophagy and carboxypeptidase Y sorting in Saccharomyces cerevisiae. J Cell Biol152, 519-530.

Kim, H.-J., Chen, C., Kabbage, M., and Dickman, M.B. (2011). Identification and characterization of *Sclerotinia sclerotiorum* NADPH oxidases. Appl Environ Microbiol 77, 7721-7729.

Klarzynski, O., Plesse, B., Joubert, J.M., Yvin, J.C., Kopp, M., Kloareg, B., and Fritig, B. (2000). Linear β-1,3 glucans are elicitors of defense responses in tobacco. Plant Physiol 124, 1027-1038.

Kloppholz, S., Kuhn, H., and Requena, N. (2011). A secreted fungal effector of *Glomus intraradices* promotes symbiotic biotrophy. Curr Biol 21, 1204-1209.

Kohler, A.C., Chen, L.-H., Hurlburt, N., Salvucci, A., Schwessinger, B., Fisher, A.J., and Stergiopoulos, I. (2016). Structural analysis of an Avr4 effector ortholog offers insight into chitin binding and recognition by the Cf-4 receptor. Plant Cell 28, 1945-1965.

Kohlmeyer, J., and Kohlmeyer, E. (1974). Distribution of *Epichloë typhina* (Ascomycetes) and its parasitic fly. Mycologia 66, 77-86.

Ktistakis, N.T., Brown, H.A., Waters, M.G., Sternweis, P.C., and Roth, M.G. (1996). Evidence that phospholipase D mediates ADP ribosylation factor-dependent formation of Golgi coated vesicles. J Cell Biol134, 295-306.

Lahrmann, U., Ding, Y., Banhara, A., Rath, M., Hajirezaei, M.R., Döhlemann, S., von Wirén, N., Parniske, M., and Zuccaro, A. (2013). Host-related metabolic cues affect colonization strategies of a root endophyte. Proc Natl Acad Sci USA 110, 13965-13970.

Lambeth, J.D., Cheng, G., Arnold, R.S., and Edens, W.A. (2000). Novel homologs of gp91phox. Trends Biochem Sci 25, 459-461.

Lambeth, J.D., and Neish, S.N. (2014). Nox enzymes and new thinking on reactive oxygen: A double-edged sword revisited. Ann Rev Pathol: Mechanisms of Disease 9, 119-145.

Lambou, K., Malagnac, F., Barbisan, C., Tharreau, D., Lebrun, M.-H., and Silar, P. (2008). The crucial role of the Pls1 tetraspanin during ascospore germination in *Podospora anserina* provides an example of the convergent evolution of morphogenetic processes in fungal plant pathogens and saprobes. Eukaryotic Cell 7, 1809-1818.

Lara-Ortiz, T., Riveros-Rosas, H., and Aguirre, J. (2003). Reactive oxygen species generated by microbial NADPH oxidase NoxA regulate sexual development in *Aspergillus nidulans*. Mol Microbiol 50, 1241-1255.

Latch, G.C., and Christensen, M.J. (1985). Artificial infection of grasses with endophytes. Ann Appl Biol 107, 1-24.

Laurindo, F.R., Araujo, T.L., and Abrahao, T.B. (2014). Nox NADPH oxidases and the endoplasmic reticulum. Antioxidants & redox signaling 20, 2755-2775.

Leuchtmann, A., Bacon, C.W., Schardl, C.L., White, J.F., and Tadych, M. (2014). Nomenclatural realignment of *Neotyphodium* species with genus *Epichloë*. Mycologia 106, 202-215.

Leuchtmann, A., Schardl, C.L., and Siegel, M.R. (1994). Sexual compatibility and taxonomy of a new species of *Epichloë* symbiotic with fine fescue grasses. Mycologia 86, 802-812.

Leuchtmann, A., Schmidt, D., and Bush, L.P. (2000). Different levels of protective alkaloids in grasses with stroma-forming and seed-transmitted *Epichloë*/*Neotyphodium* endophytes. J Chem Ecol 26, 1025-1036.

Li, J., Yen, C., Liaw, D., Podsypanina, K., Bose, S., Wang, S.I., Puc, J., Miliaresis, C., Rodgers, L., McCombie, R., *et al*. (1997). PTEN, a putative protein tyrosine phosphatase gene mutated in human brain, breast, and prostate cancer. Science 275, 1943-1947.

Li, X., Gao, M., Han, X., Tao, S., Zheng, D., Cheng, Y., Yu, R., Han, G., Schmidt, M., and Han, L. (2012). Disruption of the phospholipase D gene attenuates the virulence of *Aspergillus fumigatus*. Infect Immun 80, 429-440.

Lo Presti, L., Lanver, D., Schweizer, G., Tanaka, S., Liang, L., Tollot, M., Zuccaro, A., Reissmann, S., and Kahmann, R. (2015). Fungal effectors and plant susceptibility. Annu Rev Plant Biol 66, 513-545.

Lukito, Y., Chujo, T., and Scott, B. (2015). Molecular and cellular analysis of the pH response transcription factor PacC in the fungal symbiont *Epichloë festucae*. Fungal Genet Biol 85, 25-37.

Luo, H.R., and Mondal, S. (2015). Molecular control of PtdIns(3,4,5)P3 signaling in neutrophils. EMBO Rep 16, 149-163.

Malagnac, F., Lalucque, H., Lepere, G., and Silar, P. (2004). Two NADPH oxidase isoforms are required for sexual reproduction and ascospore germination in the filamentous fungus *Podospora anserina*. Fungal Genet Biol 41, 982-997.

Malinowski, D.P., Brauer, D.K., and Belesky, D.P. (1999). The endophyte *Neotyphodium coenophialum* affects root morphology of tall fescue grown under phosphorus deficiency. J Agron Crop Sci 183, 53-60.

Manning, B.D., and Cantley, L.C. (2007). AKT/PKB signaling: navigating downstream. Cell 129, 1261-1274.

Marschall, R., Siegmund, U., Burbank, J., and Tudzynski, P. (2016). Update on Nox function, site of action and regulation in *Botrytis cinerea*. Fungal Biol Technol 3, 8-?.

Marschall, R., and Tudzynski, P. (2016). Reactive oxygen species in development and infection processes. Sem Cell Dev Biol 57, 138-146.

Marshall, R., Kombrink, A., Motteram, J., Loza-Reyes, E., Lucas, J., Hammond-Kosack, K.E., Thomma, B.P., and Rudd, J.J. (2011). Analysis of two in planta expressed LysM effector homologs from the fungus *Mycosphaerella graminicola* reveals novel functional properties and varying contributions to virulence on wheat. Plant Physiol 156, 756-769.

Martínez-Soto, D., and Ruiz-Herrera, J. (2017). Functional analysis of the MAPK pathways in fungi. Rev Iberoam Micol 34, 192-202.

Mendgen, K., Hahn, M., and Deising, H. (1996). Morphogenesis and mechanisms of penetration by plant pathogenic fungi. Annu Rev Phytopathol 34, 367-386.

Mentlak, T.A., Kombrink, A., Shinya, T., Ryder, L.S., Otomo, I., Saitoh, H., Terauchi, R., Nishizawa, Y., Shibuya, N., Thomma, B.P., *et al.* (2012). Effector-mediated suppression of chitin-triggered immunity by *Magnaporthe oryzae* is necessary for rice blast disease. Plant Cell 24, 322-335.

Meyers, B.C., Kozik, A., Griego, A., Kuang, H., and Michelmore, R.W. (2003). Genome-wide analysis of NBS-LRR-encoding genes in *Arabidopsis*. Plant Cell 15, 809-834.

Misas Villamil, J.C., Mueller, A.N., Demir, F., Meyer, U., Okmen, B., Schulze Huynck, J., Breuer, M., Dauben, H., Win, J., Huesgen, P.F., *et al.* (2019). A fungal

substrate mimicking molecule suppresses plant immunity via an inter-kingdom conserved motif. Nat Commun 10, 1576.

Mitic, M., Berry, D., Brasell, E., Green, K., Young, C.A., Saikia, S., Rakonjac, J., and Scott, B. (2018). Disruption of calcineurin catalytic subunit (*cnaA*) in *Epichloë festucae* induces symbiotic defects and intrahyphal hyphae formation. Mol Plant Pathol 19, 1414-1426.

Mitra, P., Zhang, Y., Rameh, L.E., Ivshina, M.P., McCollum, D., Nunnari, J.J., Hendricks, G.M., Kerr, M.L., Field, S.J., Cantley, L.C., *et al.* (2004). A novel phosphatidylinositol(3,4,5)P3 pathway in fission yeast. J Cell Biol 166, 205-211.

Moon, C.D., Craven, K.D., Leuchtmann, A., Clement, S.L., and Schardl, C.L. (2004). Prevalence of interspecific hybrids amongst asexual fungal endophytes of grasses. Mol Ecol 13, 1455-1467.

Moy, M., Belanger, F., Duncan, R., Freehof, A., Leary, C., Meyer, W., Sullivan, R., and White, J.F., Jr. (2000). Identification of epiphyllous mycelial nets on leaves of grasses infected by clavicipitaceous endophytes. Symbiosis 28, 291–302.

Müller, A.N., Ziemann, S., Treitschke, S., Assmann, D., and Döhlemann, G. (2013). Compatibility in the *Ustilago maydis*-maize interaction requires inhibition of host cysteine proteases by the fungal effector Pit2. PloS Pathog 9, e1003177.

Müller, K., Carstens, A.C., Linkies, A., Torres, M.A., and Leubner-Metzger, G. (2009). The NADPH-oxidase AtrbohB plays a role in Arabidopsis seed after-ripening. New Phytol 184, 885-897.

Müller, K., Kermode, A.R., Linkies, A., and Leubner-Metzger, G. (2012). Role of a respiratory burst oxidase of *Lepidium sativum* (cress) seedlings in root development and auxin signalling. J Exp Bot 63, 6325-6334.

Nagano, N., Umemura, M., Izumikawa, M., Kawano, J., Ishii, T., Kikuchi, M., Tomii, K., Kumagai, T., Yoshimi, A., Machida, M., *et al.* (2016). Class of cyclic ribosomal peptide synthetic genes in filamentous fungi. Fungal Genet Biol 86, 58-70.

Newton, A.C., Bootman, M.D., and Scott, J.D. (2016). Second Messengers. Cold Spring Harbor Perspectives in Biology 8. pp XX

Nguyen, H.N., Afkari, Y., Senoo, H., Sesaki, H., Devreotes, P.N., and Iijima, M. (2014). Mechanism of human PTEN localization revealed by heterologous expression in *Dictyostelium*. Oncogene 33, 5688-5696.

Ogasawara, Y., Kaya, H., Hiraoka, G., Yumoto, F., Kimura, S., Kadota, Y., Hishinuma, H., Senzaki, E., Yamagoe, S., Nagata, K., *et al.* (2008). Synergistic activation of the Arabidopsis NADPH oxidase AtrbohD by Ca^{2+} and phosphorylation. J Biol Chem 283, 8885-8892.

Ökmen, B., Etalo, D.W., Joosten, M.H.A.J., Bouwmeester, H.J., de Vos, R.C.H., Collemare, J., and de Wit, P.J.G.M. (2013). Detoxification of α-tomatine by *Cladosporium fulvum* is required for full virulence on tomato. New Phytol 198, 1203-1214.

Ökmen, B., Mathow, D., Hof, A., Lahrmann, U., Aßmann, D., and Doehlemann, G. (2018). Mining the effector repertoire of the biotrophic fungal pathogen *Ustilago hordei* during host and non-host infection. Mol Plant Pathol 19, 2603-2622.

Palicz, A., Foubert, T.R., Jesaitis, A.J., Marodi, L., and McPhail, L.C. (2001). Phosphatidic acid and diacylglycerol directly activate NADPH oxidase by interacting with enzyme components. J Biol Chem 276, 3090-3097.

Park, C.H., Chen, S., Shirsekar, G., Zhou, B., Khang, C.H., Songkumarn, P., Afzal, A.J., Ning, Y., Wang, R., Bellizzi, M., *et al.* (2012). The *Magnaporthe oryzae* effector AvrPiz-t targets the RING E3 ubiquitin ligase APIP6 to suppress pathogen-associated molecular pattern-triggered immunity in rice. Plant Cell 24, 4748-4762.

Petit-Houdenot, Y., and Fudal, I. (2017). Complex interactions between fungal avirulence genes and their corresponding plant resistance genes and consequences for disease resistance management. Front Plant Sci 8, 1072-1072.

Philipson, M.N., and Christey, M.C. (1986). The relationship of host and endophyte during flowering, seed formation, and germination of *Lolium perenne*. NZ J Bot 24, 125-134.

Plett, J.M., Daguerre, Y., Wittulsky, S., Vayssieres, A., Deveau, A., Melton, S.J., Kohler, A., Morrell-Falvey, J.L., Brun, A., Veneault-Fourrey, C., *et al.* (2014). Effector MiSSP7 of the mutualistic fungus *Laccaria bicolor* stabilizes the *Populus* JAZ6 protein and represses jasmonic acid (JA) responsive genes. Proc Natl Acad Sci USA 111, 8299-8304.

Plett, J.M., Kemppainen, M., Kale, S.D., Kohler, A., Legue, V., Brun, A., Tyler, B.M., Pardo, A.G., and Martin, F. (2011). A secreted effector protein of *Laccaria bicolor* is required for symbiosis development. Curr Biol: CB 21, 1197-1203.

Plett, J.M., Khachane, A., Ouassou, M., Sundberg, B., Kohler, A., and Martin, F. (2014). Ethylene and jasmonic acid act as negative modulators during mutualistic symbiosis between *Laccaria bicolor* and *Populus* roots. New Phytol 202, 270-286.

Ponting, C.P., and Kerr, I.D. (1996). A novel family of phospholipase D homologues that includes phospholipid synthases and putative endonucleases: identification of duplicated repeats and potential active site residues. Protein Science 5, 914-922.

Potocký, M., Jones, M.A., Bezvoda, R., Smirnoff, N., and Žárský, V. (2007). Reactive oxygen species produced by NADPH oxidase are involved in pollen tube growth. New Phytol 174, 742-751.

Potocký, M., Pejchar, P., Gutkowska, M., Jimenez-Quesada, M.J., Potocka, A., Alche Jde, D., Kost, B., and Zarsky, V. (2012). NADPH oxidase activity in pollen tubes is affected by calcium ions, signaling phospholipids and Rac/Rop GTPases. J Plant Physiol 169, 1654-1663.

Pritchard, L., and Birch, P.R.J. (2014). The zigzag model of plant–microbe interactions: is it time to move on? Mol Plant Pathol 15, 865-870.

Qi, D., and Innes, R. (2013). Recent advances in plant NLR structure, function, localization, and signaling. Frontiers in Immunology 4. X-X

Quentin, M., Abad, P., and Favery, B. (2013). Plant parasitic nematode effectors target host defense and nuclear functions to establish feeding cells. Front Plant Sci 4, 53-53.

Ranf, S., Gisch, N., Schäffer, M., Illig, T., Westphal, L., Knirel, Y.A., Sánchez-Carballo, P.M., Zähringer, U., Hückelhoven, R., Lee, J., *et al.* (2015). A lectin S-

domain receptor kinase mediates lipopolysaccharide sensing in *Arabidopsis thaliana*. Nat Immunol 16, 426-X.

Rastogi, R., Geng, X., Li, F., and Ding, Y. (2017). NOX activation by subunit interaction and underlying mechanisms in disease. Front Cell Neurosci 10, 301-301.

Read, N.D., Goryachev, A.B., and Lichius, A. (2012). The mechanistic basis of self-fusion between conidial anastomosis tubes during fungal colony initiation. Fungal Biol Rev 26, 1-11.

Regier, D.S., Waite, K.A., Wallin, R., and McPhail, L.C. (1999). A phosphatidic acid-activated protein kinase and conventional protein kinase C isoforms phosphorylate p22(phox), an NADPH oxidase component. J Biol Chem 274, 36601-36608.

Rispail, N., Soanes, D.M., Ant, C., Czajkowski, R., Grünler, A., Huguet, R., Perez-Nadales, E., Poli, A., Sartorel, E., Valiante, V., *et al*. (2009). Comparative genomics of MAP kinase and calcium–calcineurin signalling components in plant and human pathogenic fungi. Fungal Gen Biol 46, 287-298.

Rittenour, W.R., and Harris, S.D. (2013). Glycosylphosphatidylinositol-anchored proteins in *Fusarium graminearum*: inventory, variability, and virulence. PLoS One 8, e81603.

Roca, M.G., Weichert, M., Siegmund, U., Tudzynski, P., and Fleißner, A. (2012). Germling fusion via conidial anastomosis tubes in the grey mould *Botrytis cinerea* requires NADPH oxidase activity. Fungal Biology 116, 379-387.

Ron, M., and Avni, A. (2004). The receptor for the fungal elicitor ethylene-inducing xylanase is a member of a resistance-like gene family in tomato. Plant Cell 16, 1604-1615.

Rooney, H.C., Van't Klooster, J.W., van der Hoorn, R.A., Joosten, M.H., Jones, J.D., and de Wit, P.J. (2005). *Cladosporium* Avr2 inhibits tomato Rcr3 protease required for Cf-2-dependent disease resistance. Science 308, 1783-1786.

Rudge, S.A., Sciorra, V.A., Iwamoto, M., Zhou, C., Strahl, T., Morris, A.J., Thorner, J., and Engebrecht, J. (2004). Roles of phosphoinositides and of Spo14p (phospholipase D)-generated phosphatidic acid during yeast sporulation. Mol Biol Cell 15, 207-218.

Ryder, L.S., Dagdas, Y.F., Mentlak, T.A., Kershaw, M.J., Thornton, C.R., Schuster, M., Chen, J., Wang, Z., and Talbot, N.J. (2013). NADPH oxidases regulate septin-mediated cytoskeletal remodeling during plant infection by the rice blast fungus. Proc Natl Acad Sci USA 110, 3179-3184.

Saed-Moucheshi, A., Pakniyat, H., Pirasteh-Anosheh, H., and Azooz, M.M. (2014). Chapter 20 - Role of ROS as signaling molecules in plants. In Oxidative Damage to Plants, P. Ahmad, ed. (San Diego: Academic Press), pp. 585-620.

Saijo, Y., Loo, E.P., and Yasuda, S. (2018). Pattern recognition receptors and signaling in plant–microbe interactions. Plant J 93, 592-613.

Saijo, Y., Loo, E.P., and Yasuda, S. (2018). Pattern recognition receptors and signaling in plant–microbe interactions. Plant J 93, 592-613.

Sansal, I., and Sellers, W.R. (2004). The biology and clinical relevance of the PTEN tumor suppressor pathway. J Clin Oncol 22, 2954-2963.

Schardl, C.L. (2001). *Epichloë festucae* and related mutualistic symbionts of grasses. Fungal Genet Biol 33, 69-82.

Schardl, C.L., Leuchtmann, A., and Spiering, M.J. (2004). Symbioses of grasses with seedborne fungal endophytes. Annu Rev Plant Biol 55, 315-340.

Schardl, C.L., Leuchtmann, A., Tsai, H.F., Collett, M.A., Watt, D.M., and Scott, D.B. (1994). Origin of a fungal symbiont of perennial ryegrass by interspecific hybridization of a mutualist with the ryegrass choke pathogen, *Epichloë typhina*. Genetics 136, 1307-1317.

Schardl, C.L., Young, C.A., Hesse, U., Amyotte, S.G., Andreeva, K., Calie, P.J., Fleetwood, D.J., Haws, D.C., Moore, N., Oeser, B., *et al*. (2013). Plant-symbiotic fungi as chemical engineers: multi-genome analysis of the *Clavicipitaceae* reveals dynamics of alkaloid loci. PLoS Genetics 9, e1003323-e1003323.

Schardl, C.L., Young, C.A., Pan, J., Florea, S., Takach, J.E., Panaccione, D.G., Farman, M.L., Webb, J.S., Jaromczyk, J., Charlton, N.D., *et al*. (2013). Currencies of mutualisms: sources of alkaloid genes in vertically transmitted *Epichloë.* Toxins 5, 1064-1088.

Schirawski, J., Mannhaupt, G., Münch, K., Brefort, T., Schipper, K., Doehlemann, G., Di Stasio, M., Rössel, N., Mendoza-Mendoza, A., Pester, D., *et al*. (2010). Pathogenicity determinants in smut fungi revealed by genome comparison. Science 330, 1546-1548.

Schmidt, S.M., Houterman, P.M., Schreiver, I., Ma, L., Amyotte, S., Chellappan, B., Boeren, S., Takken, F.L.W., and Rep, M. (2013). MITEs in the promoters of effector genes allow prediction of novel virulence genes in *Fusarium oxysporum*. BMC genomics 14, 119-119.

Sciorra, V.A., Rudge, S.A., Prestwich, G.D., Frohman, M.A., Engebrecht, J., and Morris, A.J. (1999). Identification of a phosphoinositide binding motif that mediates activation of mammalian and yeast phospholipase D isoenzymes. EMBO J 18, 5911-5921.

Scott, B. (2015). Conservation of fungal and animal nicotinamide adenine dinucleotide phosphate oxidase complexes. Mol Microbiol 95, 910-913.

Scott, B., Becker, Y., Becker, M., and Cartwright, G. (2012). Morphogenesis, growth, and development of the grass symbiont *Epichlöe festucae*. In: Morphogenesis and Pathogenicity in Fungi, Eds Pérez Martín J and Di Pietro A, Springer-Verlag. pp 243-264

Scott, B., Green, K., and Berry, D. (2018). The fine balance between mutualism and antagonism in the *Epichloë festucae*–grass symbiotic interaction. Curr Opin Plant Biol 44, 32-38.

Scott, B., and Schardl, C. (1993). Fungal symbionts of grasses: evolutionary insights and agricultural potential. Trends Microbiol 1, 196-200.

Segmüller, N., Kokkelink, L., Giesbert, S., Odinius, D., van Kan, J., and Tudzynski, P. (2008). NADPH oxidases are involved in differentiation and pathogenicity in *Botrytis cinerea*. Mol Plant Microbe Interact 21, 808-819.

Selin, C., de Kievit, T.R., Belmonte, M.F., and Fernando, W.G. (2016). Elucidating the Role of Effectors in Plant-Fungal Interactions: Progress and Challenges. Front Microbiol 7, article number 600.

Selvy, P.E., Lavieri, R.R., Lindsley, C.W., and Brown, H.A. (2011). Phospholipase D: enzymology, functionality, and chemical modulation. Chemical Reviews 111, 6064-6119.

Sharma, V.P., DesMarais, V., Sumners, C., Shaw, G., and Narang, A. (2008). Immunostaining evidence for PI(4,5)P2 localization at the leading edge of chemoattractant-stimulated HL-60 cells. J Leukoc Biol 84, 440-447.

Shi, B., Ni, L., Zhang, A., Cao, J., Zhang, H., Qin, T., Tan, M., Zhang, J., and Jiang, M. (2012). OsDMI3 is a novel component of abscisic acid signaling in the induction of antioxidant defense in leaves of rice. Molecular Plant 5, 1359-1374.

Shimizu, T., Nakano, T., Takamizawa, D., Desaki, Y., Ishii-Minami, N., Nishizawa, Y., Minami, E., Okada, K., Yamane, H., Kaku, H., *et al.* (2010). Two LysM receptor molecules, CEBiP and OsCERK1, cooperatively regulate chitin elicitor signaling in rice. Plant J 64, 204-214.

Siegmund, U., Heller, J., van Kann, J.A.L., and Tudzynski, P. (2013). The NADPH Oxidase Complexes in *Botrytis cinerea*: Evidence for a close association with the ER and the tetraspanin Pls1. PloS One 8, e55879.

Siegmund, U., Marschall, R., and Tudzynski, P. (2015). BcNoxD, a putative ER protein, is a new component of the NADPH oxidase complex in *Botrytis cinerea*. Mol Microbiol 95, 988-1005.

Skibbe, D.S., Döhlemann, G., Fernandes, J., and Walbot, V. (2010). Maize tumors caused by *Ustilago maydis* require organ-specific genes in host and pathogen. Science 328, 89-92.

Spatafora, J.W., Sung, G.H., Sung, J.M., Hywel-Jones, N.L., and White, J.F., Jr. (2007). Phylogenetic evidence for an animal pathogen origin of ergot and the grass endophytes. Mol Ecology 16, 1701-1711.

Stergiopoulos, I., van den Burg, H.A., Okmen, B., Beenen, H.G., van Liere, S., Kema, G.H.J., and de Wit, P.J.G.M. (2010). Tomato Cf resistance proteins mediate recognition of cognate homologous effectors from fungi pathogenic on dicots and monocots. Proc Natl Acad Sci USA 107, 7610-7615.

Stevenson, J.M., Perera, I.Y., Heilmann, I., Persson, S., and Boss, W.F. (2000). Inositol signaling and plant growth. Trends Plant Sci 5, 252-258.

Strahl, T., and Thorner, J. (2007). Synthesis and function of membrane phosphoinositides in budding yeast, *Saccharomyces cerevisiae*. Biochim Biophys Acta 1771, 353-404.

Suh, B.-C., and Hille, B. (2008). PIP2 is a necessary cofactor for ion channel function: how and why? Annu Rev Biophys 37, 175-195.

Sun, Y., Carroll, S., Kaksonen, M., Toshima, J.Y., and Drubin, D.G. (2007). PtdIns(4,5)P2 turnover is required for multiple stages during clathrin- and actin-dependent endocytic internalization. J Cell Biol177, 355-367.

Swanson, S., and Gilroy, S. (2010). ROS in plant development. Physiologia Plantarum 138, 384-392.

Takemoto, D., Kamakura, S., Saikia, S., Becker, Y., Wrenn, R., Tanaka, A., Sumimoto, H., and Scott, B. (2011). Polarity proteins Bem1 and Cdc24 are components of the filamentous fungal NADPH oxidase complex. Proc Natl Acad Sci USA 108, 2861-2866.

Takemoto, D., Tanaka, A., and Scott, B. (2006). A p67phox-like regulator is recruited to control hyphal branching in a fungal–grass mutualistic symbiosis. Plant Cell 18, 2807-2821.

Takken, F.L.W., and Goverse, A. (2012). How to build a pathogen detector: structural basis of NB-LRR function. Curr Opin Plant Biol 15, 375-384.

Tan, Y.Y., Spiering, M.J., Scott, V., Lane, G.A., Christensen, M.J., and Schmid, J. (2001). *In planta* regulation of extension of an endophytic fungus and maintenance of high metabolic rates in its mycelium in the absence of apical extension. Appl Environ Microbiol 67, 5377-5383.

Tanaka, A., Cartwright, G.M., Saikia, S., Kayano, Y., Takemoto, D., Kato, M., Tsuge, T., and Scott, B. (2013). ProA, a transcriptional regulator of fungal fruiting body development, regulates leaf hyphal network development in the *Epichloë festucae-Lolium perenne* symbiosis. Mol Microbiol 90, 551-568.

Tanaka, A., Christensen, M.J., Takemoto, D., Park, P., and Scott, B. (2006). Reactive oxygen species play a role in regulating a fungus-perennial ryegrass mutualistic interaction. Plant Cell 18, 1052-1066.

Tanaka, A., Takemoto, D., Chujo, T., and Scott, B. (2012). Fungal endophytes of grasses. Curr Opin Plant Biol 15, 462-468.

Tanaka, A., Takemoto, D., Hyon, G.-S., Park, P., and Scott, B. (2008). NoxA activation by the small GTPase RacA is required to maintain a mutualistic symbiotic association between *Epichloë festucae* and perennial ryegrass. Mol Microbiol 68, 1165-1178.

Tanaka, S., Brefort, T., Neidig, N., Djamei, A., Kahnt, J., Vermerris, W., Koenig, S., Feussner, K., Feussner, I., and Kahmann, R. (2014). A secreted *Ustilago maydis* effector promotes virulence by targeting anthocyanin biosynthesis in maize. eLife 3, e01355.

Tanguy, E., Wang, Q., Moine, H., and Vitale, N. (2019). Phosphatidic acid: From pleiotropic functions to neuronal pathology. Front Cell Neurosci 13, 2-2.

Thomma, B.P.H.J., Nürnberger, T., and Joosten, M.H.A.J. (2011). Of PAMPs and Effectors: The Blurred PTI-ETI Dichotomy. Plant Cell 23, 4-15.

Thomma, B.P.H.J., Van Esse, H.P., Crous, P.W., and De Wit, P.J.G.M. (2005). *Cladosporium fulvum* (syn. *Passalora fulva*), a highly specialized plant pathogen as a model for functional studies on plant pathogenic *Mycosphaerellaceae*. Mol Plant Pathol 6, 379-393.

Tian, Z., Wang, R., Ambrose, K.V., Clarke, B.B., and Belanger, F.C. (2017). The *Epichloë festucae* antifungal protein has activity against the plant pathogen *Sclerotinia homoeocarpa*, the causal agent of dollar spot disease. Scientific Reports 7, 5643-5643.

Toenjes, K.A., Sawyer, M.M., and Johnson, D.I. (1999). The guanine-nucleotide-exchange factor Cdc24p is targeted to the nucleus and polarized growth sites. Curr Biol 9, 1183-1186.

Torres, M.A., Dangl, J.L., and Jones, J.D.G. (2002). *Arabidopsis* gp91phox homologues AtrbohD and AtrbohF are required for accumulation of reactive oxygen intermediates in the plant defense response. Proc Natl Acad Sci USA 99, 517-522.

Tóth, D.I.J., Tóth, J.T., Gulyás, G., Balla, A., Balla, T., Hunyady, L., and Várnai, P. (2012). Acute depletion of plasma membrane phosphatidylinositol 4,5-bisphosphate impairs specific steps in endocytosis of the G-protein-coupled receptor. J Cell Sci 125, 2185-2197.

Tucker, S.L., and Talbot, N.J. (2001). Surface attachment and pre-penetration stage development by plant pathogenic fungi. Annu Rev Phytopathol 39, 385-417.

Tudzynski, P., Correia, T., and Keller, U. (2001). Biotechnology and genetics of ergot alkaloids. Appl Microbiol Biotechnol 57, 593-605.

Tudzynski, P., Heller, J., and Siegmund, U. (2012). Reactive oxygen species generation in fungal development and pathogenesis. Curr Opin Microbiol 15, 653-659.

van den Burg, H.A., Harrison, S.J., Joosten, M.H., Vervoort, J., and de Wit, P.J. (2006). *Cladosporium fulvum* Avr4 protects fungal cell walls against hydrolysis by plant chitinases accumulating during infection. Mol Plant Microbe Interact 19, 1420-1430.

van der Hoorn, R.A., and Kamoun, S. (2008). From Guard to Decoy: a new model for perception of plant pathogen effectors. Plant Cell 20, 2009-2017.

van Meer, G., Voelker, D.R., and Feigenson, G.W. (2008). Membrane lipids: where they are and how they behave. Nat Rev Mol Cell Biol 9, 112-124.

Voegele, R.T., and Mendgen, K. (2003). Rust haustoria: nutrient uptake and beyond. New Phytol 159, 93-100.

Wang, X. (2000). Multiple forms of phospholipase D in plants: the gene family, catalytic and regulatory properties, and cellular functions. Prog Lipid Res 39, 109-149.

Wawra, S., Fesel, P., Widmer, H., Timm, M., Seibel, J., Leson, L., Kesseler, L., Nostadt, R., Hilbert, M., Langen, G., *et al*. (2016). The fungal-specific beta-glucan-binding lectin FGB1 alters cell-wall composition and suppresses glucan-triggered immunity in plants. Nat Comm 7, article number 13188.

Weiger, M.C., and Parent, C.A. (2012). Phosphoinositides in Chemotaxis. In Phosphoinositides II: The Diverse Biological Functions, T. Balla, M. Wymann, and J.D. York, eds. (Dordrecht: Springer Netherlands), pp. 217-254.

Whisson, S.C., Boevink, P.C., Moleleki, L., Avrova, A.O., Morales, J.G., Gilroy, E.M., Armstrong, M.R., Grouffaud, S., van West, P., Chapman, S., *et al*. (2007). A translocation signal for delivery of oomycete effector proteins into host plant cells. Nature 450, 115-118.

Winter, D.J., Ganley, A.R.D., Young, C.A., Liachko, I., Schardl, C.L., Dupont, P.-Y., Berry, D., Ram, A., Scott, B., and Cox, M.P. (2018). Repeat elements organise 3D genome structure and mediate transcription in the filamentous fungus *Epichloë festucae*. PLoS Genetics 14, e1007467-e1007467.

Wong, H.L., Pinontoan, R., Hayashi, K., Tabata, R., Yaeno, T., Hasegawa, K., Kojima, C., Yoshioka, H., Iba, K., Kawasaki, T., *et al.* (2007). Regulation of rice NADPH oxidase by binding of Rac GTPase to its N-terminal extension. Plant Cell 19, 4022-4034.

Wright, G.D., Arlt, J., Poon, W.C.K., and Read, N.D. (2007). Optical tweezer micromanipulation of filamentous fungi. Fungal Gen Biol 44, 1-13.

Wu, W.N., McKown, L.A., Moyer, M.D., and Reitz, A.B. (2000). In vitro biotransformation of the new antipsychotic agent, RWJ-46344 in rat hepatic S9 fraction: API-MS/MS/MS identification of metabolites. J Pharm Biomed Anal 24, 307-316.

Xie, Z., Fang, M., Rivas, M.P., Faulkner, A.J., Sternweis, P.C., Engebrecht, J.A., and Bankaitis, V.A. (1998). Phospholipase D activity is required for suppression of yeast phosphatidylinositol transfer protein defects. Proc Natl Acad Sci USA 95, 12346-12351.

Yamamoto, A., DeWald, D.B., Boronenkov, I.V., Anderson, R.A., Emr, S.D., and Koshland, D. (1995). Novel PI(4)P 5-kinase homologue, Fab1p, essential for normal vacuole function and morphology in yeast. Mol Biol Cell 6, 525-539.

Yao, H.-Y., and Xue, H.-W. (2018). Phosphatidic acid plays key roles regulating plant development and stress responses. J Integr Plant Biol 60, 851-863.

Ye, Y., Ozaki, T., Umemura, M., Liu, C.H., Minami, A., and Oikawa, H. (2019). Heterologous production of asperipin-2a: proposal for sequential oxidative macrocyclization by a fungi-specific DUF3328 oxidase. *Org* Biomol *Chem* 17, 39-43.

Yoshie, Y., Goto, K., Takai, R., Iwano, M., Takayama, S., Isogai, A., and Che, F.-S. (2005). Function of the rice gp91phox homologs OsrbohA and OsrbohE genes in ROS-dependent plant immune responses. Plant Biotechnol 22, 127-135.

Zeniou-Meyer, M., Zabari, N., Ashery, U., Chasserot-Golaz, S., Haeberle, A.M., Demais, V., Bailly, Y., Gottfried, I., Nakanishi, H., Neiman, A.M., *et al.* (2007). Phospholipase D1 production of phosphatidic acid at the plasma membrane promotes exocytosis of large dense-core granules at a late stage. J Biol Chem 282, 21746-21757.

Zhang, J., Wang, X., Vikash, V., Ye, Q., Wu, D., Liu, Y., and Dong, W. (2016). ROS and ROS-mediated cellular signaling. Cell Longev 2016, Article ID 4350965.

Zhang, Y., Zhu, H., Zhang, Q., Li, M., Yan, M., Wang, R., Wang, L., Welti, R., Zhang, W., and Wang, X. (2009). Phospholipase dalpha1 and phosphatidic acid regulate NADPH oxidase activity and production of reactive oxygen species in ABA-mediated stomatal closure in *Arabidopsis*. Plant Cell 21, 2357-2377.

Zhao, J. (2015). Phospholipase D and phosphatidic acid in plant defence response: from protein-protein and lipid-protein interactions to hormone signalling. J Exp Bot 66, 1721-1736.

Zhao, X., Mehrabi, R., and Xu, J.-R. (2007). Mitogen-activated protein kinase pathways and fungal pathogenesis. Eukaryotic Cell 6, 1701-1714.

Zhao, Y.L., Zhou, T.T., and Guo, H.S. (2016). Hyphopodium-specific VdNoxB/VdPls1-dependent ROS-Ca^{2+} signaling is required for plant infection by *Verticillium dahliae*. PloS Pathog 12, e1005793.

Zipfel, C. (2008). Pattern-recognition receptors in plant innate immunity. Curr Opin Immunol 20, 10-16.

Appendix

Appendix 1: DRC 16 Form for Chapter 2

DRC 16

MASSEY UNIVERSITY
GRADUATE RESEARCH SCHOOL

STATEMENT OF CONTRIBUTION
DOCTORATE WITH PUBLICATIONS/MANUSCRIPTS

We, the candidate and the candidate's Primary Supervisor, certify that all co-authors have consented to their work being included in the thesis and they have accepted the candidate's contribution as indicated below in the *Statement of Originality*.

Name of candidate:	Berit Hassing
Name/title of Primary Supervisor:	Professor Barry Scott
Name of Research Output and full reference:	
Hassing, B., Winter, D., Becker, Y., Mesarich, C.H., Eaton, C.J., and Scott, B. (2019). Analysis of *Epichloë festucae* small secreted proteins in the interaction with *Lolium perenne*. PLOS ONE. doi: 10.1371/journal.pone.0209463	
In which Chapter is the Manuscript /Published work:	2
Please indicate:	
• The percentage of the manuscript/Published Work that was contributed by the candidate:	90
and	
• Describe the contribution that the candidate has made to the Manuscript/Published Work:	
The candidate carried out most of the experiments under the guidance of supervisors. The seed transmission experiment was done by Yvonne Becker (Suppl Fig S3, Suppl Table S7). David Winter carried out the Bioinformatics analysis (Fig 1 and Fig 2). The candidate and supervisors wrote and edited the manuscript.	
For manuscripts intended for publication please indicate target journal:	
published in PLOS One	
Candidate's Signature:	Berit Hassing Digitally signed by Berit Hassing Date: 2019.04.27 18:28:06 +12'00'
Date:	27 April 2019
Primary Supervisor's Signature:	Scott, Barry Digitally signed by Scott, Barry Date: 2019.04.23 08:39:13 +12'00'
Date:	23 April 2019

(This form should appear at the end of each thesis chapter/section/appendix submitted as a manuscript/ publication or collected as an appendix at the end of the thesis)

Appendix 2: DRC 16 Form for Chapter 3.

DRC 16

MASSEY UNIVERSITY
GRADUATE RESEARCH SCHOOL

STATEMENT OF CONTRIBUTION
DOCTORATE WITH PUBLICATIONS/MANUSCRIPTS

We, the candidate and the candidate's Primary Supervisor, certify that all co-authors have consented to their work being included in the thesis and they have accepted the candidate's contribution as indicated below in the *Statement of Originality*.

Name of candidate:	Berit Hassing
Name/title of Primary Supervisor:	Professor Barry Scott
Name of Research Output and full reference:	
Hassing, B., Green, K.A., Winter, D., Brandt, U. , Mesarich, C.H., Eaton, C.J., Fleissner, A., Scott, B. (2019) Phosphatidic acid produced by phospholipase D is a key signaling molecule for hyphal cell-to-cell fusion and the mutualistic interaction between *Epichloë festucae* and perennial ryegrass.	
In which Chapter is the Manuscript /Published work:	3
Please indicate:	
• The percentage of the manuscript/Published Work that was contributed by the candidate:	90
and	
• Describe the contribution that the candidate has made to the Manuscript/Published Work:	
The candidate carried out most of the experiments under the guidance of supervisors. The phylogenetic tree was constructed by David Winter. The *N. crassa* experiments were carried out by Andre Fleissner and the cellophane penetration test by Kimberly Green. Carla Eaton made the *pldA* deletion and overexpression constructs and strains. She also made the *pldB* deletion construct and designed the OE construct but the candidate made the strains. Carla Eaton made the NoxA and Bem localization constructs with the remainder made by Daigo and Aiko Takemoto and described in previous publications, which are cited in the Supplemental Table. The candidate wrote the manuscript draft, which was then edited by supervisors.	
For manuscripts intended for publication please indicate target journal:	
New Phytologist	
Candidate's Signature:	Berit Hassing Digitally signed by Berit Hassing Date: 2019.04.27 18:31:26 +12'00'
Date:	27 April 2019
Primary Supervisor's Signature:	Scott, Barry Digitally signed by Scott, Barry Date: 2019.04.23 08:25:47 +12'00'
Date:	23 April 2019

(This form should appear at the end of each thesis chapter/section/appendix submitted as a manuscript/ publication or collected as an appendix at the end of the thesis)

Appendix 3: DRC 16 Form for Chapter 4.

DRC 16

MASSEY UNIVERSITY
GRADUATE RESEARCH SCHOOL

STATEMENT OF CONTRIBUTION
DOCTORATE WITH PUBLICATIONS/MANUSCRIPTS

We, the candidate and the candidate's Primary Supervisor, certify that all co-authors have consented to their work being included in the thesis and they have accepted the candidate's contribution as indicated below in the *Statement of Originality*.

Name of candidate:	Berit Hassing
Name/title of Primary Supervisor:	Professor Barry Scott
Name of Research Output and full reference:	
Hassing, B., Mesarich, C.H., Eaton, C.J., Scott, B. (2019) A fungal homolog of the mammalian tumour suppressor protein PTEN is required for the mutualistic interaction between the filamentous ascomycete *Epichloë festucae* and perennial ryegrass.	
In which Chapter is the Manuscript /Published work:	4
Please indicate:	
• The percentage of the manuscript/Published Work that was contributed by the candidate:	90
and	
• Describe the contribution that the candidate has made to the Manuscript/Published Work:	
The candidate carried out all the experiments. Carla Eaton made the OE strains but the candidate verified them. Carla Eaton made lipid biosensor plasmids, which were transformed by Aleysha Candy. Carla Eaton made the NoxA and Bem localization constructs but the others were made by Daigo and Aiko Takemoto and described in previous publications, which are cited in the Supplemental Table. The candidate wrote the manuscript draft, which was then edited by supervisors.	
For manuscripts intended for publication please indicate target journal:	
Fungal Genetics and Biology	
Candidate's Signature:	Berit Hassing Digitally signed by Berit Hassing Date: 2019.04.27 14:31:24 +12'00'
Date:	27 April 2019
Primary Supervisor's Signature:	Scott, Barry Digitally signed by Scott, Barry Date: 2019.04.23 08:52:16 +12'00'
Date:	23 April 2019

(This form should appear at the end of each thesis chapter/section/appendix submitted as a manuscript/ publication or collected as an appendix at the end of the thesis)

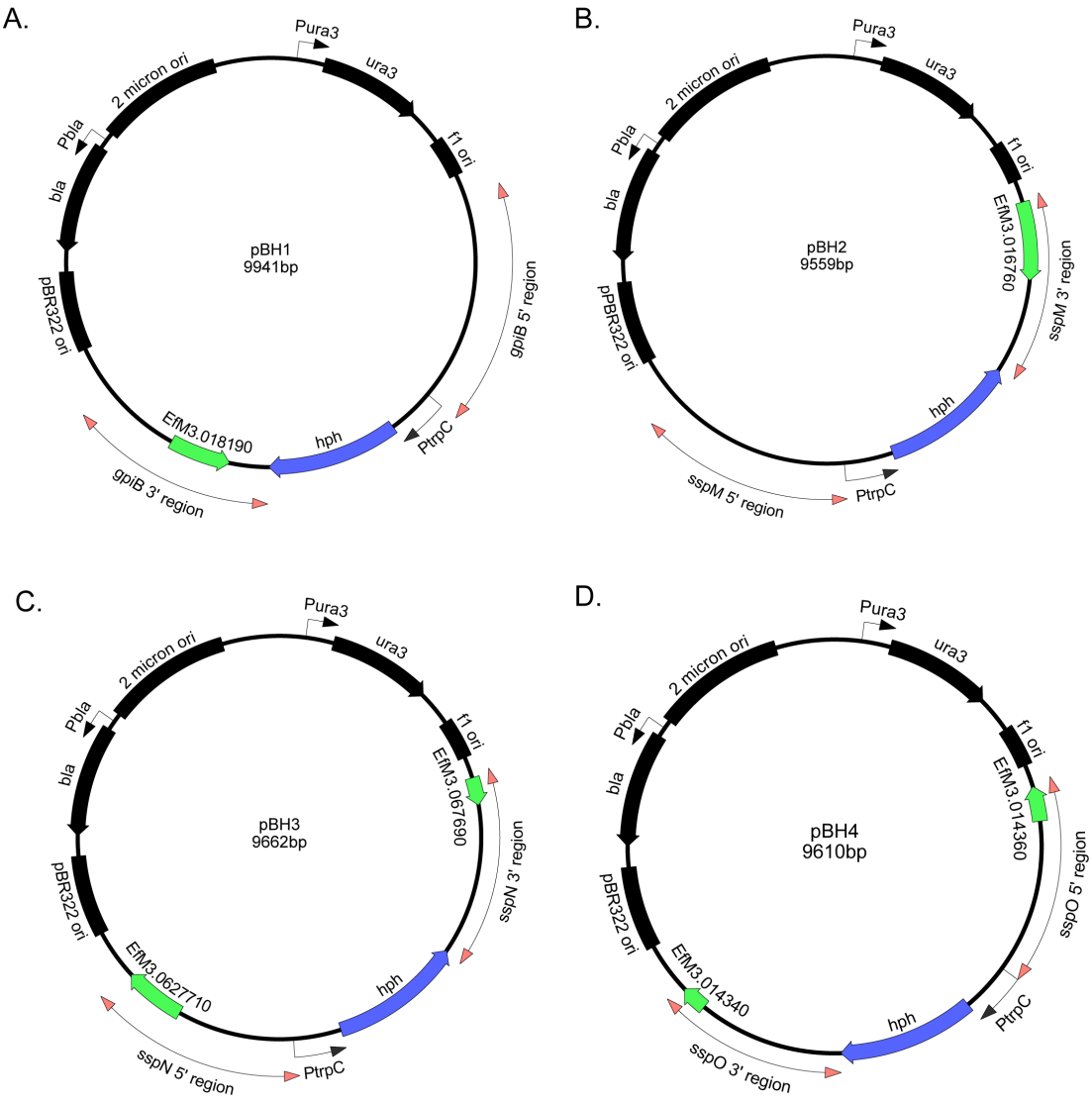

Appendix 4: *gpiB* (pBH1), *sspM* (pBH2), *sspN* (pBH3) and *sspO* (pBH4) deletion constructs.

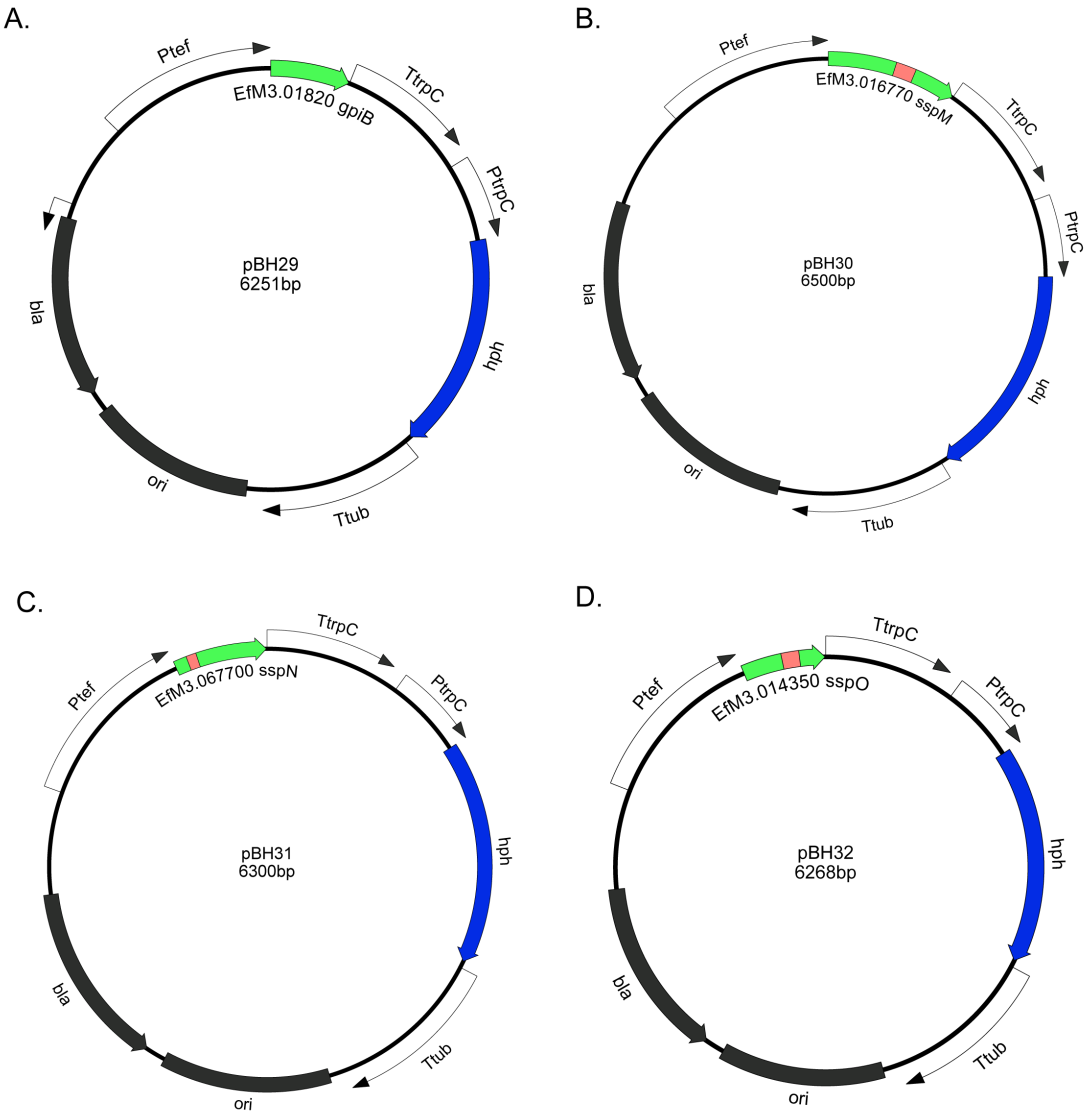

Appendix 5: *gpiB* (pBH29), *sspM* (pBH30), *sspN* (pBH31) and *sspO* (pBH32) overexpression constructs.

Red boxes indicate introns.

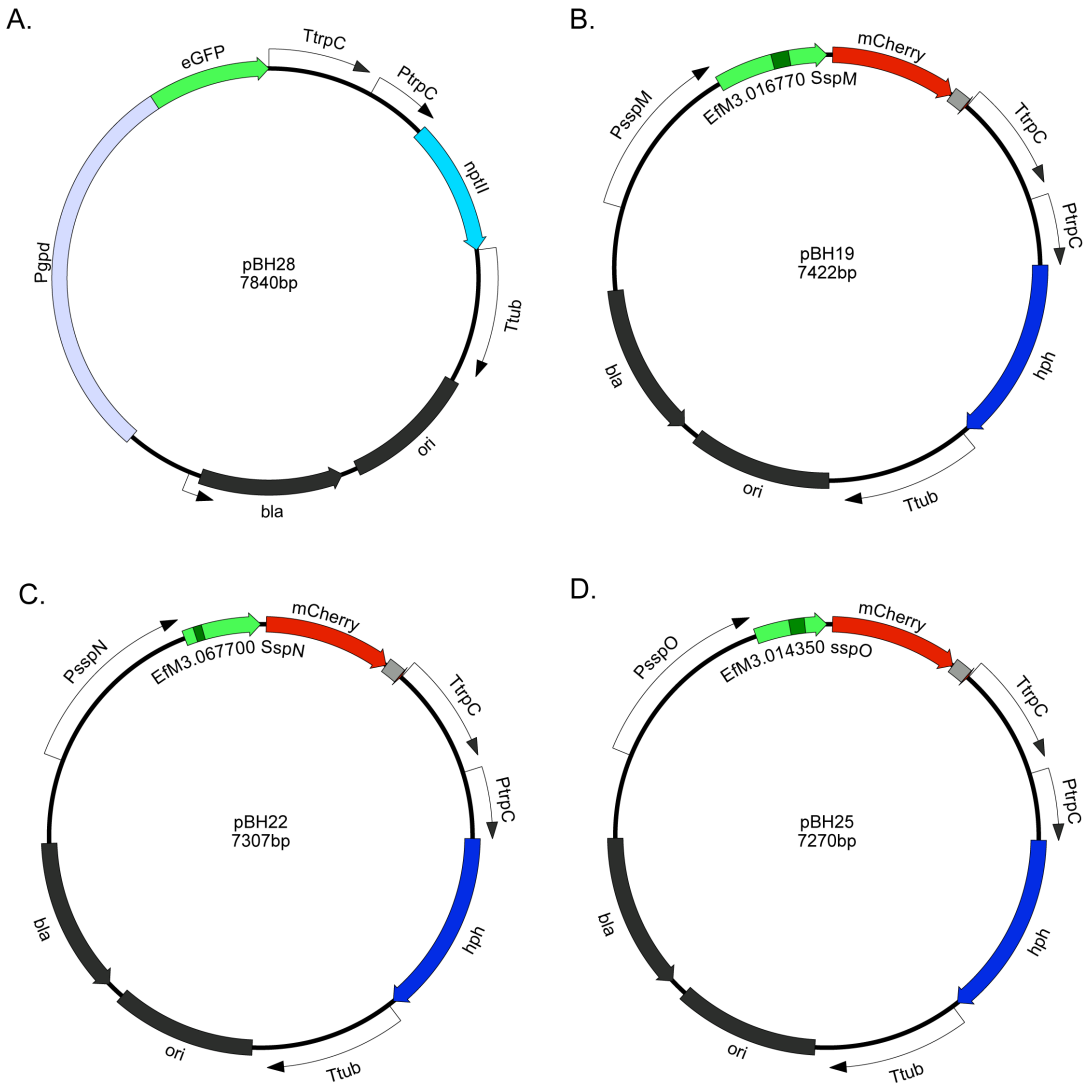

Appendix 6: cytoplasmic GFP (pBH28) and *sspM* (pBH19), *sspN* (pBH22) and *sspO* (pBH25) localization constucts.

Grey boxes indicate the nuclear localization signal, green boxes indicate introns.

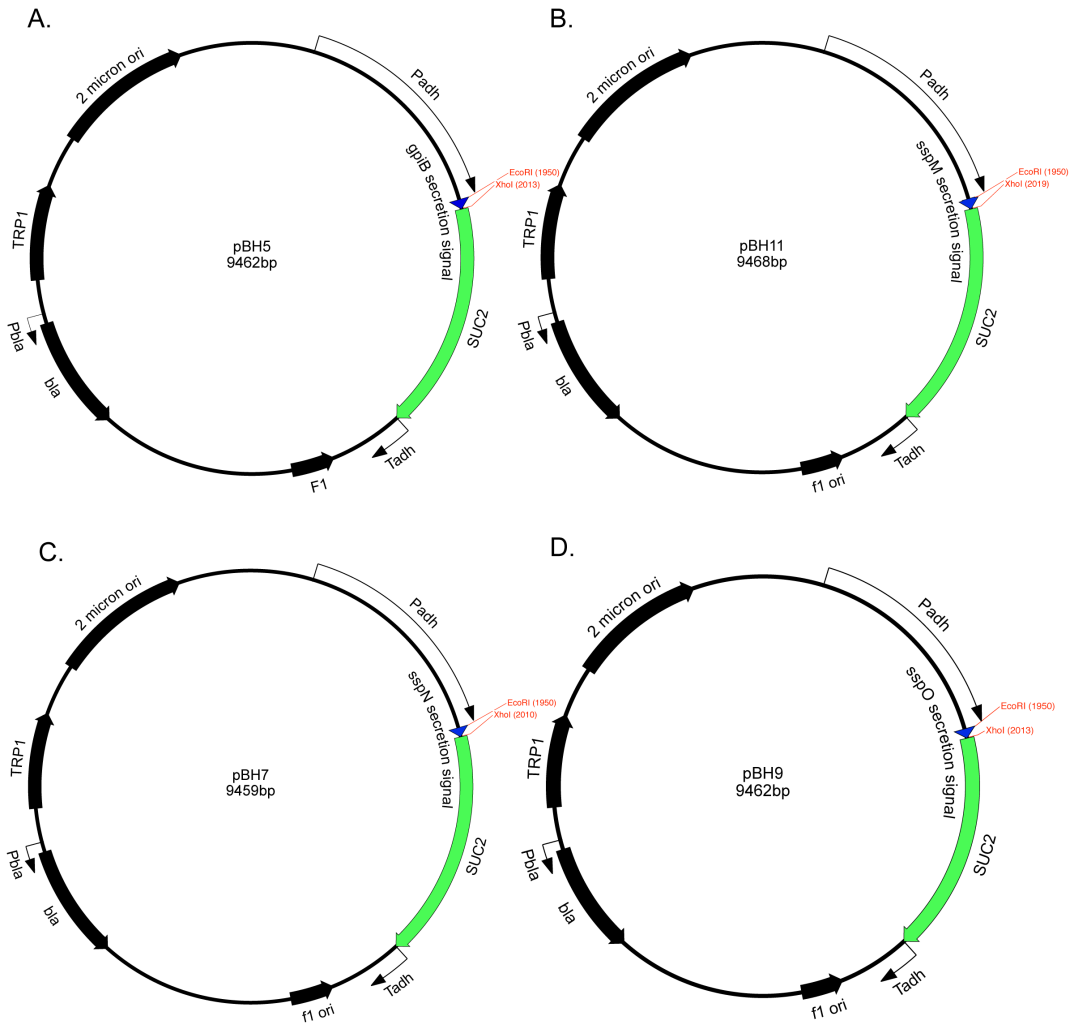

Appendix 7: *gpiB* (pBH5), *sspM* (pBH11), *sspN* (pBH7) and *sspO* (pBH9) pSUC2T7M13OR constucts.

*Eco*RI and *Xho*I restriction sites are marked.

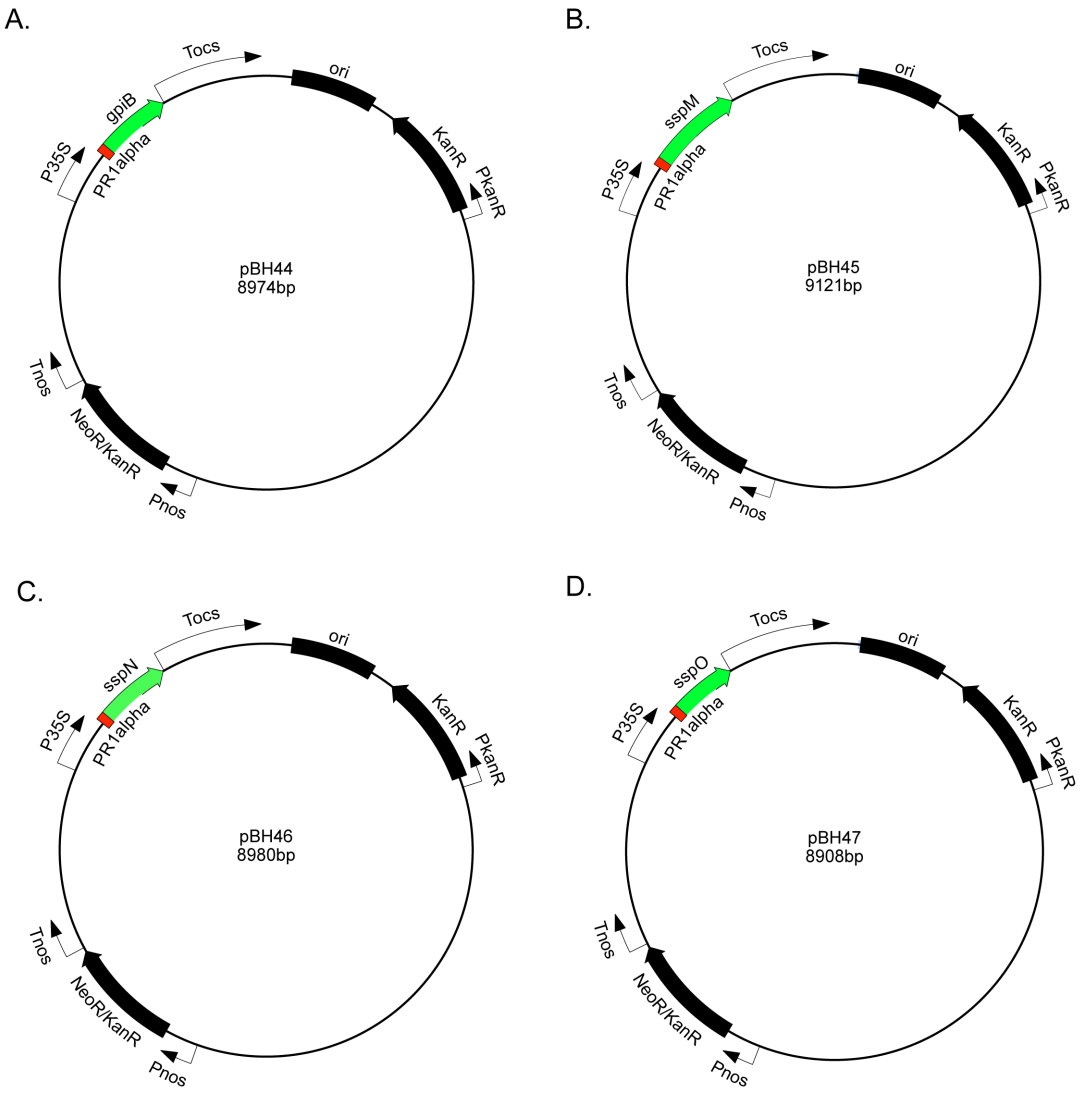

Appendix 8: *gpiB* (pBH44), *sspM* (pBH45), *sspN* (pBH46) and *sspO* (pBH47) pICH86988 constucts.

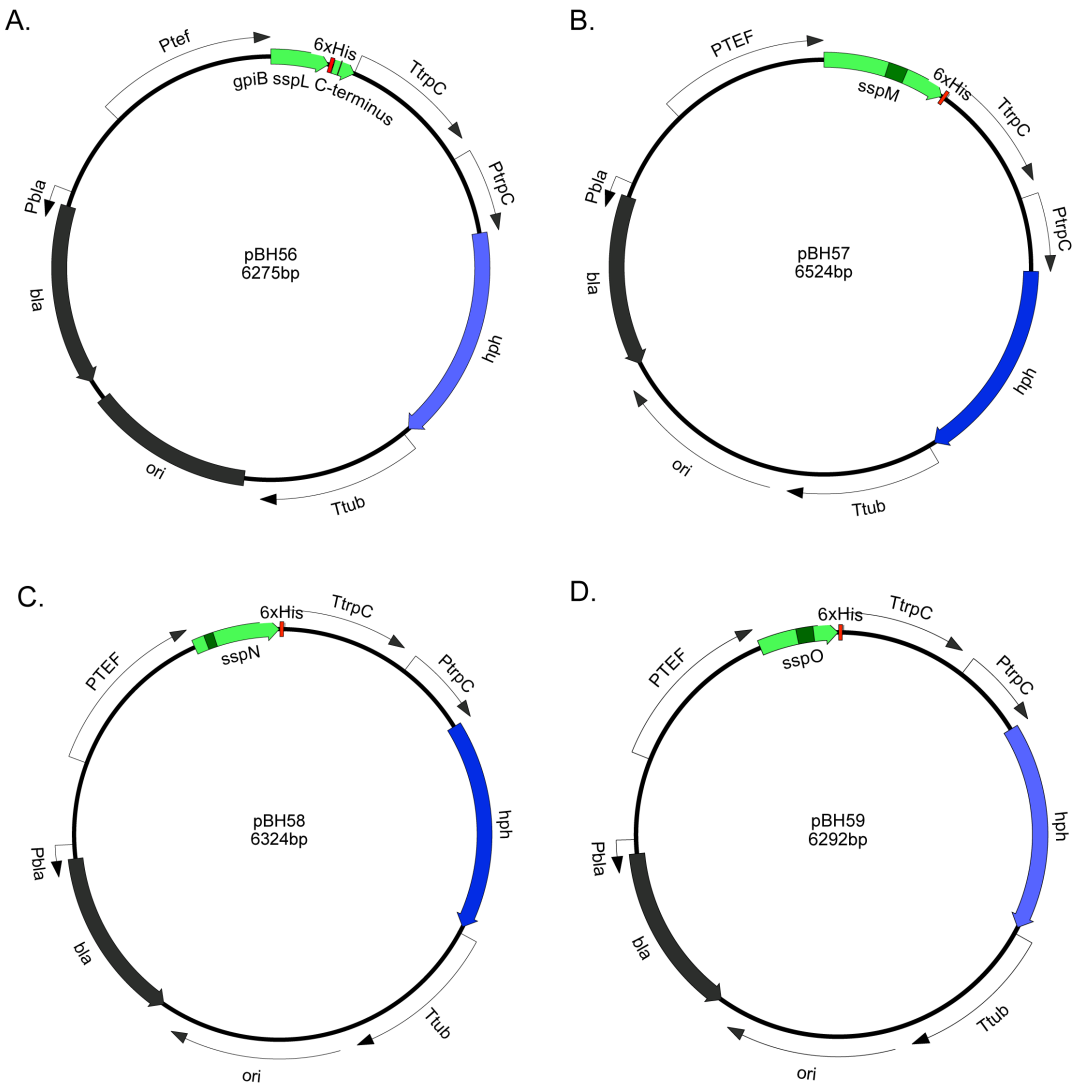

Appendix 9: *gpiB* (pBH56), *sspM* (pBH57), *sspN* (pBH58) and *sspO* (pBH59) expression constructs with 6xHis-tag.

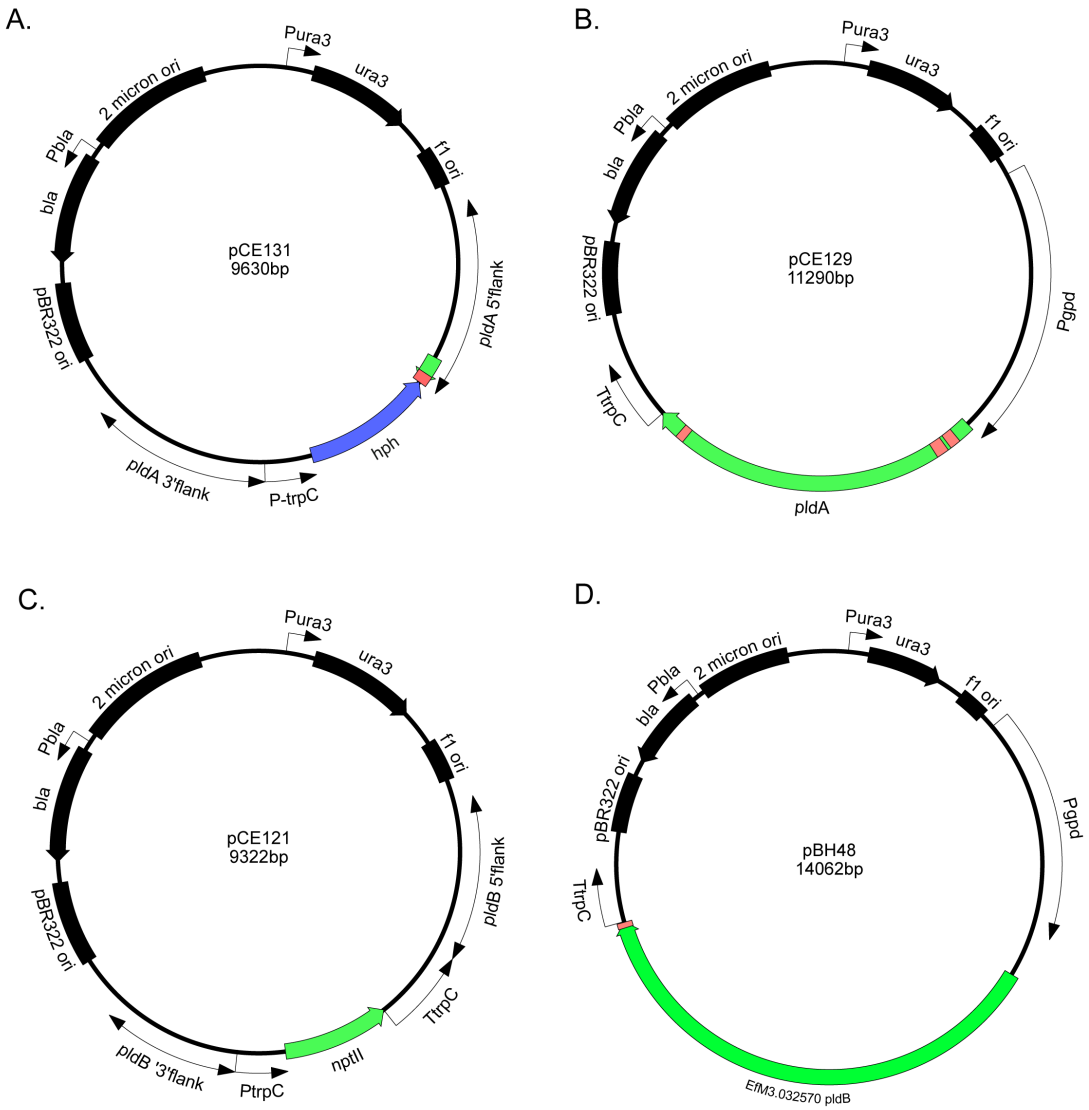

Appendix 10: *pldA* and *pldB* deletion (pCE131, pEC121) and overexpression (pCE129, pBH48) constructs.

Red boxes indicate introns.

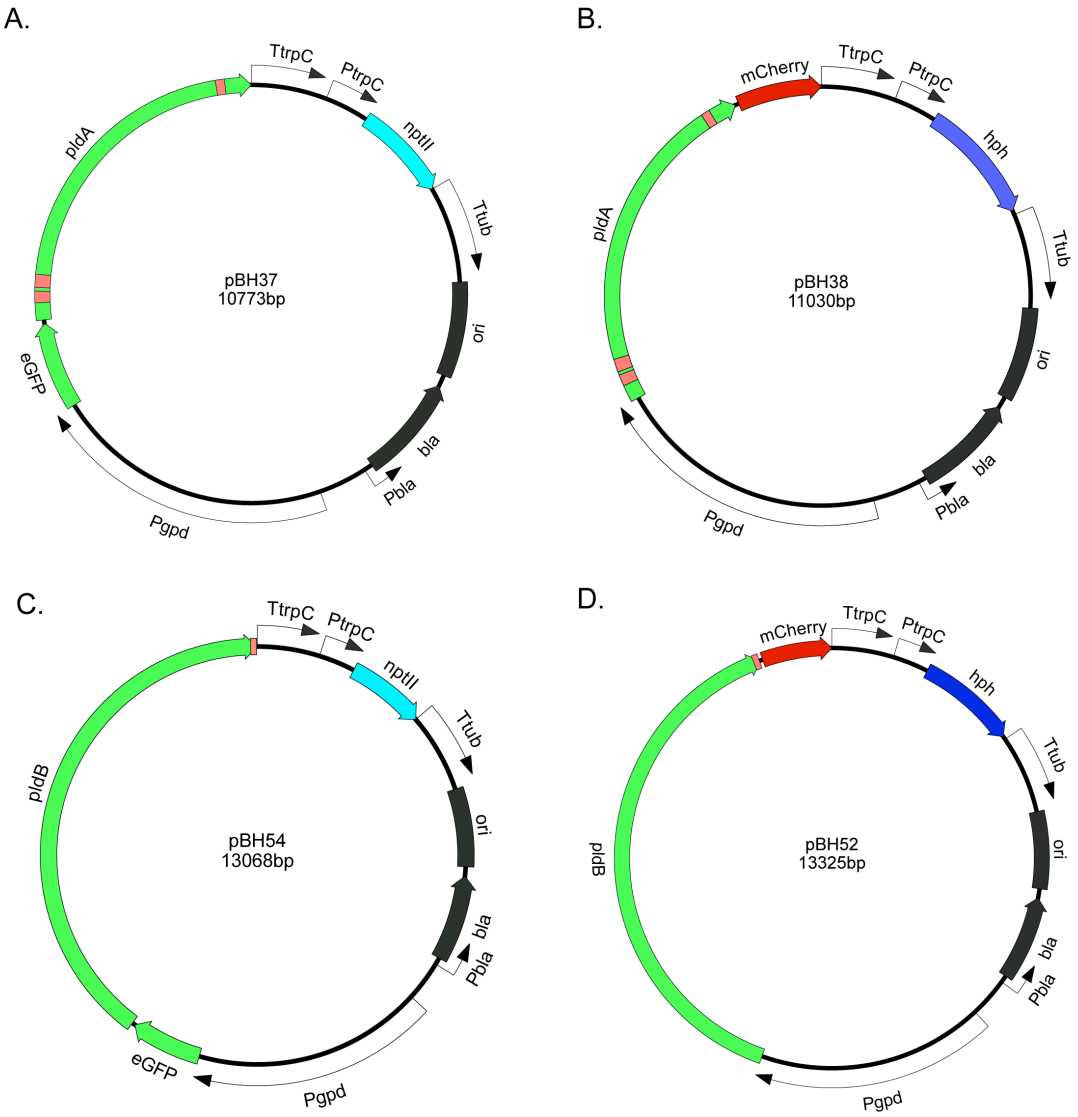

Appendix 11: *pldA* and *pldB* GFP fusion (pBH37, pBH54) and mCherry fusion (pBH38, pBH52) constructs.

Red boxes indicate introns.

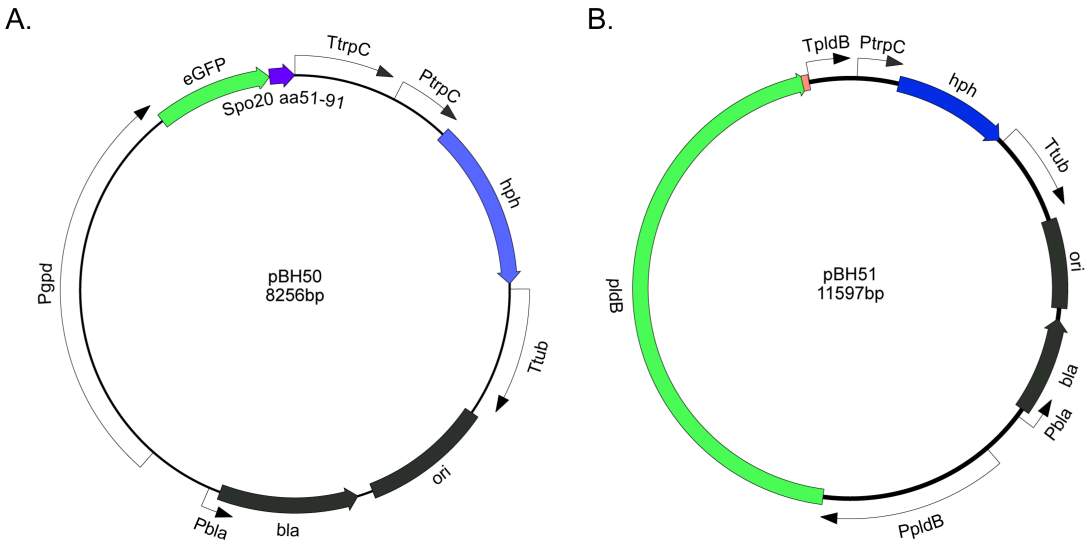

Appendix 12: *pldB* complementation (pBH51) and PA-biosensor (pBH51) constructs.

Red boxes indicate introns.

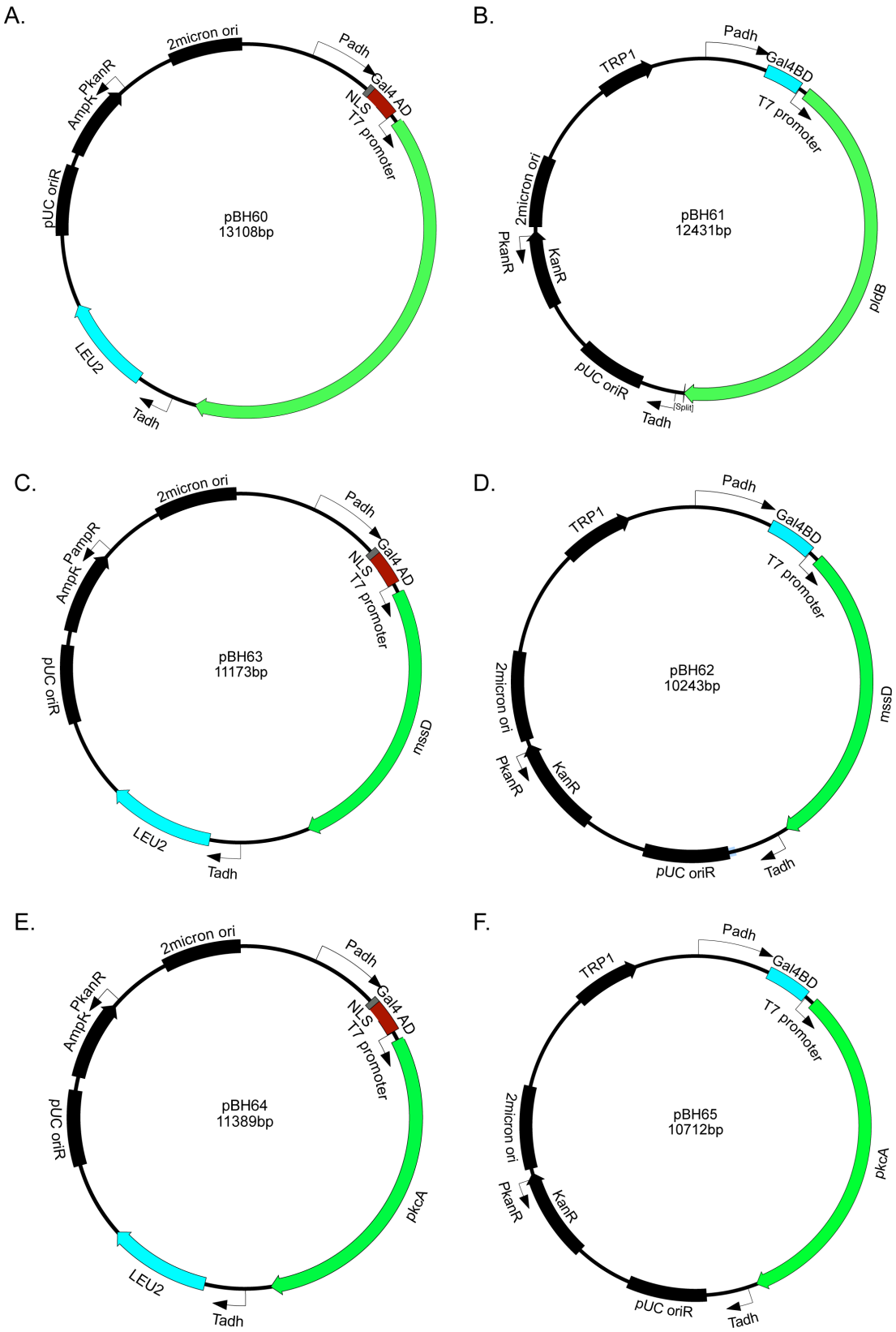

Appendix 13: *pldB* (pBH60, pBH61), *mssD* (pBH63, pBH62) and *pkcA* (pBH64, pBH65) yeast two-hybrid constructs.

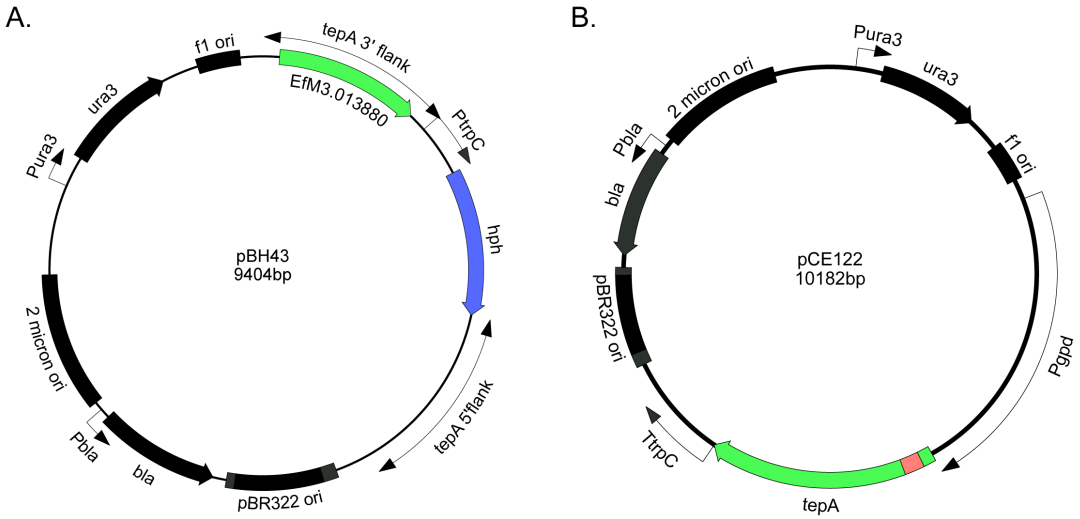

Appendix 14: *tepA* depetion (pBH43) and overexpression (pCE122) constructs.

Red boxes indicate introns.

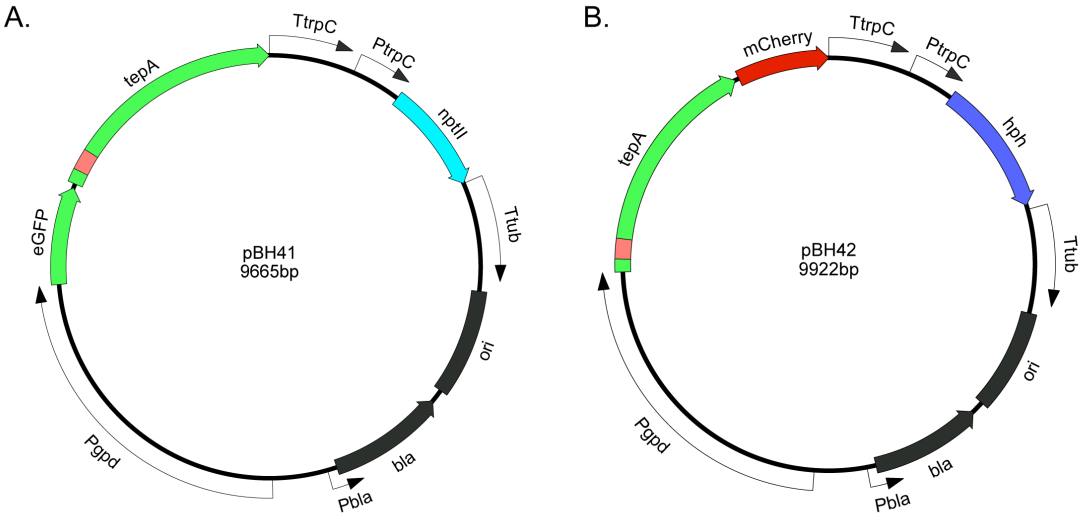

Appendix 15: *tepA* GFP fusion (pBH41) and mCherry fusion (pBH42) constructs.
Red boxes indicate introns.